SHEAR DEFORMATION IN ELASTIC BEAMS AND PLATES

Philip Reginald Stuart Speare

Thesis submitted for the degree of

Doctor of Philosophy

April 1975

ABSTRACT

Existing theories which include the effects of shear deformation in elastic beams and plates are compared and their relationship with each other examined.

Three approaches are applied to a range of problems in the bending of beams and circular and square plates. The first of these uses Reissner's theory, or, where this is not immediately applicable, a theory is developed based on his fundamental assumptions. Secondly, the possibility of employing a partial deflection method for homogeneous isotropic cases is considered, in which the effects of bending and shear can be separated. The third approach is a theory of specified order of accuracy, developed as a modification to Reissner's theory. It leads to a sixth order system of equations, thus enabling three conditions to be satisfied at each boundary of a rectangular plate, and is in terms of transverse displacement as the single variable.

The application of finite difference and localised Rayleigh-Ritz techniques to the solution of these three approaches is considered.

Two series of experimental tests are reported which investigate the effects of shear deformation on the deflection of beams and square plates.

ACKNOWLEDGEMENTS

I wish to express my gratitude for the help and advice which I have received from many people, especially the following:

Professor K.O. Kemp has shown a deep interest in this work, and has been a constant source of guidance and inspiration. I have derived great benefit from our numerous discussions, which have helped to resolve many difficulties.

The research was conducted initially while I was on the staff of Kingston Polytechnic and latterly of The City University. I am grateful for the encouragement which I have received from my colleagues and respective Heads of Department.

The laboratory and workshop staff of the Department of Civil Engineering at The City University, in particular Messrs. W.A.R. Jones, A.A. Towells and P. Bonomini, gave useful assistance in the design and manufacture of equipment for the experimental investigations.

Mrs. Kaye Ahtuam typed the thesis, and I am indebted to her for her patient and careful attention to detail.

Finally, I would like to thank my wife for her unfailing support and encouragement.

INDEX

SYMBOLS

a	radius of circular plate
	dimension of local region - localised Rayleigh-Ritz method
D	$(=Eh^3/12(1-\nu^2))$ flexural stiffness of plate
E	Young's modulus
G	shear modulus
h	depth of beam or plate
H	(= h/L) non-dimensional depth
I	second moment of area of beam
l	length of beam
L	representative length - span of beam or side of plate
M	bending moment in beam
M_n, M_t	
M_r, M_t	bending moments per unit width of plate
M_x, M_y	
M_{nt}	twisting moments per unit width of plate
M_{xy}	
n, t, z	normal and tangential orthogonal co-ordinate system
P	mesh length - finite difference method
P(= p/L)	non-dimensional mesh length
	concentrated load
q	uniformly distributed load - per unit length of beam
	or per unit area of plate
Q	shear force in beam
Q_x, Q_y	shear forces per unit width of plate

r, t, z	radial and tangential orthogonal co-ordinate system
S	shear stiffness per unit width of beam or plate
u, v, w	displacements in orthogonal co-ordinate system
U	strain energy in beam or plate
V	potential energy of beam or plate
w_b, w_s	partial deflections due to bending and shear
W(= w/L)	non-dimensional transverse displacement
X,Y,Z (=x/L, y/L, z/L)	non-dimensional co-ordinates

γ	Shear strain
$\triangle$	$(\frac{\partial^2}{\partial x^2} + \frac{\partial^2}{\partial y^2})$
$\triangle^2$	$(\frac{\partial^2}{\partial x^2} + \frac{\partial^2}{\partial y^2})^2$
$\triangle^3$	$(\frac{\partial^2}{\partial x^2} + \frac{\partial^2}{\partial y^2})^3$
ϵ	direct strain
ν	Poisson's ratio
ξ (= x/a)	non-dimensional co-ordinates in local region - localised Rayleigh-Ritz method
η (= y/a)	
σ	direct stress
ϕ	average rotation of section initially normal to the neutral surface
ψ	Reissner stress function
τ	shear stress

Subscripts:

n, t
r, t
x, y, z
} refer to relevant co-ordinate system

o (e.g. M_o, w_o) - indicates value given by classical theory

Constants: Various constants are employed as necessary and are given a temporary meaning which is defined locally.

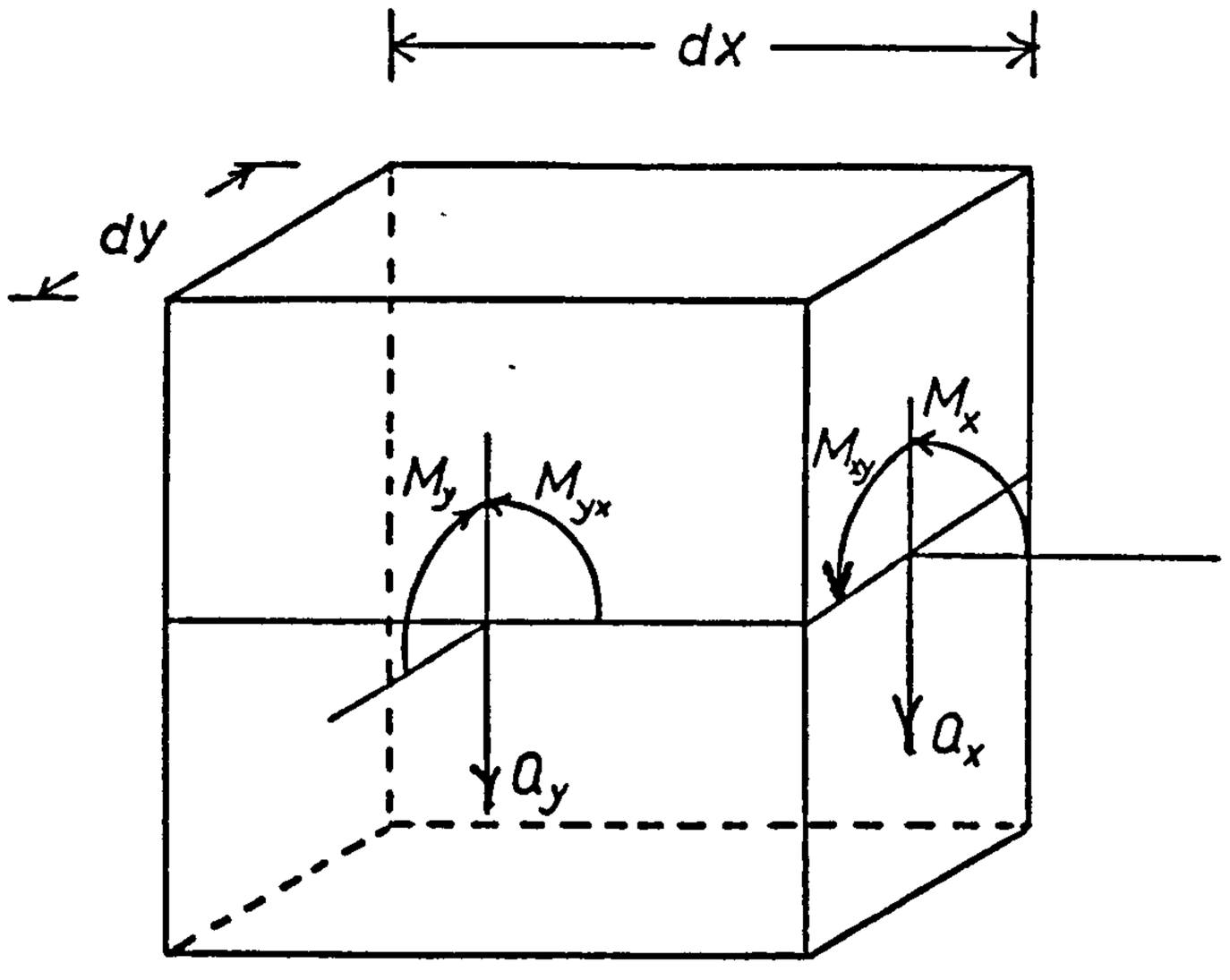

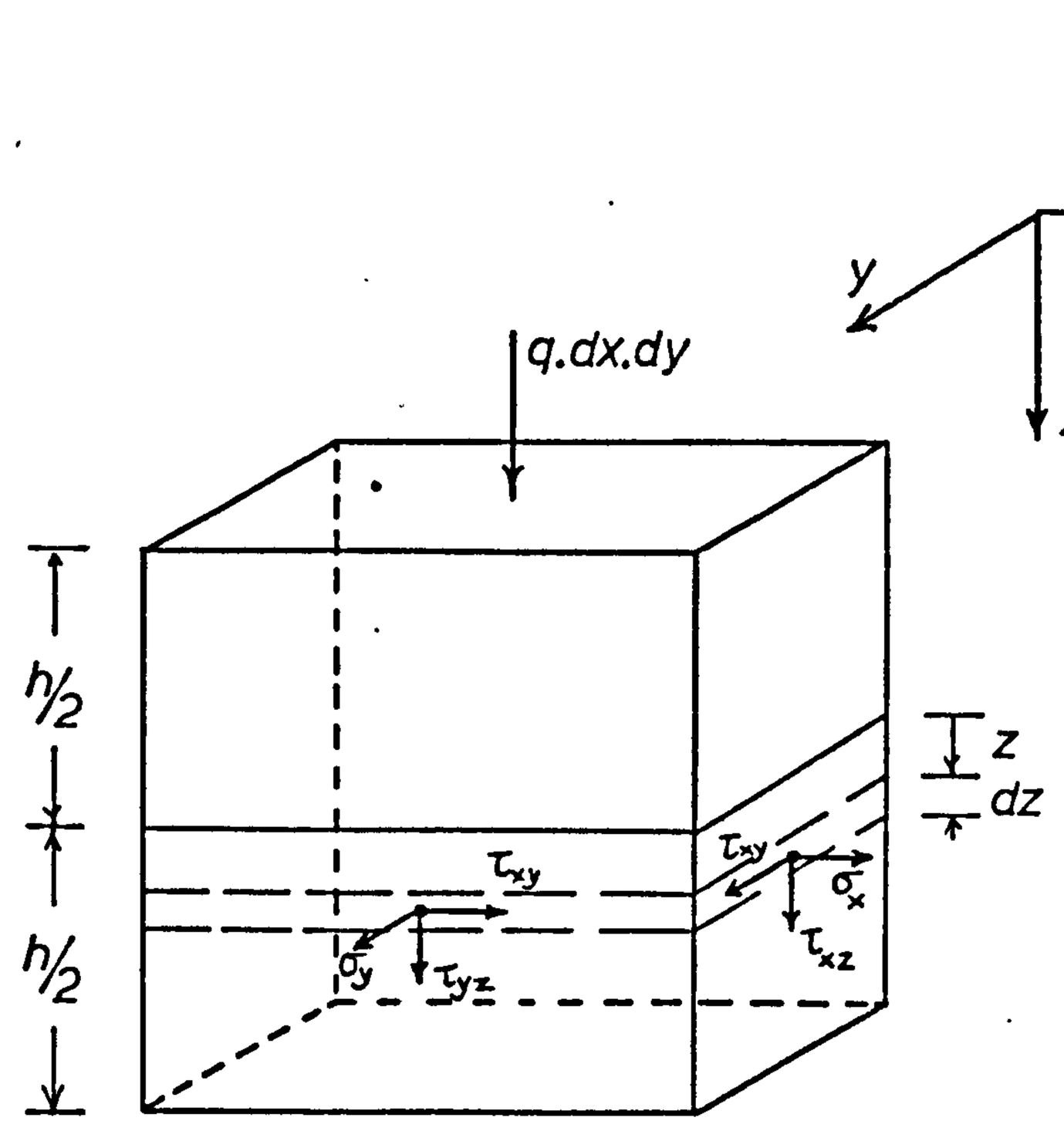

Conventions for stresses and stress resultants.

CHAPTER 1

INTRODUCTION AND HISTORICAL SURVEY

1.1 Introduction

The assumptions of classical small deflection theory of thin plates as presented, for example, by Timoshenko (1) are:

(a) there is no deformation in the plane of the neutral surface of the plate

(b) normals to the neutral surface remain straight and normal as the plate deforms

(c) direct stresses transverse to the plate may be neglected.

The first of these holds providing that there are no external forces applied in the neutral plane, and that deflections are small so that there is no membrane action, while the second implies that the effects of transverse shear on the deflection of the plate may be neglected. Thus an essentially three-dimensional elasticity problem is reduced to two dimensions since the transverse displacement is

$$w = f(x,y) \tag{1.1}$$

i.e. independent of z, and stresses and stress resultants may be expressed in terms of w and its derivatives.

A further problem is introduced, however, in that the resulting theory enables only two conditions to be satisfied at a boundary instead of three. Kirchoff's reduction of the three Poisson conditions for a free edge is the best known example of this feature.

Thus the two principal limitations of classical thin plate theory are the inconsistency in dealing with boundary conditions, and the failure to take into account the deformation due to transverse shear.

For most engineering purposes the classical theory will be adequate, but its approach cannot be applied to plates of significant thickness without at least the second of these limitations being overcome.

In the past thirty years a great deal of work has been carried out in an attempt to improve classical theory within the confines of the two-dimensional description of transverse displacement of equation (1.1), thus enabling useful results to be obtained without carrying out a fully three-dimensional analysis. The work of Reissner occupies a unique position amongst the literature of this period and will be regarded here as a standard for purposes of comparison. Reissner preserves the two-dimensional formulation of the problem by defining w, not as the transverse displacement of the neutral surface, but as a weighted average displacement through the depth of the plate, such that at any point the work done by the resultant transverse shear force acting through the average shear displacement is equal to the work of the corresponding shear stresses on the actual displacement.

1.2 Survey of previous work

This is not intended as an exhaustive survey, but simply to state the underlying assumptions of Reissner's theory and hence establish its position in relation to other important developments.

1.2.1 Reissner

Reissner first stated his theory in 1944 (2) and subsequently developed it and restated it in 1945 and 1947, (3) and (4). The starting point is the assumption of the following

distributions of stresses:

$$\sigma_x = \frac{12M_x}{h^3} z \qquad (1.2)$$

$$\sigma_y = \frac{12M_y}{h^3} z \qquad (1.3)$$

$$\tau_{xy} = \frac{12M_{xy}}{h^3} z \qquad (1.4)$$

$$\tau_{xz} = \frac{3Q_x}{2h}\left[1 - \left(\frac{2z}{h}\right)^2 \right] \qquad (1.5)$$

$$\tau_{yz} = \frac{3Q_y}{2h}\left[1 - \left(\frac{2z}{h}\right)^2 \right] \qquad (1.6)$$

$$\sigma_z = - \frac{3q}{4}\left[\frac{2}{3} - \frac{2z}{h} + \frac{1}{3}\left(\frac{2z}{h}\right)^3 \right] \qquad (1.7)$$

For a homogeneous plate, the strain energy including that due to transverse shear and transverse direct stress is given by

$$U = \frac{1}{2E}\iiint\left[\sigma_x^2 + \sigma_y^2 + \sigma_z^2 - 2\nu\,(\sigma_x\sigma_y + \sigma_x\sigma_z + \sigma_y\sigma_z)\right.$$

$$\left. + 2(1+\nu)(\tau_{xy}^2 + \tau_{xy}^2 + \tau_{yz}^2)\right] dx\,dy\,dz \qquad (1.8)$$

which may be alternatively expressed in terms of the stress resultant as

$$U = \frac{1}{2E}\iint\left[\frac{12}{h^3}\left(Mx^2 + My^2 - 2\nu\, MxMy + 2(1+\nu)\, Mxy^2\right)\right.$$

$$+\frac{12(1+\nu)}{5h}\left(Qx^2 + Qy^2\right) - \frac{12\nu q}{5h}(Mx + My)$$

$$\left.+\int_{-h/2}^{h/2} \sigma z^2 \, dz\right] dx\, dy \qquad (1.9)$$

To obtain the complementary energy the work done by the boundary stresses must be deducted, and the resulting expression is then minimised subject to the usual plate equilibrium equations

$$\frac{\partial Qx}{\partial x} + \frac{\partial Qy}{\partial y} = -q \qquad (1.10)$$

$$Qx = \frac{\partial Mx}{\partial x} + \frac{\partial Mxy}{\partial y} \qquad (1.11)$$

$$Qy = \frac{\partial My}{\partial y} + \frac{\partial Mxy}{\partial x} \qquad (1.12)$$

This minimisation is carried out by using the calculus of variations, the Lagrangian multipliers used being identified as the generalised displacements of a point, namely w, ϕ_x and ϕ_y, the average transverse displacement and average rotations. The precise form of these displacements will be discussed later; it is sufficient to note here that the rotations will take account of the shear deformation and hence will not be the slope of the neutral plane, but the average rotation of a plane initially normal to it.

The resulting equilibrium equations and stress resultants are finally established in terms of w and a stress function, ψ.

This system of partial differential equations is sixth order overall, being of fourth order in w, and second order in ψ , thus requiring that three conditions be satisfied at each boundary.

From equation (1.8) it can be seen that Reissner's theory includes the energy due to both transverse shear stress (τ_{xz}, τ_{yz}) and transverse direct stress (σ_z). The only limitation of the initial assumptions is that linear distributions are attributed to the bending stresses σ_x, σ_y whereas in thick plates with the distortion of the cross-section due to shear this will not be strictly accurate, as is demonstrated for example, by Timoshenko's analysis of beams (26) discussed in section 3.2.2.

1.2.2 Application of Reissner's theory by other writers

Among the alternative statements of Reissner's theory and applications of it the more notable are listed in references (5) - (11). Where analytical solutions are obtained these are in series form, and thus suffer the limitations of Navier or Levy type solutions - mathematical complexity and the fact that only simple geometric shapes can be treated. The need to satisfy three boundary equations adds considerably to the difficulties of obtaining solutions, and in some cases these are avoided altogether by considering infinite or semi-infinite plates. None of these papers considers the problem of concentrated loading, although this could be presented in Fourier form.

In Goodier's discussion of Reissner (3) a set of equations is derived which is almost identical with Reissner's. The only difference is a small discrepancy in some of the constants,

which is noted by Langhaar (12) and appears to arise from Reissner taking a weighted average displacement, while Goodier uses the neutral surface displacement.

1.2.3 Other advanced theories

1.2.3.1 Love (13)

Love presented a theory for moderately thick plates in which the equations for bending and twisting moments allow for shear deformation. However, the equations for shear forces are identical with those of classical theory, and hence the governing equation is the usual biharmonic allowing only two boundary equations to be satisfied.

1.2.3.2 Kromm (14) and (15)

Another approach in which initially arbitrary functions are assumed for the distribution of bending and shear stress through the depth of the plate is due to Kromm. Timoshenko (1) comments that this theory does, however, neglect the effects of transverse direct stress, σ_z. The final form of the equations shows a remarkably close resemblance to those of Reissner.

1.2.3.3 Goldenveizer and Kolos, (16 - 18)

These writers summarise the methods by which the three-dimensional stress equations have been reduced to a two dimensional form, and themselves perform this task by asymptotic integration. Again their results are very similar to those of Reissner.

1.2.3.4 Ambartsumyan, (19)

Ambartsumyan has developed a general theory for anisotropic plates which includes the effects of shear deformation,

but omits transverse direct stress, although this is included in a particular theory derived for one or two cases. It can easily be shown that the resulting equations are identical to those of Reissner when reduced to a form for homogeneous plates. The work is most notable for the fact that it is developed in anisotropic form, and for the range of solutions presented explicitly.

1.2.4 Experimental Investigations

Experimental work on plates has been largely limited to the determination of stresses by photoelastic methods, and only two papers discuss the problems of the experimental verification of Reissner's theory. Carley and Laghaar (9) attempted to confirm the predictions of Reissner's theory in respect of the distribution of shear stress, but their investigation was largely inconclusive due to lack of precision in the experimental boundary conditions. Haberland (20) formulates the relationships between the bending moments as given by Reissner's theory and the photoelastic parameters. Both of these investigations concentrate on the distributions of stress and there is no record of attempts to confirm the increase in deflection due to shear which is predicted, especially for thicker plates.

1.2.5 Special methods used for the analysis of sandwich plates

Sandwich plates represent a class of problems where the effects of shear deformation can be highly significant, and it is of interest to note here the methods of solution commonly employed.

In the partial deflection method, discussed extensively by Plantema (21) and Allen (22), two partial deflections w_b and w_s are employed.

Moment and shear stress resultants are expressed in terms of derivatives of these partial deflections, which are thus related through the equilibrium equations (1.11) and (1.12). The total deflection at any point is the sum of these two components, which in beam problems and certain plates problems can be regarded as the deflections due to bending and shear so that in these cases this approach amounts to a simple superposition of deflections due to these two effects.

Libove and Batdorf (23) adopted a different approach by developing expressions for the curvatures and twist which contain the effects of both bending and twisting moments and shear forces. Recent papers by Williams and Chapman (24) and Morley (25) have successfully applied the results to cellular problems, and the latter has found close agreement with some published experimental results.

1.3 Statement of objectives

The unique position of Reissner's theory is clear. It represents the most comprehensive investigation of the problems of the inclusion of the effects of shear deformation, and indeed of transverse direct stress, on plate flexure. But, as can be seen from the preceding historical survey, largely as a result of the mathematical form of the Reissner equations, which involve the statement of the problem in terms of both the deflection w and a stress function ψ, solutions have been obtained to only a limited range of problems.

Even more scant are references to the application of numerical techniques to the problem, and any account of experimental verification of the theoretical predictions of deflection.

The objectives of this work may, therefore, be summarised as,

(a) to compare and appraise existing improvements to thin plate theory to include the effects of shear deformation

(b) to develop a new theory as a modification of Reissner's theory which will be formulated in terms of a single variable, w, the transverse displacement.

(c) to apply finite difference and finite element methods to the solution of a range of problems, and to assess the relative merits of the various approaches in terms of the applicability of these numerical techniques.

(d) to test some of the results experimentally.

Although most of the work has been directed towards plate problems, it was found that the relationship between the various approaches and the consequences of their respective assumptions can be more readily demonstrated by applying them to a simpler class of problems, namely beams. Thus a chapter is devoted to beam problems, and these are discussed before the section dealing with square plates, although in strict chronological terms much of this latter section was completed first. An added advantage in the case of beams is that more existing solutions are available for purposes of comparison.

The work is concerned with homogeneous beams and plates, but the application to anisotropic, sandwich and cellular systems is briefly discussed.

CHAPTER 2

SHEAR DEFORMATION IN CIRCULAR PLATES.

2.1 Introduction

Timoshenko (1), Love (13) and Ambartsumyan (19) all give solutions to symetrically supported and loaded circular plate problems in which the effects of shear deformation are included. Reissner did not apply his theory to this class of problem, but a theory is developed here, employing his assumptions, thus enabling theories so based to be assessed in relation to other approaches.

There are three particular advantages in first considering circular plates.

(a) Because of symmetry, three boundary conditions are automatically satisfied by all solutions, and thus in comparing the theory with those already existing any disparity, at least for simply supported plates, must derive from differences in the initial assumptions rather than the statement of boundary conditions.

(b) It is found that there is no need to introduce Reissner's stress function, ψ, in this case and a solution is obtained in terms of transverse displacement, w, only.

(c) As has been noted in Section 1.2.1, Reissner's theory includes both the effects of shear and transverse direct stress. For these problems it is possible to quantify the influence of these effects separately, so that their relative importance can be assessed.

After a brief discussion of existing solutions, the theory is applied to uniformly loaded circular plates with simply

supported and clamped boundaries. From the results obtained the accuracy of theories based on Reisner's assumptions is assessed, and the influence of shear and transverse direct stress on the deflection and state of stress of the plate examined.

In essence it is found that while Timoshenko's method is the superposition of deflections due to bending, shear and transverse direct stress, the utilisation of Reissner's approach involves a superposition of curvatures due to these three effects. For circular plates these approaches are identical in effect, and the differences which arise here are shown to result from a different definition of shear stiffness. In the case of clamped boundaries the disparities are found to arise from differences in the assumed mode of action of this type of support.

The results obtained from the theory are identical with those of Ambartsumyan, but differ slightly from Love's solution, due to the latter's use of a more refined non-linear distribution of bending stress.

2.2 Existing solutions for circular plates including the effects of shear deformation

2.2.1 Timoshenko (1)

Timoshenko gives two simple corrections to be superimposed on the classical solution, one for deformation due to shear, and the other for transverse direct stress. Assuming a parabolic distribution of shear stress through the depth of the plate the maximum shear stress occurs at the neutral surface, and at radius r is given by

$$\tau_{rz\ max} = \frac{3}{2}\frac{qr}{2h} \qquad (2.1)$$

and the corresponding shear strain is

$$\frac{dw_1}{dr} = -\frac{3qr}{4Gh} \qquad (2.2)$$

where w_1 is the additional deflection at the mid surface due to shear deformation.

Integrating and setting $w_1 = 0$ at $r = a$ gives

$$w_1 = \frac{qh^2}{16D(1-\nu)}(a^2 - r^2) \qquad (2.3)$$

For transverse direct stress the usual cubic distribution for uniform loading is assumed, giving the following values for transverse direct stress, σ_z, and radial strain ϵ_r:

upper surface $\sigma_z = -q$ $\epsilon_r = \frac{\nu q}{E}$

mid-surface $\sigma_z = -q/2$ $\epsilon_r = \frac{\nu q}{2E}$

lower surface $\sigma_z = 0$ $\epsilon_r = 0$

The distribution of radial strain is approximated to a linear form, giving a curvature at the mid-surface of $\nu q/Eh$. Noting that this positive curvature will produce negative (i.e. upward) deflection, the correction w_2 to be applied to the midplane deflection is found on integration to be

$$w_2 = \frac{\nu q h^2}{24D(1 - \nu^2)} \qquad (2.4)$$

Timoshenko argues that a clamped boundary would prevent in-plane radial strains which would eliminate w_2, so that the deflection of a plate with such boundaries would be the sum of the normal classical expression,

$$\frac{q}{64D} (a^2 - r^2)^2,$$

and the shear correction, w_1

$$\text{i.e.} \quad w = \frac{q}{64D}\left[(a^2 - r^2)^2 + \frac{4h^2}{(1 - \nu)} (a^2 - r^2) \right] \qquad (2.5)$$

For a simply supported plate, however, these radial strains would be free to occur and hence corrections due to both shear and transverse direct stress have to be applied giving

$$w = \frac{q}{64D} (a^2 - r^2)\left(\frac{5 + \nu}{1 + \nu} a^2 - r^2\right) + \frac{qh^2(3 + \nu)}{48D\ (1 - \nu^2)}(a^2 - r^2) \qquad (2.6)$$

2.2.2 Love (13)

Love presents a theory for moderately thick plates which includes the effects of both shear and transverse direct stress. In the case of circular plates a solution is presented which is not limited by the assumption of a linear distribution of radial or tangential strain. The resulting formulae for the deflection of the mid-surface of uniformly loaded plates are:

(a) simply supported edges

$$w = \frac{q}{64D}(a^2 - r^2)\left(\frac{5 + \nu}{1 + \nu} a^2 - r^2\right) + \frac{qh^2}{160} \frac{8 + \nu + \nu^2}{1 - \nu^2}(a^2 - r^2) \qquad (2.7)$$

(b) clamped edges

$$w = \frac{q}{64D}\left[(a^2 - r^2)^2 + \frac{4}{1-\nu} h^2 (a^2 - r^2)\right] \qquad (2.8)$$

2.2.3 Ambartsumyan (19)

Ambartsumyan applies both his general and particular theories to circular plates, so that solutions are available for uniform loading omitting and including the effects of transverse direct stress.

(a) For a simply supported plate the deflection is defined by one of the two following functions. If the effects of transverse direct stress are included the deflection is

$$w = \frac{q}{64D}(a^2 - r^2)\left(\frac{5+\nu}{1+\nu} a^2 - r^2\right) + \frac{qh^2}{20D(1-\nu^2)}(a^2 - r^2) \qquad (2.9)$$

and if these effects are omitted this expression is modified to

$$w = \frac{q}{64D}(a^2 - r^2)\left(\frac{5+\nu}{1+\nu} a^2 - r^2\right) + \frac{qh^2}{20D(1-\nu)}(a^2 - r^2) \qquad (2.10)$$

(b) For a plate with clamped edges the deflection is the same whether or not the effects of transverse direct stress are included and is given by

$$w = \frac{q}{64D}(a^2 - r^2)^2 + \frac{qh^2}{16D(1-\nu)}(a^2 - r^2) \qquad (2.11)$$

2.3 Development of a theory based on Reissner's assumptions

2.3.1 Basic assumptions

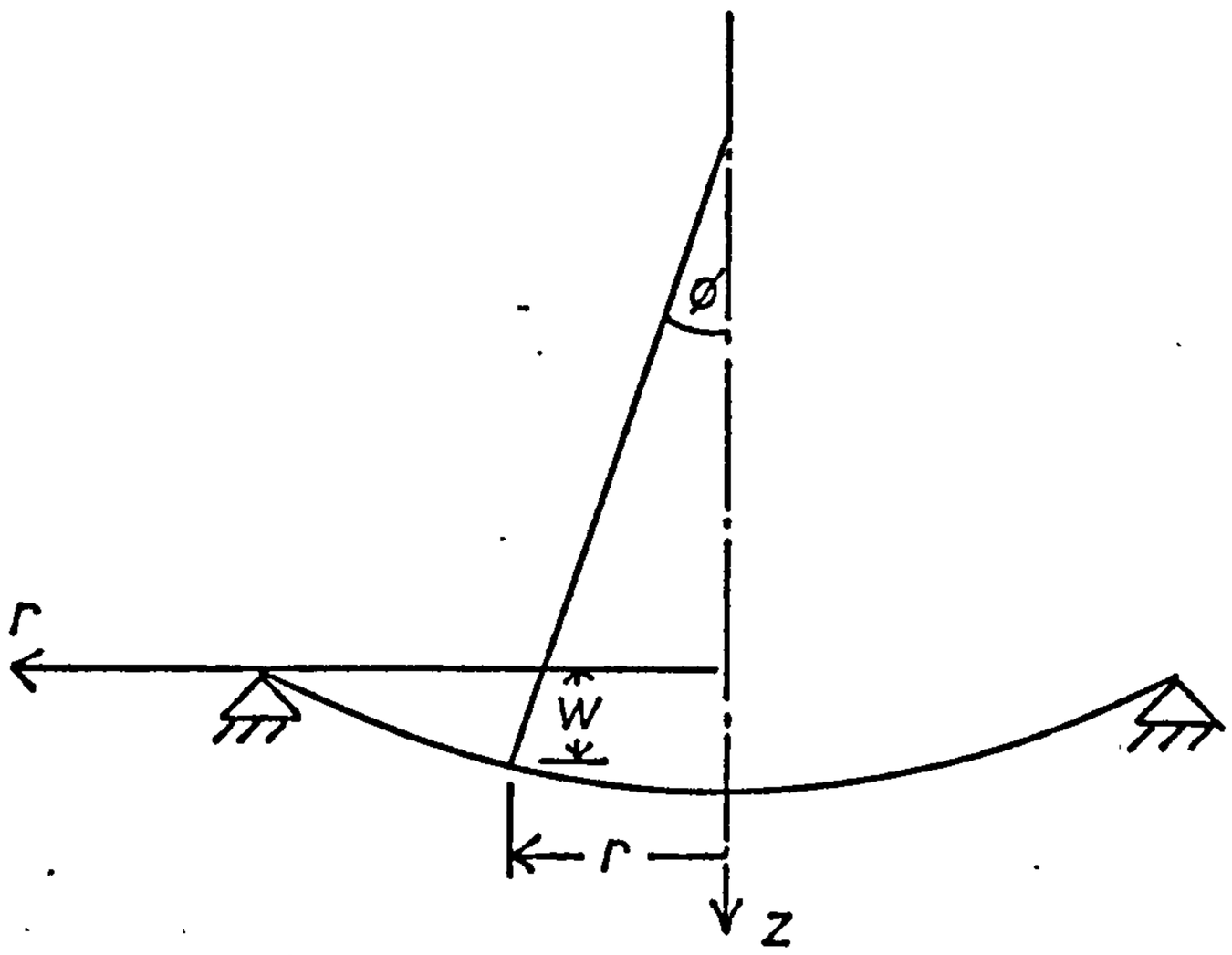

Figure 2.1

Diametral section of circular plate.

In the classical theory of circular plates as given, for example, by Timoshenko (1) the principal curvatures of radial and tangential sections at radius r are defined as

$$\frac{1}{R_n} = \frac{d\phi}{dr} \qquad (2.12)$$

$$\frac{1}{R_t} = \frac{\phi}{r} \qquad (2.13)$$

where ϕ is the rotation of a plane initially normal to the neutral plane. In classical theory this is equal to the neutral plane slope, dw/dr, but when the effects of shear deformation are included a relative rotation between the neutral plane and the plane initially normal to it will occur. In keeping with

Reissner's work, $12(1 + \nu)Q_r/5Eh$ is adopted for the average value of this relative rotation through the depth of the plate due to shear force Q_r. Thus the angle ϕ in Figure 2.1 is the total average rotation of an initially vertical plane due to both bending and shear, and will therefore be given by

$$\phi = -\frac{dw}{dr} - \frac{12(1 + \nu)}{5Eh} Q_r \qquad (2.14)$$

in which, for a uniformly distributed load

$$Q_r = \frac{qr}{2} \qquad (2.15)$$

If the radial and tangential bending moments M_r and M_t are now expressed in terms of the principal curvatures in the usual manner, then

$$M_r = D(\frac{d\phi}{dr} + \frac{\nu\phi}{r}) \qquad (2.16)$$

$$M_t = D(\frac{\phi}{r} + \nu\frac{d\phi}{dr}) \qquad (2.17)$$

and by virtue of the new definition of ϕ these expressions include the effects of shear deformation.

These relationships are consistent with Reissner's assumptions in respect of shear deformation, but no account has yet been taken of transverse direct stress. Inspection of Reissner's equations for bending moments indicates that the additional curvature caused by this stress is $6\nu(1 + \nu)q/5Eh$ and including this term would modify equations (2.16) and (2.17) to

$$M_r = D\left(\frac{d\phi}{dr} + \frac{\nu\phi}{r} + \frac{6\nu(1 + \nu)}{5Eh} q\right) \qquad (2.18)$$

$$M_t = D\left(\frac{\phi}{r} + \nu\frac{d\phi}{dr} + \frac{6\nu(1 + \nu)}{5Eh} q\right) \qquad (2.19)$$

In the following two sections solutions will be developed for uniformly loaded circular plates with clamped and simply supported boundaries, firstly including the effects of shear deformation and secondly transverse direct stress in addition. In each case the usual form of the equilibrium equation will apply, namely

$$M_r + \frac{dM_r}{dr} r - M_t + Qr = 0 \qquad (2.20)$$

and it only remains to substitute the appropriate expressions for M_r and M_t and to satisfy the relevant boundary conditions.

2.3.2 Deflection of circular plates including the effects of shear deformation.

Substituting for M_r and M_t from (2.16) and (2.17) in (2.20) leads to the classical form of the equilibrium equation

$$\frac{d}{dr}\left(\frac{1}{r}\frac{d}{dr}(r\phi)\right) = -Q/D \qquad (2.21)$$

but with ϕ now defined by equation (2.14).

2.3.2.1 Clamped boundary

At a clamped boundary it will be assumed that the average rotation of an initially vertical plane is zero, although such a plane will clearly be distorted by shear stresses and hence this condition is only satisfied on average rather than that the radial displacement at every point on the boundary is zero, (See figure 2.2(a)). It is worth noting that if the mid-plane slope, $\frac{dw}{dr}$, is set equal to zero at the boundary, then the deflection function which results is the normal classical expression. The physical explanation of this is that in order to produce the latter boundary condition, the initially vertical boundary surface plane would have

to be rotated outwards through an angle equal to the average

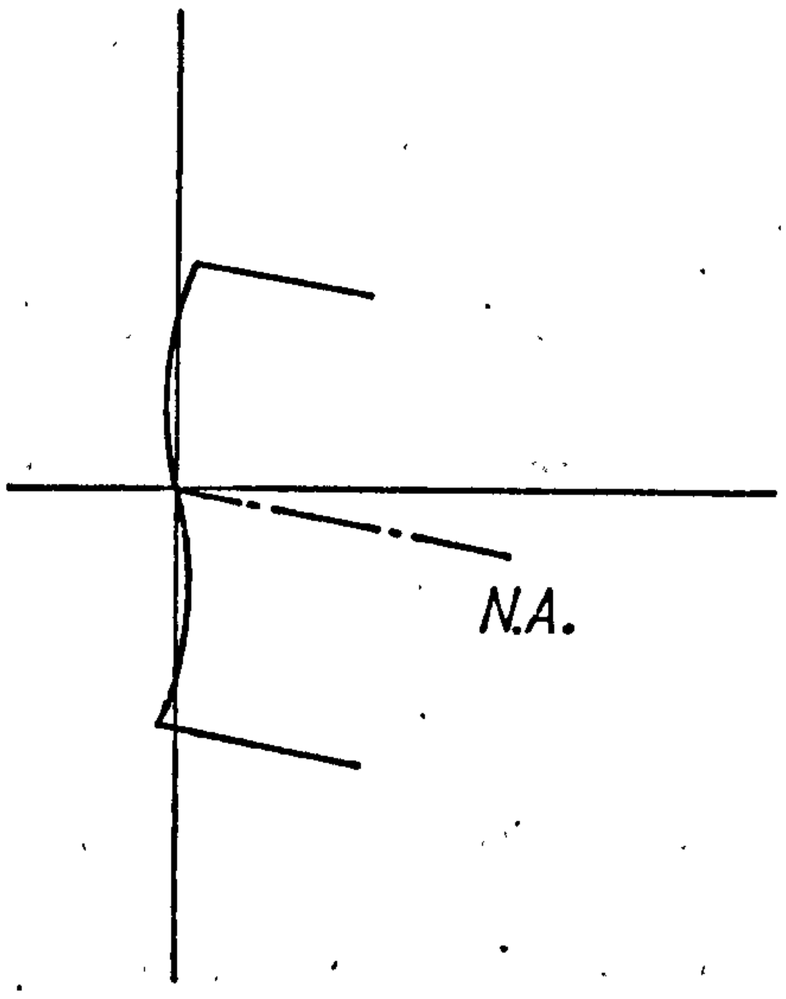

Figure 2.2 (a)

Clamped boundary Type 1: $\phi = 0$

Mid-plane slope $\neq 0$, average shear strain permitted.

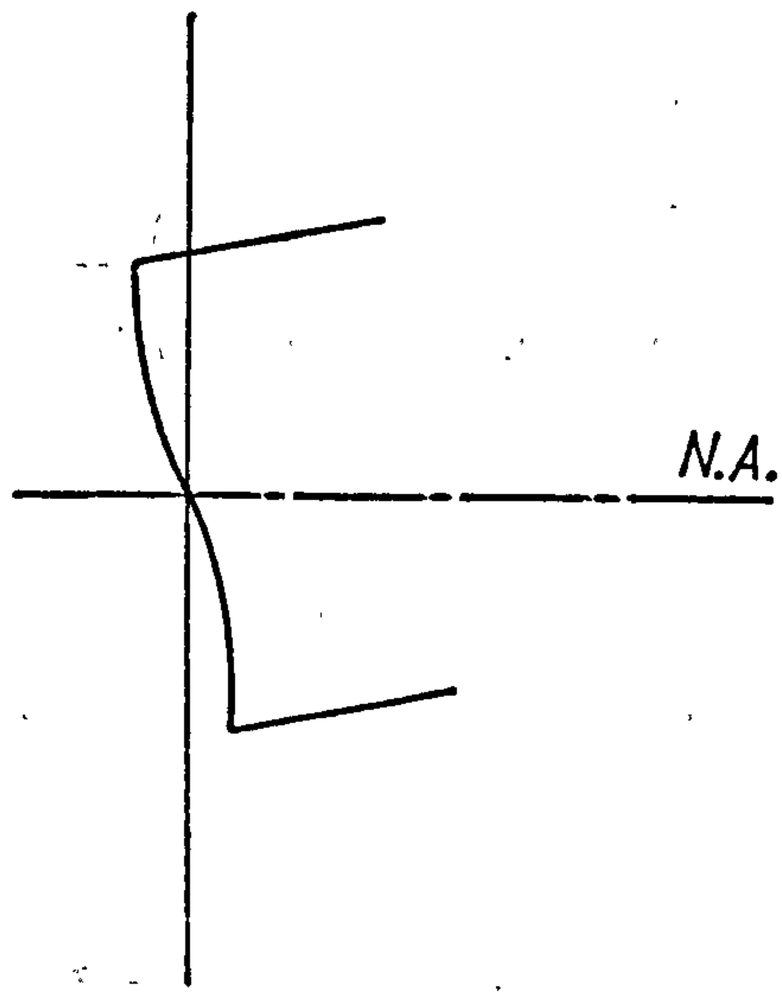

Figure 2.2 (b)

Clamped boundary Type 2: $\frac{dw}{dr} = 0$

'Outward' rotation of initially vertical section necessary to eliminate average shear strain.

shear strain at the boundary as shown in Figure 2.2 (b). This is tantamount to giving a vertically upwards displacement to the interior of the plate which in this case of uniform loading is equal at all points to the downwards displacement which would be caused by shear deformation.

Substituting for Q from (2.15) integrating twice and satisfying $\phi = 0$ at $r = 0$ and $r = a$ gives

$$\phi = -\frac{qr^3}{16D} + \frac{qa^2r}{16D} \qquad (2.22)$$

Hence, noting (2.14)

$$\frac{dw}{dr} = \frac{qr^3}{16D} - \frac{qa^2r}{16D} - \frac{qh^2r}{10D(1-\nu)} \qquad (2.23)$$

Integrating and satisfying w = 0 at r = a the final form of the displacement function is

$$w = \frac{q}{64D}(a^2 - r^2)^2 + \frac{qh^2}{20D(1-\nu)}(a^2 - r^2) \qquad (2.24)$$

where the first term is the normal classical expression and the second the additional deflection due to shear.

Since the expressions for ϕ, M_r and M_t given in equations (2.22), (2.16) and (2.17) are the same as in classical theory the distributions of radial and tangential moment throughout the plate are given by the usual classical expressions.

2.3.2.2 Simply supported boundary

Integrating the equilibrium equation (2.21) twice and satisfying the conditions $\phi = 0$ at r = 0, and M_r as given by equation (2.16) equals zero at r = a gives

$$\phi = -\frac{qr^3}{16D} + \frac{qa^2r}{16D}\quad\frac{(3+\nu)}{(1+\nu)} \qquad (2.25)$$

which is identical in form to classical theory, but ϕ is now given by equation (2.14). Substituting this expression for ϕ, integrating and satisfying the boundary condition w = 0 at r = a leads to

$$w = \frac{q}{64D}(a^2 - r^2)\left(\frac{5+\nu}{1+\nu}a^2 - r^2\right) + \frac{qh^2(a^2 - r^2)}{20D(1-\nu)} \qquad (2.26)$$

Again the second term in this expression can be identified as the additional deflection due to shear deformation. As would be expected this is identical to the additional deflection in the clamped plate, since the distribution of shear is the same in both cases.

For the same reasons as given for the clamped plate, the distribution of radial and tangential moment will be unaffected by shear and identical to the expressions given by classical theory.

2.3.3 Deflection of a circular plate including the effects of shear deformation and transverse direct stress

Substituting the expressions for M_r and M_t from equations (2.18) and (2.19) in the equilibrium equation (2.20) gives

$$\frac{d}{dr}\left(\frac{1}{r}\frac{d}{dr}(r\phi)\right) = -\frac{Q}{D} - \frac{\nu h^2}{10D(1-\nu)}\frac{dq}{dr} \qquad (2.27)$$

but with uniform loading $\frac{dq}{dr} = 0$ and this becomes identical with (2.21).

2.3.3.1 Clamped boundary

In this case the deflection is the same as that given by equation (2.13) of section 2.2.2.1 for the case with transverse direct stress omitted. The equations giving the distribution of moments will be slightly modified on account of the further curvature caused by transverse direct stress, becoming

$$M_r = \frac{q}{16}\left(a^2(1+\nu) - r^2(3+\nu)\right) + \frac{\nu q h^2}{10(1-\nu)} \qquad (2.28)$$

$$M_t = \frac{q}{16}\left(a^2(1+\nu) - r^2(1+3\nu)\right) + \frac{\nu q h^2}{10(1-\nu)} \qquad (2.29)$$

2.3.3.2 Simply supported boundary

Integrating the equilibrium equation (2.21) twice and satisfying the conditions $\phi = 0$ at $r = 0$ and M_r as given by equation (2.18) equals zero at $r = a$ results in the following

$$\phi = -\frac{qr^3}{16D} + \frac{qa^2r}{16D}\left(\frac{3+\nu}{1+\nu}\right) - \frac{\nu q h^2 r}{10D(1-\nu^2)} \qquad (2.30)$$

Substituting in (2.14), integrating and satisfying the boundary condition $w = 0$ at $r = a$ gives the deflection function as

$$w = \frac{q}{64D}(a^2 - r^2)\left(\frac{5 + \nu}{1 + \nu}a^2 - r^2\right) + \frac{qh^2(a^2 - r^2)}{20D(1 - \nu^2)} \qquad (2.31)$$

The distribution of radial and tangential moment throughout the plate can then be found by substituting for ϕ from (2.30) in equations (2.18) and (2.19) giving the usual classical values.

2.4 Summary of theoretical results

2.4.1 Circular plate with simply supported edges

The formulae for the central deflection of uniformly loaded circular plates with simply supported edges are summarised in Table 2.1, and the relationships compared graphically in Figures 2.2 to 2.6

Theory	Central deflection
Classical.	$\frac{qa^4}{64D}\left(\frac{5+\nu}{1+\nu}\right)$
Timoshenko with shear correction.	$\frac{qa^4}{64D}\left(\frac{5+\nu}{1+\nu}\right)\left(1+\frac{4(3+\nu)}{3(1-\nu)(5+\nu)}\frac{h^2}{a^2}\right)$
Ambartsumyan and present theory (ignoring the effects of σ_z).	$\frac{qa^4}{64D}\left(\frac{5+\nu}{1+\nu}\right)\left(1+\frac{16(1+\nu)}{5(1-\nu)(5+\nu)}\frac{h^2}{a^2}\right)$
Ambartsumyan and present theory (including the effects of σ_z).	$\frac{qa^4}{64D}\left(\frac{5+\nu}{1+\nu}\right)\left(1+\frac{16}{5(1-\nu)(5+\nu)}\frac{h^2}{a^2}\right)$
Love	$\frac{qa^4}{64D}\left(\frac{5+\nu}{1+\nu}\right)\left(1+\frac{2(8+\nu+\nu^2)}{5(1-\nu)(5+\nu)}\frac{h^2}{a^2}\right)$

Table 2.1

Central deflection of simply supported circular plates.

2.4.2 Circular plate with clamped edges

The formulae for central deflection of uniformly loaded circular plates with clamped edges are summarised in Table 2.2, and the relationships compared graphically in Figures 2.7 - 2.10.

Theory	Central deflection
Classical	$\frac{qa^4}{64D}$
Timoshenko with shear correction	$\frac{qa^4}{64D}\left(1 + \frac{4}{1-\nu}\frac{h^2}{a^2}\right)$
Ambartsumyan and Love	$\frac{qa^4}{64D}\left(1 + \frac{16}{5(1-\nu)}\frac{h^2}{a^2}\right)$
Present theory	

Table 2.2

Central deflection of clamped circular plates.

2.4.3 Bending moment

There is only one case in which bending moments different from those of classical theory are predicted and that is for clamped plates when the effects of transverse direct stress are included. From equations (2.28) and (2.29) it can be seen that the classical values obtain when $\nu = 0$, but that a difference develops which increases with Poisson's ratio. Values of the radial moments at the centre and at the boundary expressed as ratios of the classical values are given in Table 2.3 for $\nu = 0.3$ and a range of values of the ratio of depth to radius, h/a.

h/a	$\frac{M}{M_o}$ at centre	$\frac{M}{M_o}$ at boundary
0.0	1.000	1.000
0.1	1.005	0.997
0.2	1.021	0.986
0.3	1.047	0.969
0.4	1.084	0.945
0.5	1.132	0.914
0.6	1.190	0.876
0.7	1.258	0.832

Table 2.3

Radial moment at the centre and boundary of a clamped circular plate subjected to uniform loading expressed as a ratio of the classical values. ($\nu = 0.3$).

Figure 2.11 illustrates the manner in which the radial bending moment is altered along a radius for a typical case in which Poisson's ratio is 0.3 and the depth/radius ratio 0.6.

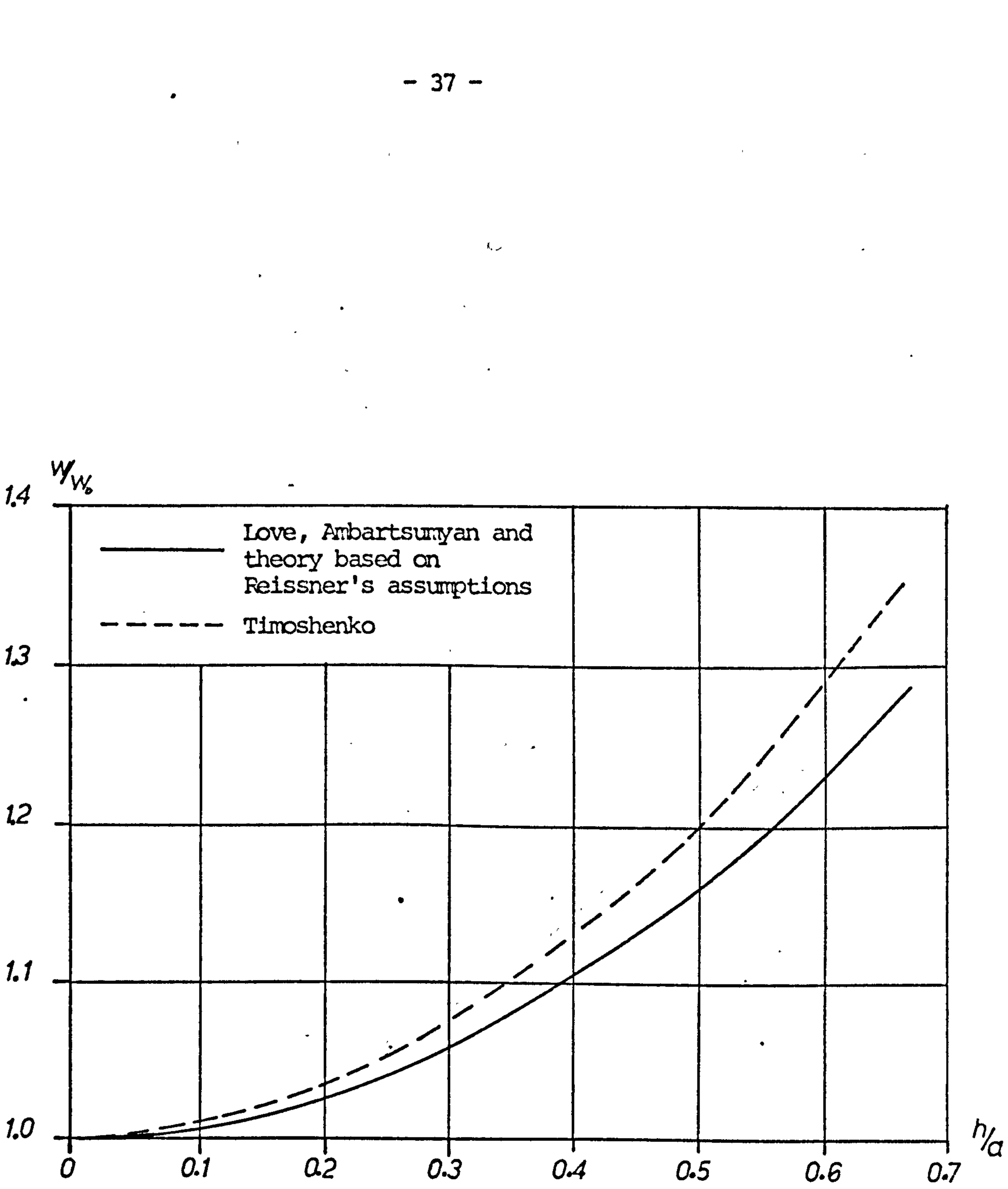

Figure 2.3

Central deflection ratio.

Simply supported circular plate carrying

uniformly distributed load ($\nu = 0$)

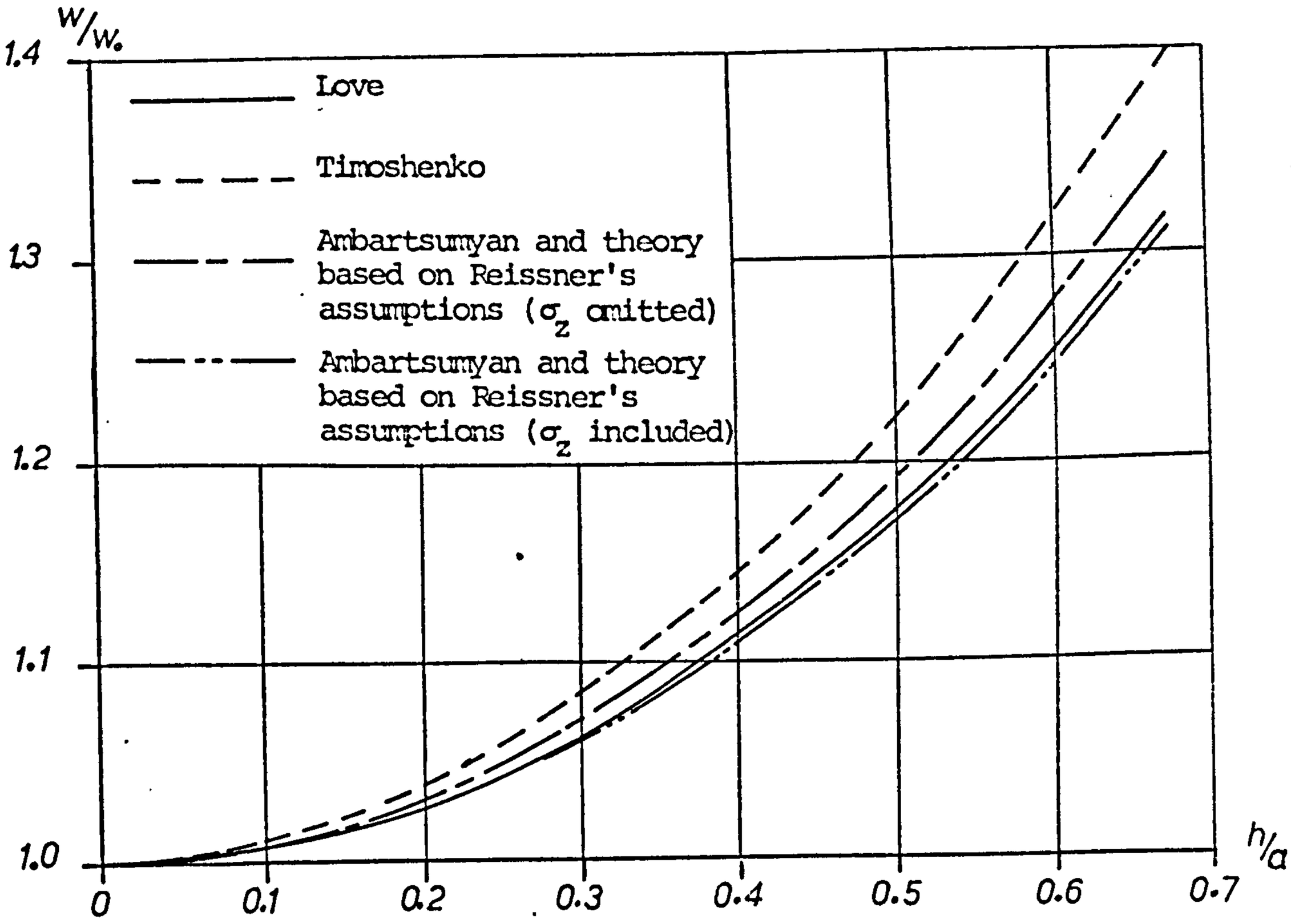

Figure 2.4

Central deflection ratio.

Simply supported circular plate carrying

uniformly distributed load (ν = 0.1)

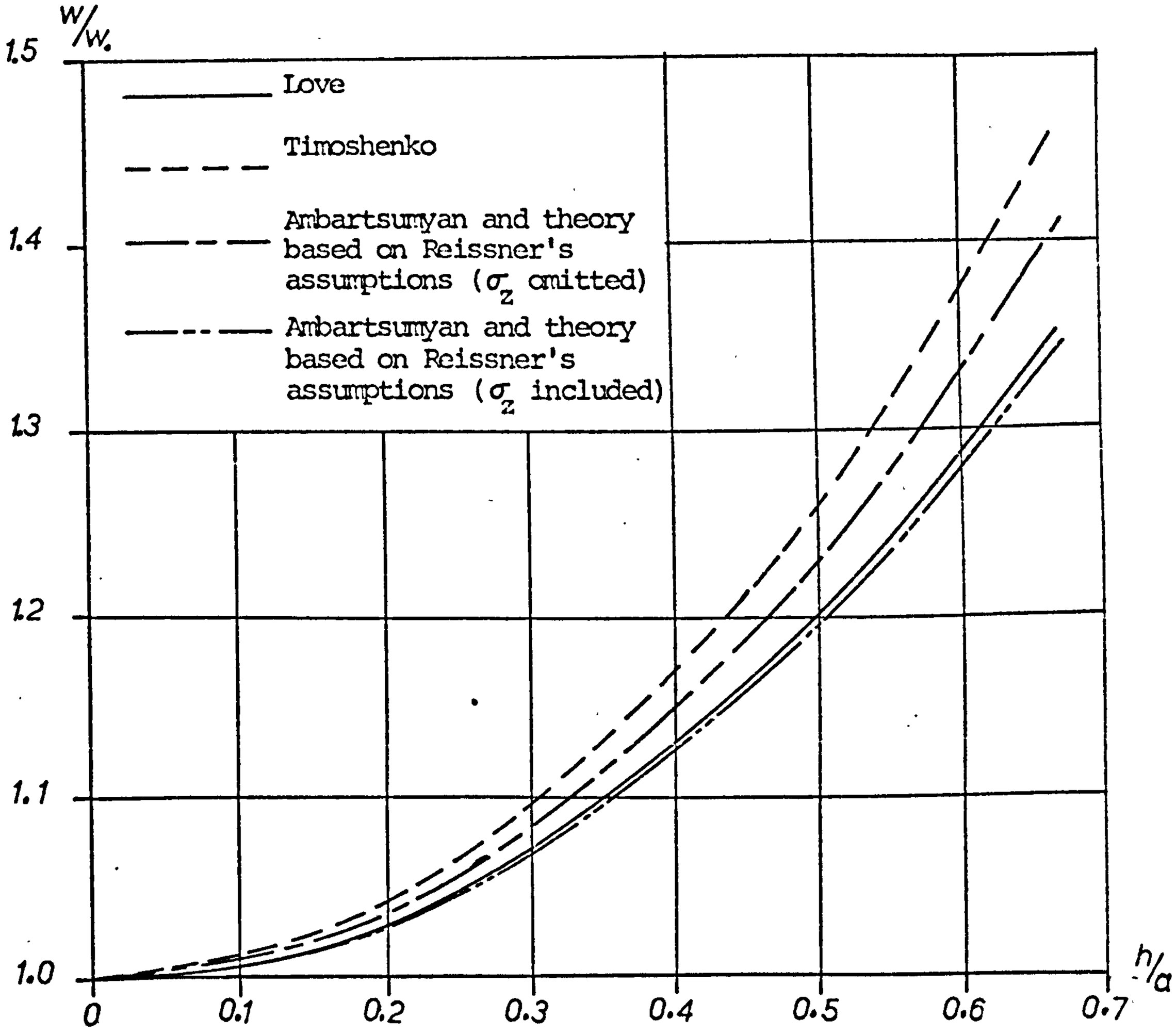

Figure 2.5

Central deflection ratio

Simply supported circular plate carrying

uniformly distributed load ($\nu = 0.2$)

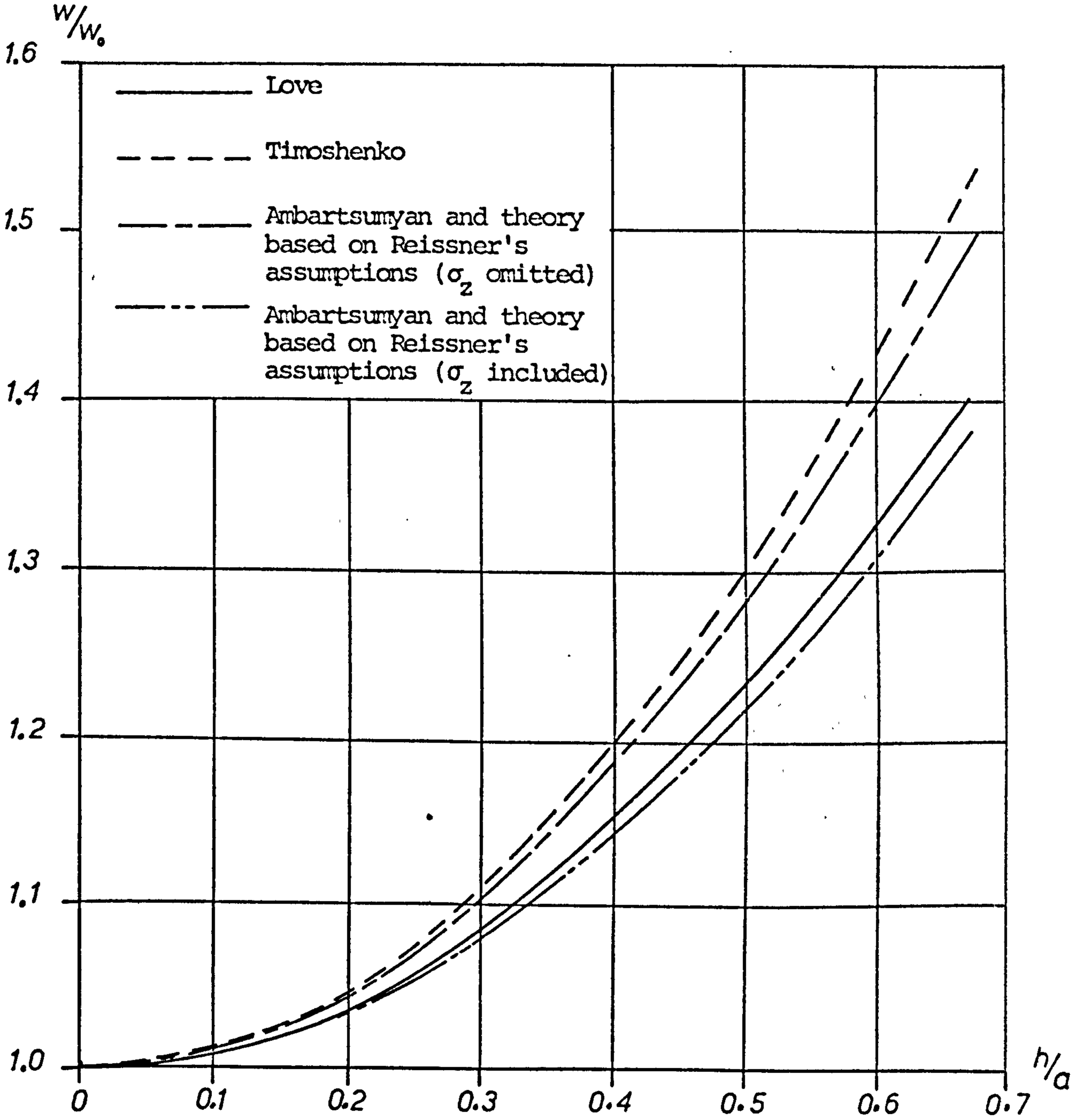

Figure 2.6

Central deflection ratio

Simply supported circular plate carrying

uniformly distributed load (ν = 0.3)

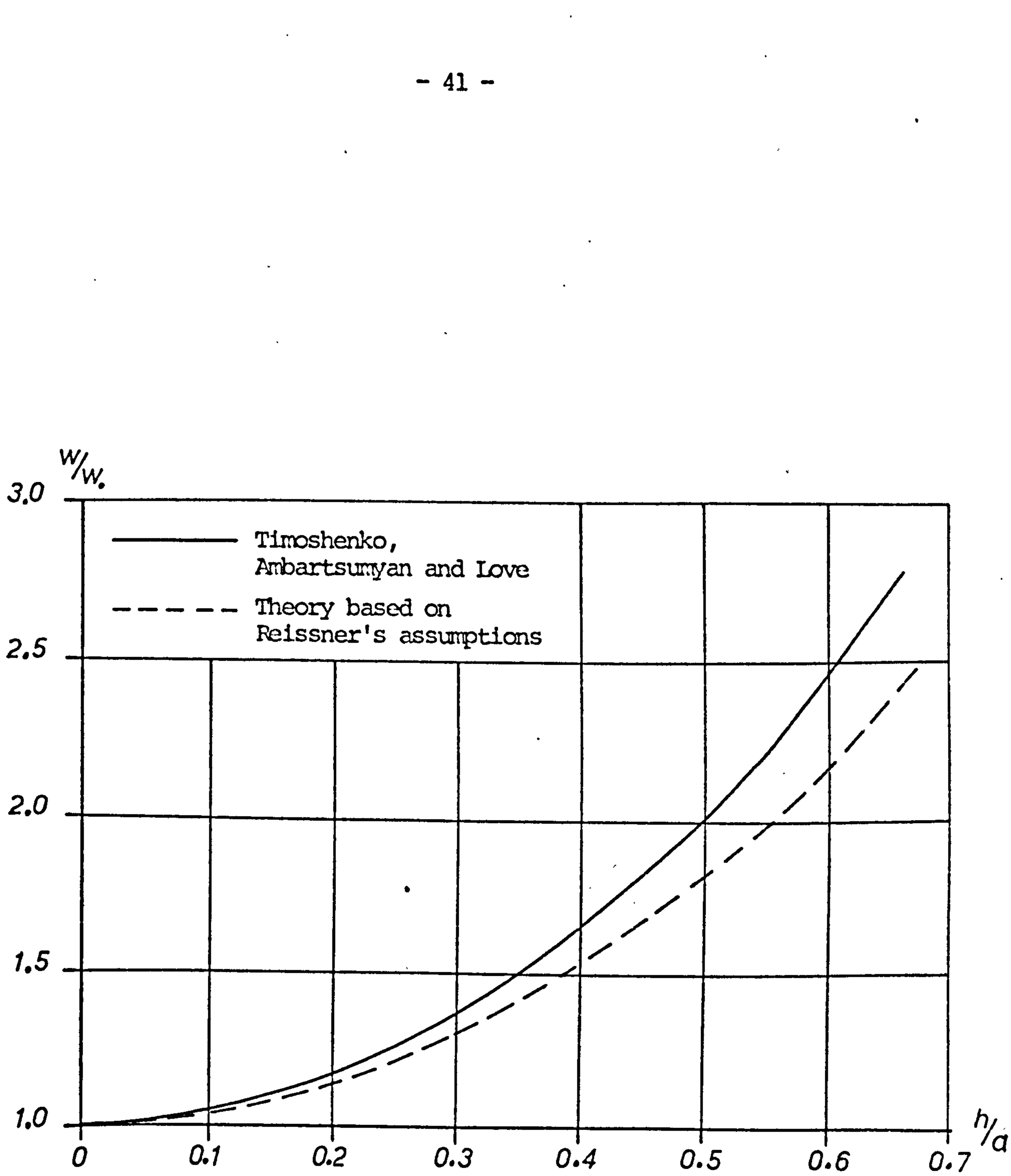

Figure 2.7

Central deflection ratio.

Clamped circular plate carrying

uniformly distributed load ($\nu = 0$)

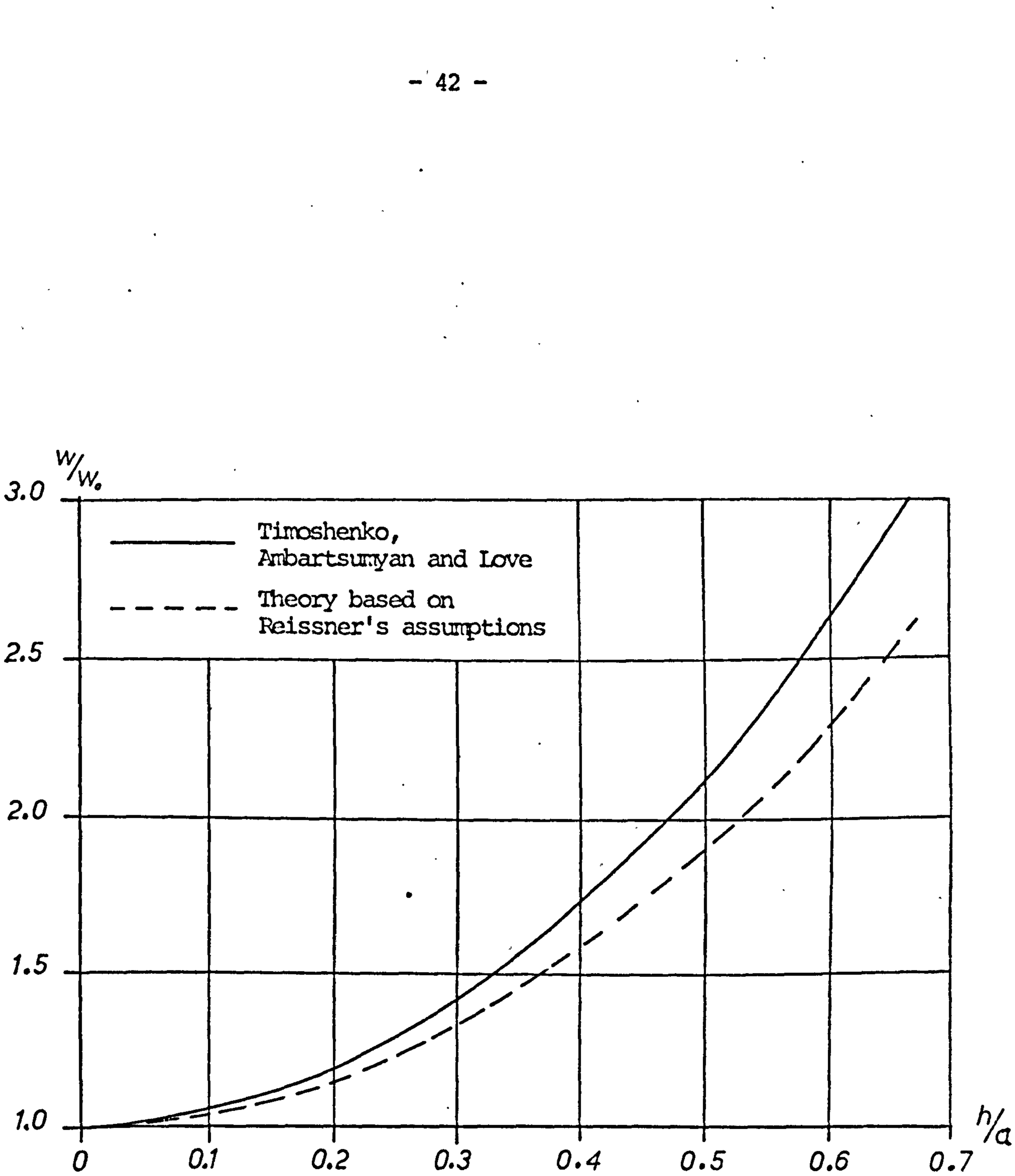

Figure 2.8

Central deflection ratio.

Clamped circular plate carrying

uniformly distributed load ($\nu = 0.1$)

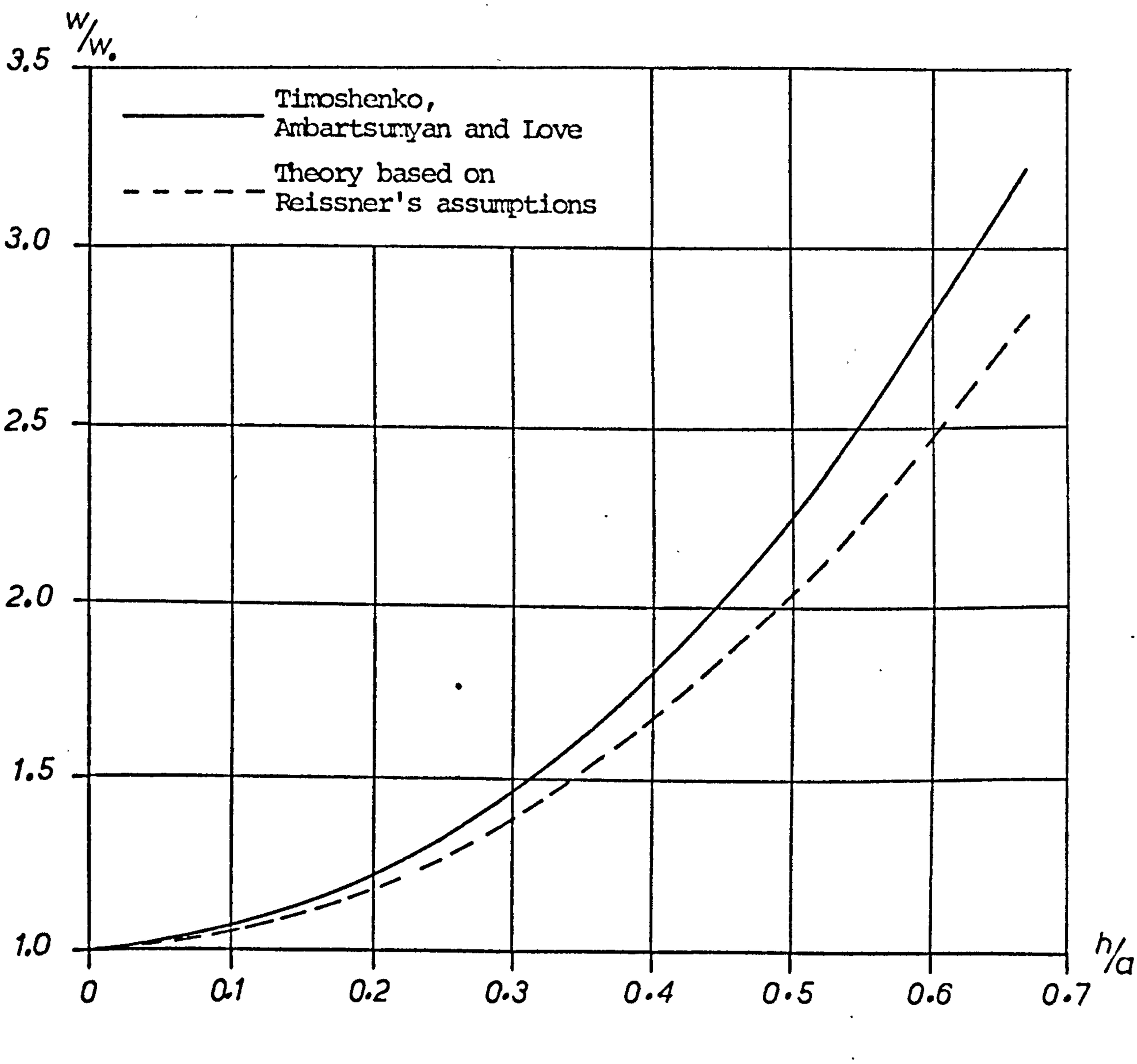

Figure 2.9

Central deflection ratio.

Clamped circular plate carrying

uniformly distributed load ($\nu = 0.2$)

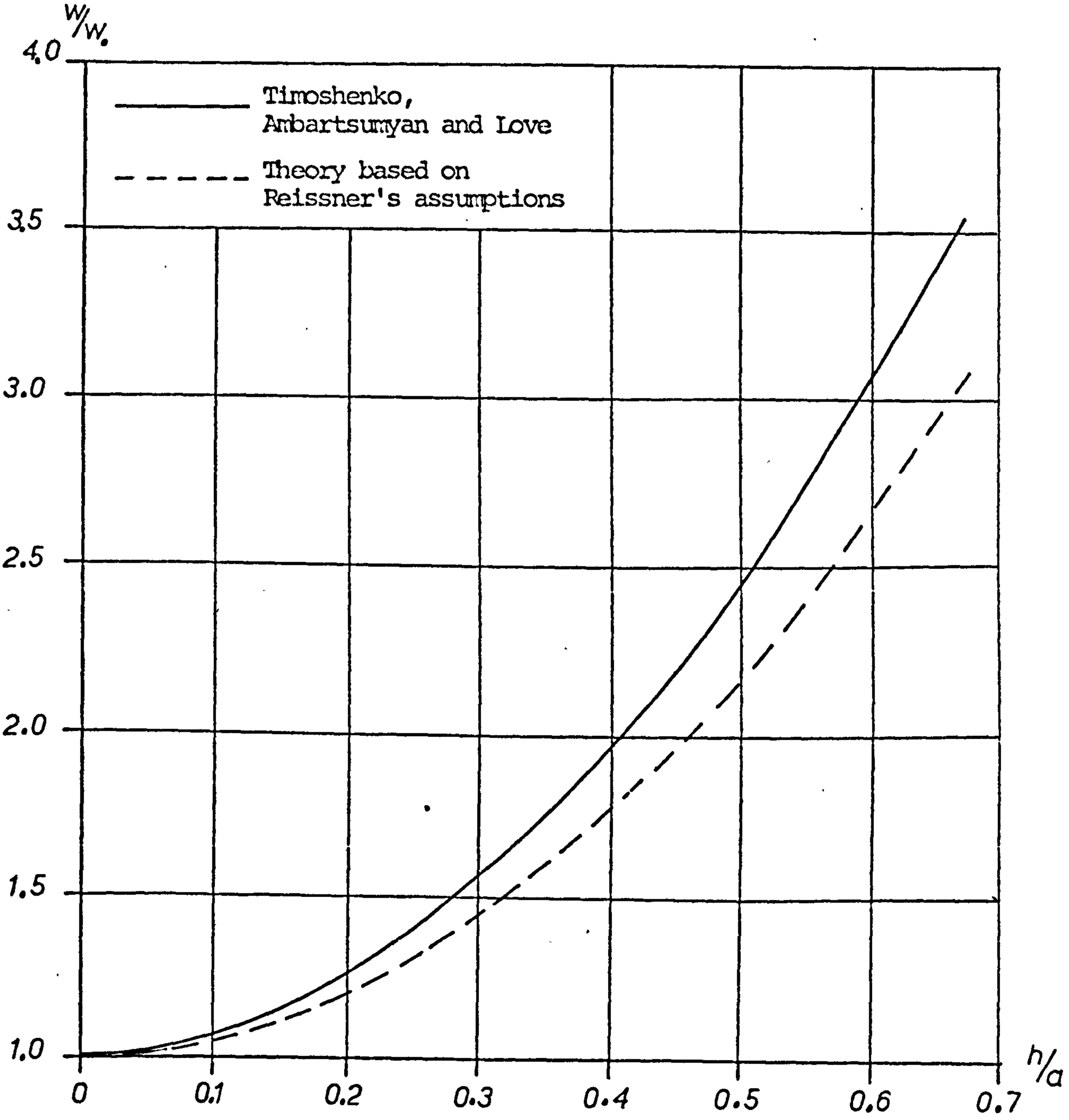

Figure 2.10

Central deflection ratio.

Clamped circular plate carrying

uniformly distributed load (ν = 0.3)

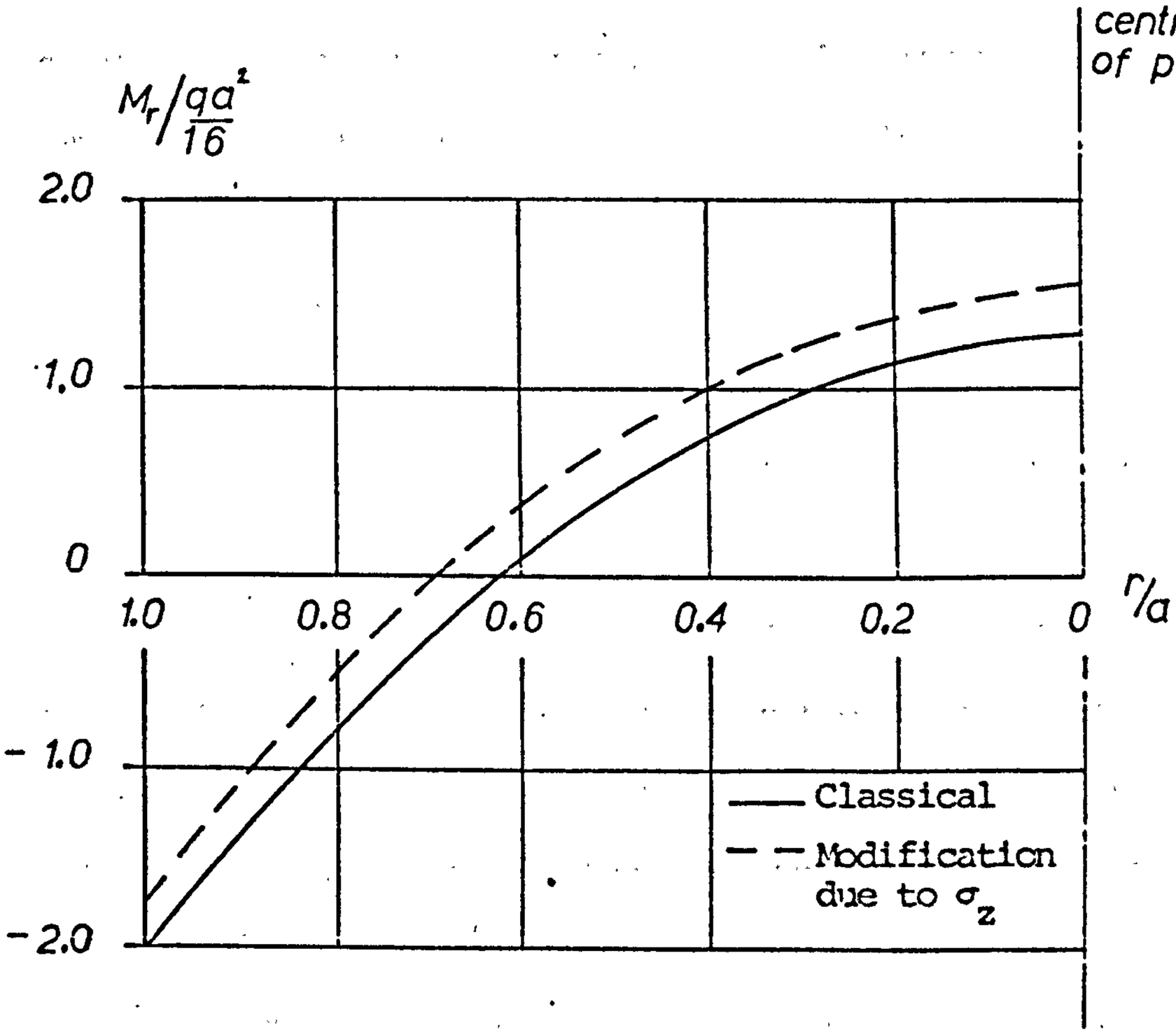

Figure 2.11

Modification to distribution of

Radial bending moment due to the effects of σ_z.

($h/a = 0.6$, $\nu = 0.3$)

2.5 Discussion

2.5.1 Simply supported boundaries

Considering Figures 2.2 - 2.5 and Table 2.1, and taking Love's solution as the standard for purposes of comparison two general characteristics may be observed:

(a) Timoshenko's corrections consistently lead to an overestimate of deflection.

(b) the other theories give identical results when $\nu = 0$ and diverge to an increasing extent from Love's solution as Poisson's ratio increases.

The first of these features arises because in making the shear correction Timoshenko has taken the neutral plane shear strain and evaluated an additional deflection based on this. Choice of a maximum rather than an average value through the depth of the plate leads to an overestimate of the deflection.

As far as the second characteristic is concerned, those solutions which omit the effects of σ_z lead to an overestimate of the deflection, which is to be expected since the resulting curvature and related negative deflection have been ignored. The results obtained from using Reissner's assumptions and Ambartsumyan's solution in which σ_z terms have been included lead to a very small underestimate of the deflection predicted by Love, and the difference in this case would be due to the latter's allowance of greater refinement in the non-linear distributions of σ_r, σ_t and τ_{rt} with depth.

The extent of the differences in the results of the various theories is summarised in Table 2.4 for a thickness ratio, h/a, of 0.6 and $\nu = 0.3$.

Theory	Difference in central deflection compared with Love
Timoshenko	+ 7.8%
Present theory and Ambartsumyan	
(a) transverse direct stress omitted	+ 5.5%
(b) transverse direct stress included	- 1.3%

Table 2.4

Comparison of theoretical results for central deflection. Simply supported circular plate carrying uniform loading h/a = 0.6, $\nu = 0.3$.

2.5.2 Clamped boundaries

Turning now to the clamped plates, for which the results are summarised in Table 2.2 and Figures 2.7 - 2.10, for this type of boundary the results of Love, Timoshenko and Ambartsumyan are identical while the new work based on Reissner's assumptions predicts a smaller value of deflection. When h/a = 0.6 and $\nu = 0.3$ the central deflection is about 13% less. This disparity is accounted for by a difference in the condition of clamping which is illustrated in Figure 2.12.

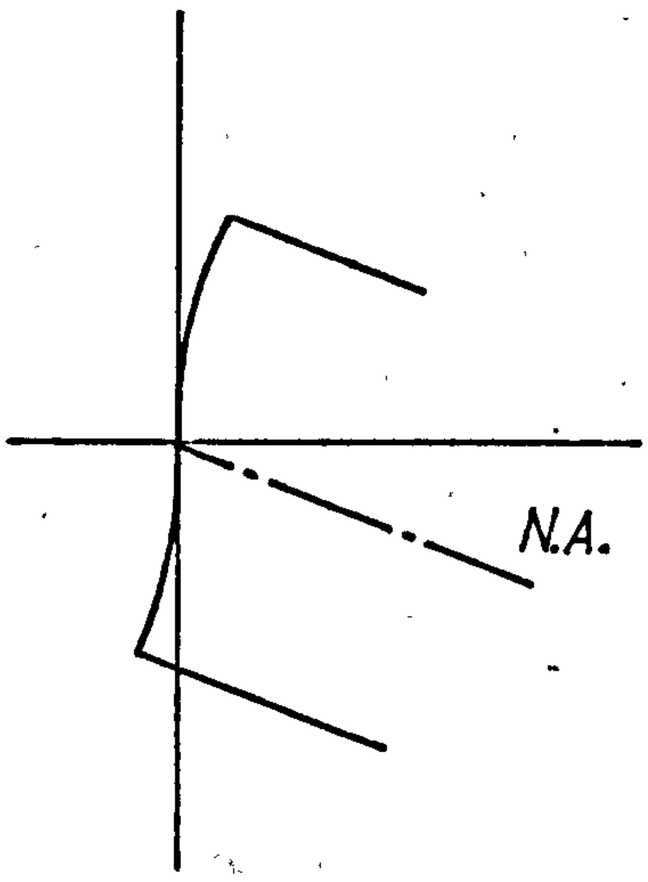

Figure 2.12(a)

$\frac{\partial u}{\partial z} = 0$ at the neutral surface

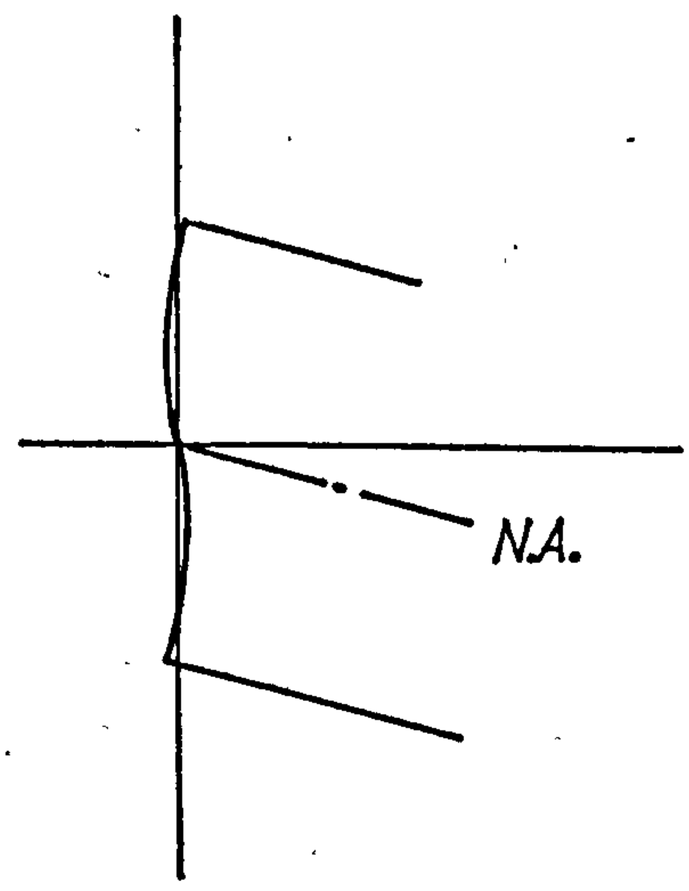

Figure 2.12(b)

average rotation $\phi = 0$

Love defines the effect of the clamp as restraining a tangent initially normal to the neutral surface at the boundary in its original position, so that restraint is applied only at the neutral surface and not throughout the depth of the plate. Distortion due to shear then results in a net rotation at the clamp as illustrated in Figure 2.12(a), causing additional deflections throughout the plate. In this present work the clamp has been assumed to cause the average rotation ϕ to be zero. This situation is illustrated in Figure 2.12(b), and clearly results in a greater degree of restraint at the boundary and hence smaller deflections elsewhere.

The fact that Timoshenko's correction leads to a solution in exact agreement with that of Love is consistent with this explanation in that a neutral surface slope equal to the maximum shear strain will be permitted by the support.

The precise action of a practical support is more likely to produce restraint of the type $\phi = 0$ than the local neutral surface restraint assumed by Love, although neither model may be a perfect representation of the real situation.

2.5.3 Effect of shear deformation and transverse direct stress on stress resultants.

It is found that no changes in the classical distribution of bending moment result from the inclusion of the effects of shear alone for either simple or clamped supports. Transverse direct stress also has no effect on bending moments in the simply supported case, since the resulting curvature can develop without generating in-plane stresses. The clamped boundary, however, prevents radial straining from transverse direct stress, but in doing so generates an additional system of in-plane stresses which for large values of Poisson's ratio and depth/radius ratio can significantly change the distribution of bending moment.

In these symmetric cases the shear force at any point is determined by equilibrium considerations alone, and will therefore remain unchanged by either of these effects.

2.6 Conclusions

The purpose of this chapter has been to develop a theory for circular plates which has as its basis the same assumptions as Reissner used, and to compare the results with those obtained by other means. For plates with clamped boundaries some differences arose from the differing action assumed for the support, but these difficulties do not arise with simple supports, and therefore a true comparison can be made in this case.

First, considering the differing nature of the approaches, Timoshenko uses superposition of three components of deflection due to bending, shear and transverse direct stress, while use of Reissner's approach involves expressing the bending moments in terms of a superposition of curvatures due to these effects.

In principle these two approaches are the same in this case, differences arising because of the approximate manner in which Timoshenko evaluates his corrections. As far as shear is concerned, by taking the mid-plane shear strain instead of an average value through the depth of the plate calculated in the manner of Reissner, Timoshenko calculated a correction in deflection due to shear which is 25% greater than that which is obtained in this present work.

In dealing with transverse direct stress by approximating the actual distribution of strain to a linear form, Timoshenko calculates the curvature produced as $\nu q/Eh$. On the other hand Reissner uses the usual cubic distribution with depth in the energy function and the resulting curvature produced is found to be $6\nu(1 + \nu)q/5Eh$, and this again leads to a difference in final values of deflection.

Love's solution comes from a stress function approach and thus is not limited by an initial assumption of a linear distribution of bending stress, but it has been shown that the disparity is very small for even quite large values of depth/span ratio.

Thus the present approach is found to be simple to apply to symmetrically loaded and supported circular plates, and to give excellent results for the modification in deflection due to shear and transverse direct stress. It is found that there is no change in the distribution of moment and shear stress resultants for simply supported plates, but that for clamped plates transverse direct stress causes a minor modification to the distribution of bending moment when Poisson's ratio is non-zero.

CHAPTER 3

SHEAR DEFORMATION IN BEAMS.

3.1 Introduction

In this chapter all the methods which will be used later for square plates are applied to beams. The reasons for so doing are:

(a) There are existing solutions in a number of cases with which the results can be compared.

(b) Solutions can be derived analytically, without the need to resort to numerical methods. Hence the differences in the results obtained from the various theories can be genuinely attributed to differences in the assumptions made or the general approach, rather than possibly being introduced by the numerical technique.

(c) Numerical methods can then be employed and any associated problems investigated.

(d) Experimental tests can be used to illustrate the validity of the theoretical results, without the difficulties associated with plate tests of physically reproducing the theoretical boundary conditions.

After the opening discussion of existing solutions three theories are developed for beams which take into account the effects of shear deformation, and in two cases transverse direct stress also. The first is based on the partial deflection method while the others are based on Reissner's assumptions, in one case following his theoretical development for plates and in the other introducing a modification which produces a final solution of specified order of accuracy. Each of these three approaches is applied in turn to a range of beam problems, the results compared and an assessment of them made.

Finite difference and localised Rayleigh Ritz techniques are then used, and the results compared with those obtained analytically.

Finally a series of experimental tests was conducted for one support and loading condition, and excellent agreement found with the deflection predicted by the various theories.

3.2 Exisiting solutions

3.2.1 Simply supported beam carrying a uniformly distributed load

The solution to this case is also given by Timoshenko and Goodier (26), and this is examined first in some detail as it is probably the most refined consideration of this type of problem available.

The general arrangement and dimensions are shown in Figure 3.1.

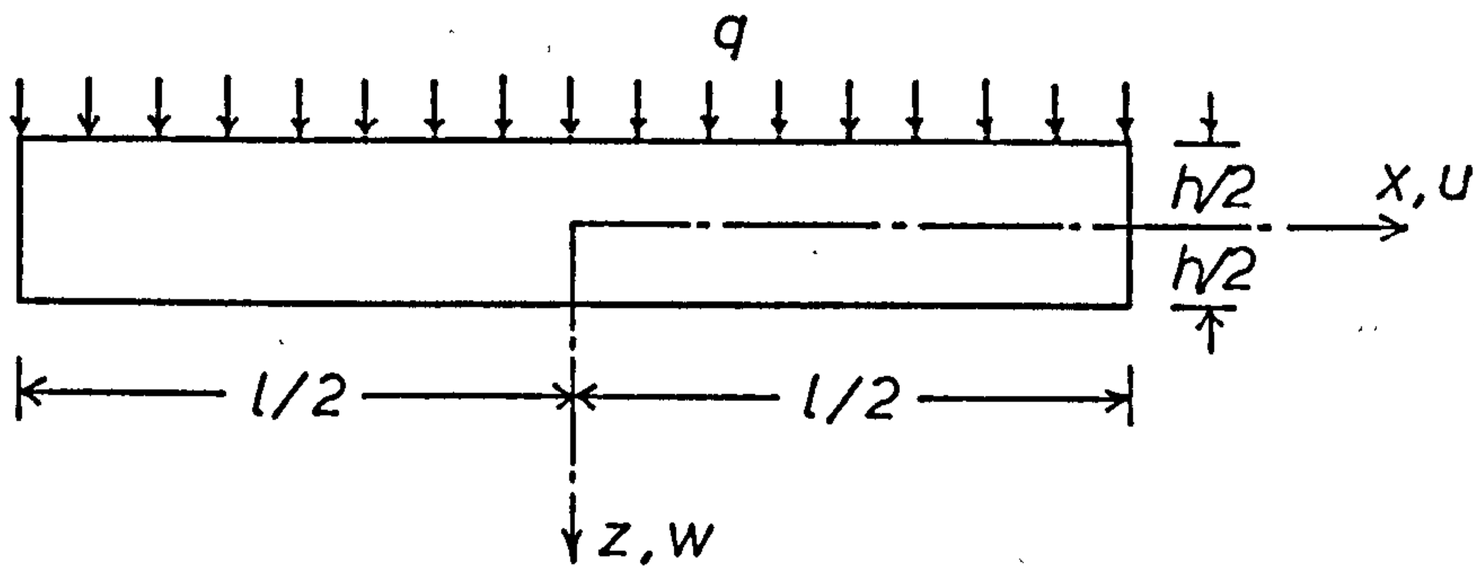

Figure 3.1

Simply supported beam carrying uniformly distributed load.

The stress boundary conditions to be satisfied are:

upper face $z = -\frac{h}{2}$; $\tau_{xy} = 0$, $\sigma_z = -q$

lower face $z = +\frac{h}{2}$; $\tau_{xy} = 0$, $\sigma_z = 0$

ends $x = \pm \frac{l}{2}$; $\int_{-\frac{h}{2}}^{\frac{h}{2}} \tau_{xz} dz = \mp \frac{ql}{2}$ (end shear)

$\int_{-\frac{h}{2}}^{\frac{h}{2}} \sigma_x dz = 0$ (no net longitudinal force)

$$\int_{-\frac{h}{2}}^{\frac{h}{2}} \sigma_x z \, dz = 0 \qquad \text{(no end moment)}$$

By superposition of stress distributions to satisfy these conditions, expressions for stresses (σ_x, σ_z, τ_{xz}) and displacements (u, w) at any point in the beam are found.

For longitudinal stress, the equation is

$$\sigma_x = \frac{q}{2I}\left(\frac{l^2}{4} - x^2\right)z + \frac{q}{2I}\left(\frac{2}{3}z^3 - \frac{1}{10}h^2 z\right) \qquad (3.1)$$

which in addition to the linear distribution assumed in elementary theory represented by the first term in this equation, contains a cubic term.

From the expression for vertical displacement, w, the central deflection, defined as the vertical displacement of the point (0, 0) relative to the points $(\pm \frac{l}{2}, 0)$ is found to be

$$\delta = \frac{5}{384}\,\frac{q l^4}{EI}\left(1 + \frac{12}{5}\,\frac{h^2}{l^2}\left(\frac{4}{5} + \frac{\nu}{2}\right)\right) \qquad (3.2)$$

compared with the normal classical expression, $\delta = 5ql^4/384EI$.

The usual parabolic distribution of shear stress, τ_{xz}, is obtained and the transverse direct stress, σ_z, is found to be distributed with depth according to a cubic law. From the equation (3.1) and (3.2) the influence of the other effects can be seen.

Detailed examination of Timoshenko's equations sheds light on some important issues, on the basis of which an assessment of the assumptions made by other theories can be made later.

(i) The non-linearity of longitudinal stress.

Considering (3.1), it can be seen that on the centre line σ_x is given by

$$\sigma_x = \frac{ql^2z}{8I} + \frac{q}{2I}\left(\frac{2}{3}z^3 - \frac{h^2z}{10}\right) \qquad (3.3)$$

If σ_{x_o} $\left(= \frac{ql^2z}{8I}\right)$ is the corresponding value given by elementary theory, then the deviation from linearity is:

$$\frac{\sigma_x - \sigma_{x_o}}{\sigma_{x_o}} = 4\left(\frac{2}{3}\frac{z^2}{l^2} - \frac{h^2}{10l^2}\right) \qquad (3.4)$$

The departure from the classical linear distribution is $+\frac{4h^2}{15l^2}$ at $z = \pm\frac{h}{2}$. Values of the ratio $\frac{\sigma_x}{\sigma_{x_o}}$ for a range of values of $\frac{h}{l}$ are given in Table 3.1.

h/l	$\frac{\sigma_x}{\sigma_{x_o}}$ at $z = \pm\frac{h}{2}$
0	1.0
0.1	1.003
0.2	1.011
0.3	1.024
0.4	1.043
0.5	1.067

Table 3.1

Deviation from linear of longitudinal stress on the centre-line of a simply supported beam of rectangular section carrying a uniformly distributed load.

A sketch of the distribution of stress for $h/l = 0.3$ is shown in Figure 3.2. The greatest departures from linearity in this case are +2.4% and -4.9%.

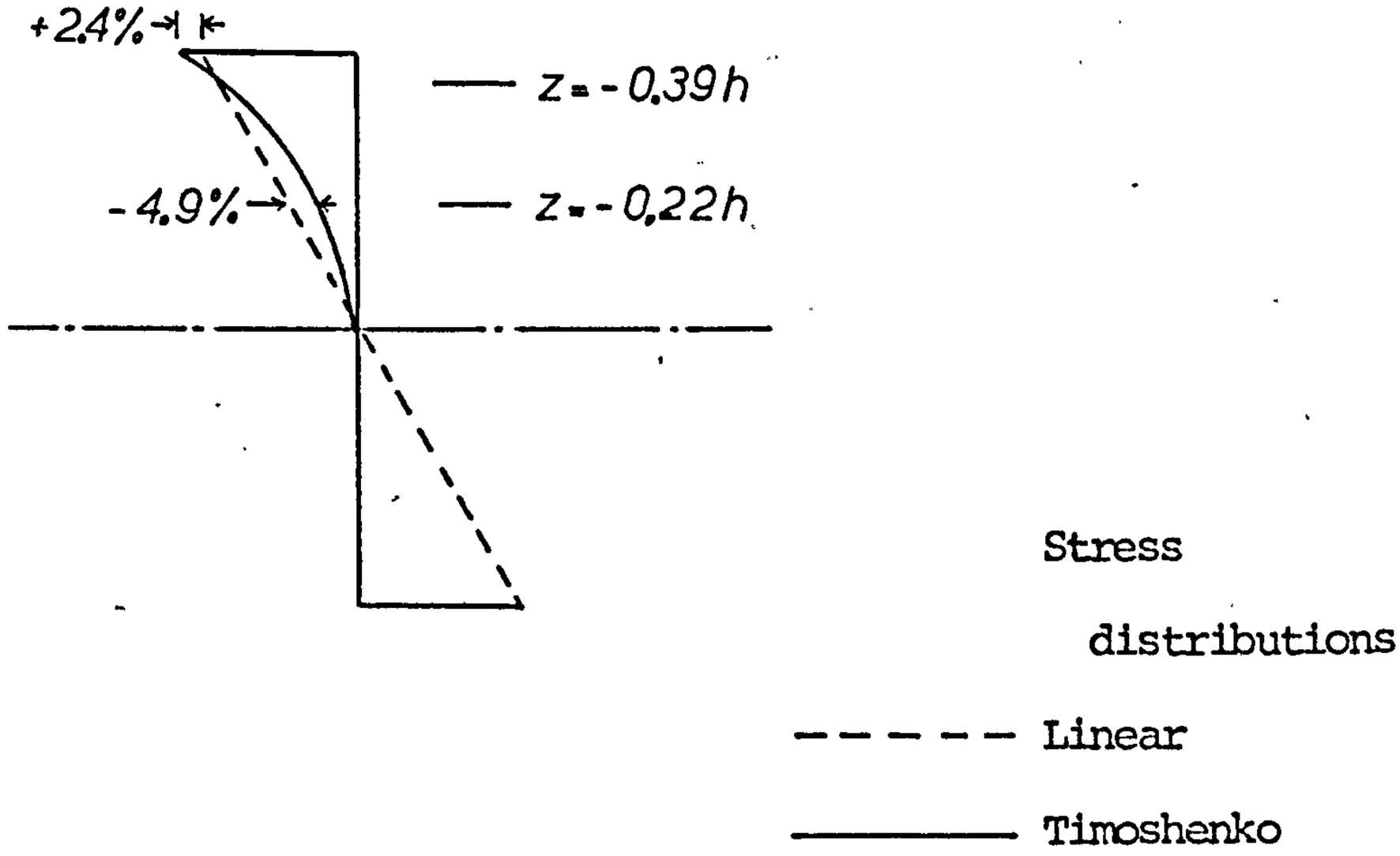

Figure 3.2

Distribution of σ_x for $h/l = 0.3$.

(ii) The non-linearity of longitudinal strain.

Timoshenko and Goodier give an expression for u, the displacement in the x-direction at any point in the beam. From this the longitudinal strain can be calculated as $\epsilon_x = \frac{\partial u}{\partial x}$.

On the centre-line of the beam ϵ_x is given by

$$\epsilon_x = \frac{q}{2EI}\left(\frac{l^2 z}{4} + \left(\frac{2}{3}z^3 - \frac{1}{10}h^2 z\right) + \nu\left(\frac{1}{3}z^3 - \frac{1}{4}h^2 z + \frac{1}{12}h^3\right)\right) \qquad (3.5)$$

The first of these terms gives the linear strain distribution of elementary theory, and the second the modification due to shear deformation. The third term is a further modification due to the inclusion of transverse direct stress σ_z, and if $\nu \neq 0$ this term will cause differences in the value of ϵ_x at the upper and lower faces, and cause ϵ_x to be non-zero on the centroidal axis. Observing the magnitude of the modifications made to elementary theory the correction for shear is seen to be of order h^2, and the correction due to transverse direct stress of order νh^2.

Evaluation of the difference between the value of ϵ_x given by this theory and that of elementary theory (ϵ_{x_o}) gives

$$\frac{\epsilon_x - \epsilon_{x_o}}{\epsilon_{x_o}} = \frac{\frac{2}{3}Z^3 - \frac{1}{10}h^2Z + \nu(\frac{1}{3}Z^3 - \frac{1}{4}h^2Z + \frac{1}{12}h^3)}{\frac{1}{4}l^2Z} \qquad (3.6)$$

The departure from linearity at the lower face is

$$\frac{\epsilon_x - \epsilon_{x_o}}{\epsilon_{x_o}} = \frac{4}{15}\frac{h^2}{l^2} \qquad (3.7)$$

and at the upper face is

$$\frac{\epsilon_x - \epsilon_{x_o}}{\epsilon_{x_o}} = \frac{h^2}{l^2}(\frac{4}{15} - \frac{4\nu}{3}) \qquad (3.8)$$

The values of the ratio $\epsilon_x/\epsilon_{x_o}$ for a range of values of h/l and ν are given in Table 3.2.

h/l	$\frac{\epsilon_x}{\epsilon_{x_o}}$ at $Z = +\frac{h}{2}$	$\epsilon_x/\epsilon_{x_o}$ at $Z = -h/2$				
		$\nu = 0$	$\nu = 0.1$	$\nu = 0.2$	$\nu = 0.3$	$\nu = 0.4$
0	1.0	1.0	1.0	1.0	1.0	1.0
0.1	1.003	1.003	1.001	1.0	0.999	0.997
0.2	1.011	1.011	1.005	1.0	0.995	0.989
0.3	1.024	1.024	1.012	1.0	0.988	0.976
0.4	1.043	1.043	1.021	1.0	0.979	0.957
0.5	1.067	1.067	1.034	1.0	0.966	0.933

Table 3.2

Deviation from linear of longitudinal strain on the centre-line of a simply supported beam of rectantular section carrying a uniformly distributed load.

On the centroidal axis, the longitudinal strain at mid-span is $\frac{\nu q h^3}{24EI}$.

(iii) Variation of vertical displacement through the depth of the beam.

From Timoshenko and Goodier's equations for the vertical displacement at any point in the beam, it can be shown that on the centre-line of the beam the variation displacement w with depth is defined by the following ratios:

$$\frac{\text{vertical displacement of lower face}}{\text{vertical displacement of mid-plane}}$$

$$= \frac{w_{z=h/2}}{w_{z=0}} = 1 - \frac{\frac{3}{5}\left(\frac{h^4}{l^4} + \nu\left(\frac{2h^2}{l^2} - \frac{2h^4}{15l^4}\right)\right)}{1 + \frac{12}{5}\frac{h^2}{l^2}\left(\frac{4}{5} + \frac{\nu}{2}\right)} \qquad (3.9)$$

$$\frac{\text{vertical displacement of upper face}}{\text{vertical displacement of mid-plane}}$$

$$= \frac{w_{z=h/2}}{w_{z=0}} = 1 + \frac{\frac{13}{12}\left(\frac{h^4}{l^4} + \nu\left(\frac{2h^2}{l^2} - \frac{2h^4}{15l^4}\right)\right)}{1 + \frac{12}{5}\frac{h^2}{l^2}\left(\frac{4}{5} + \frac{\nu}{2}\right)} \qquad (3.10)$$

Table 3.3 shows the values of these ratios for a range of values of the ratio h/l for $\nu = 0$ and $\nu = 0.4$.

h/l	ν = 0		ν = 0.4	
	$w_{z=h/2}/w_{z=0}$	$w_{z=-h/2}/w_{z=0}$	$w_{z=h/2}/w_{z=0}$	$w_{z=-h/2}/w_{z=0}$
0	1.0	1.0	1.0	1.0
0.1	1.000	1.000	0.995	1.009
0.2	0.999	1.001	0.980	1.036
0.3	0.996	1.007	0.964	1.065
0.4	0.988	1.020	0.944	1.100
0.5	0.975	1.042	0.924	1.137

Table 3.3

Values of $\frac{\text{lower face deflection}}{\text{mid-plane deflection}}$ and $\frac{\text{upper face deflection}}{\text{mid-plane deflection}}$ on the centre-line of a simply supported beam carrying a uniformly distributed load.

(iv) Moment-curvature relationship.

Timoshenko and Goodier show that at the mid-point of the beam the curvature is

$$\frac{\partial^2 w}{\partial x^2} = - \frac{ql^2}{8EI} \left(1 + \frac{2h^2}{l^2} \left(\frac{4}{5} + \frac{\nu}{2}\right)\right) \qquad (3.11)$$

The bending moment at this point is $ql^2/8$ and is therefore not proportional to curvature when the effects of shear are included.

(v) State of stress at the ends of the beam.

The boundary equation at the ends of the beam is $\int_{-h/2}^{h/2} \sigma_x Z dZ = 0$, (i.e. M = 0) not $\sigma_x = 0$, and hence there will be a residual longitudinal stress at $x = \pm l/2$. This is

$$\sigma_{x_{x=\pm l/2}} = \frac{q}{2I} \left(\frac{2}{3}Z^3 - \frac{1}{10}h^2 Z\right) \qquad (3.12)$$

which, from equation (3.1) can be seen to be the departure from the linearity of elementary theory.

Parabolic distributions of shear stress τ_{xz} at the ends provide the supporting forces, in contrast to the simple support reactions.

3.2.1 Cantilever with end load.

Timoshenko and Goodier (26) also give a two dimensional elastic analysis of the end-loaded cantilever problem, and as this gives an opportunity to consider the conditions at a fixed support this is examined here.

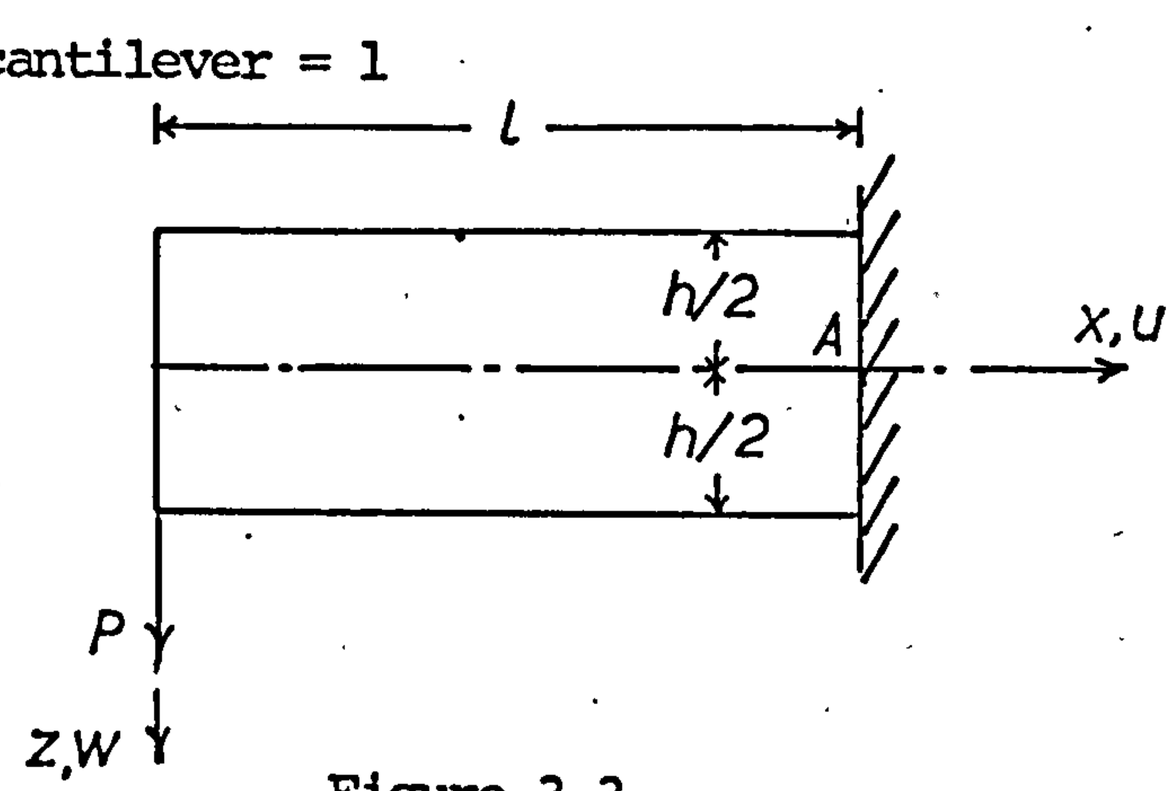

Figure 3.3

Cantilever under end load, P.

The solution is obtained by the superposition of various stress distributions in order to achieve the following boundary stress conditions:

(i) upper and lower faces free from load and shear stress

(ii) a parabolic distribution of shear stress, τ_{xz}, at x = 0, the point of load application

(iii) a linear distribution of longitudinal stress through the depth of the beam.

Equations for displacements u and w are then derived for the appropriate displacement boundary conditions at the support at point A on the axis of the beam ($x = \ell$, $z = 0$), which are:

(i) $u = 0$

(ii) $w = 0$

(iii) $\frac{\partial w}{\partial x} = 0$ or $\frac{\partial u}{\partial z} = 0$

This third condition represents a choice between either the tangent or the normal to the neutral surface of the beam remaining fixed, while relative rotation of the other is permitted. If the first of these ($\partial w/\partial x = 0$) is chosen, it transpires that the vertical deflection of the tip is $P\ell^3/3EI$, which is the usual classical expression. Thus, in requiring a tangent to the neutral surface at A to remain fixed, the beam has to be given a clockwise rigid body rotation about A, eliminating the additional deflection due to shear deformation, which is proportional to the distance from A.

If the second possibility ($\partial u/\partial z = 0$) is chosen, then by contrast a tangent to the neutral surface at A is free to rotate in an anticlockwise direction, and the tip deflection is found to be

$$w = \frac{P\ell^3}{3EI}\left(1 + \frac{3(1+\nu)}{4}\,\frac{h^2}{\ell^2}\right) \qquad (3.13)$$

There is an important difficulty associated with this solution resulting from the assumed state of deformation at the support, which is illustrated in Figure 3.4 and is clearly different from that which would actually occur at a practical support.

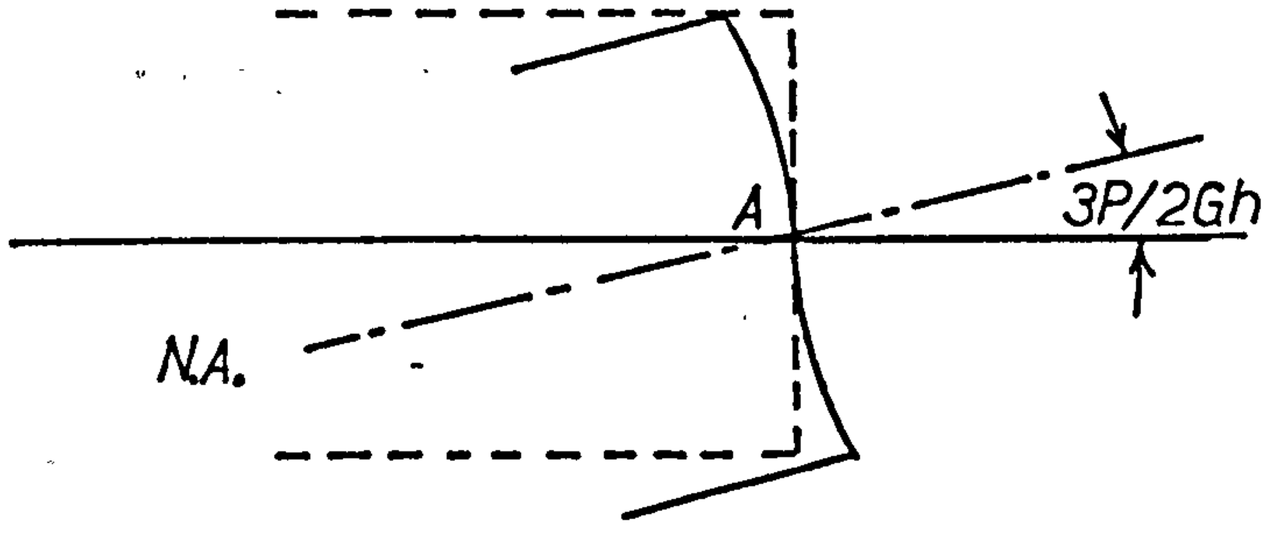

Figure 3.4

The essential features are:

(a) the normal to the initial position of the neutral surface at A remaining vertical

(b) the tangent to the neutral surface at A rotating through an angle of 3P/2Gh

But, in addition, there is a distortion in which longitudinal displacements occur at points away from the neutral axis, which would not occur physically at a fixed support.

As a consequence of this distortion being permitted, the additional vertical deflection due to shear takes the form of that resulting from a rigid body rotation about A, equal in magnitude to the neutral surface shear strain. Since the effect of shear on the overall deflection of the cantilever is therefore evaluated on the basis of the greatest shear strain, any theory which takes account of the actual distribution of shear strain through the depth of the beam would be expected to predict a smaller increase in deflection.

3.2.3 Simply supported beam carrying a central point load

This problem has received less attention than the two previously discussed, presumably because of the difficulties associated with the stress distribution due to the concentrated load.

Three approaches are available:

(i) Correcting the mid-plane slope to allow for shear deformation. Timoshenko adopts this approach (27), but also points out its limitations in another place (26). The maximum shear strain is calculated at the neutral axis, and used to determine the increase in curvature and hence in deflection. In effect, this attributes the maximum shear strain to the entire depth of the section, and consequently results in a considerable over-estimate of deflection.

The central deflection calculated on this basis would be

$$\delta = \frac{Pl^3}{48EI}\left(1 + 3(1+\nu)\frac{h^2}{l^2}\right) \qquad (3.14)$$

(ii) The use of strain energy considerations, assuming linear bending and parabolic shear stress distribution, and ignoring stress concentrations in the region of the load (e.g. Sechler (28)).

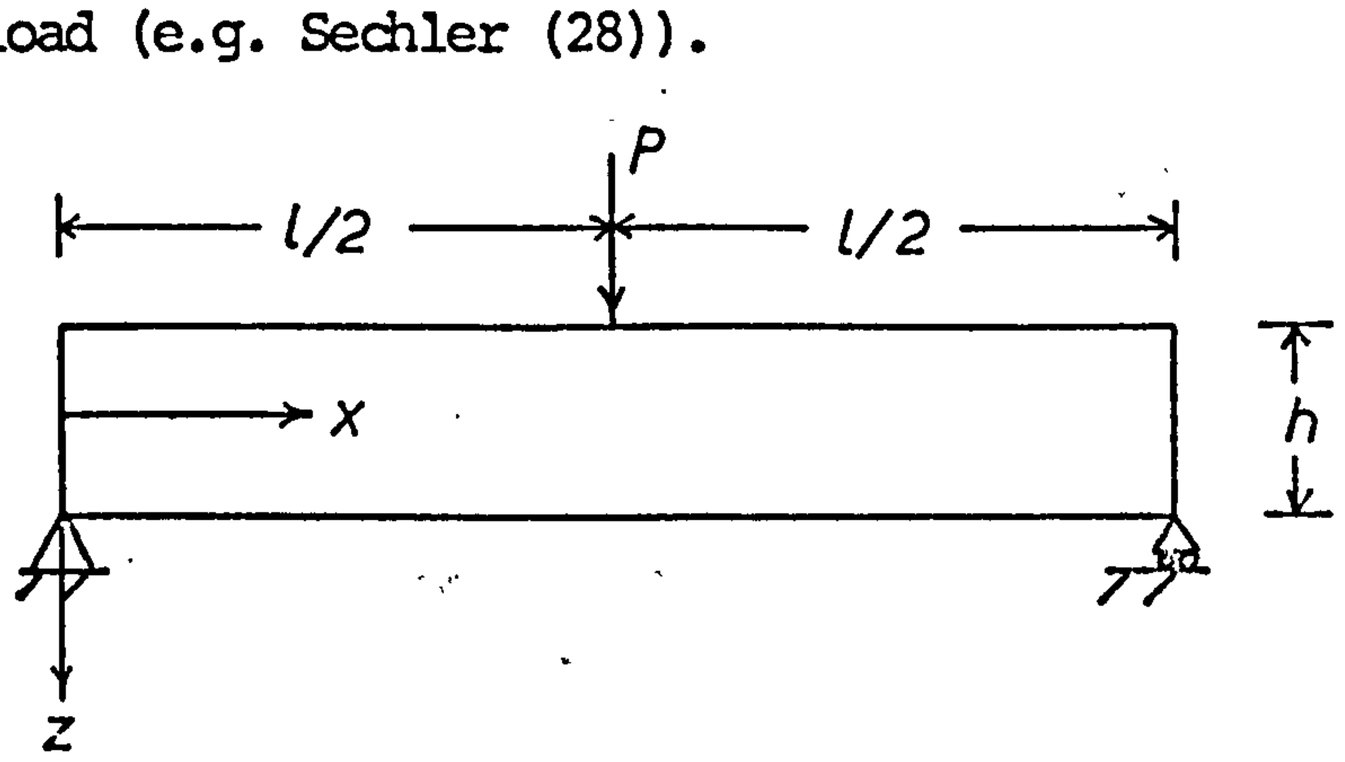

Figure 3.5

In this method the strain energy is taken as

$$U = \tfrac{1}{2} \iiint (\sigma_x \epsilon_x + \tau_{xz} \gamma_{xz}) \, dx \, dy \, dz \qquad (3.15)$$

$$= \frac{1}{2EI} \int_0^l M^2 dx + \frac{3}{5Gh} \int_0^l Q^2 dx \qquad (3.16)$$

Taking the usual longitudinal distribution of shear force and bending moment gives finally

$$U = \frac{P^2 l^3}{96EI} + \frac{(1 + \nu)}{40EI} P^2 l h^2 \qquad (3.17)$$

The deflection under the load is $\frac{\partial U}{\partial P}$ whence the central deflection is

$$\delta = \frac{Pl^3}{48EI} \left(1 + \frac{12(1 + \nu)}{5} \frac{h^2}{l^2}\right) \qquad (3.18)$$

(iii) Seewald's work on this problem, which is fully discussed by Timoshenko and Goodier (26), considers in detail the local distributions of stress in the region of the load. From these an additional local curvature is evaluated and the corresponding correction to the deflection of the beam calculated. It is found that the deflected form of the beam then contains a discontinuity of slope at the load, and hence a small second correction is subtracted which removes this sharp change of slope. For the case under consideration here the central deflection would be

$$\delta = \frac{Pl^3}{48EI} \left(1 + (\frac{12}{5} + \frac{3\nu}{2}) \frac{h^2}{l^2} - 0.84 \frac{h^3}{l^3}\right) \qquad (3.19)$$

3.2.4 Summary and Conclusions

Existing solutions to three beam problems have been studied in the foregoing sections, and it is now possible to

assess the importance of certain factors in developing other theories.

There are two issues of some importance concerning the state of deformation within the beam:

(a) When the effects of shear deformation are included an initially plane section will warp, and the distribution of bending stress with depth will no longer be linear as assumed in simple classical bending theory.

(b) If the effects of transverse direct stress are also considered, then a variation in vertical displacement through the depth of the beam is introduced, and, unless Poisson's ratio is zero, a further modification made to the distribution of longitudinal strain.

Now it is important to establish whether in future work these two modifications to the deformed state of the beam need be defined in this precise manner, or whether the effects from which they result can be taken into account in principle in some average way without considering the detailed changes in the distributions of stress and strain implicit in Timoshenko's treatment of the uniformly loaded beam discussed in Section 3.2.1.

As far as non-linearity in the distribution with depth of longitudinal stress is concerned, the variation from a statically equivalent linear distribution has been shown in Table 3.1 and Figure 3.2 to amount to only a few percent for even quite large values of depth ratio h/l. It seems unlikely that this would have a very significant effect on the overall deflection of the beam, and an equivalent linear distribution would probably give good results for deflection, while for stress the difference between actual and assumed values can be estimated from Timoshenko's

results.

The variation in displacement through the depth of the beam was described in Table 3.3. It is necessary to assess here whether these variations can be neglected, and the displacement represented by either the value at the mid-plane or an appropriate average value, without serious error. The error introduced increases with depth/span ratio and Poisson's ratio, and is always greatest at the upper face. Taking a typical value of h/l of 0.3, the error at the upper face is 0.7% for $\nu = 0$ and 6.5% for $\nu = 0.4$, so that Poisson's ratio is seen to have a significant influence. There may therefore be a case for giving special consideration to a situation involving large values of both h/l and ν, but otherwise the mid-plane or an average deflection will be adequate. This consideration could consist simply of applying a correction to the mid-plane or average deflection to obtain the deflection of the upper or lower face, based on the results derived from Timoshenko's analysis.

Considering next the state of stress and deformation at the ends of the beams, the following points are important:

(a) The action of simple supports has been assumed to prevent vertical displacement of the mid-plane and to supply the end reaction as a parabolic distribution of shear stress.

(b) The end of a simply supported beam is not free from longitudinal stress, as is shown by equation 3.1, but only the moment stress resultant is zero.

(c) Clamped boundaries present a serious problem of representing accurately in theory the true physical action of a fixed support.

No improvement in the theoretical description of a simple support can really be made, but it is unlikely that these very local differences will have any significant effect on the overall deflection or on the state of stress away from the support. The exception to this will be the deflection due to local deformation at a real support consisting of a concentrated vertical reaction rather than an end shear, and this is more conveniently investigated experimentally than theoretically.

The possible models of a clamped boundary discussed represent two extremes, and it is likely that if the warping due to shear is replaced by an average rotation of a normal to the neutral surface in the manner already discussed, setting this rotation equal to zero may come much closer to predicting the correct overall deflected form of a beam with practical fixed supports.

Turning now to problems involving concentrated loads, it is necessary to assess the effects of local stress concentrations on the overall deflection of the beam. A cursory comparison of equations (3.18) and (3.19) shows that an approach which avoids altogether consideration of local stress concentration leads to a final result for overall deflection which is very similar to that obtained by taking them into account, and typical values of the difference when h/l is 0.3 can be shown to be 1.9% for $\nu = 0$ and 3.9% for $\nu = 0.3$.

With such small discrepancies involved for depth/span ratios of this order, it is clear that theories not taking local effects into account will be sufficiently accurate for predicting the overall deflected form of the beam.

From this discussion the following will be accepted as reasonable assumptions on which theories including the effects of shear deformation to be developed in the following sections can be based:

(a) The warping of sections initially normal to the neutral surface due to shear may be replaced by an equivalent average rotation of such a section relative to the mid-plane.

(b) When the effects of transverse direct stress are included in addition to those of shear, theories may be based on the mid-plane or on an average vertical displacement through the depth of the beam.

(c) At simple supports it may be regarded as sufficiently accurate for the moment stress resultant to be zero, rather than requiring the bending stress to vanish throughout the depth of the beam.

(d) In theoretical work support reactions may be assumed to provide a parabolic distribution of shear stress over the end face of the beam, the effects of replacing this by a concentrated transverse direct stress reaction becoming a matter for experimental investigation.

(e) The most likely description of a clamped support to be physically accurate may be taken as one which provides

for the average rotation described in (a) to be set equal to zero.

(f) The local stress concentrations associated with concentrated loading may be assumed to have negligible effect on the overall behaviour of the beam.

On the basis of the earlier detailed consideration, the adoption of these assumptions may be expected to lead to reasonably accurate results for values of depth/span ratio up to 0.3 or 0.4.

3.3 Application of the method of partial deflections

3.3.1 Introduction

This method has been used extensively in the analysis of sandwich beams and plates, e.g. Plantema (21) and Allen (22). Essentially no interaction between bending moment and shear is assumed; the effects of each are evaluated separately and then added to find the overall deflection.

In its usual form this approach is applicable only to problems where

(a) the core has a low shear stiffness

(b) the transverse direct stiffness is high

The core is assumed to carry the shear force, and the faces the bending moment. A uniform shear stress is assumed in the core, giving a shear strain which is independent of depth at a given section. In cases where there is a longitudinal variation of shear force, a curvature due to shear will be induced causing additional bending moments in the faces. A further assumption is that these are small and may therefore be neglected.

In this section the possibility of applying this general method of approach to homogeneous isotropic beams is investigated. In order to do this there are two problems which have to be resolved:

(a) The basis on which the shear deformation is to be assessed has to be established. This will be expressed as an average shear strain through the depth of the beam, γ_{ave}, defined by

$$\int_{-h/2}^{h/2} \tau \gamma \, dz = Q \gamma_{ave} \qquad (3.20)$$

i.e. that the shear strain energy produced by the shear force Q acting through γ_{ave}, is the same as that produced by the actual distribution of shear stress and strain.

Taking $\tau = \frac{3Q}{2h}\left(1 - (\frac{2z}{h})^2\right)$ and $\gamma = \frac{\tau}{G}$

gives $$\gamma_{ave} = \frac{6Q}{5Gh} \qquad (3.21)$$

(b) It must be established in which situations this method amounts to a simple superposition of the deflections due to bending and shear effects. Such an approach means that no interaction between bending and shear is permitted, and hence the distributions of stress resultants will be unchanged from those given by simple bending theory. This will be the case in statically determinate beams, and in indeterminate cases in which the reactions, and hence distribution of shear force, is known because of symmetry. (In this context, it may be recalled that in the symmetrical circular plates considered in Chapter 2, the only change in bending moment found was due to transverse direct stress.) However, in non-symmetric indeterminate beams interaction between bending and shear may occur, and then an approach consisting of a simple superposition of two separately assessed partial deflections could not be used. In such situations the deflections w_b and w_s would not necessarily vanish separately at a rigid support, but only their sum would be zero.

They would then no longer have the simple physical significance of being the deflections due to bending and shear.

The assumptions to be made may be summarised in mathematical form as:

$$w_b = \text{partial deflection due to bending} \tag{3.22}$$

$$w_s = \text{partial deflection due to shear} \tag{3.23}$$

$$w = w_b + w_s = \text{total deflection} \tag{3.24}$$

$$M = -EI \frac{d^2 w_b}{dx^2} \tag{3.25}$$

$$Q = S \frac{dw_s}{dx} \tag{3.26}$$

$$\text{where } \frac{dw_s}{dx} = \gamma_{ave} \text{ and } S = 5Gh/6 = \frac{5}{h^2(1 + \nu)} EI \tag{3.27}$$

The following load and support cases are investigated for the reasons stated:

(a) simply supported beam with uniformly distributed load - to give an indication of the general accuracy of the approach by comparison with the most refined solution available (Timoshenko and Goodier, see Section 3.2.1).

(b) simply supported beam with central point load - to reveal any problems associated with concentrated loads

(c) cantilever carrying an end load - to investigate the behaviour of a clamped support

(d) clamped beam with uniformly distributed load - as an example of an indeterminate, symmetric case

(e) propped cantilever with uniformly distributed load - to investigate the possibility of changes in the

distributions of stress resultants due to shear deformation in an indeterminate, non-symmetric case. In the solution of these cases in the following sections, the working is presented in full in the first case, and only significant points of difference noted in the others.

3.3.2 Simply supported beam carrying a uniformly distributed load

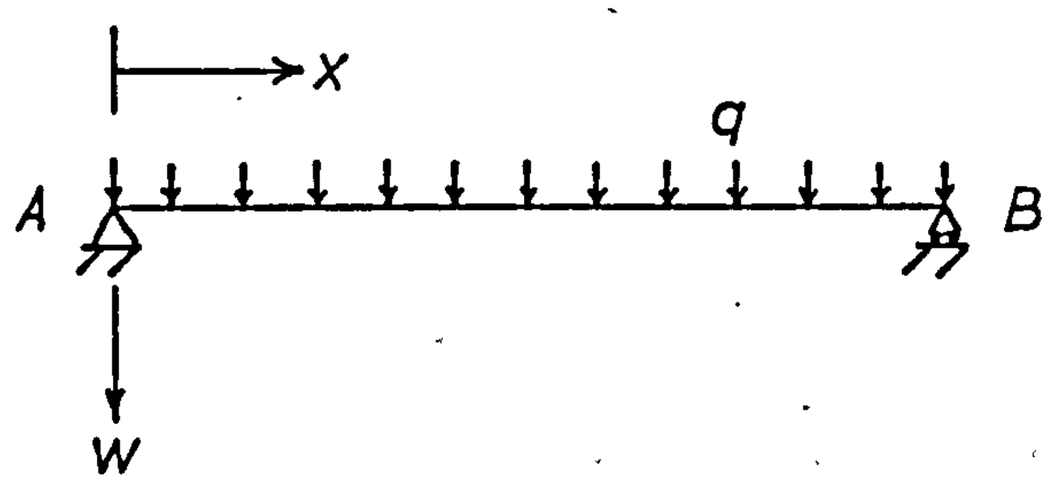

Figure 3.6

The basic equation of equilibrium is

$$\frac{dQ}{dx} = -q \tag{3.28}$$

with $$Q = \frac{dM}{dx} \tag{3.29}$$

Substituting for M and Q from (3.25) and (3.26) gives

$$\frac{d^4 w_b}{dx^4} = q/EI \tag{3.30}$$

$$\frac{d^2 w_s}{dx^2} = -q/s \tag{3.31}$$

Integrating (3.28) four times and satisfying the boundary conditions $w_b = \frac{d^2 w_b}{dx^2} = 0$ at $x = 0$ and $x = l$ gives

$$w_b = \frac{1}{EI}\left(\frac{qx^4}{24} - q\frac{lx^3}{12} + \frac{ql^3 x}{24}\right) \tag{3.32}$$

Integrating (3.29) twice and satisfying boundary conditions

$w_s = 0$ at $x = 0$ and $x = l$ gives

$$w_s = \frac{1}{S}\left(-\frac{qx^2}{2} + \frac{qlx}{2}\right) \tag{3.33}$$

so that finally the total deflection is given by

$$w = w_b + w_s = \frac{1}{EI}\left(\frac{qx^4}{24} - \frac{qlx^3}{12} + \frac{ql^3x}{24}\right) + \frac{1}{S}\left(-\frac{qx^2}{2} + \frac{qlx}{2}\right) \tag{3.34}$$

Substituting for S from (3.27), the deflection at the centre is then found to be

$$\delta = \frac{5ql^4}{384EI}\left(1 + \frac{48(1+\nu)}{25}\frac{h^2}{l^2}\right) \tag{3.35}$$

3.3.3 Simply supported beam carrying a central point load

In this case the rate of loading tends to infinity under the load and is zero everywhere else. The issue of local effects is easily avoided by working directly from the expressions for shear force and bending moment, i.e.

$$Q = S\frac{dw_s}{dx} = \frac{P}{2} - \Phi P \qquad \text{where } \Phi = 0,\ 0 < x < l/2$$

$$\Phi = 1,\ l/2 < x < l \tag{3.36}$$

$$\text{and } M = -EI\frac{d^2w_b}{dx^2} = \frac{Px}{2} - P\left|x - \frac{l}{2}\right|$$

$$\text{where } \left|x - \frac{l}{2}\right| = 0 \text{ if } \left(x - \frac{l}{2}\right) < 0 \tag{3.37}$$

Integrating as required, and satisfying $w_b = w_s = 0$ at $x = 0$ and $x = l/2$ gives the central deflection as

$$w_{x = l/2} = \frac{Pl^3}{48EI}\cdot\left(1 + \frac{12}{5}(1+\nu)\frac{h^2}{l^2}\right) \tag{3.38}$$

3.3.4 Cantilever carrying an end load

The method is the same as used in 3.3.3. The initial expressions for M and Q are

$$M = -EI\frac{d^2w_b}{dx^2} = -P(l - x) \tag{3.39}$$

$$Q = S\frac{dw_s}{dx} = P \tag{3.40}$$

The boundary conditions to be satisfied in this case are $w = 0$ and $\frac{dw_b}{dx} = 0$ at $x = 0$. In accordance with the discussion relating to slope boundary conditions in 3.2.2

$$\frac{dw}{dx} \quad \left(= \frac{dw_s}{dx} \right)$$

is non-zero at the support; since there is shear force at the support shear strain must also be permitted and hence the total neutral axis slope is non-zero. It is that part of the slope due to bending (i.e. the rotation of an initially vertical element) which is zero.

The final value for the deflection at the tip is

$$w_{x=l} = \frac{Pl^3}{3EI} \left(1 + \frac{3}{5}(1 + \nu) \frac{h^2}{l^2}\right) \tag{3.41}$$

3.3.5 Clamped beam carrying uniformly distributed load

The solution in this case is obtained in the same manner as the simply supported beam of 3.3.2, excepting that the boundary conditions in this case are $w_b = w_s = \frac{dw_b}{dx} = 0$ at $x = 0$ and $x = l$. The choice of the slope boundary condition is governed by the same considerations as the cantilever of 3.3.4. The result obtained for the central deflection is

$$w_{x = l/2} = \frac{ql^4}{384EI} \left(1 + \frac{48(1 + \nu)}{5} \frac{h^2}{l^2}\right) \tag{3.42}$$

The accompanying distributions of shear force and bending moment are the same as those given by elementary theory.

3.3.6 Propped cantilever carrying uniformly distributed load

From equations (3.30) and (3.31) it is clear that w_b and w_s are related by

$$EI \frac{d^4 w_b}{dx^4} = q = -S \frac{d^2 w_s}{dx^2} \tag{3.43}$$

The solution is obtained by integrating this equation and satisfying as boundary conditions,

at the fixed support $\quad w_b + w_s = \frac{dw_b}{dx} = 0$

at the propped support $\quad w_b + w_s = \frac{d^2w_b}{dx^2} = 0$

Of more interest in this case than the deflected form are the distributions of shear force and bending moment. These may be evaluated from the values of the reactions at the fixed support, which are found to be:

$$\text{vertical reaction} = \frac{5ql}{8}\left(1 + \frac{12(1+\nu)}{25}\frac{h^2}{l^2}\right)\left(1 + \frac{3(1+\nu)}{5}\frac{h^2}{l^2}\right)^{-1} \quad (3.44)$$

$$\text{moment reaction} = -\frac{ql^2}{8}\left(1 + \frac{3(1+\nu)}{5}\frac{h^2}{l^2}\right)^{-1} \quad (3.45)$$

3.4 Development of a theory for beams based on Reissner's assumptions

3.4.1 Introduction

Reissner presented his theory for plates, but his assumptions can readily be adopted for beams. A theory for beam bending including the effects of shear and transverse direct stress based on the assumptions and approach of Reissner is developed in Appendix A.

It is important here to note the assumptions associated with this solution:

(a) bending stress $\sigma_x = \frac{Mz}{I}$ (3.46)

(b) shear stress $\tau_{xz} = \frac{3Q}{2h}\left(1 - (\frac{2z}{h})^2\right)$ (3.47)

(c) transverse direct stress $\sigma_z = -\frac{3q}{4}\left(\frac{2}{3} - \frac{2z}{h} + \frac{1}{3}(\frac{2z}{h})^3\right)$ (3.48)

Timoshenko and Goodier's exact solution for the simply supported beam carrying a uniformly distributed load discussed in 3.2.1 offers the further refinement that non-linearity in the distribution of bending stress is permitted, but otherwise it has exactly the same assumptions regarding shear stress and transverse direct stress.

In the applications which follow, the solution is worked in full in the first case, and any important points of difference noted in subsequent examples.

3.4.2 Simply supported beam carrying uniformly distributed load

(See Figure 3.6)

From Appendix A equation (A.22) the governing equilibrium equation for a uniformly distributed load (q = constant) is

$$EI \frac{d^4w}{dx^4} = q \tag{3.49}$$

Integrating gives

$$EI \frac{d^2w}{dx^2} = qx^2 + Ax + B \tag{3.50}$$

$$\text{and } EI\, w = \frac{qx^4}{24} + \frac{Ax^3}{6} + \frac{Bx^2}{2} + Cx + D \tag{3.51}$$

The boundary equations are $w = M = 0$ at $x = 0$ and $x = l$. From equation (A20) and (3.50) the bending moment is

$$M = -\frac{qx^2}{2} - Ax - B - \frac{(2+\nu)}{10} h^2 q \tag{3.52}$$

The deflected form is finally found to be

$$EIw = \frac{qx^4}{24} - \frac{qlx^3}{12} + \frac{ql^3x}{24} - \frac{qh^2}{20}(2+\nu)x^2 + \frac{qh^2}{20}(2+\nu)lx$$

From which the central deflection is

$$w_{x = l/2} = \frac{5ql^4}{384EI}\left(1 + \frac{24(2+\nu)}{25}\frac{h^2}{l^2}\right) \tag{3.53}$$

3.4.3 Simply supported beam carrying central point load

The main problem associated with concentrated loads is that terms such as q, $\frac{dq}{dx}$, $\frac{d^2q}{dx^2}$ become indeterminate at the load. A solution can only be obtained if the loading is represented in the form of a Fourier Series. The appropriate form of such a series for a central point load is

$$q = \sum_{n=1,3,5\cdots} \frac{2P}{l} \sin\frac{n\pi}{2} \sin\frac{n\pi x}{l} \tag{3.54}$$

substituting this expression into the Reissner equilibrium equation (A.22) gives

$$EI \frac{d^4w}{dx^4} = \sum_{n=1,3,5\cdots}^{\infty} \lambda \sin\frac{n\pi}{2} \sin\frac{n\pi x}{l} \tag{3.55}$$

where $\lambda = \frac{2P}{l}\left(1 + \frac{n^2\pi^2}{l^2}\,\frac{h^2(2+\nu)}{10}\right)$ (3.56)

Equation (3.55) may be integrated in the usual manner, and satisfying the boundary conditions $w = M = 0$ at $x = 0$ and $x = l$, where M is given by (A.20), the deflected form is finally found to be

$$w = \frac{1}{EI}\sum_{n=1,3\cdots}^{\infty} \frac{2P}{l}\left(1 + \frac{h^2(2+\nu)}{10}\,\frac{n^2\pi^2}{l^2}\right)\frac{l^4}{n^4\pi^4}\sin\frac{n\pi}{2}\sin\frac{n\pi x}{l} \qquad (3.57)$$

Form this the central deflection is

$$w_{x=l/2} = \frac{1}{EI}\,\frac{2Pl^3}{\pi^4}\left[1 + \frac{1}{3^4} + \frac{1}{5^4} + \cdots + \frac{h^2(2+\nu)}{10}\,\frac{\pi^2}{l^2}\left(1 + \frac{1}{3^2} + \frac{1}{5^2} + \cdots\right)\right]$$

$$= \frac{Pl^3}{48EI}\left(1 + \frac{6(2+\nu)}{5}\,\frac{h^2}{l^2}\right) \qquad (3.58)$$

3.4.4 Centilever carrying an end load

(See Figure 3.3)

It is supposed that the load is applied as an end shear, so that $q = 0$ throughout the cantilever. From (A.20) it follows that the bending moment is

$$M = -EI\frac{d^2w}{dx^2} = -Px \qquad (3.59)$$

Integrating twice and satisfying the boundary conditions $w = \phi = 0$ at $x = l$ where ϕ is equal to the average rotation of an initially vertical element. ϕ is equivalent to β of equation (A.19) and hence

$$\phi = -\frac{dw}{dx} + \frac{12(1+\nu)}{5Eh}\,Q \qquad (3.60)$$

In this case the shear force, Q, is equal to -P. The deflected form is found to be

$$w = \frac{1}{EI}\left(\frac{Pl^3}{3} - \frac{Pl^2x}{2} + \frac{Px^3}{6} - \frac{(1+\nu)}{5}Ph^2x + \frac{(1+\nu)}{5}Ph^2l\right) \quad (3.61)$$

Hence the deflection at the tip is given by

$$w_{x=0} = \frac{Pl^3}{3EI}\left(1 + \frac{3(1+\nu)}{5}\frac{h^2}{l^2}\right) \quad (3.62)$$

3.4.5 Clamped beam carrying uniformly distributed load

The solution in this case is obtained in a manner similar to that used for the simply supported beam of Section 3.4.2, but in this case satisfying the boundary conditions $w = \phi = 0$. The deflected form is then found to be

$$w = \frac{1}{EI}\left(\frac{qx^4}{24} - \frac{qlx^3}{12} + \frac{ql^2x^2}{24} + \frac{q(1+\nu)h^2}{10}(lx - x^2)\right) \quad (3.63)$$

and the central deflection is

$$w_{x=l/2} = \frac{ql^4}{384EI}\left(1 + \frac{48(1+\nu)}{5}\frac{h^2}{l^2}\right) \quad (3.64)$$

The bending moment can be obtained from (A.20) and (3.63), and is

$$M = -\left(\frac{qx^2}{2} - \frac{qlx}{2} + \frac{ql^2}{12} - \frac{(1+\nu)}{5}h^2q\right) - \frac{qh^2}{10}(2+\nu) \quad (3.65)$$

Of particular interest are the values of M at the support and at mid-span.

$$\text{At } x = 0 \text{ and } x = l \qquad M = -\frac{ql^2}{12}\left(1 - \frac{6\nu}{5}\frac{h^2}{l^2}\right) \quad (3.66)$$

$$\text{and at } x = l/2 \qquad M = \frac{ql^2}{24}\left(1 + \frac{12\nu}{5}\frac{h^2}{l^2}\right) \quad (3.67)$$

So that in this indeterminate case the distribution of bending moment differs from that given by elementary theory, the correction taking the form of a constant, $\nu qh^2/10$ to be added to the classical value at any point.

The magnitude of these differences is shown in Tables 3.4 and 3.5.

h/ℓ	ν=0.1	ν=0.2	ν=0.3	ν=0.4
0.1	0.9988	0.9976	0.9964	0.9952
0.2	0.9952	0.9904	0.9856	0.9804
0.3	0.9892	0.9784	0.9676	0.9568
0.4	0.9808	0.9616	0.9424	0.9232
0.5	0.9700	0.9400	0.9100	0.8800

Table 3.4

Values of $\frac{M}{M_o}$ at support for clamped beam carrying distributed load.

h/ℓ	ν=0.1	ν=0.2	ν=0.3	ν=0.4
0.1	1.0024	1.0048	1.0072	1.0096
0.2	1.0096	1.0192	1.0288	1.0384
0.3	1.0216	1.0432	1.0648	1.0864
0.4	1.0384	1.0768	1.1152	1.1536
0.5	1.0600	1.1200	1.1800	1.2400

Table 3.5

Values of $\frac{M}{M_o}$ at mid-span for clamped beam carrying uniformly distributed load.

M = bending moment as calculated from theory based on Reissner's assumptions

M_o = bending moment as calculated from elementary theory

3.4.6 Propped cantilever carrying uniformly distributed load

The solution in this case is obtained in the same manner as for the simply supported beam of Section 3.4.2, but with the appropriate boundary conditions substituted. The point at issue here is the distribution of shear force and bending moment. These are determined from the reactions at the fixed support, which are found to be

$$\text{vertical reaction } \frac{-5ql}{8}\left(1+\frac{6(2+\nu)}{25}\frac{h^2}{l^2}\right)\left(1+\frac{3(1+\nu)}{5}\frac{h^2}{l^2}\right)^{-1} \quad (3.68)$$

$$\text{moment reaction } \frac{ql^2}{8}\left(1-\frac{2(4+5\nu)}{5}\frac{h^2}{l^2}-\frac{12(1+\nu)(2+\nu)}{25}\frac{h^4}{l^4}\right)\left(1+\frac{3(1+\nu)}{5}\frac{h^2}{l^2}\right)^{-1} \quad (3.69)$$

3.5 A modified form of the theory based on Reissner's assumptions

3.5.1 Introduction

In Chapter I it was mentioned that Reissner's theory for plates involves the use of a stress function in its solution, and it was listed as an objective of this work to develop a theory based on Reissner's assumptions whose solution did not require the use of a stress function. A theory based on Reissner's assumptions has been developed for beams in Appendix A, and the cases considered in Section 3.4 show that there is no need for the introduction of a stress function to obtain a solution for beams. However a modification to this theory is developed here in the form which will be required in order to avoid the stress function in plate problems, so that the general characteristics of the approach can be observed and the accuracy of its results assessed.

3.5.2 Theoretical development

Consider equation (A.21) for shear force. Since $q = -\frac{dQ}{dx}$ this may be rewritten as

$$Q = -EI\frac{d^3w}{dx^3} + \frac{(2+\nu)}{10}h^2\frac{d^2Q}{dx^2} \qquad (3.70)$$

Differentiating twice

$$\frac{d^2Q}{dx^2} = -EI\frac{d^5w}{dx^5} + \frac{(2+\nu)}{10}h^2\frac{d^4Q}{dx^4} \qquad (3.71)$$

Substituting for d^2Q/dx^2 from (3.71) in (3.70) yields

$$Q = -EI\left(\frac{d^3w}{dx^3} + \frac{h^2(2+\nu)}{10}\frac{d^5w}{dx^5} + (\text{terms in } h^4 \text{ and higher powers of } h)\right) \qquad (3.72)$$

In considering the required degree of accuracy at this stage, two points must be borne in mind:

(a) The initial assumption of a linear distribution of bending stress and the averaging of shear deformation through the depth of the beam are themselves approximations.

(b) Finite difference techniques will later be employed, and the normal central difference formulae are themselves accurate only to order (mesh length)^2.

Clearly the inclusion of terms in equation (3.72) of high powers of h would attribute a degree of accuracy to the expression for shear force which is not justified by the accuracy of other parts of the analysis or solution. Terms in the fourth and higher powers of h will therefore be ignored. So that, considering equations (A.20 - A.22) the final form of the equations for bending moment and shear force to be used here are

$$Q = -EI\left(\frac{d^3w}{dx^3} + \frac{h^2(2+\nu)}{10}\frac{d^5w}{dx^5}\right) \tag{3.73}$$

$$M = -EI\left(\frac{d^2w}{dx^2} + \frac{h^2(2+\nu)}{10}\frac{d^4w}{dx^4}\right) \tag{3.74}$$

and for the equilibrium equation

$$\frac{d^4w}{dx^4} + \frac{h^2(2+\nu)}{10}\frac{d^6w}{dx^6} = \frac{q}{EI} \tag{3.75}$$

where $q = q(x)$.

This theory will be referred to as the modified Reissner theory, and owing to the close similarity with the theory based directly on Reissner's assumptions only simply supported beams carrying uniformly distributed and central point loading will be investigated.

3.5.2 Simply supported beam carrying uniformly distributed load

As it stands the problem is the solution of a sixth order partial differential equation, which demands three boundary conditions to be satisfied, while strictly only two such conditions will apply in the case of a beam. This difficulty can be overcome by separation of the contributions to total deflection of bending and shear and setting each equal to zero at a support.

The general solution to (3.75) is

$$w = \frac{1}{EI}\left(\frac{qx^4}{24} + \frac{Ax^3}{6} + \frac{Bx^2}{2} + Cx + D + F\cos\mu x + G\sin\mu x\right) \qquad (3.76)$$

where $\frac{1}{\mu^2} = \frac{h^2(2+\nu)}{10}$

Differentiating this expression as required and substituting in (3.73) and (3.74) gives the following expressions for shear force and bending moment.

$$M = -\frac{qx^2}{2} - Ax - B - \frac{h^2(2+\nu)}{10}q \qquad (3.77)$$

$$Q = -qx + A \qquad (3.78)$$

From statics $Q = 0$ at $x = \frac{l}{2}$ and hence $A = -q\,l/2$

$$M = 0 \text{ and hence } B = -\frac{h^2(2+\nu)}{10}q$$

The boundary conditions at $x = 0$ require $w = 0$, i.e.

$$0 = D + F \qquad (3.79)$$

If the contribution to total deflection of bending deflection is to be zero then D = 0 and hence F = 0 also.

Therefore, since w = 0 at x = l.

$$0 = \frac{ql^4}{24} + (\frac{-ql}{2})\frac{l^3}{6} - \frac{h^2(2+\nu)}{10}\frac{ql^2}{2} + Cl + G\sin\mu l \qquad (3.80)$$

If bending and shear deflections are to be separately zero then G = 0 and hence

$$C = \frac{ql^3}{24} + \frac{h^2(2+\nu)}{20}ql \qquad (3.81)$$

So that finally the deflected form is given by

$$w = \frac{1}{EI}\left(\frac{qx^4}{24} - \frac{qlx^3}{12} + \frac{ql^3x}{24} + \frac{h^2(2+\nu)}{20}qlx - \frac{h^2(2+\nu)}{20}qx^2\right) \qquad (3.82)$$

from which the central deflection is

$$w_{x = l/2} = \frac{5ql^4}{384EI}\left(1 + \frac{24(2+\nu)}{25}\frac{h^2}{l^2}\right) \qquad (3.83)$$

3.5.3 Simply supported beam carrying central point load

Representing the point load in Fourier form as before (3.54), the governing equilibrium equation (3.75) becomes

$$\frac{d^4w}{dx^4} + \frac{h^2(2+\nu)}{10}\frac{d^6w}{dx^6} = \sum_{1,3\cdots}^{\infty} \frac{2P}{EIl}\sin\frac{n\pi}{2}\sin\frac{n\pi x}{l} \qquad (3.84)$$

Integrating four times gives

$$w + \frac{h^2(2+\nu)}{10}\frac{d^2w}{dx^2} = \frac{2P}{EIl}\sum_{1,3\cdots}^{\infty}(\frac{l}{n\pi})^4\sin\frac{n\pi}{2}\sin\frac{n\pi x}{l} +$$

$$\frac{Ax^3}{6} + \frac{Bx^2}{2} + Cx + D \qquad (3.85)$$

so that the shear force and bending moment are

$$Q = \frac{2P}{l} \sum_{1,3\cdots}^{\infty} \frac{l}{n\pi} \sin\frac{n\pi}{2} \cos\frac{n\pi x}{l} + A \qquad (3.86)$$

$$M = \frac{2P}{l} \sum_{1,3\cdots}^{\infty} \left(\frac{l}{n\pi}\right)^2 \sin\frac{n\pi}{2} \sin\frac{n\pi x}{l} + Ax + B \qquad (3.87)$$

The general solution to (3.85) is

$$w = \frac{2P}{EIl} \sum_{1,3\cdots}^{\infty} \frac{1}{\left(\frac{n\pi}{l}\right)^4 \left(1 - \frac{h^2(2+\nu)}{10} \left(\frac{n\pi}{l}\right)^2\right)} \sin\frac{n\pi}{2} \sin\frac{n\pi x}{l} \qquad (3.88)$$

$$+ Cx + D + F\cos\lambda x + G\sin\lambda x$$

where λ is given by (3.56).

Applying the arguments similar to those used in section 3.5.2 this equation can then be solved, and gives for the central deflection

$$w_{x = l/2} = \frac{Pl^3}{48EI} \left(1 + \frac{6(2+\nu)}{5} \frac{h^2}{l^2}\right) \qquad (3.89)$$

3.6 Summary of theoretical results

3.6.1 Introduction

At this stage the results obtained by the three theories developed in Sections, 3.3, 3.4 and 3.5 can be compared with the existing solutions discussed in Section 3.2, and also the results for other cases examined. Before doing so it may be noted that the results obtained from both theories based on Reissner's assumptions are identical (compare equation (3.53) with (3.83) and equation (3.58) with (3.89). The results from these theories will therefore be referred to together as the results obtained from the application of Reissner's assumptions.

3.6.2 Summary of deflection results

The expressions for central deflection obtained for each load and support case considered are summarised below, and illustrated graphically in Figures 3.7 - 3.10.

(a) Simply supported beam with uniformly distributed load

(See Figure 3.7 and 3.8)

Timoshenko and Goodier (3.2) $\frac{5ql^4}{384EI}\left(1+\frac{48}{25}(1+\frac{5\nu}{8})\frac{h^2}{l^2}\right)$

Partial deflection method (3.35) $\frac{5ql^4}{384EI}\left(1+\frac{48}{25}(1+\nu)\frac{h^2}{l^2}\right)$

Theories based on Reissner's assumptions (3.53) and (3.83) $\frac{5ql^4}{384EI}\left(1+\frac{48}{25}(1+\frac{\nu}{2})\frac{h^2}{l^2}\right)$

(b) Simply supported beam with central point load

(See Figures 3.9 and 3.10)

Timoshenko (3.14) $\frac{Pl^3}{48EI}\left(1+3(1+\nu)\frac{h^2}{l^2}\right)$

Sechler (3.18)	$\frac{Pl^3}{48EI}\left(1+\frac{12}{5}(1+\nu)\frac{h^2}{l^2}\right)$
Seewald (3.19)	$\frac{Pl^3}{48EI}\left(1+\frac{12}{5}(1+\frac{5\nu}{8})\frac{h^2}{l^2}-0.85\frac{h^3}{l^3}\right)$
Partial deflection method (3.38)	$\frac{Pl^3}{48EI}\left(1+\frac{12}{5}(1+\nu)\frac{h^2}{l^2}\right)$
Theories based on Reissner's assumptions (3.58) and (3.89)	$\frac{Pl^3}{48EI}\left(1+\frac{12}{5}(1+\frac{\nu}{2})\frac{h^2}{l^2}\right)$

(c) Cantilever with end load

(See Figures 3.11 and 3.12)

Timoshenko and Goodier (3.13)	$\frac{Pl^3}{3EI}\left(1+\frac{3(1+\nu)}{4}\frac{h^2}{l^2}\right)$
Partial deflection method (3.41)	$\frac{Pl^3}{3EI}\left(1+\frac{3(1+\nu)}{5}\frac{h^2}{l^2}\right)$
Theories based on Reissner's assumptions (3.62)	$\frac{Pl^3}{3EI}\left(1+\frac{3(1+\nu)}{5}\frac{h^2}{l^2}\right)$

(d) Clamped beam with uniformly distributed load

(See Figure 3.13)

Partial deflection method (3.42)	$\frac{ql^4}{384EI}\left(1+\frac{48(1+\nu)}{5}\frac{h^2}{l^2}\right)$
Theories based on Reissner's assumptions (3.64)	$\frac{ql^4}{384EI}\left(1+\frac{48(1+\nu)}{5}\frac{h^2}{l^2}\right)$

———— Timoshenko and Goodier (3.3)

—— —— Theories based on Reissner's assumptions (3.53) and (3.83)

------ Partial deflection method (3.35)

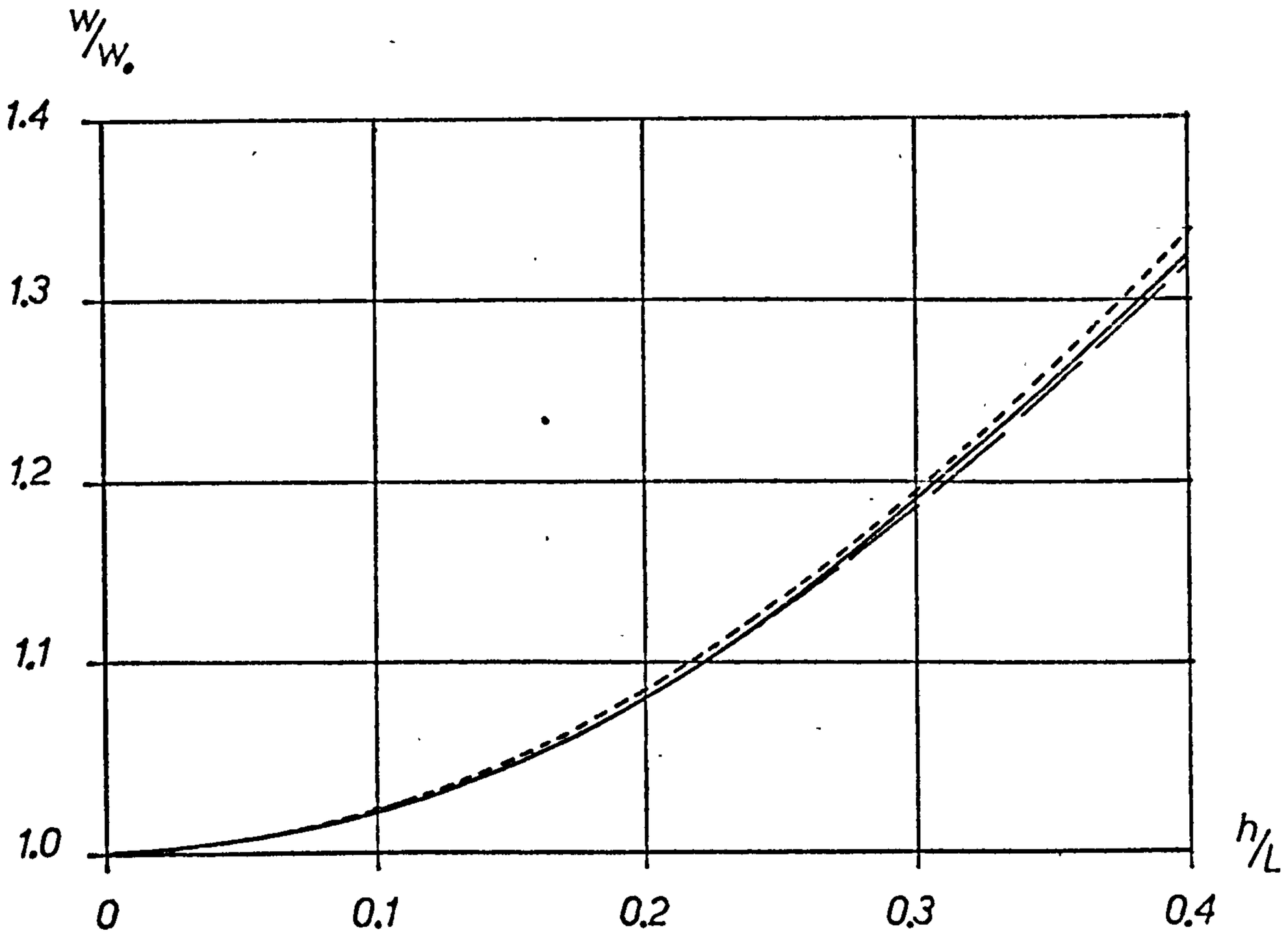

Figure 3.7

Central deflection ratio.

Simply supported beam carrying uniformly distributed load ($\nu = 0.1$)

———— Timoshenko and Goodier (3.3)

—— —— Theories based on Reissner's assumptions (3.53) and (3.83)

------- Partial deflection method (3.35)

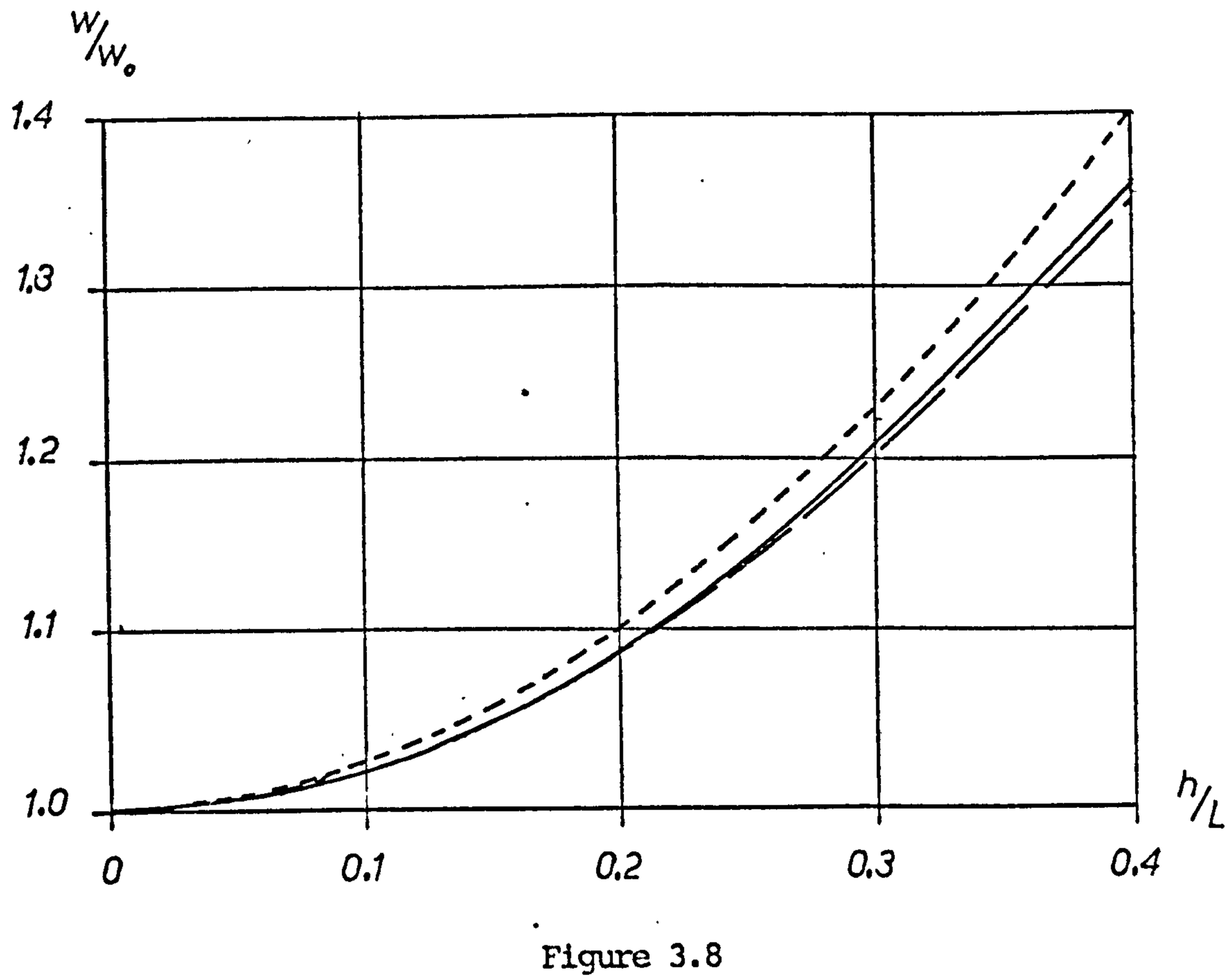

Figure 3.8

Central deflection ratio.

Simply supported beam carrying uniformly distributed load ($\nu = 0.3$)

———— Seewald (3.19)

—— —— Theories based on Reissner's assumptions (3.58) and (3.89)

- - - - - - Partial deflection method (3.38)

———-——— Timoshenko (3.14)

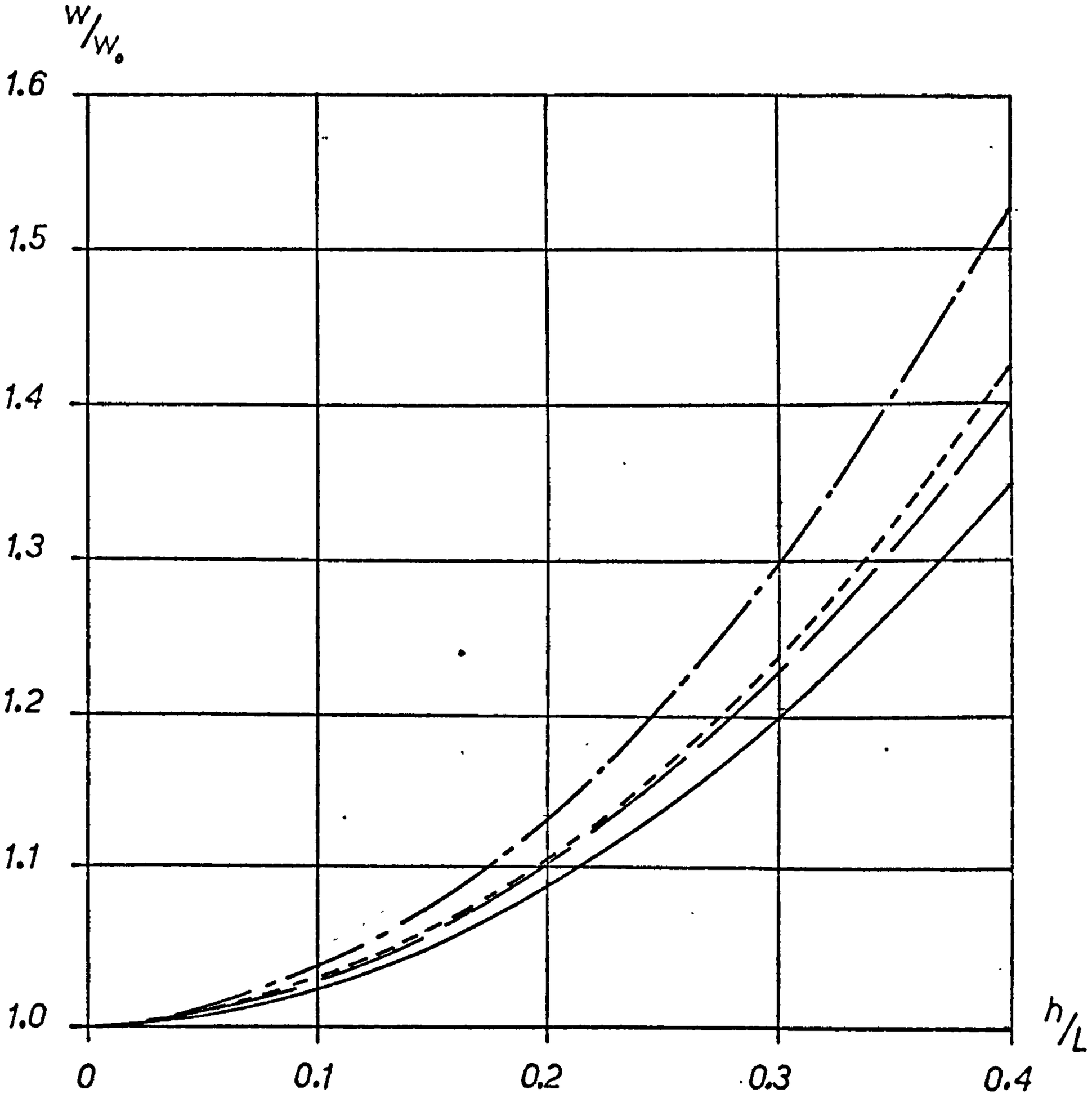

Figure 3.9

Central deflection ratio

Simply supported beam carrying

a central point load ($\nu = 0.1$)

——————— Seewald (3.19)

———— ———— Theories based on Reissner's assumptions (3.58) and (3.89)

— — — — — — Partial deflection method (3.38)

————·———— Timoshenko (3.14)

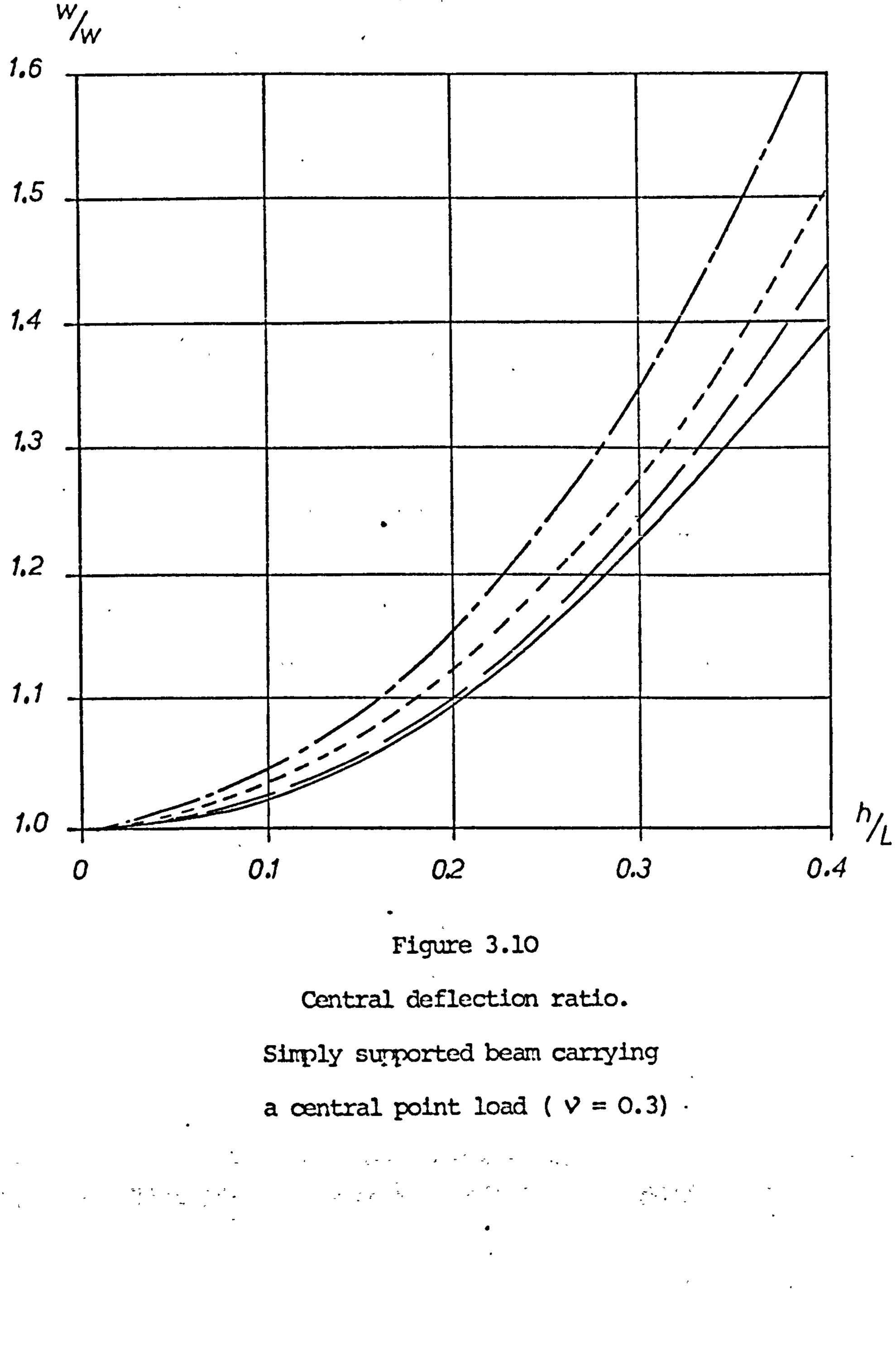

Figure 3.10

Central deflection ratio.

Simply supported beam carrying

a central point load ($\nu = 0.3$)

———— Timoshenko and Goodier (3.13)

—— —— Partial deflection method (3.41) and theory based on Reissner's assumptions (3.62)

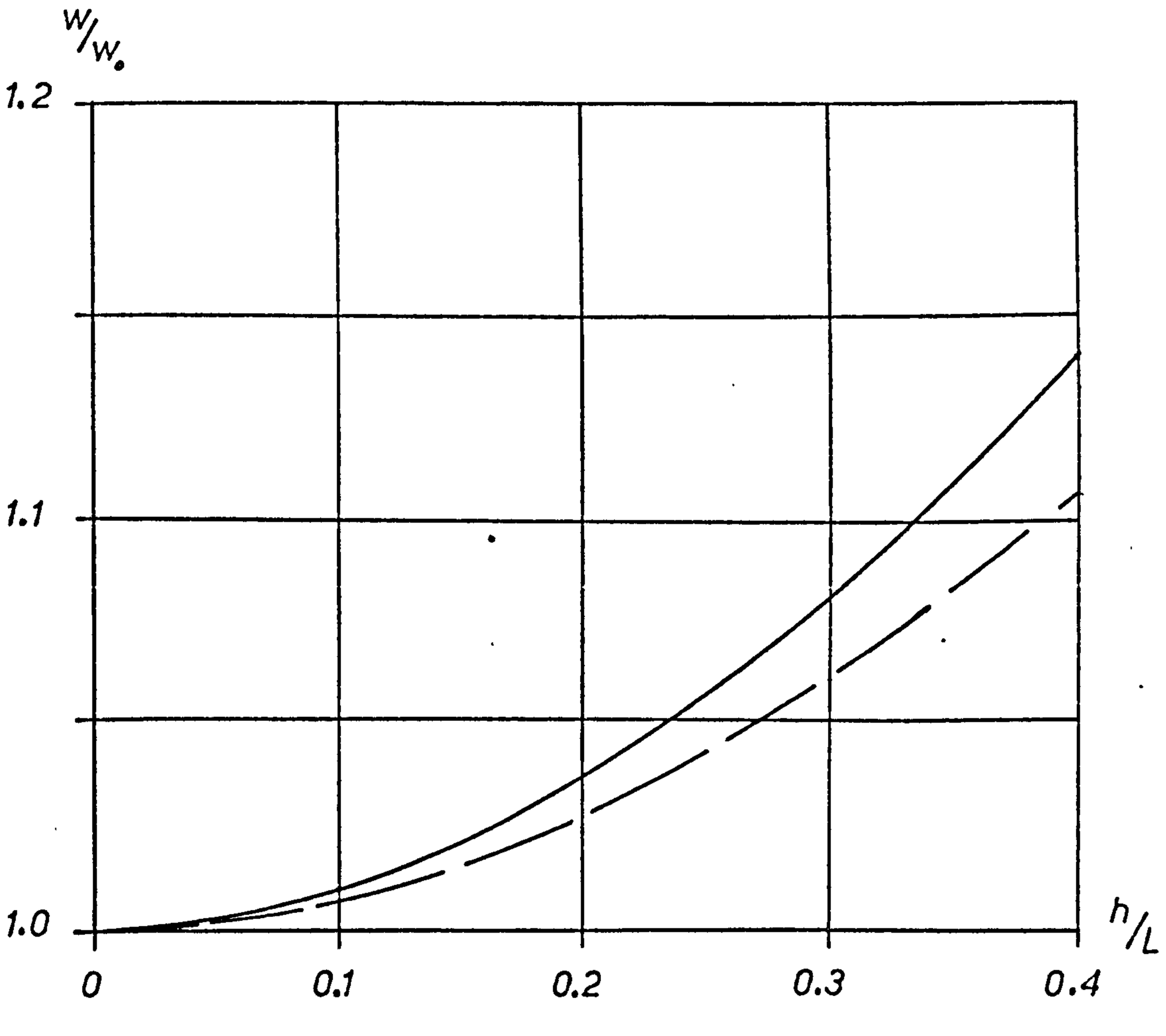

Figure 3.11

Tip deflection ratio

Cantilever with end load (ν = 0.1)

———— Timoshenko and Goodier (3.13)

—— —— Partial deflection method (3.41) and theory based on Reissner's assumptions (3.62)

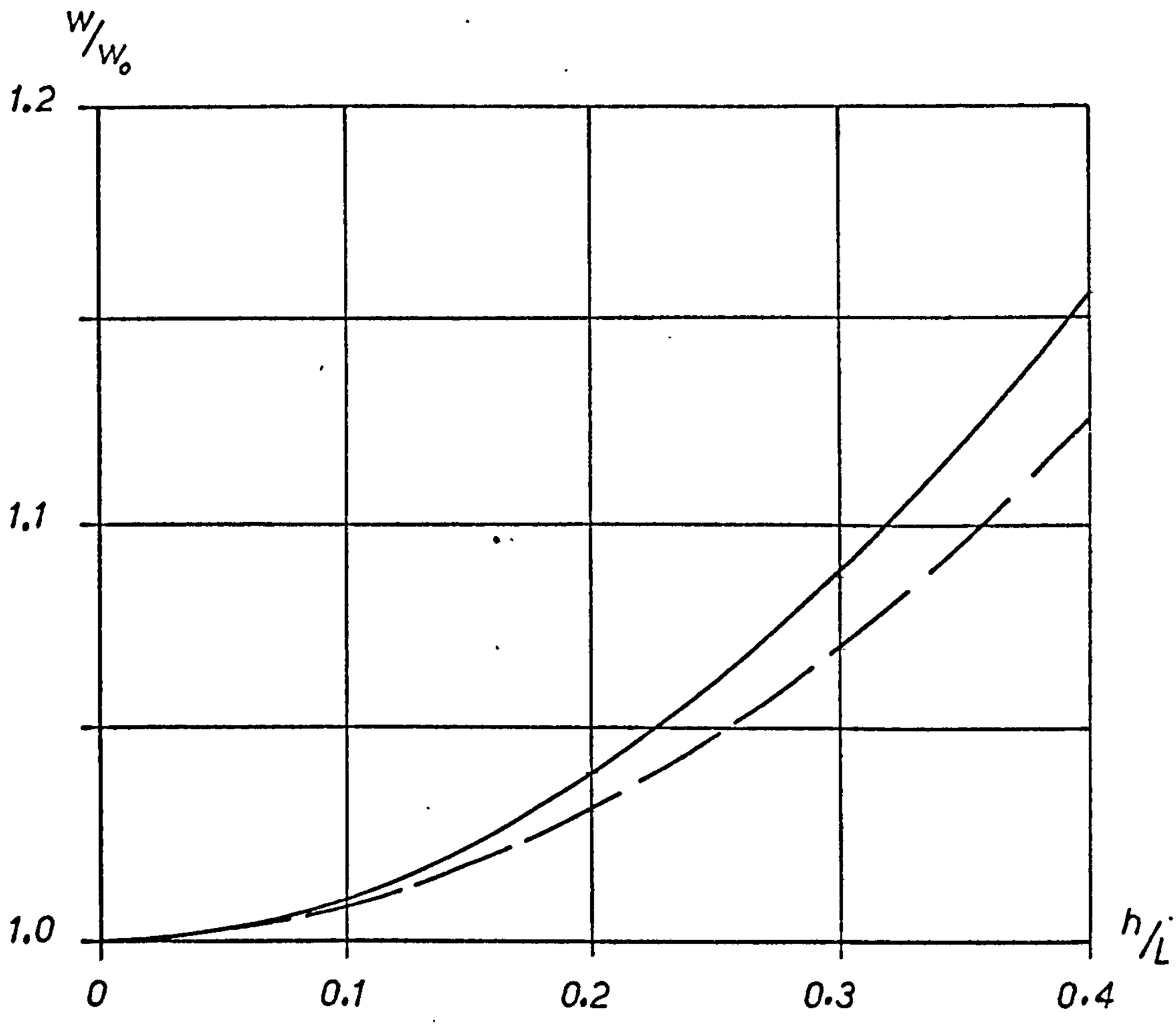

Figure 3.12

Tip deflection ratio

Cantilever with end load (ν = 0.3)

———— Partial deflection method (3.42) and theory based on Reissner's assumptions (3.64)

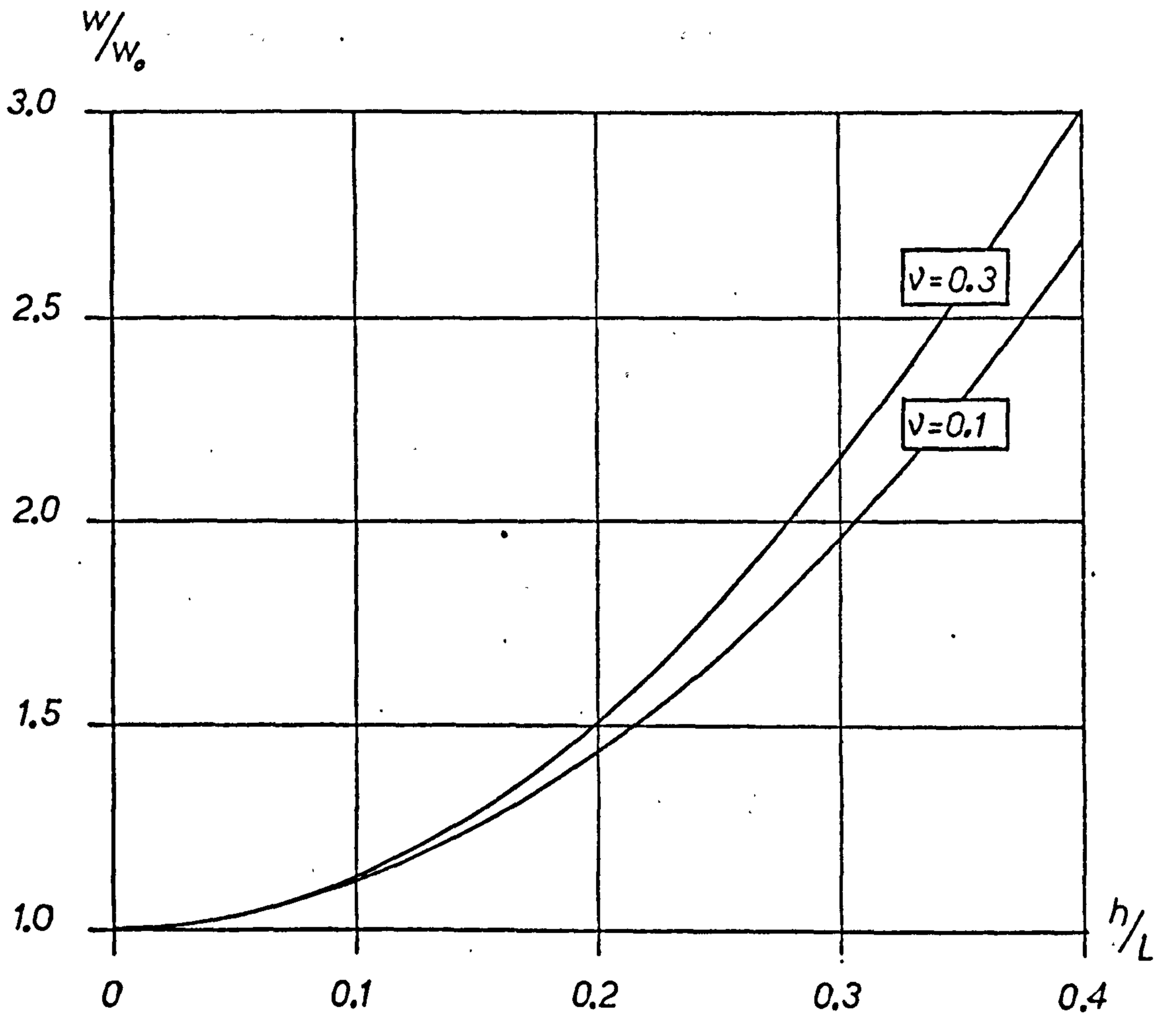

Figure 3.13

Central deflection ratio.

Clamped beam carrying uniformly distributed load.

3.6.3 Discussion of deflection results

Before comparing the formulae developed in this chapter with the results of existing work, it is convenient to note first the relationship between the partial deflection method and the theories based on Reissner's assumptions. The latter include the effects of transverse direct stress, but two cases have been considered in which these have no effect on deflection, namely the end-loaded cantilever ($\sigma_z = 0$ throughout) and the clamped beam with uniformly distributed load (the clamped boundary prevents the associated in-plane strain - see discussion relating to circular plates in Section 2.2.1). The results for these cases are summarised in cases (c) and (d) above and in Figures 3.11 - 3.13. Comparing the formulae it is observed that the partial deflection method and the theories based on Reissner's assumptions give identical results, and it may be deduced that in estimating the effects of shear both approaches are essentially the same. Thus, any differences between the results that these two approaches give in other cases will be due to effects other than shear deformation.

Comparing next the results given by these two theories for the simply supported beams (Summary cases (a) and (b) and Figures 3.7 - 3.10), it is found that they are the same when $\nu = 0$, but, due to the inclusion of transverse direct stress in the theories based on Reissner's assumptions, they differ for other values of Poisson's ratio. It may be observed that the Reissner based theories predict a slightly smaller deflection, which is consistent with the general effect of transverse direct stress.

If this term had been omitted from the development of the theory in Appendix A, the deflection results given by the partial deflection method and the theories based on Reissner's assumptions would have been the same in all cases.

Having discovered the common ground between the theories developed in this chapter, it is now possible to compare them with existing solutions.

Considering first case (a), the simply supported beam with uniform loading, it is found that the results obtained in this work are the same as those given by Timoshenko and Goodier when $\nu = 0$, but differ slightly for other values of Poisson's ratio. The magnitudes of the differences for $h/l = 0.3$ are shown in Table 3.6, and can be seen to be very small

	$\nu = 0.1$	$\nu = 0.3$
Partial deflection method	+ 0.35%	+.1.66%
Theories based on Reissner's assumptions	- 0.14%	- 0.5%

Table 3.6

Differences in central deflection compared with Timoshenko and Goodier. Simply supported beam with uniform load, $h/l = 0.3$.

Turning next to case (b), the simply supported beam with central point load, it is not surprising that Sechler's result (3.18) is the same as that obtained by the partial deflection method, since it is derived from energy considerations based on

the same assumed distributions of bending stress and shear stress. However, Timoshenko's formula (3.14) gives a greater increase in deflection due to shear than any of the others, and this is because his estimate is based on the mid-plane shear strain, rather than an average value taken through the depth of the beam. Undoubtedly Seewald's consideration is the most detailed, and regarding his solution as the standard for comparison, the results obtained in this chapter differ slightly, typical values of the differences for $h/l = 0.3$ being indicated in Table 3.7.

	$\nu = 0.1$	$\nu = 0.3$
Partial deflection method	+2.9%	+3.8%
Theories based on Reissner's assumptions	+1.7%	+1.2%

Table 3.7

Differences in central deflection compared with Seewald. Simply supported beam with central point load, $h/l = 0.3$

The only remaining result to be considered is Timoshenko and Goodier's equation (3.13) for case (c), the end-loaded cantilever, and this is seen to indicate a deflection due to shear 25% greater than that predicted by the methods developed in this work. This disparity is attributable purely to the difference in the assumed action of the boundary clamp. Timoshenko's assumption, illustrated in Figure 3.4, is that a tangent to an initially vertical element at the neutral axis remains vertical, and this obviously allows a greater deflection to occur than with the prevention of an average rotation of an initially vertical section.

3.6.4 Theoretical results for stress resultants

It has been established that inclusion of shear deformation can only alter the distributions of stress resultants from those of classical theory in non-symmetric indeterminate beams. For the propped cantilever considered in Sections 3.3.6 and 3.4.6 both the partial deflection method and the theory based on Reissner's assumptions are seen to predict such a modification to the distributions of both shear force and bending moment. The relevant equations are (3.44), (3.45) and (3.68), (3.69) and while the first pair contain the effects of shear deformation only, the second pair, based on Reissner's assumptions, take into account transverse direct stress as well. Omitting these last terms from the Reissner based theory developed in Appendix A would again lead to identical results to those given by the partial deflection method. The modifications due to shear alone are small, and typical values for $h/l = 0.3$ and $\nu = 0.3$ are reductions of 1% and 6% in the fixed support reaction and moment respectively, with corresponding changes in the shear force and bending moment throughout the beam.

Transverse direct stress has a more significant effect on the distribution of bending moment in all indeterminate cases, except when Poisson's ratio is zero. In symmetric beams the modification takes the form of a constant correction throughout, since the distribution of shear force must remain unchanged. In non-symmetric cases the distributions of both shear force and bending moment are modified, although changes in shear force are only slight. The order of magnitude of the change in bending

moment can be quite significant for large values of both h/ℓ and ν together, as indicated in the typical values shown in Tables 3.4 and 3.5 for the uniformly loaded, clamped beam.

3.6.5 Conclusions

At the end of this theoretical discussion some general conclusions can be drawn before proceeding to an examination of the application of numerical methods and experimental verification.

Three theories have been developed in this chapter, the first based on the partial deflection method and the other two on Reissner's assumptions. It is found that all three give the same values for the additional deflection due to shear, whilst the last two give an additional correction due to transverse direct stress. The main conclusions reached are:

(a) Estimation of the effects of shear deformation by taking either an overall shear stiffness or by evaluating an average rotation of a section initially normal to the neutral surface gives extremely accurate results when compared with a more refined solution. The averaging in both cases is carried out by equating the work done by the shear force acting through the average distortion to that done by the actual distributions of shear stress and strain.

(b) Consideration of transverse direct stress can, in some cases, lead to a small reduction in deflection. The theories based on Reissner's assumptions take this factor into account, and again make very accurate predictions of the correction to deflection involved.

(c) A modification to the theory based on Reissner's assumptions has been made, the order of accuracy of which has been specified as h^2. The results confirm that this accuracy has been achieved, and any errors involved would be of order h^4.

(d) The partial deflection method amounts to a simple superposition of deflections due to bending and shear, except in non-symmetric indeterminate beams. In such cases the two partial deflections do not separately vanish at a rigid support. For example w_b and w_s are not separately zero at the fixed support in the propped cantilever considered in Section 3.3.6.

(e) Both types of theory developed indicate modifications in the distributions of stress resultants due to shear in cases where the distribution of shear force is not determinate by consideration of equilibrium and symmetry. These have been evaluated, but compared with the changes in deflection due to shear, are relatively insignificant.

(f) Transverse direct stress has been found to have an effect on the distribution of bending moment in indeterminate beams which can be fairly important when large values of both h/l and ν occur together.

3.7 Solution of the modified Reissner theory by numerical methods.

3.7.1 Introduction.

The modified Reissner theory has no particular advantage to offer for beam problems; its potential lies in the field of plates. The purpose in developing it in the context of beams has been to assess its accuracy, and this has been found to be excellent in the cases considered. Although analytical solutions are possible for beams it is useful to consider the application of numerical methods to the theory here, so that any fundamental difficulties can be resolved before considering the more complex problems associated with plates.

Thus in this section, finite difference and localised Rayleigh Ritz techniques will be applied to simply supported beams with both uniformly distributed and central point loading.

3.7.2 Solution by finite differences

Non-dimensionalising equations (3.73) - (3.75) in accordance with the method given in Appendix C, the bending moment, shear force and equilibrium equations become

$$\frac{ML}{EI} = -\frac{d^2W}{dX^2} - \frac{H^2(2+\nu)}{10}\frac{d^4W}{dX^4} \qquad (3.90)$$

$$\frac{QL^2}{EI} = -\frac{d^3W}{dX^3} - \frac{H^2(2+\nu)}{10}\frac{d^5W}{dX^5} \qquad (3.91)$$

$$\frac{d^4W}{dX^4} = \frac{H^2(2+\nu)}{10}\frac{d^6W}{dX^6} = \frac{qL^3}{EI} \qquad (3.92)$$

The finite difference forms of these equations are obtained by substituting the finite difference equivalents of the derivatives given in Appendix C. They then become

$$\frac{ML}{EI} = \boxed{-C} - \boxed{-1+4C} - \boxed{2-6C} - \boxed{-1+4C} - \boxed{-C} \qquad (3.93)$$

$$\frac{QL^2}{EI} = \boxed{\frac{C}{2}} - \boxed{\frac{1}{2}-2C} - \boxed{-1+\frac{5C}{2}} \quad | \quad \boxed{1-\frac{5C}{2}} - \boxed{-\frac{1}{2}+2C} - \boxed{-\frac{C}{2}} \qquad (3.94)$$

$$\frac{qL^3}{EI} = \boxed{C} - \boxed{1-6C} - \boxed{-4+15C} - \boxed{6-20C} - \boxed{-4+15C} - \boxed{1-6C} - \boxed{C} \qquad (3.95)$$

N+3 N+2 N+1 N N-1 N-2 N-3

where $C = \frac{H^2(2+\nu)}{10P^2}$

A reasonably accurate result can probably be obtained using a fairly coarse mesh for a uniformly distributed load, but in order to give a good representation of a point load a finer mesh is required. $P = \frac{1}{12}$ was finally selected after investigating the convergence of the solution. The scheme of mesh points required is as shown in Figure 3.14.

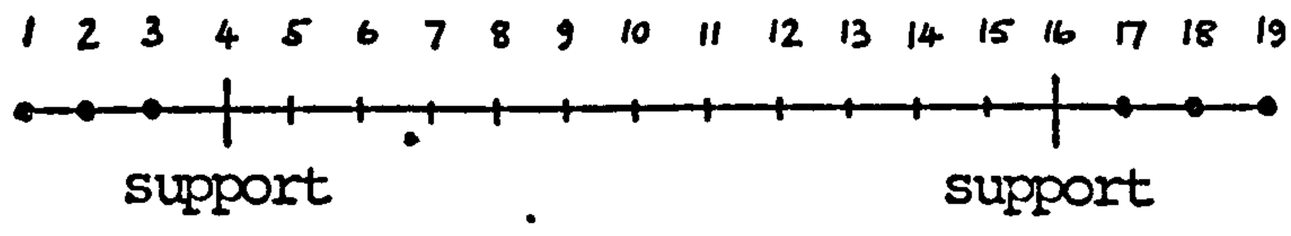

Figure 3.14

Finite difference mesh used for solution of beam problems.

Points marked.are fictitious points. 19 equations are required for solution, and these are

equilibrium	13
boundary equation w = 0	2
M = 0	2

Two further equations are therefore needed, and these can be found by extrapolating for W_1 and W_{19}. Alternatively points 1 and 19 can be eliminated altogether by using an off-centre finite difference equivalent for $\frac{d^6w}{dx^6}$ in the equilibrium equations at points 4 and 16. Forms of this type are described in Appendix C. The numerical results obtained are the same in either case, and are given in Section 3.8. Methods of solution used for the set of simultaneous equations are described in Appendix E.

3.7.3 Solution by the use of Localised Rayleigh-Ritz techniques

The basis of this method is given by Thompson (30). Some aspects relevant to this work are discussed in detail in Appendix D.

The deflected form of the beam is defined by local Rayleigh functions over a number of regions. The displacement functions will be continuous between regions at the nodes up to the nth order derivative, $\frac{d^nw}{dx^n}$. The least value of n required is one less than the highest order derivative contained in the energy function, so that integration does not involve indeterminate quantities.

For a beam of unit width, the strain energy due to bending and shear in region i, of length a, is

$$U_i = \frac{a}{2EI}\int_0^1 M_i^2 d\xi + \frac{3a}{5Gh}\int_0^1 Q_i^2\, d\xi \qquad (3.97)$$

where the non-dimensionalisation is achieved by setting $\xi = x/a$.

Substituting for G and h in terms of E and I gives

$$U_i = \frac{a}{2EI}\left(\int_0^1 M_i^2 d\xi + \frac{(1+\nu)}{5} h^2 \int_0^1 Q_i^2\, d\xi\right) \tag{3.98}$$

Substituting for M and Q from (3.73) and (3.74) gives

$$U_i = \frac{EI}{2a^3}\int_0^1 \left[\left(\frac{d^2w}{d\xi^2}\right)^2 + 2\frac{(2+\nu)}{10}\frac{h^2}{a^2}\frac{d^2w}{d\xi^2}\frac{d^4w}{d\xi^4} + \left(\frac{(2+\nu)}{10}\frac{h^2}{a^2}\right)^2\left(\frac{d^4w}{d\xi^4}\right)^2\right.$$

$$+ \frac{(1+\nu)}{5}\frac{h^2}{a^2}\left(\frac{d^3w}{d\xi^3}\right)^2 + 2\frac{(1+\nu)}{5}\frac{h^2}{a^2}\frac{(2+\nu)}{10}\frac{h^2}{a^2}\frac{d^3w}{d\xi^3}\frac{d^5w}{d\xi^5}$$

$$\left. + \frac{(1+\nu)}{5}\frac{h^2}{a^2}\left(\frac{(2+\nu)}{10}\frac{h^2}{a^2}\right)^2\left(\frac{d^5w}{d\xi^5}\right)^2\right] d\xi \tag{3.99}$$

The question now arises as to whether all the terms in equation (3.99) need to be retained or not. The expressions for M_i and Q_i are themselves correct to order h^2, but because they are squared and the shear further multiplied by $\frac{(1+\nu)}{5}h^2$ the resulting equation for U_i contains terms in h^2, h^4, and h^6. Once the order of accuracy of M_i and Q_i is fixed at h^2, U_i can also only be accurate to this same order, even though it contains some higher powers of h. A number of possibilities arise:

(a) U_i is made accurate to order h^2. All terms in h^4 and h^6 in equation (3.99) are then omitted, leaving

$$U_i = \frac{EI}{2a^3}\int_0^1 \left[\left(\frac{d^2w}{d\xi^2}\right)^2 + \frac{2(2+\nu)}{10}\frac{h^2}{a^2}\frac{d^2w}{d\xi^2}\frac{d^4w}{d\xi^4} + \frac{(1+\nu)}{5}\frac{h^2}{a^2}\left(\frac{d^3w}{d\xi^3}\right)^2\right] d\xi \tag{3.100}$$

The main disadvantage of this approach is that U_i contains an incomplete description of the bending moment.

The shear force, however is simply equal to $-EI\frac{d^3w}{dx^3}$.

(b) M_i is made accurate to order h^2. Equation (3.99) would then become

$$U_i = \frac{EI}{2a^3}\int_0^1 \left[\left(\frac{d^2w}{d\xi^2}\right)^2 + \frac{2(2+\nu)}{10}\frac{h^2}{a^2}\frac{d^2w}{d\xi^2}\frac{d^4w}{d\xi^4} + \left(\frac{h^2(2+\nu)}{a^2 10}\right)^2\left(\frac{d^4w}{d\xi^4}\right)^2 \right.$$

$$\left. + \frac{(1+\nu)}{5}\frac{h^2}{a^2}\left(\frac{d^3w}{d\xi^3}\right)^2 \right] d\xi \qquad (3.101)$$

At least the expression for M_i is now complete, but another inconsistency is introduced, in that only some of the h^4 terms have now been included.

(c) U_i contains all the terms in h^2 and h^4 which arise from establishing the accuracy of M_i and Q_i at order h^2.

Equation (3.99) then becomes

$$U_i = \frac{EI}{2a^3}\int_0^1 \left[\left(\frac{d^2w}{d\xi^2}\right)^2 + \frac{2(2+\nu)}{10}\frac{h^2}{a^2}\frac{d^2w}{d\xi^2}\frac{d^4w}{d\xi^4} + \left(\frac{(2+\nu)}{10}\frac{h^2}{a^2}\right)^2\left(\frac{d^4w}{d\xi^4}\right)^2 \right.$$

$$+ \frac{(1+\nu)}{5}\frac{h^2}{a^2}\left(\frac{d^3w}{d\xi^3}\right)^2 + \frac{2(1+\nu)}{5}\frac{h^2}{a^2}\frac{(2+\nu)}{10}$$

$$\left. \frac{h^2}{a^2}\frac{d^3w}{d\xi^3}\frac{d^5w}{d\xi^5} \right] d\xi \qquad (3.102)$$

If this expression is adopted then the expression for Q_i is incomplete.

(d) U_i contains all terms in h^2, h^4 and h^6 which arise from establishing the order of accuracy of M_i and Q_i at h^2. Equation (3.99) then stands. The only qualification is that if more accurate expressions for M_i and Q_i were taken,

further terms in h^4 and h^6 would arise, so that even this expression contains inconsistencies.

(a) and (b) would require local Rayleigh Functions to be continuous at least in $\frac{d^3w}{d\xi^3}$, while obviously more accurate results and more rapid convergence would be expected with functions which are continuous in $\frac{d^4w}{d\xi^4}$ as well. (c) and (d) would require this additional degree of continuity in any case.

Each of these was tried, and the eventual choice was made purely on numerical grounds, as it was found that in certain cases the inclusion of higher powers of h led to an ill-behaved system of equations. A comparison of the results is given in Section 3.8.2.

Whichever course is followed, the general procedure is the same. If continuity up to and including $\frac{d^nw}{d\xi^n}$ is required then the displacement function in region i (see Figure 3.15) is

$$w_i = \sum_{i=0}^{m} a_i \xi^i = [A][\xi] \qquad (3.103)$$

where $m = (2n + 1)$

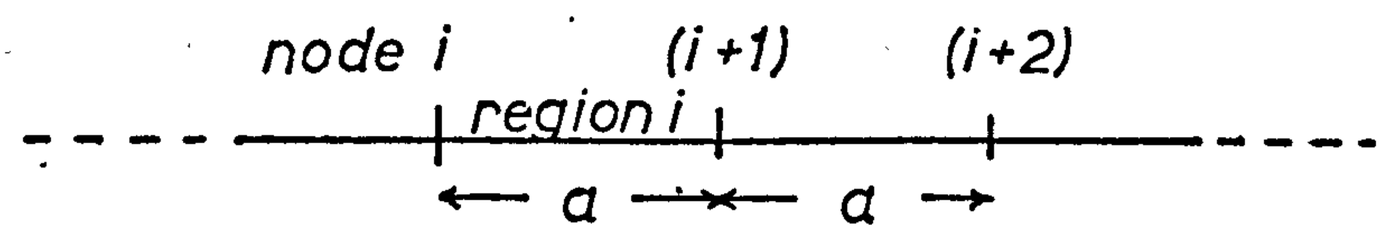

Figure 3.15

Region and node notation for local Rayleigh functions for a beam.

Local Rayleigh functions are formed giving freedom to each derivative as required. Two sets of such functions are associated with node i, $\bar{f}^k$ and f^k. These give freedom to $\frac{d^k w}{d\xi^k}$ at i. $\bar{f}^k$ extends from node i to node (i + 1) and is such that

$$\frac{d^l \bar{f}^k}{d\xi^l} = 0 \text{ for } 0 \leq l \leq n \text{ at } \xi = 0$$

$$\frac{d^l \bar{f}^k}{d\xi^l} = 0 \text{ for } 0 \leq l \leq n \text{ but } l \neq k \text{ at } \xi = 1$$

$$\frac{d^l \bar{f}^k}{d\xi^l} = 1 \text{ for } l = k \text{ at } \xi = 1$$

Similarly f^k extends from node (i + 1) to node (i + 2) and has the following properties

$$\frac{d^l f^k}{d\xi^l} = 0 \text{ for } 0 \leq l \leq n \text{ but } l \neq k \text{ at } \xi = 0$$

$$\frac{d^l f^k}{d\xi^l} = 1 \text{ for } l = k \text{ at } \xi = 0$$

$$\frac{d^l f^k}{d\xi^l} = 0 \text{ for } 0 \leq l \leq n \text{ at } \xi = 1$$

Q_i^k is the coefficient associated with f^k at node i, so that the deflection in region i is given by

$$w_i = \sum_{k=0}^{n} Q_i^{k-k} \bar{f}^k + \sum_{k=0}^{n} Q_{i+1}^k f^k \qquad (3.104)$$

Hence $[A] = [B][Q]$

where $$[Q] = \{Q_i^0, Q_i^1, \ldots Q_i^n, Q_{i+1}^0, \ldots Q_{i+1}^n\} \qquad (3.105)$$

Figure (3.16a) shows the value for [B] for continuity up to $\frac{d^3 w}{d\xi^3}$ and Figure (3.16b) for continuity up to and including $\frac{d^4 w}{d\xi^4}$.

$$\begin{bmatrix}
1 & 0 & 0 & 0 & 0 & 0 & 0 & 0 \\
0 & 1 & 0 & 0 & 0 & 0 & 0 & 0 \\
0 & 0 & \frac{1}{2} & 0 & 0 & 0 & 0 & 0 \\
0 & 0 & 0 & \frac{1}{6} & 0 & 0 & 0 & 0 \\
-35 & -20 & -5 & -\frac{2}{3} & 35 & -15 & \frac{5}{2} & -\frac{1}{6} \\
84 & 45 & 10 & 1 & -84 & 39 & -7 & \frac{1}{2} \\
-70 & -36 & -\frac{15}{2} & -\frac{2}{3} & 70 & -34 & \frac{13}{2} & -\frac{1}{2} \\
20 & 10 & 2 & \frac{1}{6} & -20 & 10 & -2 & \frac{1}{6}
\end{bmatrix}$$

Figure 3.16a Matrix [B] for continuity of $\frac{d^3w}{d\xi^3}$

$$\begin{bmatrix}
1 & 0 & 0 & 0 & 0 & 0 & 0 & 0 & 0 & 0 \\
0 & 1 & 0 & 0 & 0 & 0 & 0 & 0 & 0 & 0 \\
0 & 0 & \frac{1}{2} & 0 & 0 & 0 & 0 & 0 & 0 & 0 \\
0 & 0 & 0 & \frac{1}{6} & 0 & 0 & 0 & 0 & 0 & 0 \\
0 & 0 & 0 & 0 & \frac{1}{24} & 0 & 0 & 0 & 0 & 0 \\
-126 & -70 & -\frac{35}{2} & -\frac{5}{2} & -\frac{5}{24} & 126 & -56 & \frac{21}{2} & -1 & \frac{1}{24} \\
420 & 224 & -\frac{105}{2} & \frac{20}{3} & \frac{5}{12} & -420 & 196 & -\frac{77}{2} & \frac{23}{6} & -\frac{1}{6} \\
-540 & -280 & -63 & -\frac{15}{2} & -\frac{5}{12} & 540 & -260 & 53 & -\frac{11}{2} & \frac{1}{4} \\
315 & 160 & 35 & 4 & \frac{5}{24} & -315 & 155 & -\frac{65}{2} & \frac{7}{2} & -\frac{1}{6} \\
-70 & -35 & -\frac{15}{2} & -\frac{5}{6} & -\frac{1}{24} & 70 & -35 & \frac{15}{2} & -\frac{5}{6} & \frac{1}{24}
\end{bmatrix}$$

Figure 3.16b Matrix [B] for continuity of $\frac{d^4w}{d\xi^4}$

The strain energy associated with region i can then be written in the form

$$U_i = \frac{EI}{2a^3} [A^T C A] = \frac{EI}{2a^3} [Q^T] [B^T C B] [Q] \qquad (3.106)$$

where the coefficients of [C] are found in the manner described in Appendix E.

The total potential energy of the whole system of N regions is

$$V = \sum_{i=1}^{N} U_i - [P][\delta] \qquad (3.107)$$

where $[P][\delta]$ is the loss of potential energy of the loads. For a concentrated load, P, acting at node i this is simply $P.Q_i^o$. If the load is q per unit length uniformly distributed, then the loss of potential energy is q x (volume of deflection function). This can be expressed in terms of the coefficients Q as shown in Appendix D.

The potential energy is then minimized with respect to each coefficient Q_i^k, and this gives the system of simultaneous equations, which when solved gives the values of these coefficients. The form of these equations is

$$\frac{EI}{a^3}\begin{bmatrix} B^TCB & & & \\ B^TCB & B^TCB & & \\ & B^TCB & \ddots & \\ & & & \end{bmatrix} \times \begin{bmatrix} Q_1^o \\ \vdots \\ \\ \end{bmatrix} = \begin{bmatrix} R \\ R \\ \\ \end{bmatrix}$$

where $R_i = \sum_{k=1}^{m+1} \frac{B_{ki}}{k}$ for uniformly distributed load (3.108)

At the boundaries the appropriate rows of the matrix are replaced by the boundary equations. These may be expressed in terms of coefficients from [B] and [Q] as follows. At node i

$$w_i = Q_i^o \tag{3.109}$$

$$M_i = -\frac{EI}{a^2}\left(\frac{d^2w}{d\xi^2} + \frac{h^2(2+\nu)}{10}\frac{d^4w}{d\xi^4}\right)$$

$$= -\frac{EI}{a^2}\sum_{j=1}^{m+1}\left((2!)B_{3,j} + (4!)\frac{(2+\nu)}{10}\frac{h^2}{a^2}B_{5,j}\right)Q_i^j \tag{3.110}$$

$$\phi_i = -\frac{1}{a}\left(\frac{dw}{d\xi} + \frac{(1+\nu)}{5}\frac{h^2}{a^2}\frac{d^3w}{d\xi^3} + \frac{(1+\nu)}{5}\frac{h^2}{a^2}\frac{(2+\nu)}{10}\frac{h^2}{a^2}\frac{d^5w}{d\xi^5}\right)$$

$$= -\frac{1}{a}\sum_{j=1}^{m+1}\left(B_{2j} + (3!)\frac{(1+\nu)}{5}\frac{h^2}{a^2}B_{4,j} + (5!)\frac{(1+\nu)(2+\nu)}{50}\frac{h^4}{a^4}B_{6,j}\right)Q_i^j \qquad (3.111)$$

$$Q_i = -\frac{EI}{a^2}\left(\frac{d^3w}{d\xi^3} + \frac{(2+\nu)}{10}\frac{h^2}{a^2}\frac{d^5w}{d\xi^5}\right)$$

$$= -\frac{EI}{a^3}\sum_{j=1}^{m+1}\left((3!)\,B_{4,j} + (5!)\frac{(2+\nu)}{10}\frac{h^2}{a^2}B_{6,j}\right)Q_i^j \qquad (3.112)$$

The last term in the equations for ϕ_i and Q_i would be omitted if h^4 and h^6 terms arising from the shear are omitted from the expression for U_i, as discussed in points (a), (b) and (c) above. After solution of the equations (3.108) the bending moment and shear force at any node can be evaluated from equations (3.110) and (3.112).

3.8 Comparison of numerical results

3.8.1 Comments on the finite difference solution

In the case of uniformly distributed loading the finite difference equations are almost always well behaved. The only occasional exception to this is when a particular value of H causes a critical coefficient (e.g. the central coefficient of the molecule) in equation (3.95) to become very nearly zero.

But, with a central point load, the equations become unstable at certain values of depth/span ratio, H, and no meaningful solution can be obtained for higher values of H. The precise reason for this remains obscure.

3.8.2 Comments on the localised Rayleigh-Ritz solution

Since continuity is required up to relatively high order derivatives the deflection function is itself very accurate, so that the Rayleigh functions need not be highly localised. Using $a = \frac{l}{2}$ or possibly $a = \frac{l}{4}$ was found to be quite satisfactory. In any case numerical problems arise if a is too small, since the ratios $(\frac{h}{l})^2$ and $(\frac{h}{l})^4$ can then become very large, and in the energy function shear terms dominate to an extent which makes the solution very unstable.

The results obtained by the various methods outlined in Section 3.6.2 are compared in Figures 3.17 to 3.20. For a simply supported beam carrying a uniformly distributed load, Figures 3.17 and 3.18 show that with continuity of $\frac{d^3w}{dx3}$ or $\frac{d^4w}{dx^4}$ very close agreement with the theoretical values is obtained by using U_i as given by equation (3.101), where h^4 terms arising from M_i are included in addition to all h^2 terms.

——————— Theoretical

—— —— U_i contains h^2 terms only

------- U_i contains h^2 terms and h^4 terms from M_i

——-—— U_i contains h^2 terms and h^4 terms from M_i and Q_i

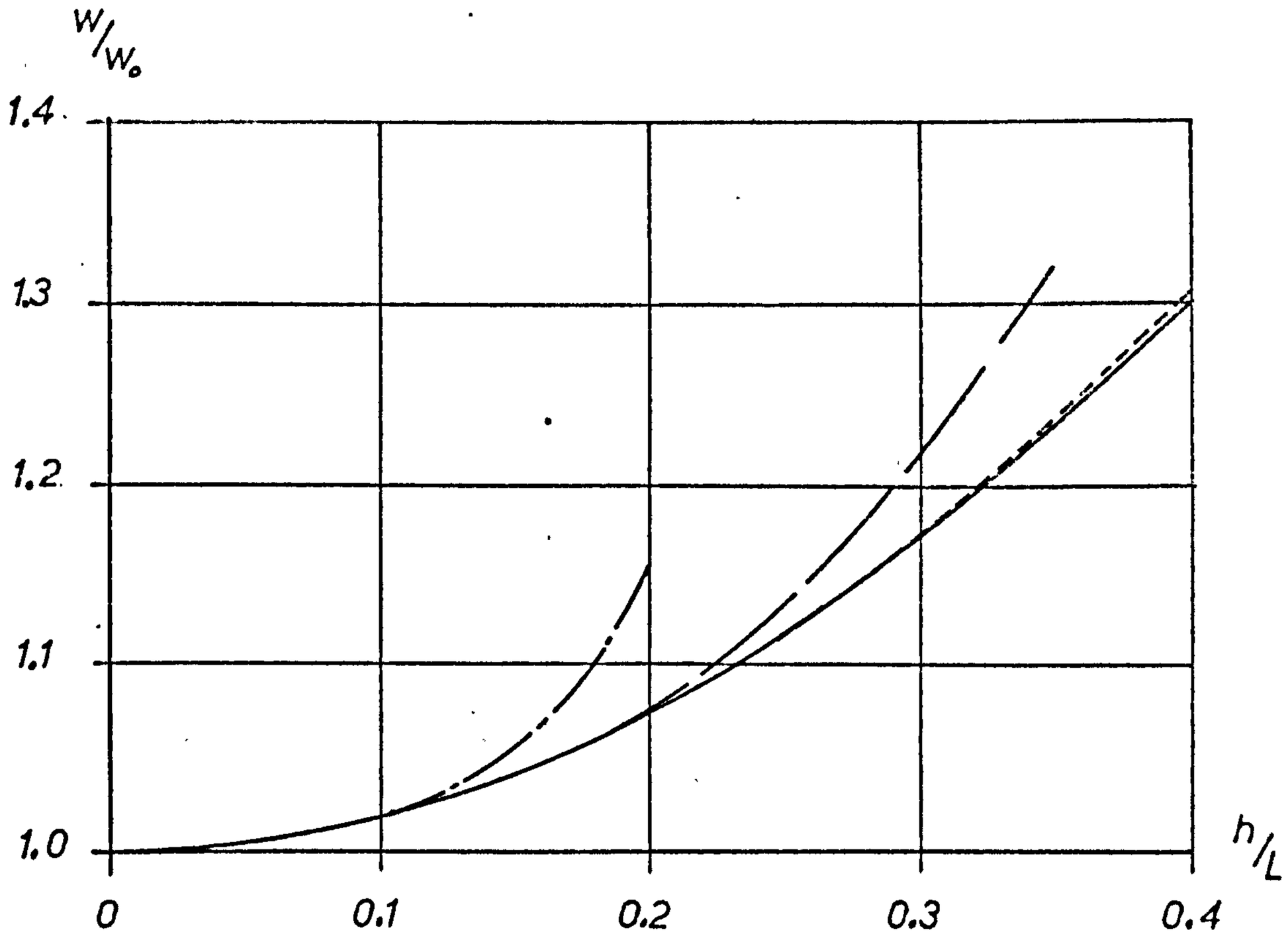

Figure 3.17

Central deflection ratio

Simply supported beam carrying

uniformly distributed load ($\nu = 0$)

Localised Rayleigh-Ritz results - continuity of $\frac{d^3w}{dx^3}$

——————— Theoretical

—— —— U_i contains h^2 terms only

– – – – – – – U_i contains h^2 terms and h^4 terms from M_i

——– —— U_i contains h^2 terms and h^4 terms from M_i and Q_i

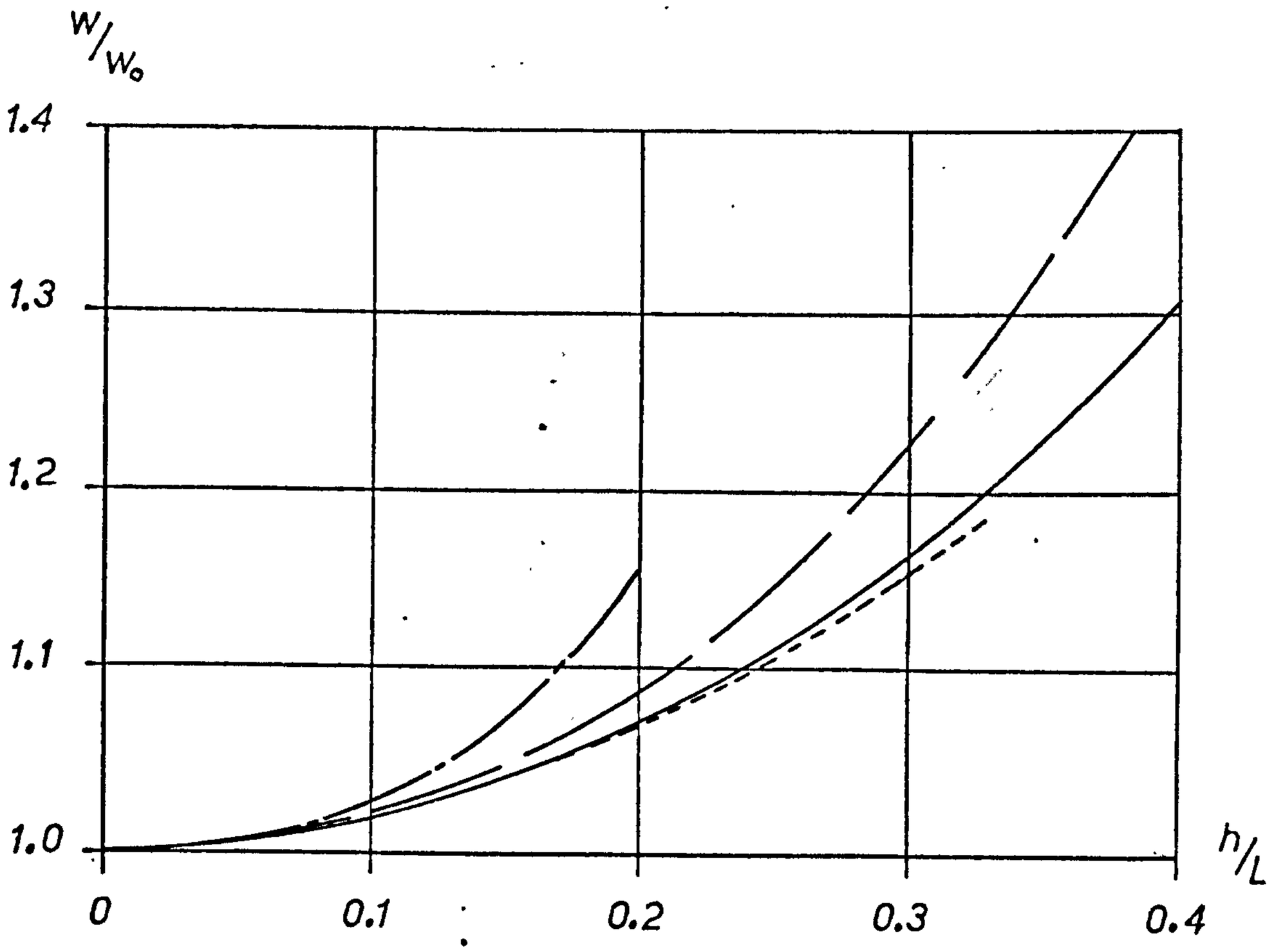

Figure 3.18

Central deflection ratio

Simply supported beam carrying

uniformly distributed load ($\nu = 0$)

Localised Rayleigh-Ritz results - continuity of $\frac{d^4w}{dx^4}$

———— Theoretical

—— —— U_i contains h^2 terms only

- - - - - - - U_i contains h^2 terms and h^4 terms from M_i

——- —— U_i contains h^2 terms and h^4 terms from M_i and Q_i

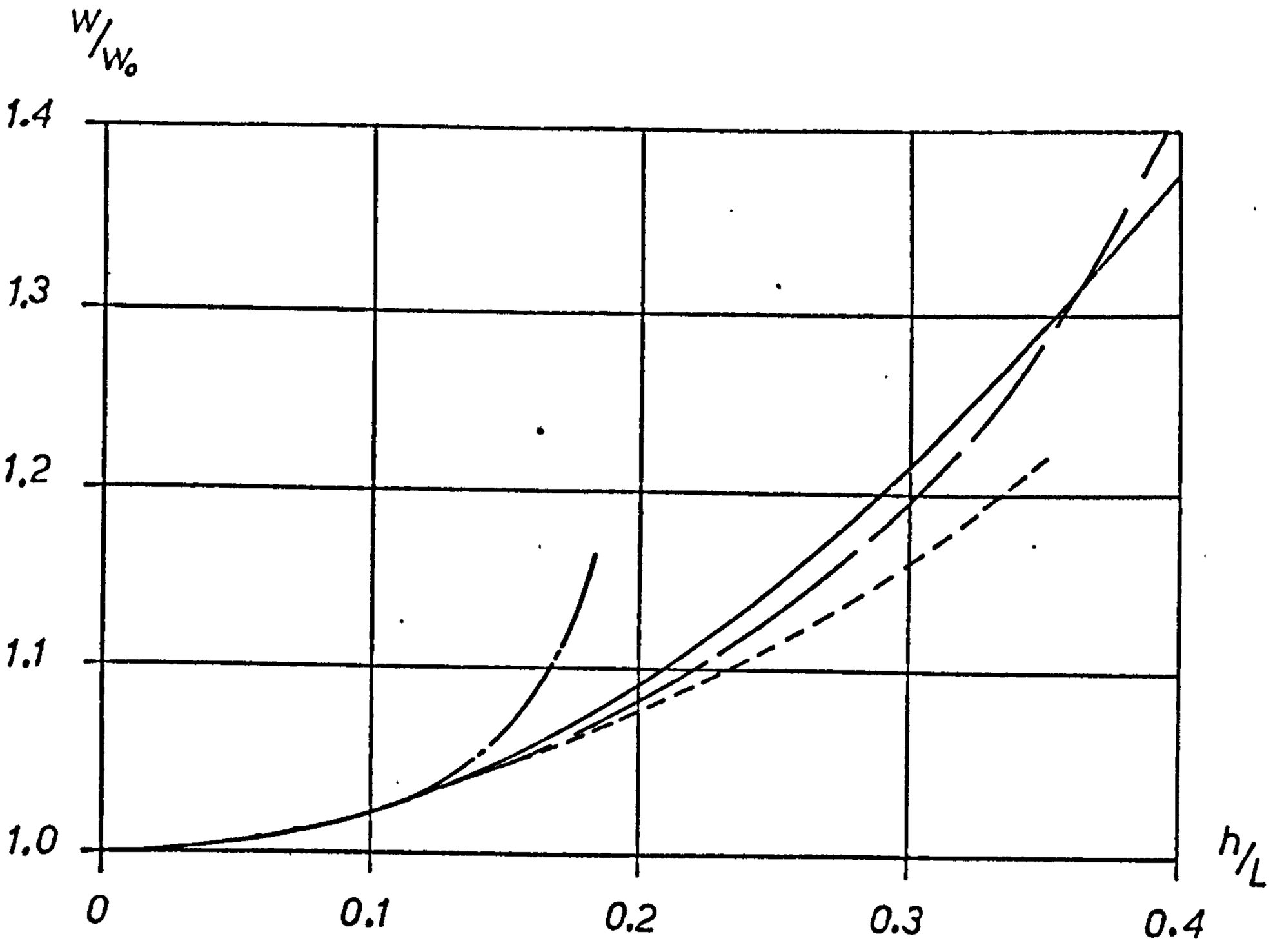

Figure 3.19

Central deflection ratio

Simply supported beam carrying

central point load ($\nu = 0$)

Localised Rayleigh-Ritz results - continuity of $\frac{d^3w}{dx^3}$

———— Theoretical

—— —— U_i contains h^2 terms only

-------- U_i contains h^2 terms and h^4 terms from M_i

——-—— U_i contains h^2 terms and h^4 terms from M_i and Q_i

——--—— U_i contains h^2, h^4 and h^6 terms from M_i and Q_i

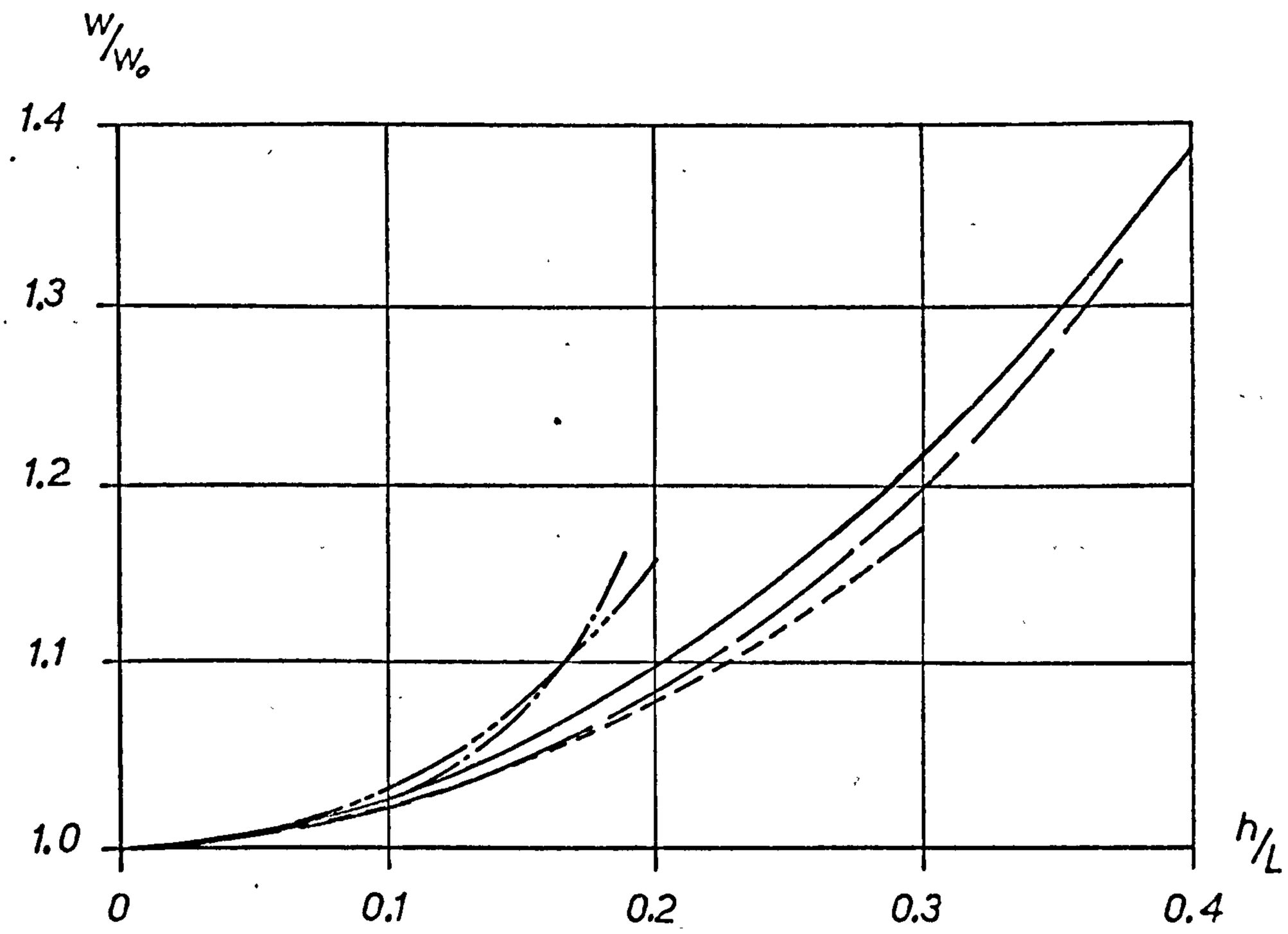

Figure 3.20

Central deflection ratio

Simply supported beam carrying

central point load ($\nu = 0$)

Localised Rayleigh-Ritz results - continuity of $\frac{d^4w}{dx^4}$

Comparison of these two Figures also shows that with continuity of $\frac{d^4w}{dx^4}$ a solution is unobtainable for values of $\frac{h}{l}$ greater than 0.325, so that the use of a higher order of accuracy in the deflection function can be disadvantageous. The reason for this is again numerical. Assuming that the scaling of the matrix [B] is roughly related to the ratio of its greatest to smallest coefficients, this ratio is approximately 13×10^3 for continuity of $\frac{d^4w}{dx^4}$ but only 0.5×10^3 for continuity of $\frac{d^3w}{dx^3}$, indicating that while the former should theoretically give more accurate results, numerically it may have some disadvantages.

In all other cases the results begin to show substantial deviation from theoretical values for ratios of $\frac{h}{l}$ greater than 0.2. In some cases, as can be seen from the termination of the graph at a relatively low value of $\frac{h}{l}$ stable numerical results can only be obtained for a limited range.

A similar pattern of results is seen in Figures 3.19 and 3.20 for a central point load. Taking U_i as given by equation (3.101) does not give such close agreement in this case, however, and the range of values of $\frac{h}{l}$ for which a solution can be obtained is more limited. In fact, closer agreement with theory in this case is obtained by using equation (3.100) for U_i, that is including h^2 terms only.

3.8.3 Conclusions.

From this brief examination of the applicability of numerical methods it is seen that the finite difference approach is excellent for uniformly distributed load, but for concentrated loading will only give results for values of h/l up to 0.2.

On the other hand, by careful selection of the degree of continuity and the terms to be included in the energy function, the localised Rayleigh-Ritz method gives results of reasonable accuracy. It is found that

(a) Continuity to $\frac{d^3w}{dx^3}$ is sufficiently accurate, a higher order of continuity offering no clear advantages, and even introducing its own numerical problems.

(b) Of the possible expressions for U_i, use of that given by equation (3.101) leads to the greatest consistency in the numerical results, while equation (3.100) gives the most accurate results for the point loaded case.

3.9 Experimental tests on beams

3.9.1 Description of tests

Tests were carried out on a series of beams simply supported over a span of 260 mm and carrying a central point load. The depths of the beams ranged from 10 mm to 100 mm in intervals of 10 mm, giving depth/span ratios from 0.0385 to 0.385. Central deflections and mid-span strains on the lower face were measured.

The beams were made from Araldite CY219, a cold setting resin. Square plates 300 mm x 300 mm x 25 mm deep were cast in the mould shown in Plate 1, which were then cut into strips of varying width to give the range of beam specimens required. A vacuum pump was used to extract air entrained during mixing, and after curing the beams were machined flat and square to the required dimensions before testing.

The tests were conducted in a Clockhouse testing machine which delivers the load by screw jacks and can be controlled either manually or by motor. The load was measured by a load cell connected to a digital voltmeter. The load range was 0-800 N with a sensitivity of 1 N.

Displacement measurements were made using a displacement transducer of infinite resolution, and with the associated digital voltmeter enabled displacements to be measured to an accuracy of 0.5×10^{-4} mm.

2 mm foil resistance strain gauges were used to determine the strains, and on two beams rosettes were incorporated so that Poisson's ratio could be found.

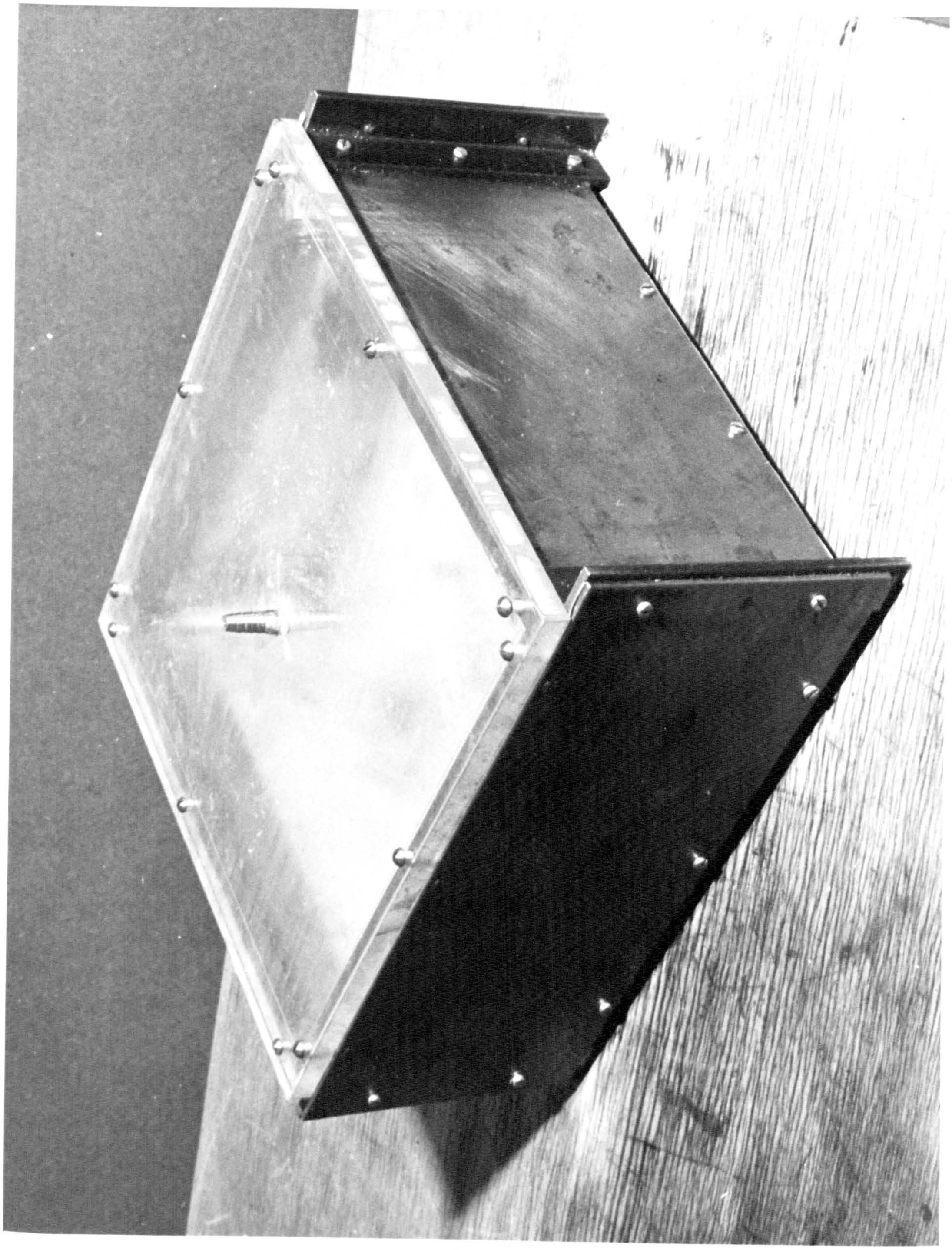

Plate 1

Mould used for casting Araldite test specimens.

(The tapping on the cover is for connection to a vacuum pump)

The test rig used is shown in Plate 2 and Figure 3.21. A rectangular hollow section resting on the bed of the test machine carried two saddles which in turn support the beam on 25 mm diameter rollers. The load was delivered to the beam via a fixed 25 mm diameter roller.

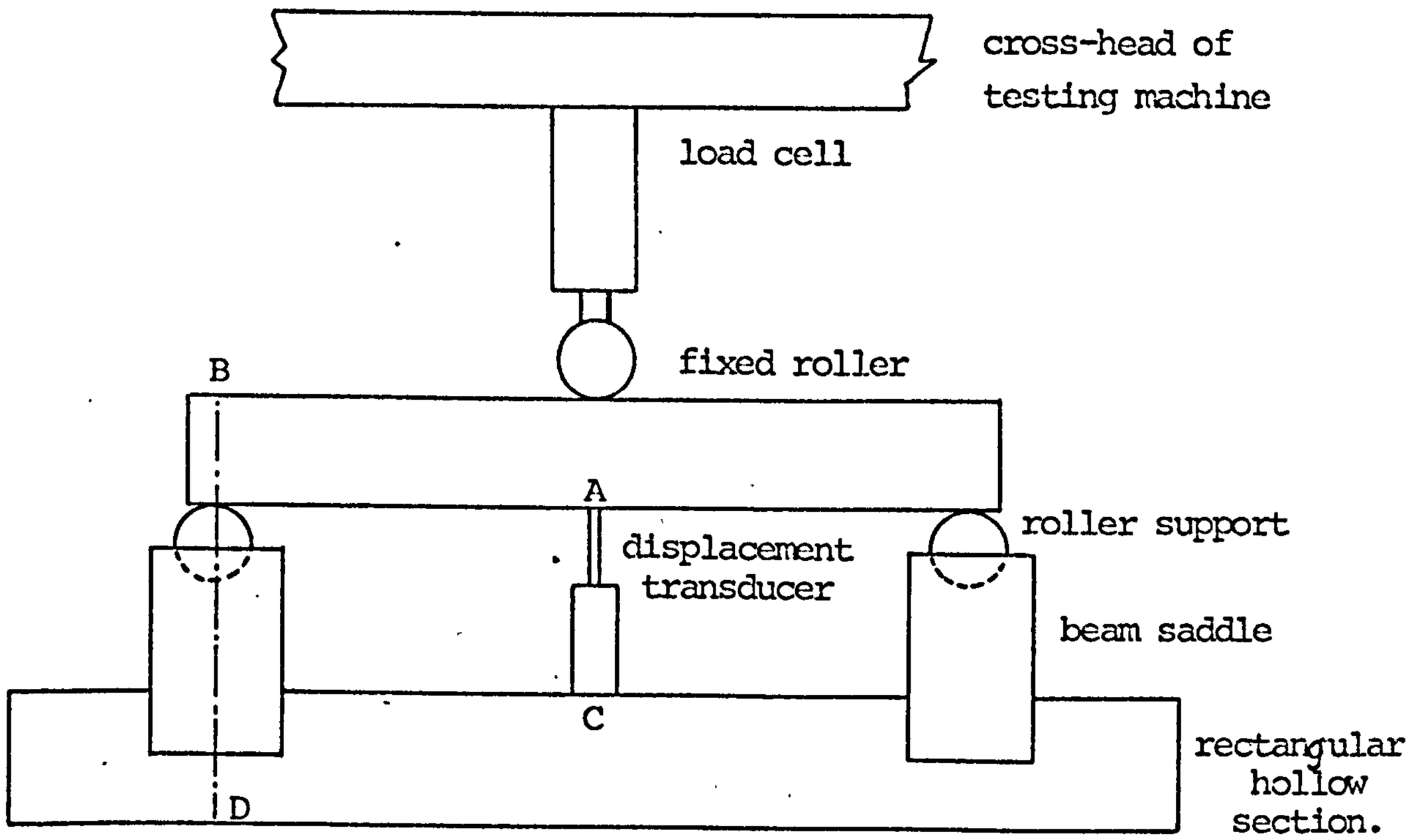

Figure 3.21

Test rig for simply supported beams.

In some of the deeper beams the deflections involved are very small and secondary effects from other movements in the general arrangement of the rig become increasingly significant.

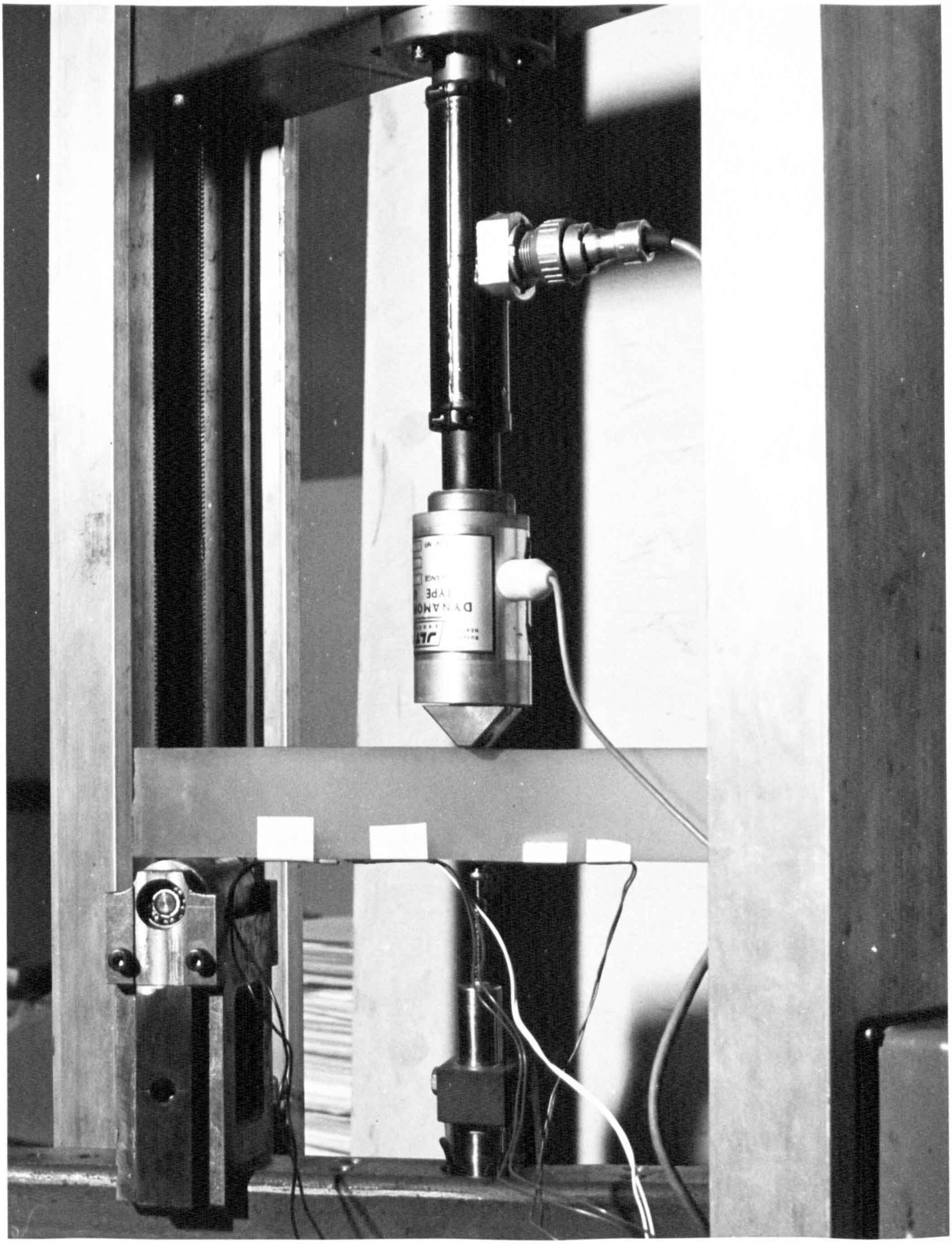

Plate 2

General arrangement for beam tests.

Assessing such effects and making the necessary corrections called for extreme care.

The vertical deflection recorded at point A in Figure 3.21 by a displacement transducer mounted at C contains the following components,

(a) The vertical deflection of the beam

(b) the embedment of the beam on the roller supports

(c) the relative displacement between the saddles and point C (the rectangular hollow section showed a slight tendency to hog under load).

To obtain the true deflection of the beam it is necessary to assess the components (b) and (c) and apply a correction to the actual measurement recorded by the transducer. In order to obtain the embedment the displacement of B relative to D was measured, and measurement of the displacement of C relative D gives the hogging movement of point C.

Pure bending tests were carried out on some of the beams to determine the value of Young's modulus. The arrangement used for these tests is shown diagrammatically in Figure 3.22.

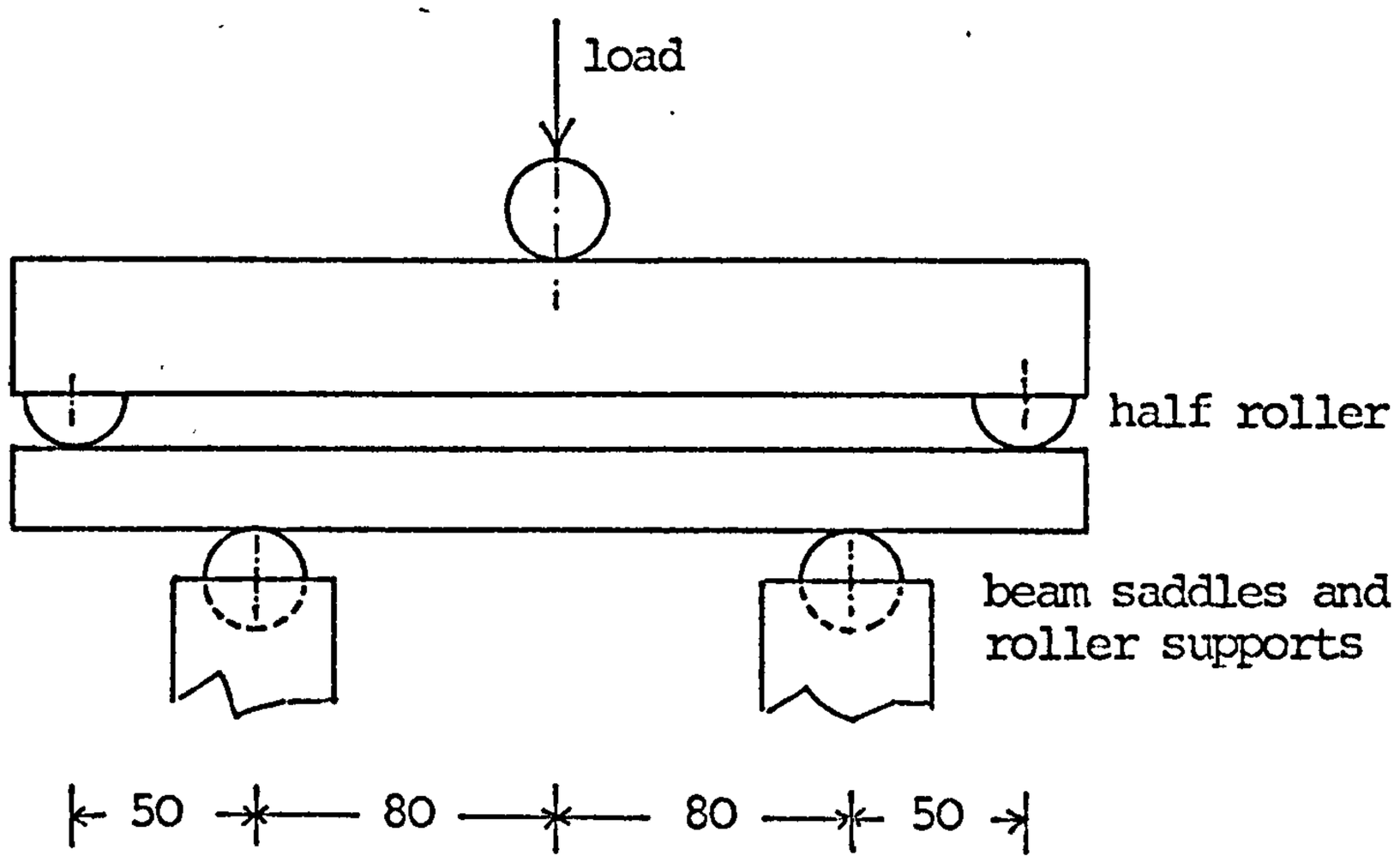

Figure 3.22

General arrangement for pure bending tests.

Lower beam is in a state of pure bending between

the saddle supports.

3.9.2 Experimental results

A summary of the dimensions of the beams, the displacement measurements and corrections is given in Table 3.8.

h (mm) (1)	I (mm⁴) (2)	Displacement per unit load (mm/N)		(5) (2) x (4)	(5) 133
		measured (3)	corrected (4)		
10	1.925×10^{3}	69.1×10^{-3}	69.1×10^{-3}	133	1.0
20	15.92×10^{3}	8.67×10^{-3}	8.65×10^{-3}	138	1.035
30	52.0×10^{3}	2.72×10^{-3}	2.70×10^{-3}	140.5	1.065
40	123.0×10^{3}	1.18×10^{-3}	1.162×10^{-3}	143	1.075
50	240.3×10^{3}	0.64×10^{-3}	0.617×10^{-3}	148.5	1.117
60	418×10^{3}	0.38×10^{-3}	0.358×10^{-3}	150	1.13
70	661×10^{3}	0.27×10^{-3}	0.246×10^{-3}	162.5	1.22
80	991×10^{3}	0.20×10^{-3}	0.174×10^{-3}	172	1.29
90	1401×10^{3}	0.15×10^{-3}	0.125×10^{-3}	175	1.315
100	1920×10^{3}	0.12×10^{-3}	0.097×10^{-3}	187	1.405

Table 3.8

Summary of experimental results for simply supported beam carrying central point load.

From the pure bending tests an average value of $2.7 \times 10^{3} N/mm^{2}$ was obtained for Young's modulus, and 0.38 for Poisson's ratio.

There are two ways in which the experimental results can be compared with the theoretical values. Firstly, for each beam, from a knowledge of Young's modulus and the span, the deflection which would be given by elementary bending theory can be calculated and the present results expressed as a ratio of these. The main disadvantage of this method is that it is highly sensitive to any error in the span measurements.

For example, in the pure bending test an error of 1 mm in each of the four parts of the span would lead to an error of about 6.5% in the value finally obtained for Young's modulus. Setting up supports with a relatively large radius roller to an accuracy of 1 mm is extremely difficult.

An alternative method is used here, in which the actual values of the span and Young's modulus do not need to be known, providing they are constant for all tests, which they are in this case. If w_o is the central deflection predicted by elementary bending theory for a beam of second moment of area I, carrying a central point load P, then for any beam having a material of the same Young's modulus and Poisson's ratio and the same span

$$\frac{w_o I}{P} = k = \text{constant}$$

If w is the deflection measured experimentally then

$$\frac{w}{w_o} = \frac{(W/P)}{(W_o/P)} = \frac{wI}{kP}$$

If it is assumed that for the 10 mm beam the shear deformation has negligible effect on the deflection (it actually accounts for about 0.4% of the total deflection) then for this beam

$$\frac{w}{P} = \frac{w_o}{P} \qquad \text{i.e. } k = \left(\frac{wI}{P}\right)_{10}$$

where the suffix refers to the depth of the beam.

Therefore for any other beam of depth i

$$\frac{w}{w_o} = \frac{\left(\frac{wI}{P}\right)_i}{\left(\frac{wI}{P}\right)_{10}}$$

giving the required ratio of experimental deflection to that given by elementary bending theory, without involving the errors associated with span measurement.

The final column of Table 3.8 and the graph of Figure 3.23 show the results presented in this manner, the experimental results are compared with the theoretical values predicted by equation (3.19). Close agreement is found, all the experimental results lying within 3% of the theoretical values.

Table 3.9 gives a summary of the strain measurements.

h (mm)	Strain per unit load $\mu\epsilon/N$	(Strain per unit load) x h^2
10	62.2	6220
20	14.7	5990
30	6.67	6010
40	3.78	6050
50	2.45	6120
60	1.64	5920
70	1.21	5950
80	0.905	5980
90	0.718	5820
100	0.595	5950

Table 3.9

Strain measurements on the lower face of the beams at mid-span.

For beams of constant span, breadth and Young's modulus, the strain per unit load at mid-span on the lower face will be proportional to $\frac{1}{h^2}$ if the distribution of longitudinal strain is linear.

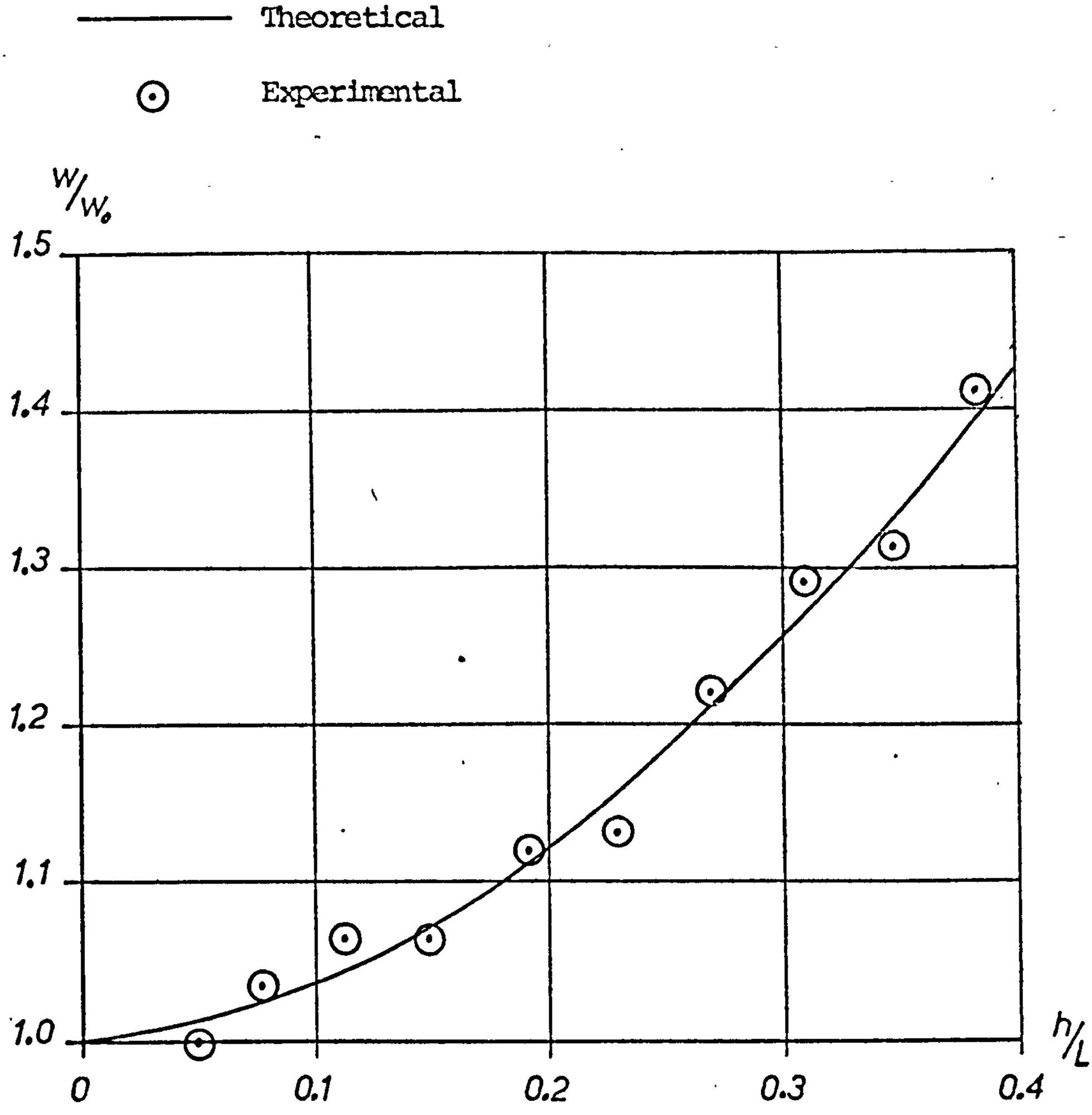

Figure 3.23

Central deflection ratio

Simply supported beam carrying

central point load.

Experimental Results

Although no theoretical results are available for this load case, it was found in Section 3.2.1 that for the uniformly loaded beam longitudinal stress at the extreme fibres was 2.4% greater than a linear distribution would predict when $h/\ell = 0.3$. Obviously a variation of the same order would be expected in the point loaded case considered here, and since this is within the range of normal error of strain gauge work the ratio $h^2(\frac{\epsilon}{P})$ would be expected to be more or less the same for all values of h. This is borne out by the last column of Table 3.9 where values of this ratio are given.

3.10 Conclusions

Detailed discussions and conclusions have been included at the end of the sections dealing with existing work (Section 3.2.4), the new theories developed in this work (Section 3.6) and the application of numerical methods (Section 3.8.3). It merely remains here to summarise the principal conclusions in general terms.

(a) The theories developed here are approximate in that the warping due to shear has been replaced by an average shear distortion. The error introduced by this assumption in the estimation of the overall deflection is found to be insignificant.

(b) Both approaches used here (the partial deflection method and the theories based on Reissner's assumptions) have identical effect in their treatment of deflection due to shear deformation.

(c) Theories based on Reissner's assumptions are shown to deal very adequately with the modification to overall deflection caused by transverse direct stress.

(d) Some changes from the classical distributions of stress resultants occur in certain cases and the theories developed have been shown to be capable of taking these into account.

(e) The modified Reissner theory, developed specifically for later use in connection with plate problems, has been

shown to be fundamentally amenable to solution by finite difference and localised Rayleigh-Ritz methods, although some difficulties have been found to be associated with concentrated loads.

(f) For one load and support case experimental tests have confirmed the theoretical results to within the limits of experimental error.

CHAPTER 4

SHEAR DEFORMATION IN SQUARE PLATES

4.1 Introduction

The assumptions which Reissner made in his plate theory have been outlined in Section 1.2.1, and the limited range of solutions noted in Section 1.2.2. The purpose of this chapter is to develop two further theories, one employing the partial deflection method and the other as a modification to Reissner's theory in the manner adopted for beams in Section 3.5. The possibility of applying numerical methods to these two theories, and to Reissner's theory itself, are then to be investigated.

After a summary of the principal formulae associated with Reissner's theory it is compared with various other theories and approaches. A modification to this theory is presented which is in the form of a sixth order system of partial differential equations in terms of transverse displacement only, so that the use of a stress function is avoided. An application of the method of partial deflections to homogeneous plates is then also developed.

Next these three theories are assessed in relation to each other and some general observations made concerning their respective fundamental theoretical bases.

Numerical methods are then applied to obtain solutions to a range of problems. In one case it is possible to assess the accuracy of these solutions by comparison with an existing series solution to Reissner's theory. The problems associated with the application of numerical methods to each of these three theories are discussed and their potential evaluated on this basis.

A series of experimental tests for one support and loading case is described, which indicates the extent to which the theoretical predictions are verified practically.

4.2 Reissner's theory

The basic assumptions and derivation of Reissner's theory have been summarised in Section 1.2.1, and it is only necessary here to state the principal results.

The shear deformation causes an additional rotation of sections initially normal to the neutral plane, and these sections are also distorted by shear, so that their average rotations are given by

$$\phi_x = -\frac{\partial w}{\partial x} + \frac{12(1+\nu)}{5Eh} Q_x \tag{4.1}$$

$$\phi_y = -\frac{\partial w}{\partial y} + \frac{12(1+\nu)}{5Eh} Q_y \tag{4.2}$$

The bending and twisting moments may then be expressed in terms of these average rotations as,

$$M_x = D\left(\frac{\partial \phi_x}{\partial x} + \nu\frac{\partial \phi_y}{\partial y} + \frac{6\nu(1+\nu)}{5Eh}q\right) \tag{4.3}$$

$$M_y = D\left(\frac{\partial \phi_y}{\partial y} + \nu\frac{\partial \phi_x}{\partial x} + \frac{6\nu(1+\nu)}{5Eh}q\right) \tag{4.4}$$

$$M_{xy} = -\frac{D(1-\nu)}{2}\left(\frac{\partial \phi_x}{\partial y} + \frac{\partial \phi_y}{\partial x}\right) \tag{4.5}$$

These relationships reflect two features of Reissner's theory,

(a) the bending and twisting moments are no longer proportional to neutral surface curvatures and twist, since a part of these is now caused by shear

(b) the final term in equations (4.3) and (4.4) shows that an additional curvature is caused by transverse direct stress.

Substitution of (4.1) and (4.2) in (4.3) - (4.5) and then of the resulting expressions in the plate equilibrium equations (1.11) and (1.12) leads to the following relationships

$$Q_x - \frac{h^2}{10}\Delta Q_x = -D\left(\frac{\partial^3 w}{\partial x^3} + \frac{\partial^3 w}{\partial x \partial y^2}\right) - \frac{h^2}{10(1-\nu)}\frac{\partial q}{\partial x} \tag{4.6}$$

$$Q_y - \frac{h^2}{10}\Delta Q_y = -D\left(\frac{\partial^3 w}{\partial y^3} + \frac{\partial^3 w}{\partial x^2 \partial y}\right) - \frac{h^2}{10(1-\nu)}\frac{\partial q}{\partial y} \tag{4.7}$$

These expressions and the remaining equilibrium equation (1.10) are satisfied by expressing the shear forces in terms of transverse displacement and a stress function as

$$Q_x = -D\left(\frac{\partial^3 w}{\partial x^3} + \frac{\partial^3 w}{\partial x \partial y^2}\right) + \frac{\partial \psi}{\partial y} \tag{4.8}$$

$$Q_y = -D\left(\frac{\partial^3 w}{\partial y^3} + \frac{\partial^3 w}{\partial x^2 \partial y}\right) - \frac{\partial \psi}{\partial x} \tag{4.9}$$

Hence the final expressions for the bending and twisting moments are

$$M_x = -D\left(\frac{\partial^2 w}{\partial x^2} + \nu\frac{\partial^2 w}{\partial y^2}\right) - \frac{h^2 D}{5}\left(\frac{\partial^4 w}{\partial x^4} + \frac{\partial^4 w}{\partial x^2 \partial y^2}\right) + \frac{h^2}{5}\frac{\partial^2 \psi}{\partial x \partial y} - \frac{qh^2}{10}\frac{\nu}{1-\nu} \tag{4.10}$$

$$M_y = -D\left(\frac{\partial^2 w}{\partial y^2} + \nu\frac{\partial^2 w}{\partial x^2}\right) - \frac{h^2 D}{5}\left(\frac{\partial^4 w}{\partial y^4} + \frac{\partial^4 w}{\partial x^2 \partial y^2}\right) + \frac{h^2}{5}\frac{\partial^2 \psi}{\partial x \partial y} - \frac{qh^2}{10}\frac{\nu}{1-\nu} \tag{4.11}$$

$$M_{xy} = (1-\nu)D\frac{\partial^2 w}{\partial x \partial y} + \frac{h^2 D}{5}\left(\frac{\partial^4 w}{\partial x^3 \partial y} + \frac{\partial^4 w}{\partial x \partial y^3}\right) - \frac{h^2}{10}\left(\frac{\partial^2 \psi}{\partial y^2} - \frac{\partial^2 \psi}{\partial x^2}\right) \tag{4.12}$$

The governing equations for the transverse displacement and the stress function are then found to be

$$\Delta^2 w = \frac{q}{D} - \frac{h^2(2-\nu)}{10D(1-\nu)}\Delta q \tag{4.13}$$

and

$$\Delta\psi - \frac{10}{h^2}\psi = 0 \tag{4.14}$$

so that the system of equations is fourth order in w and second order in ψ, that is sixth order overall.

4.3 Comparison with other theories and approaches

4.3.1 Libove and Batdorf (23)

This theory is presented for sandwich plates in terms of flexural and shear stiffnesses; curvature due to shear is included, but not that due to transverse direct stress in line with the normal sandwich plate assumption of transverse incompressibility of the core. Bending and shear stiffnesses, D_n and S_n respectively, are defined as

$$D_n = -M_n / \frac{\partial^2 w}{\partial n^2} \qquad \text{when } M_n \text{ acts alone}$$

$$S_n = Q_n / \gamma_n \qquad \text{when } Q_n \text{ acts alone}$$

where, in the original application to sandwich plates γ_n is the mid-plane slope $\partial w / \partial n$. The resulting expressions for moments and shears are not given in a form which can be directly compared with Reissner's equations, but both sets can be reduced to a common format as shown in Table 4.1.

If Libove and Batdorf's theory were to be applied to homogeneous plates an appropriate value for the shear stiffness, S, would have to be chosen. Clearly the normal sandwich plate assumptions would not be valid and a value of S related to neutral-plane slope alone could not therefore be used. If an average rotation of the Reissner type is chosen so that the shear strain energy produced by the shear force acting through the average rotation is the same as that produced by the actual distributions of shear stress and shear strain then

$$S = \frac{5Eh}{12(1+\nu)} \qquad (4.25)$$

On this basis the ratio of bending stiffness to shear stiffness is

Equations for stress resultants derived from Libove and Batdorf

$$M_x = -D\left(\frac{\partial^2 w}{\partial x^2} + \nu\frac{\partial^2 w}{\partial y^2}\right) + \frac{D}{S}\left(\frac{\partial Q_x}{\partial x} + \nu\frac{\partial Q_y}{\partial y}\right) \tag{4.15}$$

$$M_y = -D\left(\frac{\partial^2 w}{\partial y^2} + \nu\frac{\partial^2 w}{\partial x^2}\right) + \frac{D}{S}\left(\frac{\partial Q_y}{\partial y} + \nu\frac{\partial Q_x}{\partial x}\right) \tag{4.16}$$

$$M_{xy} = D(1-\nu)\frac{\partial^2 w}{\partial x \partial y} - \frac{D(1-\nu)}{2S}\left(\frac{\partial Q_x}{\partial y} + \frac{\partial Q_y}{\partial x}\right) \tag{4.17}$$

$$Q_x = -D\left(\frac{\partial^3 w}{\partial x^3} + \frac{\partial^3 w}{\partial x \partial y^2}\right) + \frac{D}{2S}\left(2\frac{\partial^2 Q_x}{\partial x^2} + (1-\nu)\frac{\partial^2 Q_x}{\partial y^2} + (1+\nu)\frac{\partial^2 Q_y}{\partial x \partial y}\right) \tag{4.18}$$

$$Q_y = -D\left(\frac{\partial^3 w}{\partial y^3} + \frac{\partial^3 w}{\partial x^2 \partial y}\right) + \frac{D}{2S}\left(2\frac{\partial^2 Q_y}{\partial y^2} + (1-\nu)\frac{\partial^2 Q_y}{\partial x^2} + (1+\nu)\frac{\partial^2 Q_x}{\partial x \partial y}\right) \tag{4.19}$$

Equations for stress resultants derived from Reissner.

$$M_x = -D\left(\frac{\partial^2 w}{\partial x^2} + \nu\frac{\partial^2 w}{\partial y^2}\right) + \frac{h^2}{5(1-\nu)}\left(\frac{\partial Q_x}{\partial x} + \nu\frac{\partial Q_y}{\partial y}\right) + \frac{\nu h^2 q}{10(1-\nu)} \tag{4.20}$$

$$M_y = -D\left(\frac{\partial^2 w}{\partial y^2} + \nu\frac{\partial^2 w}{\partial x^2}\right) + \frac{h^2}{5(1-\nu)}\left(\frac{\partial Q_y}{\partial y} + \nu\frac{\partial Q_x}{\partial x}\right) + \frac{\nu h^2 q}{10(1-\nu)} \tag{4.21}$$

$$M_{xy} = (1-\nu)\,D\frac{\partial^2 w}{\partial x \partial y} - \frac{h^2}{10}\left(\frac{\partial Q_x}{\partial y} + \frac{\partial Q_y}{\partial x}\right) \tag{4.22}$$

$$Q_x = -D\left(\frac{\partial^3 w}{\partial x^3} + \frac{\partial^3 w}{\partial x \partial y^2}\right) + \frac{h^2}{10(1-\nu)}\left(2\frac{\partial^2 Q_x}{\partial x^2} + (1-\nu)\frac{\partial^2 Q_x}{\partial y^2} + (1+\nu)\frac{\partial^2 Q_y}{\partial x \partial y}\right) + \frac{\nu h^2}{10(1-\nu)}\frac{\partial q}{\partial x} \tag{4.23}$$

$$Q_y = -D\left(\frac{\partial^3 w}{\partial y^3} + \frac{\partial^3 w}{\partial x^2 \partial y}\right) + \frac{h^2}{10(1-\nu)}\left(2\frac{\partial^2 Q_y}{\partial y^2} + (1-\nu)\frac{\partial^2 Q_y}{\partial x^2} + (1+\nu)\frac{\partial^2 Q_x}{\partial x \partial y}\right) + \frac{\nu h^2}{10(1-\nu)}\frac{\partial q}{\partial y} \tag{4.24}$$

Table 4.1 Comparison of stress resultants derived from Libove and Batdorf and Reissner.

$$\frac{D}{S} = \frac{h^2}{5(1 - \nu)} \tag{4.26}$$

The two sets of equations in Table 4.1 can now be compared using this value for the ratio D/S and the following points noted:

(a) the expressions for the bending moments M_x and M_y as given by the two theories are the same except for an additional term $\frac{\nu h^2 q}{10(1 - \nu)}$ in the Reissner equations.

(b) the expressions for the twisting moment M_{xy} are identical

(c) the expressions for the shear forces Q_x and Q_y are the same except for an additional term $\frac{\nu h^2}{10(1 - \nu)} \frac{\partial q}{\partial x}$ in the Reissner equations.

If the origin of these additional terms in the Reissner equations is traced it becomes clear that these are due solely to the inclusion of transverse direct stress, and that the two theories are the same in the modification resulting from consideration of transverse shear. The difference in the equations for shear forces would in any case vanish in the case of uniform loading.

4.3.2 Ambartsumyan (19)

As mentioned in Section 1.2.3.4 the assumptions and results of the general theory are identical to those of Reissner with the effects of transverse direct stress omitted. For example, it can easily be shown that Ambartsumyan's equations for bending and twisting moments are identical with those derived from Libove and Batdorf's equations, (4.15) - (4.17), which, as has just been demonstrated, are those which would result from Reissner's theory if the σ_z terms are omitted. Further it may be shown that the three equations of equilibrium are the same as those of Libove and Batdorf.

In the particular theory, when the effects of transverse direct stress are included, Ambartsumyan himself shows that his results are identical with those of Reissner.

In one case of the general theory the consequence of selecting a fourth order rather than parabolic distribution of shear stress is examined and found to make an almost negligible difference to the values of deflection obtained.

4.3.3 Love (13)

In his theory for moderately thick plates, derived initially for plane stress problems, Love includes the deformation due to shear, but the resulting expressions for the shear forces are the usual classical form, and hence the governing equation for deflection is the normal biharmonic. The equations for bending and twisting moments are, however, modified by the consideration of shear, and the resulting expressions are in terms of transverse displacement alone.

4.3.4 Finite element approaches

4.3.4.1 Clough and Felippa (30)

One approach which has been used for the inclusion of shear deformation in the finite element solution of plate bending problems is based on the usual 12 term polynomial which gives three degrees of freedom at each node. An example of this approach is that of Clough and Felippa, but from the discussions to references (31) and (24) it is evident that very similar methods have been used elsewhere.

The general technique is to maintain continuity of transverse displacement and rotation of a plane initially normal to the neutral surface at the interface between elements. In Reissner terms this is equivalent to the three degrees of freedom at a node being w, ϕ_x, and ϕ_y. This means that there is a discontinuity in the slope of the neutral surface between elements, so that a typical element interface would be as shown in Figure 4.2. Further, only two conditions can be satisfied at each boundary.

Figure 4.2

Continuity conditions between elements. (Clough and Felippa)

No extensive numerical results are given, but for a simply supported square homogeneous plate with a thickness equal to 1/10 of the span increases in deflection due to shear distortion are reported of 10% for a uniformly distributed load

and 294% for a concentrated load at the centre. It may be noted in passing that the first of these figures is approximately twice the increase which series solutions to Reissner's theory predict, while the second would appear to be out of all proportion. No comment is made about this value, but it could be due to a serious overestimate of the deformation local to the concentrated load, or to ill-behaviour of the system of equations which was not detected.

In the discussions to references (31) and (24) various writers have described how this general method has been applied to sandwich plates, and close agreement with series solutions is reported for a range of shear stiffnesses. Their results, however, only cover uniform loading and thus do not shed any light on the strange result obtained by Clough and Felippa for concentrated loading.

4.3.4.2 Pryor, Barker and Frederick (32)

Reissner's theory is used in this case with two simplifications:

(a) terms arising from transverse direct stress are omitted

(b) plane sections are assumed to remain plane after bending, so that shear distortion is prevented and the rotations ϕ_x, ϕ_y of planes initially normal to the neutral surface are actual and not average values. However, average shear strains are taken in calculating ϕ although the basis for averaging is not stated, and so the net effect may in the end be the same as taking average rotations.

Two additional degrees of freedom are permitted at each mesh point, namely $\bar{\gamma}_x$ and $\bar{\gamma}_y$, the average shear strains, giving 5 degrees of freedom in all, w, ϕ_x, ϕ_y, $\bar{\gamma}_x$, $\bar{\gamma}_y$. The usual 12 term polynomial is deemed to be adequate and this results in linear variations of γ_x and γ_y in the x and y directions so that continuity of these terms is achieved along the element interfaces, while ϕ_x and ϕ_y are continuous only at the mesh points.

Results for the central deflection of a simply supported plate carrying a uniformly distributed load are compared with those obtained by Salerno and Goldberg in a series solution (6), and close agreement is found for values of thickness ratio h/l up to 0.25. Care should be taken in comparing the two sets of results, however, since the series solution contains the effects of transverse direct stress while the finite element solution omits them. This would be unimportant for small values of Poisson's ratio but Pryor, Barker and Frederick's results appear to be for a value of 0.3, and omitting the effects of σ_z in this case should lead to deflections which are greater than Salerno and Goldberg's by up to about 5%, whereas they are actually slightly smaller.

In the cases of a concentrated load there is no basis for comparison for values of h/l in excess of 0.1. Up to this value the deflections are considerably in excess of those found by Smith (36), who argues in the discussion that the author's solution overestimates the true deflection for this loading case due to incompatibility of the elements.

4.3.4.3 Smith (33)

Smith has developed a finite element method based on Love's theory which is notable for the fact that it uses seventh order displacement functions and 10 generalised displacements per node

$$w,\ \frac{\partial w}{\partial x},\ \frac{\partial w}{\partial y},\ \frac{\partial^2 w}{\partial x^2},\ \frac{\partial^2 w}{\partial x \partial y},\ \frac{\partial^2 w}{\partial y^2},\ \frac{\partial^3 w}{\partial x^3},\ \frac{\partial^3 w}{\partial x^2 \partial y},\ \frac{\partial^3 w}{\partial x \partial y^2},\ \frac{\partial^3 w}{\partial y^3}$$

For a plate with a thickness ratio h/l of 0.1 the following increases in deflection over those given by classical theory are found,

simply supported	uniform load	3.5%
	central point load	4.0%
clamped	uniform load	8.5%
	central point load	7.0%

Referring to his own results in the discussion of reference (32) Smith regards his deflections due to point loads as being underestimates of the true values.

4.3.5 Conclusions

A wide range of theories and approaches for the inclusion of shear deformation in plate problems has been proposed, some of which have been discussed here. Although it is not possible to classify them in a systematic manner some useful observations can be made:

(a) None of the approaches considered offers any fundamental improvement on Reissner's theory, which must therefore still be regarded as the best of its type available from a theoretical point of view.

(b) From the standpoint of shear deformation alone the Libove and Batdorf approach of curvature superposition can lead to the same formulae as Reissner if an appropriate shear stiffness is chosen.

(c) Among the finite element solutions some considerable variations occur in the results for deflections, especially for concentrated load.

4.4 A modification to Reissner's theory

As has been mentioned before the usual formulation of Reissner's theory in terms of transverse displacement and stress function imposes a number of difficulties in obtaining a solution. Hence a modification to Reissner's theory has been developed which is expressed in terms of transverse displacement alone.

The basis of this modification is to include in the various equations and relationships only those terms which are independent of the plate thickness, h, or of order h^2; all terms containing higher powers of h are excluded. If equations (4. 6) and (4. 7) are differentiated to form expressions for ΔQ_x and ΔQ_y and these are substituted back into (4.6) and (4.7) and terms in h^4 and higher powers omitted, then the new expressions for shear forces become

$$Q_x = -D\left(\frac{\partial^3 w}{\partial x^3} + \frac{\partial^3 w}{\partial x \partial y^2}\right) - \frac{h^2(2-\nu)}{10(1-\nu)} D \left(\frac{\partial^5 w}{\partial x^5} + 2\frac{\partial^5 w}{\partial x^3 \partial y^2} + \frac{\partial^5 w}{\partial x \partial y^4}\right) \quad (4.27)$$

$$Q_y = -D\left(\frac{\partial^3 w}{\partial y^3} + \frac{\partial^3 w}{\partial x^2 \partial y}\right) - \frac{h^2(2-\nu)}{10(1-\nu)} D \left(\frac{\partial^5 w}{\partial y^5} + 2\frac{\partial^5 w}{\partial x^2 \partial y^3} + \frac{\partial^5 w}{\partial x^4 \partial y}\right) \quad (4.28)$$

Substituting these relationships for shear forces in equations (4.3) - (4.5), noting (1.10), (4.1) and (4.2) and again omitting terms in h^4 and higher degrees, the following expressions for bending and twisting moments result,

$$M_x = -D\left(\frac{\partial^2 w}{\partial x^2} + \nu\frac{\partial^2 w}{\partial y^2}\right) - \frac{h^2 D}{10(1-\nu)}\left((2-\nu)\frac{\partial^4 w}{\partial x^4} + 2\frac{\partial^4 w}{\partial x^2 \partial y^2} + \nu\frac{\partial^4 w}{\partial y^4}\right) \quad (4.29)$$

$$M_y = -D\left(\frac{\partial^2 w}{\partial y^2} + \nu\frac{\partial^2 w}{\partial x^2}\right) - \frac{h^2 D}{10(1-\nu)}\left((2-\nu)\frac{\partial^4 w}{\partial y^4} + 2\frac{\partial^4 w}{\partial x^2 \partial y^2} + \nu\frac{\partial^4 w}{\partial x^4}\right) \quad (4.30)$$

$$M_{xy} = (1-\nu)D\frac{\partial^2 w}{\partial x \partial y} + \frac{h^2 D}{5}\left(\frac{\partial^4 w}{\partial x^3 \partial y} + \frac{\partial^4 w}{\partial x \partial y^3}\right) \quad (4.31)$$

The sixth order governing equation for w is found by substituting (4.27) and (4.28) in (1.10) and is

$$\Delta^2 w + \frac{h^2(2 - \nu)}{10(1 - \nu)} \Delta^3 w = \frac{q}{D} \tag{4.32}$$

The main part of this work is limited to a consideration of homogeneous plates, as is the original statement of Reissner's theory, but a development of the above modification in an anisotropic form is given in Appendix B.

4.5 Solution by the method of partial deflections

The basis of this method has been outlined in relation to beams in Section 3.3. The process can easily be extended to the study of plate problems, and the fundamental relationships for displacements in stress resultants are:

$$w = w_b + w_s \tag{4.33}$$

$$M_x = -D\left(\frac{\partial^2 w_b}{\partial x^2} + \nu \frac{\partial^2 w_b}{\partial y^2}\right) \tag{4.34}$$

$$M_y = -D\left(\frac{\partial^2 w_b}{\partial y^2} + \nu \frac{\partial^2 w_b}{\partial x^2}\right) \tag{4.35}$$

$$M_{xy} = (1 - \nu) D \frac{\partial^2 w_b}{\partial x \partial y} \tag{4.36}$$

$$Q_x = S \frac{\partial w_s}{\partial x} \tag{4.37}$$

$$Q_y = S \frac{\partial w_s}{\partial y} \tag{4.38}$$

Combining the equilibrium equations (1.11) and (1.12) and noting (1.10) leads to

$$\frac{\partial^2 M_x}{\partial x^2} + \frac{\partial^2 M_y}{\partial y^2} - 2 \frac{\partial^2 M_{xy}}{\partial x \partial y} = -q \tag{4.39}$$

Substituting from (4.34) - (4.36) leads to the usual biharmonic equation

$$\Delta^2 w_b = \frac{q}{D} \tag{4.40}$$

which is in terms of the partial deflection w_b rather than the overall deflection.

There are now two possible approaches. The first amounts to a simple superposition of deflections due to bending and shear, w_b and w_s having their own separate governing equations and boundary conditions. The governing equation for w_s is found by substituting for Q_x and Q_y from equations (4.37) and (4.38) in (1.10) giving

$$\Delta w_s = -\frac{q}{S} \tag{4.41}$$

and it follows from (4.40) and (4.41) that the relationship between w_b and w_s may be expressed as

$$\Delta w_s = -\frac{D}{S}\Delta^2 w_b \tag{4.42}$$

or

$$w_s = -\frac{D}{S}\Delta w_b + C \tag{4.43}$$

where C is an arbitrary constant. This gives rise to the second approach in which the governing equation is written for w_b only, the boundary equations are written in terms of w_b and w_s together, and w_s defined by equation (4.43). In this case w_s will automatically take its boundary conditions from those set for w_b.

Obviously the superposition approach can only be used when the boundary conditions imposed for w_s coincide with those implied by equation (4.43), otherwise the boundary values of moments and shears will not satisfy the equilibrium requirements of equations (1.11) and (1.12). The only type of boundary for which this approach is valid is a simply supported case, where $\Delta w_b = 0$ and hence from (4.43) w_s is constant along the boundary. This results in $Q_t = 0$ being the implied boundary condition and is compatible with w_s being set arbitrarily equal to zero.

The solution is therefore a simple superposition of the separately assessed deflections due to bending and shear, with both vanishing independently at the boundary and the boundary conditions amounting to $w = M_n = \phi_t = 0$.

By contrast, at a clamped boundary $\Delta w_b \neq 0$ and so w_s will not be constant and hence w_b and w_s cannot separately vanish but only their sum is zero.

The use of numerical techniques in applying this method to the solution of plate problems will be discussed in the following sections, where the shear stiffness will be defined by

$$S = \frac{5Gh}{6}$$

for the reasons already discussed in the application to beams.

4.6 Discussion and conclusions

The place of the modified Reissner theory and the partial deflection method can now be discussed in relation to Reissner's theory. From the above the following points emerge:

(a) The form of Reissner's equations indicates that, in essence, it results in a superposition of curvatures due to bending, shear and transverse direct stress to give the total curvature at any point. The modified Reissner theory will therefore be the same in concept.

(b) The partial deflection method for simply supported boundaries amounts to a simple superposition of deflections due to bending and shear, but in other cases w_b and w_s cannot be given this simple physical interpretation, and then they do not vanish separately at a rigid boundary.

(c) The Reissner, modified Reissner and partial deflection theories are the same in their treatment of shear deformation, since the first two take an average rotation of a section initially normal to the neutral surface, thereby averaging out the distortion due to shear, while the partial deflection method takes an overall shear stiffness which defines an average shear strain through the depth of the section, and hence the same net average rotation.

(c) The Reissner and modified Reissner theories, being sixth order systems, enable three conditions to be satisfied at each boundary, while in cases where w_b and w_s cannot

be considered independently the partial deflection method permits only two. In certain circumstances this will lead to differences in the results, and the extent of these remains to be assessed.

(e) Therefore, from a theoretical point of view, differences in results given by these three theories can arise only from the omission of transverse direct stress in the partial deflection method and from differences in the statement of boundary conditions. Other discrepancies which may occur in the numerical results can only be due to computational factors.

4.7 Boundary conditions

Where a sixth order system of equations is under consideration three boundary conditions must be satisfied at any boundary. Three support cases must be considered:

(a) Free edge

A free edge must be stress free at all points and will therefore require as boundary conditions zero normal and twisting moments and zero normal shear, that is

$$M_n = M_{nt} = Q_n = 0 \tag{4.44}$$

Thus the Kelvin-Tait combination of M_{nt} and Q_n into a single total shear V_n ($= Q_n - \frac{\partial M_{nt}}{\partial t}$) is no longer necessary and each will be separately set equal to zero.

(b) Simply supported edge

In classical theory two boundary conditions are imposed, namely zero transverse displacement and zero normal moment,

$$w = M_n = 0 \tag{4.45}$$

For the third boundary condition, either the tangential edge rotation, ϕ_t, or the twisting moment, M_{nt}, is set equal to zero.

Timoshenko (1) conceives a simple support as a knife edge of the type shown in Figure 4.1.

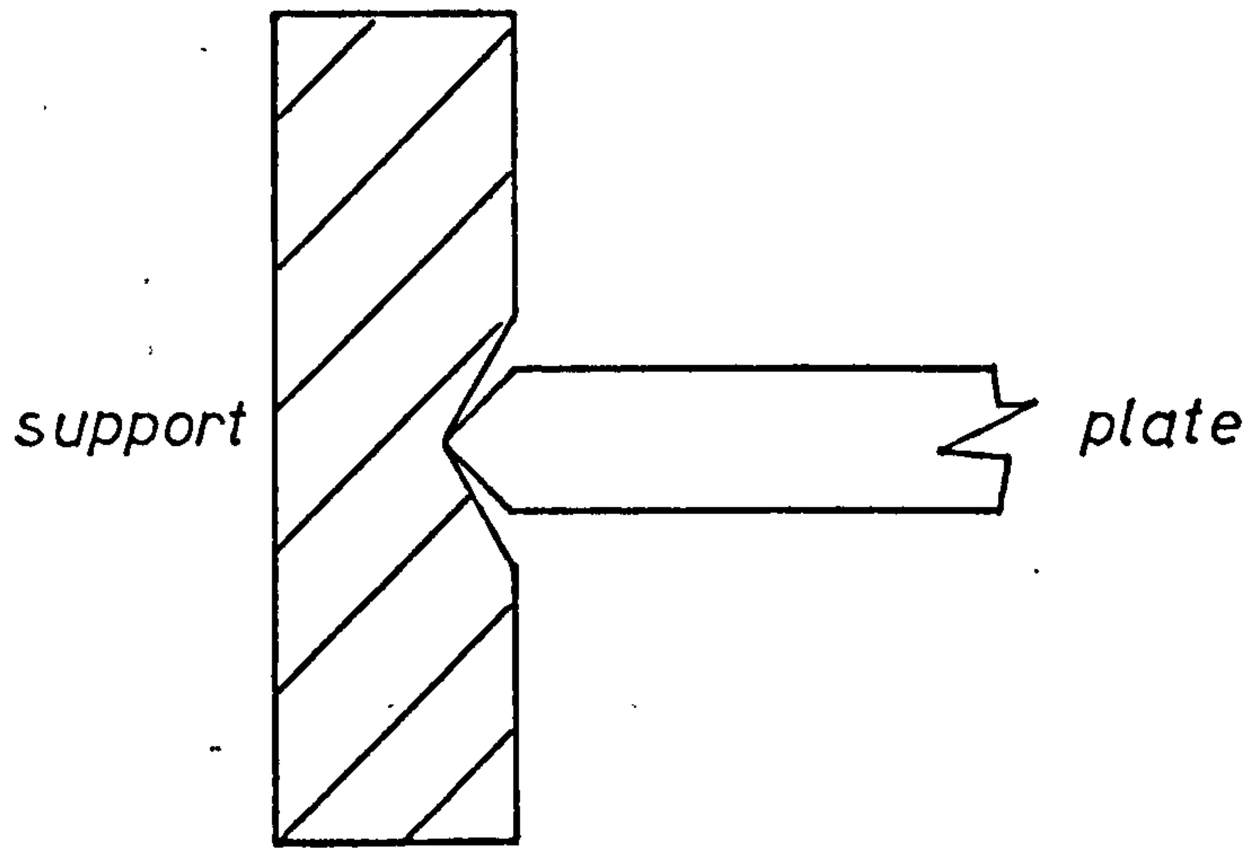

Figure 4.1

Action of a simple support.

Such a support clearly prevents rotation of an initially vertical tangent about an axis perpendicular to the edge plane, that is

$$\phi_t = 0 \tag{4.46}$$

Now in Reissner's theory this would be identical to the average rotation defined as

$$\phi_t = -\frac{\partial w}{\partial t} + \frac{12(1+\nu)}{5Eh} Q_t \tag{4.47}$$

and as the first term is zero at a simply supported edge then Q_t will also be zero. In fact this condition is automatically satisfied in classical theory, since Q_t is given by

$$Q_t = -D\left(\frac{\partial^3 w}{\partial t^3} + \frac{\partial^3 w}{\partial n^2 \partial t}\right) \tag{4.48}$$

and both the derivatives are zero along the boundary, the first because w is zero and the second because the normal moment is zero, requiring $\partial^2 w/\partial n^2$ to be zero. In theories in which shear deformation is included, however, $\phi = 0$ is valid as a third independent boundary condition because

the bending moment is no longer proportional to curvature.

This type of support generates twisting moments, M_{nt}, along the boundary, and analysis using classical theory also predicts such forces. Equilibrium is achieved only by applying corner reactions.

Thus as an alternative third boundary condition, the twisting moment can be set equal to zero,

$$M_{nt} = 0 \tag{4.49}$$

It is difficult to visualise a physical support which would produce this set of boundary conditions since the only stresses it may generate are vertical shear stresses, and yet tangential rotation of initially vertical filaments must be permitted.

It seems unlikely that any practical simple support could be properly described by either of two possible sets of theoretical boundary conditions described.

(c) Fixed edge.

A fixed edge will prevent transverse displacement and rotation of a vertical tangent about both normal and tangential axes. Thus the boundary conditions are

$$w = \phi_n = \phi_t = 0 \tag{4.50}$$

In using Reissner type theories the rotations are average rotations, that is, distortion of tangents initially normal to the neutral plane may still occur, but in

such a way that the average rotations resulting are zero. As has already been observed in dealing with circular plates and beams (see Section 2.3.2.1 and 3.2.2) rotation of the neutral plane is not prevented by fixed supports, that is $\partial w / \partial n \neq 0$.

4.8 Finite difference solutions

In this section techniques will be used to find solutions to square plate problems based on the partial deflection method, Reissner's theory and the modified Reissner theory. The mesh size used is 12 x 12 in all cases, and for dealing with symmetric loading and support conditions only a triangular portion forming 1/8 of the plate need be considered, as indicated in Figure 4.2.

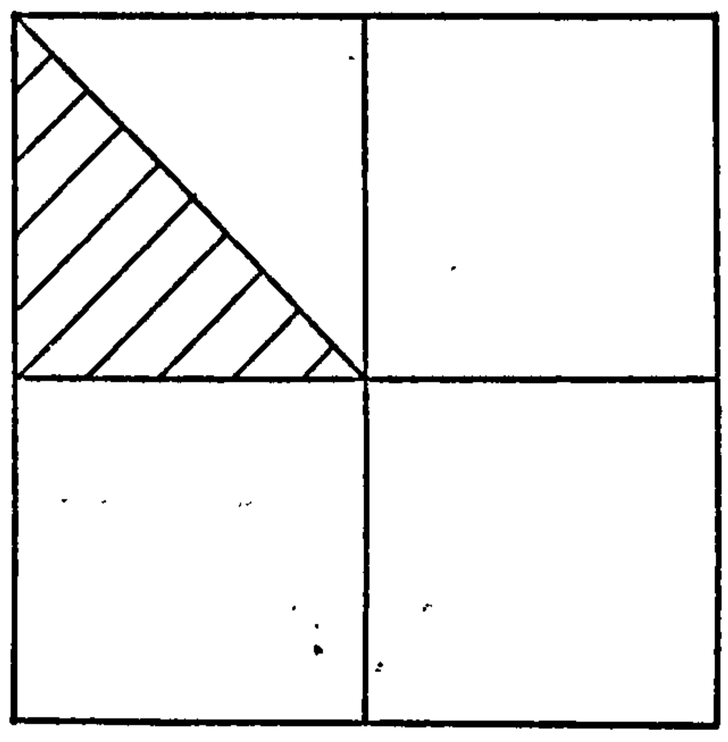

Figure 4.2

1/8 plate used for finite difference analysis of symmetrically loaded and supported square plates.

Gaussian elimination was used for solving the resulting system of equations in each case, the details of which are discussed in Appendix E.

4.8.1 Application of finite differences to the partial deflection method

The equations to be used are shown in non-dimensional finite difference form in Figures 4.3 - 4.6. A square mesh of

non-dimensional mesh length P (= p/ℓ = 1/12), and the normal central difference formulae are used.

Since this solution is in terms of two variables, w_b and w_s, there will be two unknowns at each real mesh point. As the highest order derivatives of w_b and w_s involved are 4th and 2nd respectively, using the normal central difference formulation will involve values of w_b at fictitious mesh points up to two mesh lengths outside the 1/8 plate region, but values of w_s at only one mesh length away. The term 'fictitious' is used to mean external to the 1/8 plate region being considered; some such mesh points lie within the boundary of the complete plate and are therefore not fictitious in the normal sense. This is illustrated in the scheme of mesh points shown in Figure 4.7, from which it may be seen that 126 unknowns are involved.

The equations to be solved for simple supports are summarised in Table 4.2.

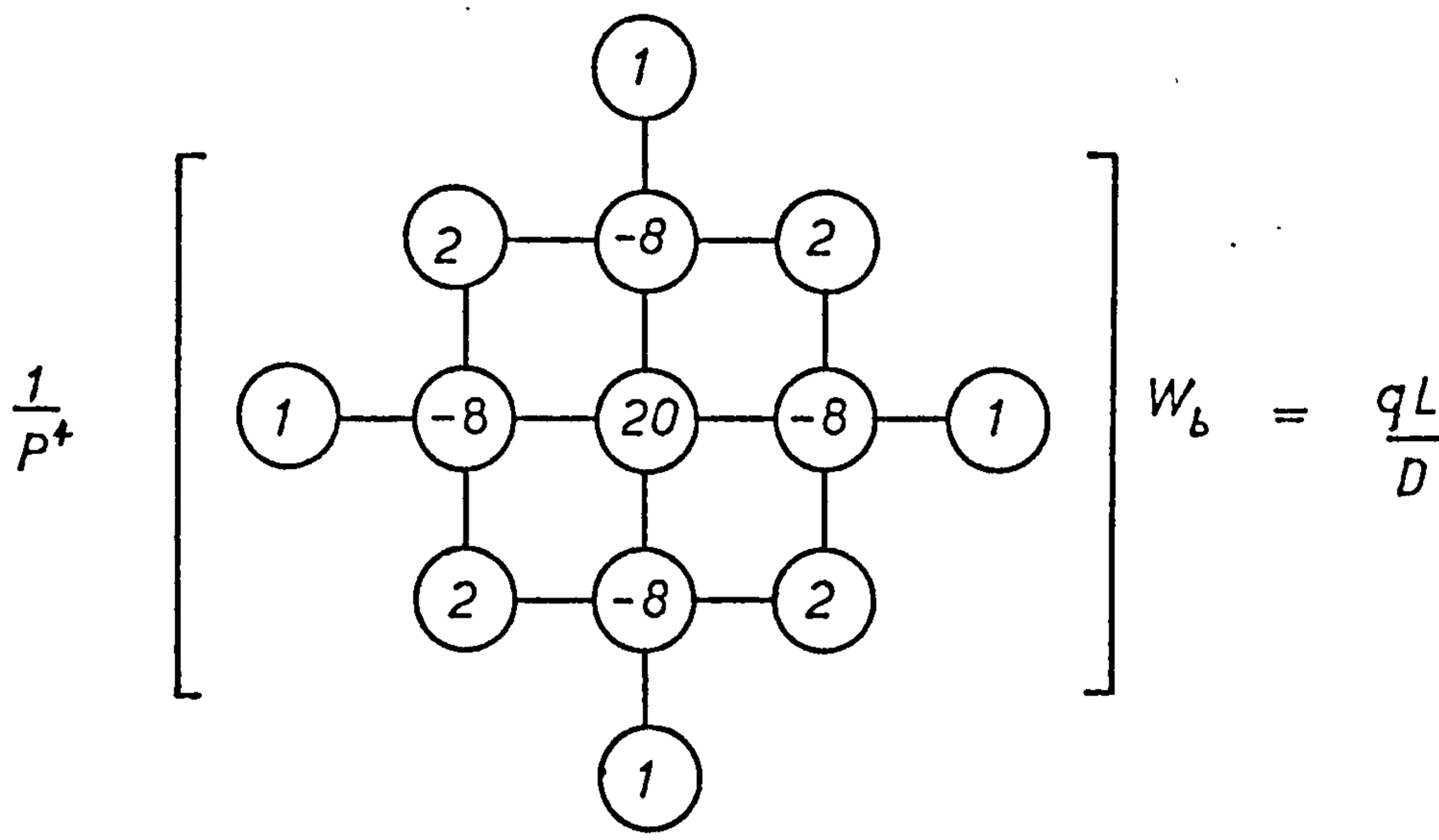

Figure 4.3

Partial deflection method.

Finite difference form of governing equation for W_b.

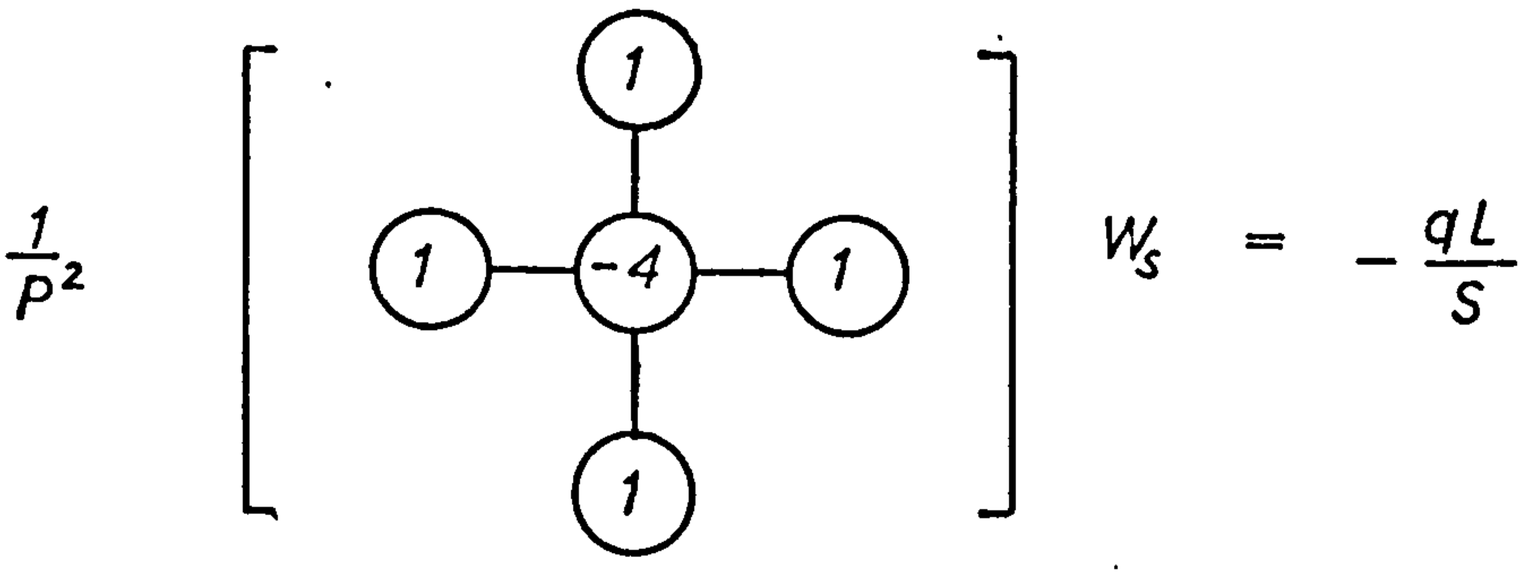

Figure 4.4

Partial deflection method.

Finite difference form of governing equation for W_s.

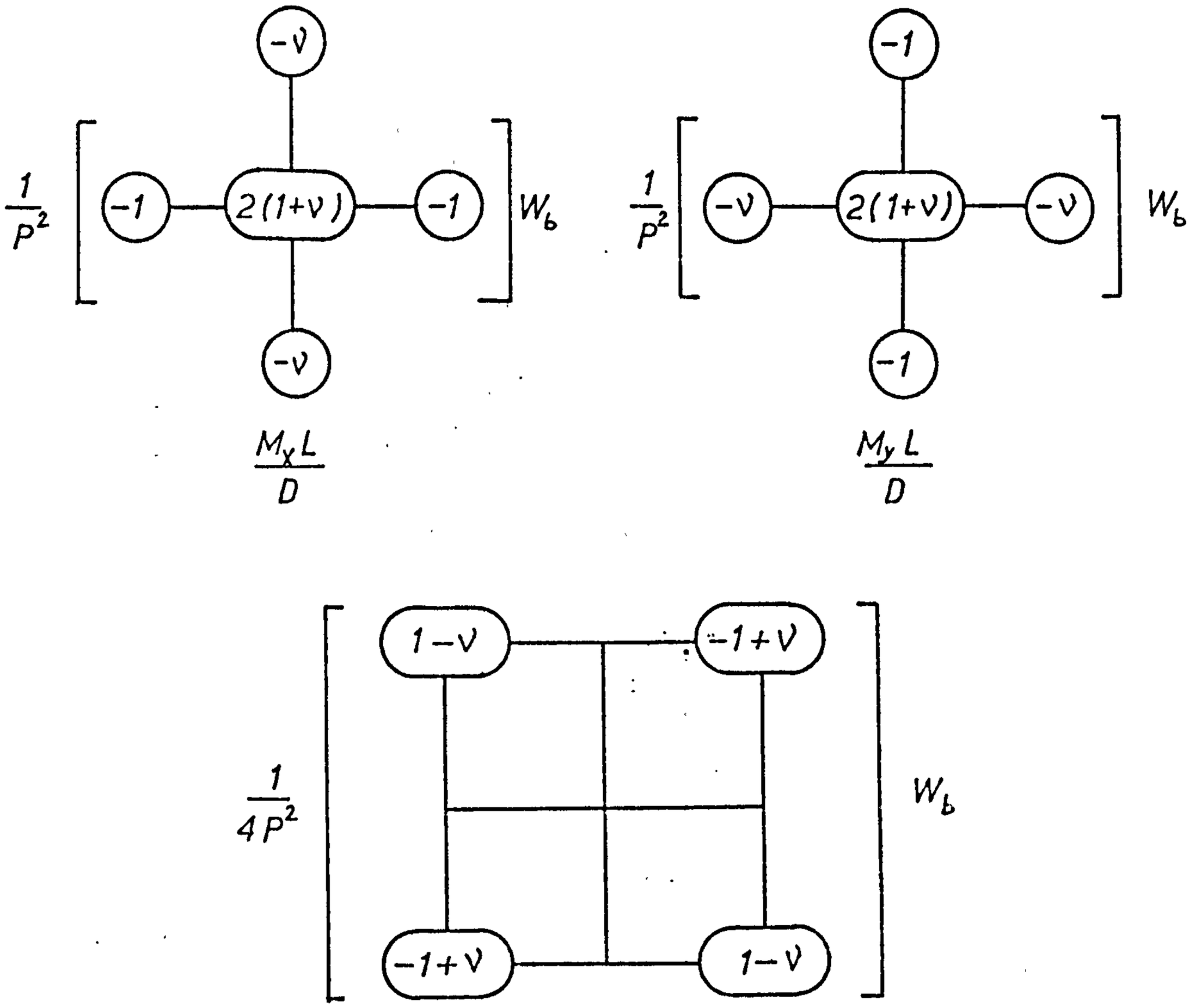

Figure 4.5

Partial deflection method.

Finite difference equivalents for bending and twisting moments.

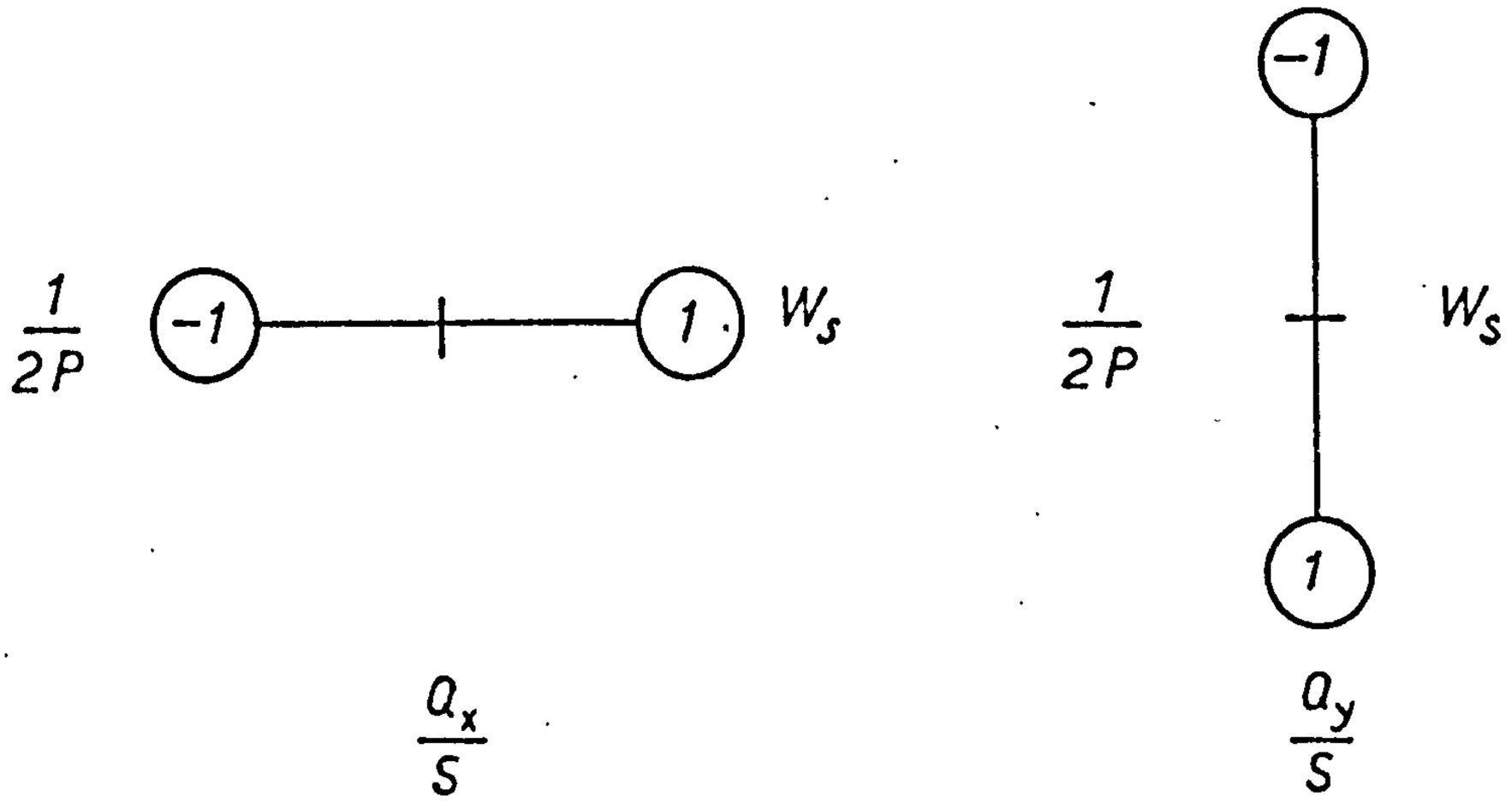

Figure 4.6

Partial deflection method.

Finite difference equivalents for shear forces.

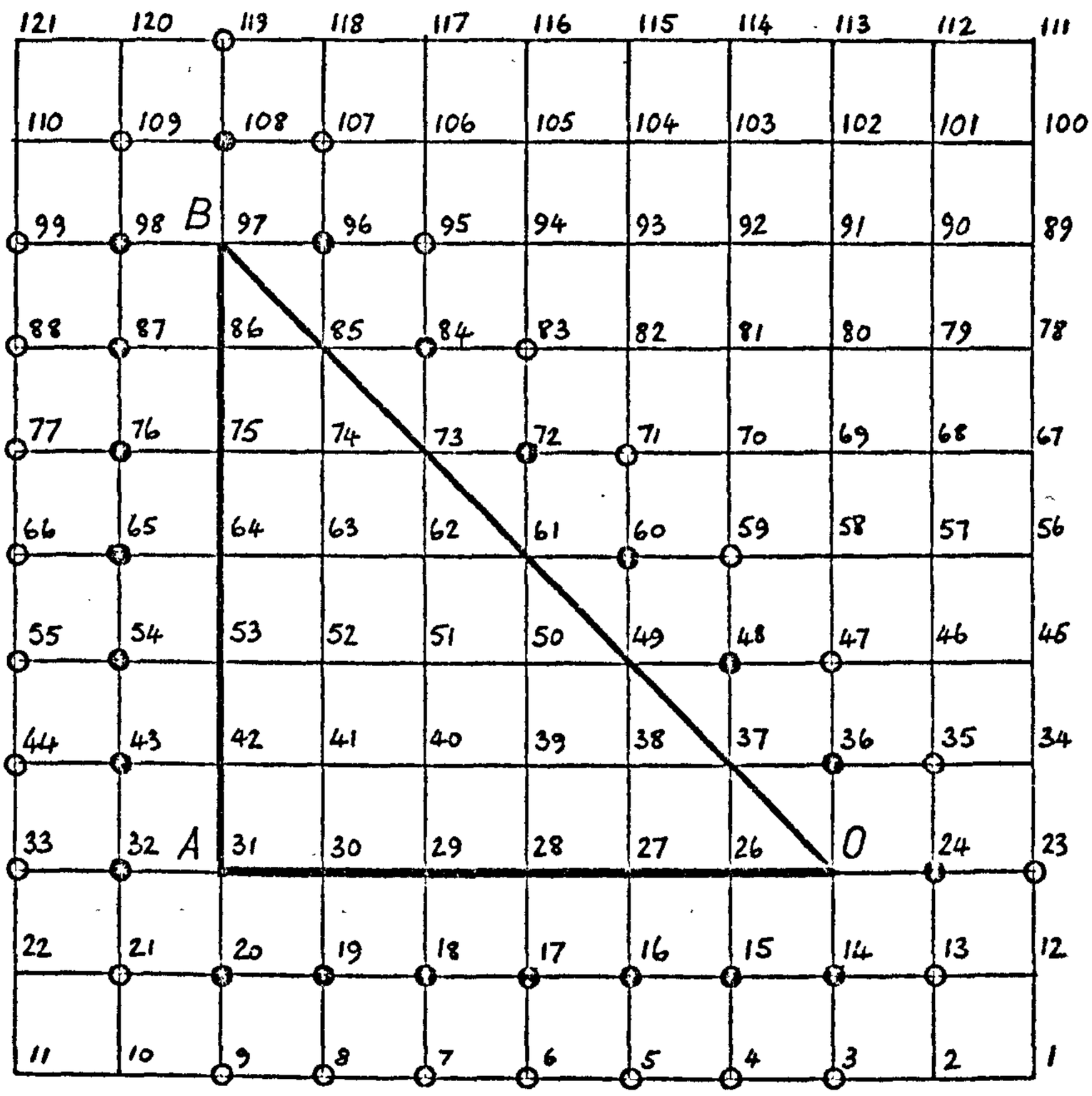

o fictitious value of W_b

● fictitious values of W_b and W_s

Figure 4.7

Finite difference mesh for the partial deflection method.

Number of unknowns	
W_b	28 real and 48 fictitious values 76
W_s	28 real and 22 fictitious values 50
Total number of unknowns	126

Equation	Number
Governing equation for W_b	28
Governing equation for W_s	28
Boundary equations on AB $W = 0$	7
$M_x = 0$	7
$\phi_y = 0$	6
Symmetry equations for W_b	33
Symmetry equations for W_s	15
Additional equations: $W_s = 0$ at mesh point 97	
and extrapolation along OB to find W_b at 109	2
Total	126

Table 4.2

Equations for the partial deflection method.

The following points should be noted:

(a) The third condition on AB at mesh point 31 is automatically satisifed by the statement of symmetry about OA, and hence this equation is only written at the remaining six mesh points on this boundary.

(b) To obtain a solution it is necessary to fix the value of W_b or W_s at one point. In this case W_s was set equal to zero at mesh point 97, the corner of the plate.

(c) The governing equations for W_b and W_s, the boundary and symmetry equations and the fixing of one point give a total of 125 equations leaving one further equation to be found, and this can be done in one of two ways.

Firstly the need for one unknown can be eliminated by the use of backward differences (for example, W_b at mesh point 109 could be eliminated by the use of backward or off-centre differences for some terms in the equation $\Delta^2 W_b = qL^3/D$ at point 97). Alternatively, an additional equation can be formed by extrapolation to determine a fictitious value of one variable. This was found from a programming point of view to be the simplest method, and W_b at mesh point 109 was determined by extrapolation along the diagonal OB.

This sets out the procedure for a superposition solution. When this is not applicable equation (4.50) replaces the governing equation for W_s, and fictitious values of W_s will no longer be required, so that the total number of equations is reduced to 104.

4.8.2 Application of the finite difference method to Reissner's theory.

The non-dimensional forms of the equations used in this case are shown in Figure 4.8 - 4.10. The governing equation for W for uniform loading is the usual biharmonic, and is the same as that shown in Figure 4.3 for W_b.

The scheme of mesh points used in this solution is shown in Figure 4.11. There are 150 unknowns and the equations used to determine these are summarised in Table 4.3.

Equation	Number
Governing equation for W	28
Governing equation for ψ	28
Boundary equations on AB: $W = 0$	7
$M_x = 0$	7
$\phi_y = 0$ or $M_{xy} = 0$	7
Symmetry equations for W	46
Symmetry equations for ψ	24
Special equations: W = 0 at mesh points 108 and 119, and extrapolation along OB to find W at mesh point 109	3
Total	150

Table 4.3

Equations for Reissner's theory.

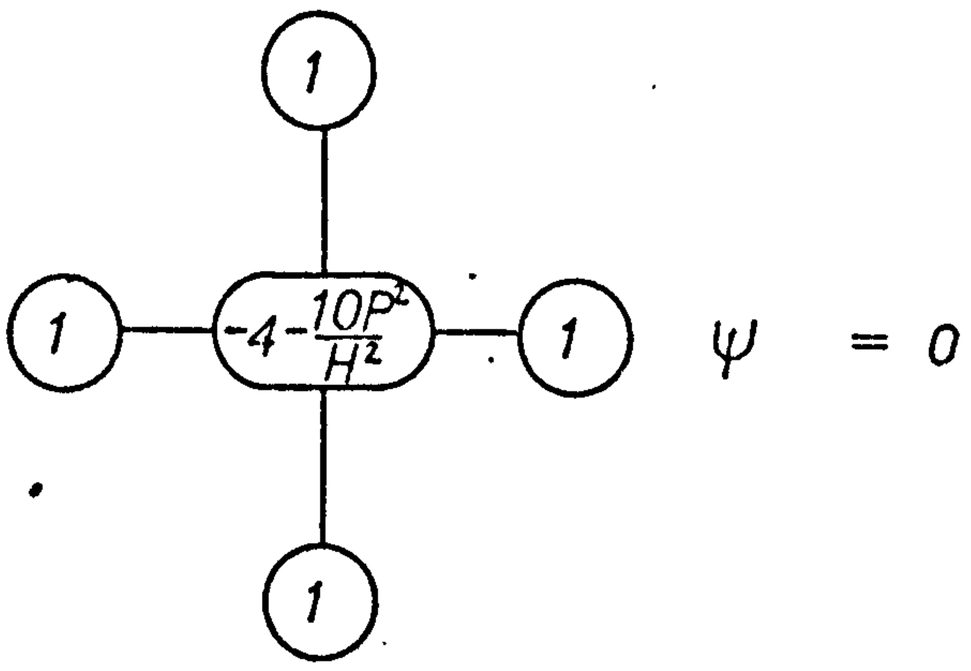

Figure 4.8

Reissner Theory

Finite difference form of governing equation for ψ

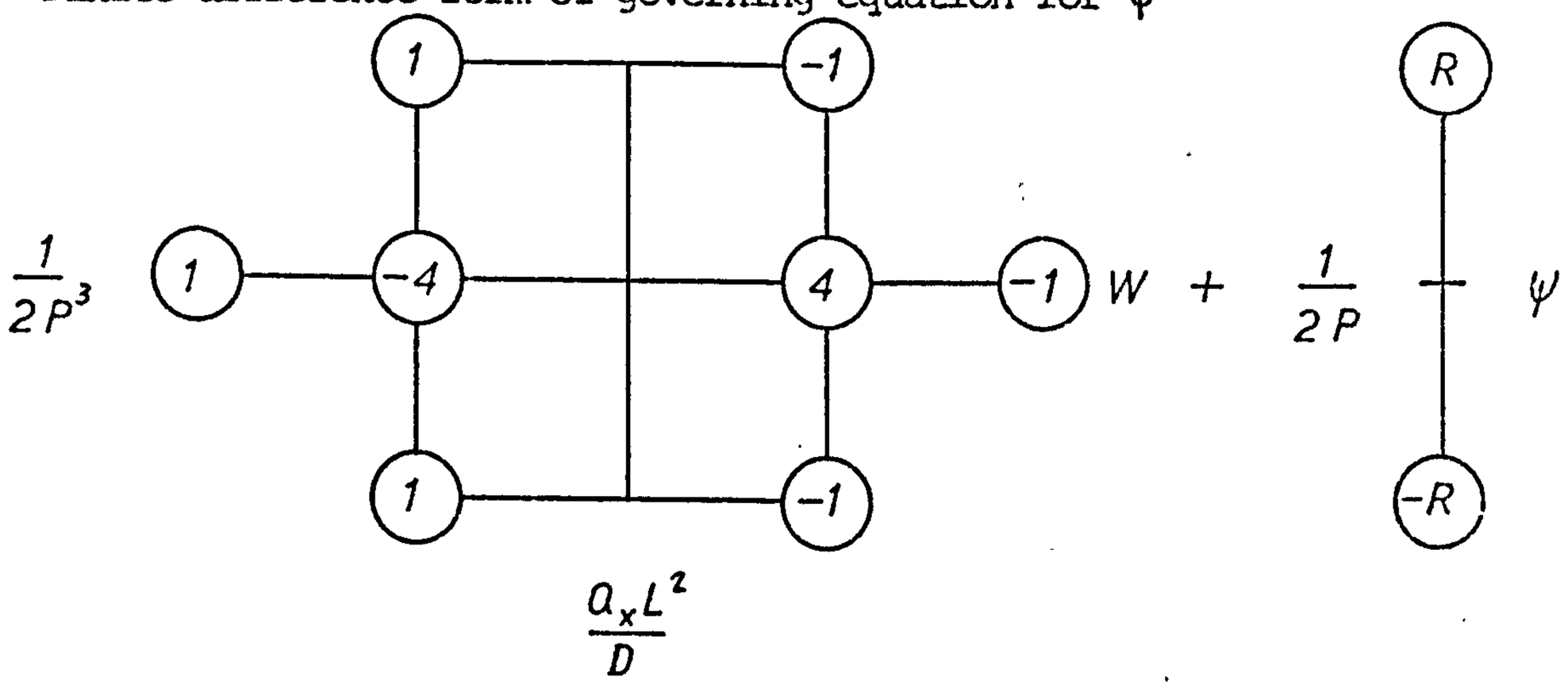

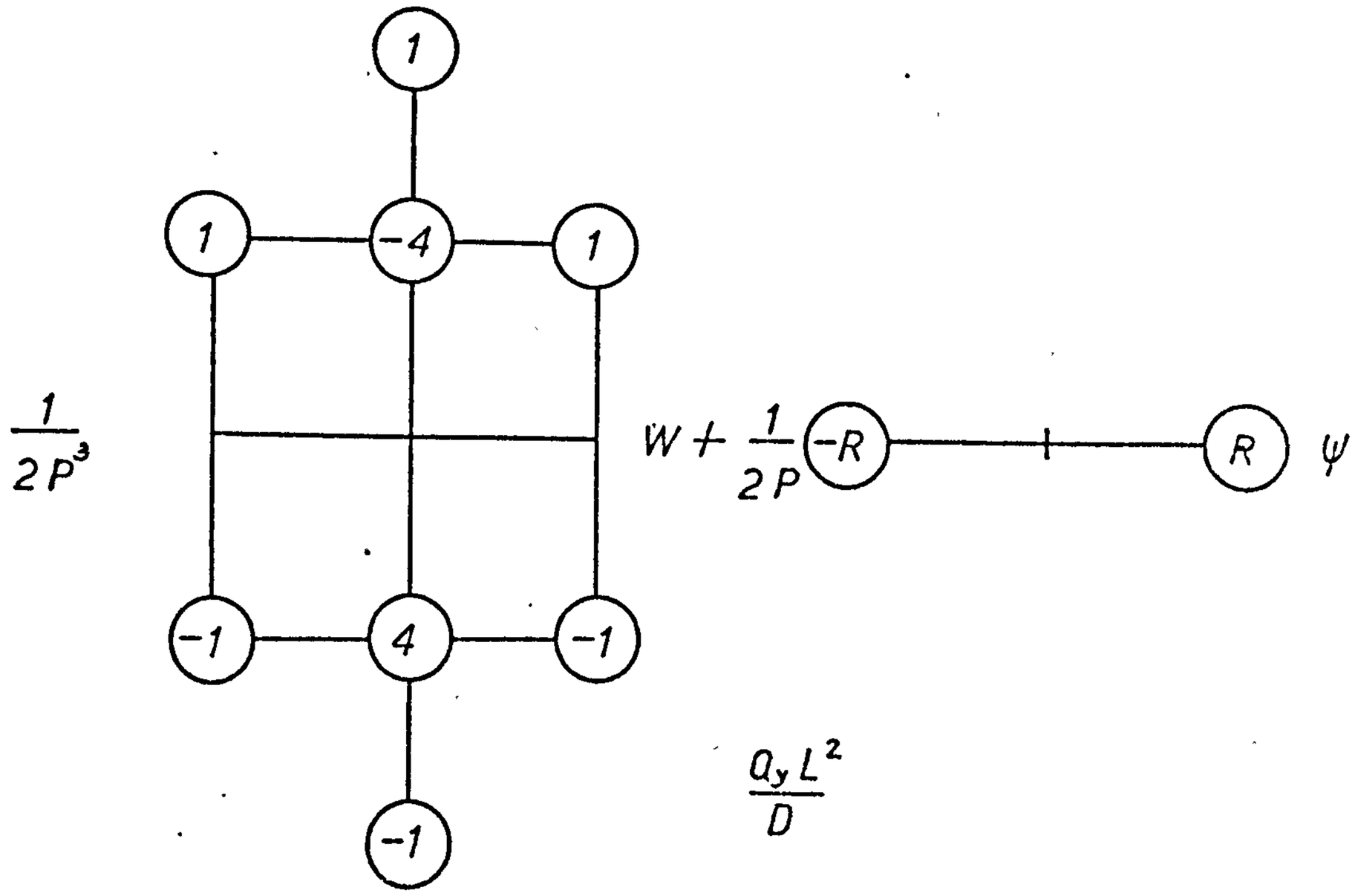

Figure 4.9

Reissner Theory

Finite difference equivalents for shear forces.

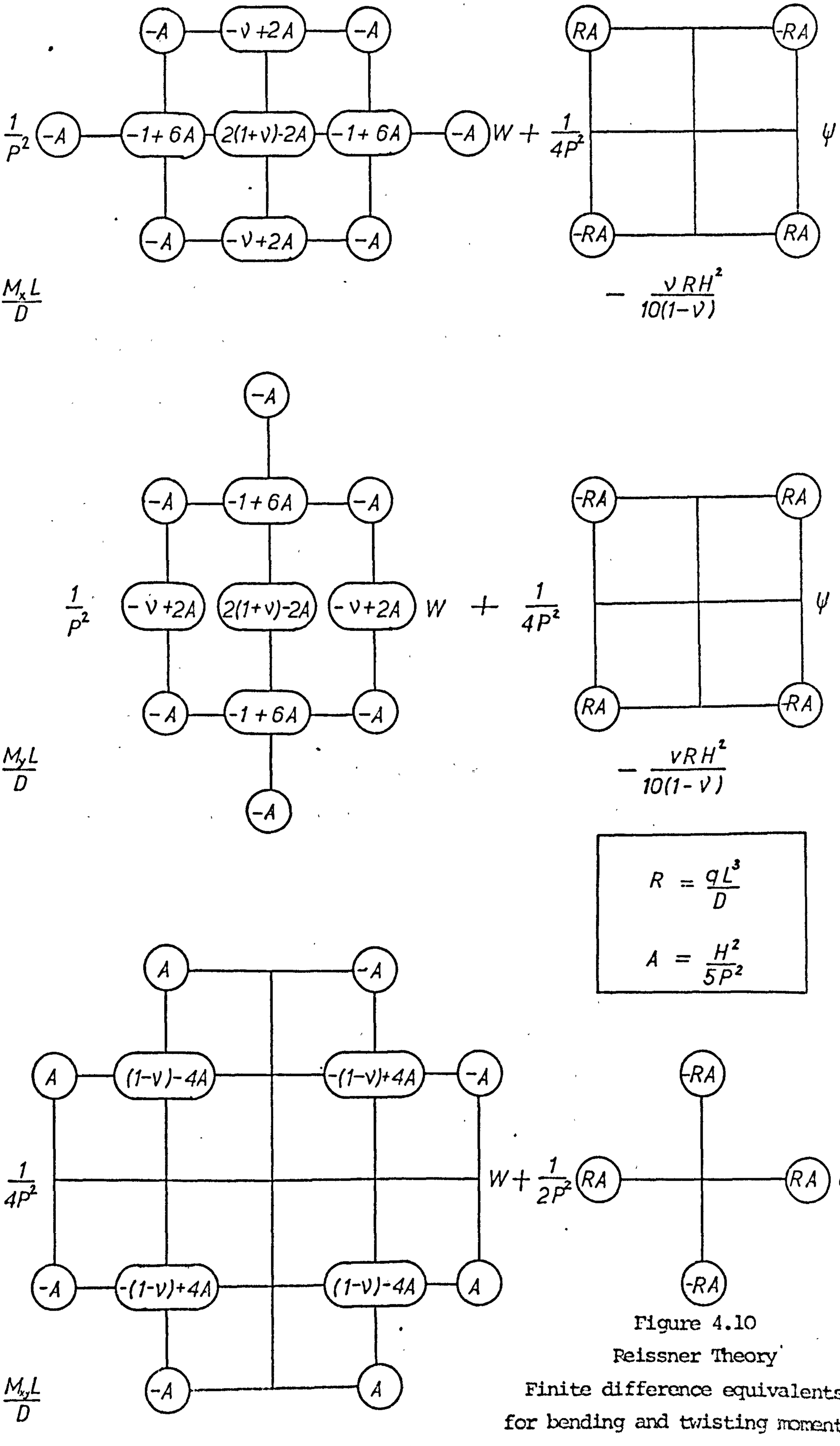

Figure 4.10

Reissner Theory

Finite difference equivalents

for bending and twisting moments.

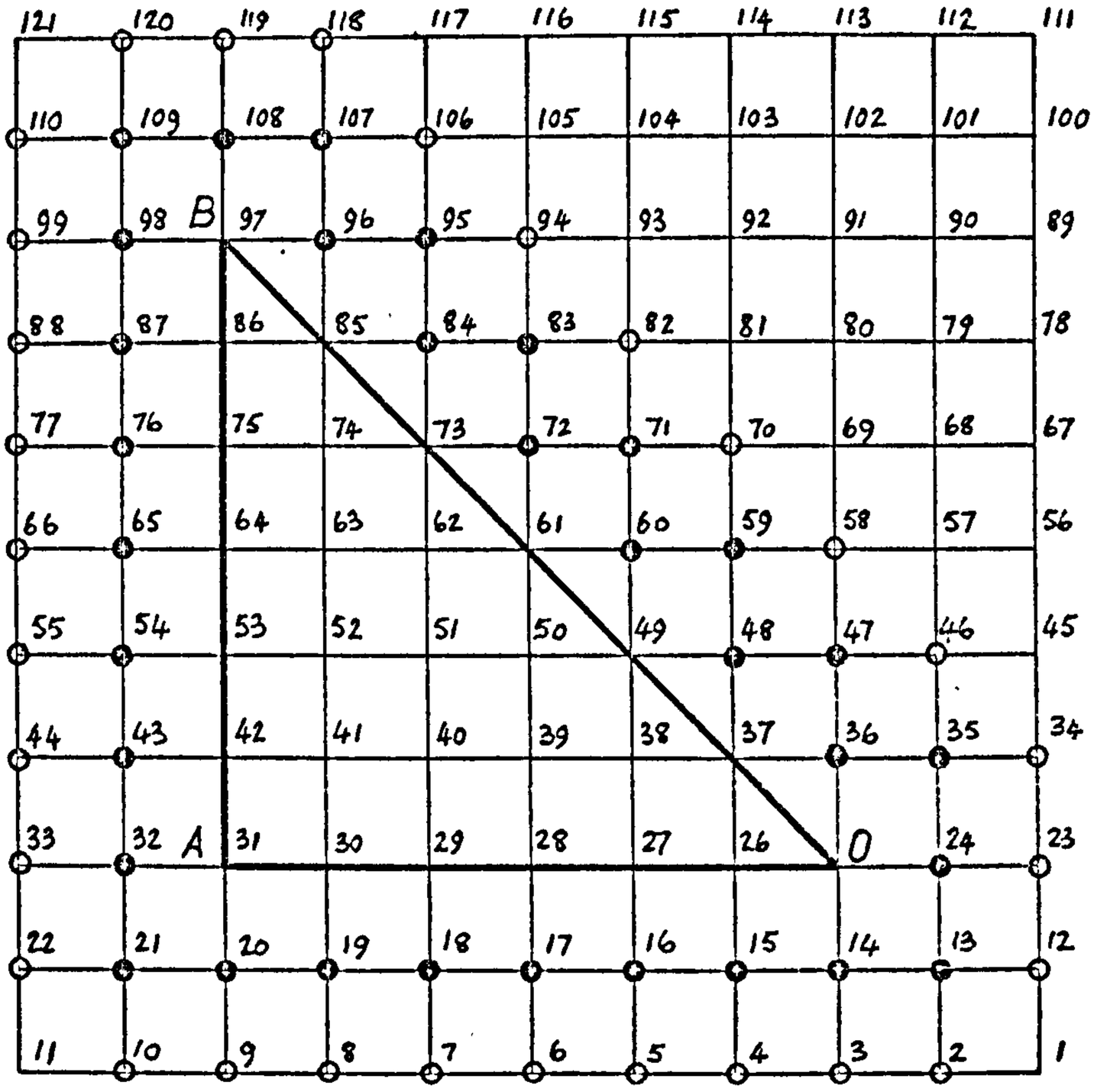

o fictitious values of W

• fictitious values of W and ψ

Figure 4.11

Finite difference mesh for Peissner theory.

Number of unknowns:

W	28 real and 62 fictitious values	90
ψ	28 real and 32 fictitious values	60
	Total number of unknowns	150

The following points should be noted:

(a) Three additional equations are required in this case. It is permissible to use W = 0 at mesh points 108 and 119 on the grounds that along the line AB W = 0 and thus all derivatives of W with respect to Y are zero at all points including the corner. The form of the classical finite difference equation for $M_x = 0$ would automatically establish this but the form used here does not and so these zero values may be stated as separate equations. The third additional equation is again extrapolation along OB to establish the value of W at mesh point 109.

(b) It is not necessary to give an arbitrary value to ψ at one point because the governing equation does not contain only its derivatives but ψ itself.

(c) The finite difference forms of the equations $\phi_y = 0$ or $M_{xy} = 0$ are not symmetric about a line X = constant and hence these equations are not automatically satisfied at mesh point 31 by general symmetry about OA. Hence the third boundary equation has to be applied at all 7 mesh points from A to B, in contrast to only 6 in the previous case.

(d) Not all the fictitious values shown in Figure 4.11 are strictly required in order to solve the governing equations; the values of W at mesh points 34, 46, 58, 70, 82, 94 and 106 and of ψ at 35, 47, 59, 71, 83 and 95 are required only for subsequent calculation of

bending and twisting moments along the diagonal OB if the usual finite difference forms are to be used. Similarly, when the third boundary condition used is $\phi_y = 0$ then the values of W at mesh points 110, 118 and 120 are not required.

However since all these values are governed by symmetry relationships it is convenient to include them in the analysis.

4.8.3 Application of the finite difference method to the modified Reissner theory.

The non-dimensional finite difference form of the equations required in this case using the normal central difference formulae are shown in Figures 4.12 - 4.14.

Examination of these finite difference molecules shows that for certain values of H^2 large differences in the magnitude of the various coefficients in a particular molecule can exist. While this would not be a disadvantage if the large coefficients lay on or near the leading diagonal of the solution matrix and the smaller coefficients further away, the nature of the set of equations involved in a finite difference solution is such that the reverse will often be true, with the possibility of illconditioning in certain cases. The general form of the equations involved here is

$$f_1 + H^2 f_2 = \text{constant} \qquad (4.51)$$

where f_1 and f_2 are functions of derivatives of W, and from equations (4.27) - (4.32) it may be seen that f_1 contains lower order derivatives than f_2.

Now the usual central difference forms used so far are of order of accuracy (mesh length)^2 that is they contain an error term of order p^2, where p is the mesh length, but more accurate forms can be derived which will always involve additional mesh points and thus enlarge the finite difference molecules. It was thought that by using finite difference forms of order of accuracy p^4 for those derivatives contained in f_1 of equation (4.51) the

numerical imbalance in the magnitude of the coefficients could to some extent be redressed, the only constraint being that the resulting molecules should not involve any mesh points other than those used in Figures 4.12 - 4.14. The reason for this last condition is that otherwise additional fictitious points would be introduced, with no further equations available to enable their values to be determined. This meant that not all the derivatives contained in f_1 could be written in a form where all the finite difference equivalents were of order of accuracy p^4. In some cases ($\frac{\partial^2 W}{\partial x \partial y}$, $\frac{\partial^3 W}{\partial x^2 \partial y}$, $\frac{\partial^3 W}{\partial x \partial y^2}$ and $\frac{\partial^4 W}{\partial x^2 \partial y^2}$) a mixture of p^2 and p^4 accuracy terms were used in such a way that the difference in magnitude between the coefficients of a particular molecule was kept as small as possible and no points additional to those of Figures 4.12 - 4.14 were introduced.

The derivation of a typical finite difference equivalent of order of accuracy p^4 is given in Appendix C together with molecules for this and the other derivatives involved. The actual forms of the finite difference equations finally used are shown in Figures 4.15 - 4.17.

Figure 4.18 shows the finite difference mesh used for this theory, from which it can be seen that a total of 106 unknown values of W are involved. The equations to be solved for simple supports are shown in Table 4.4.

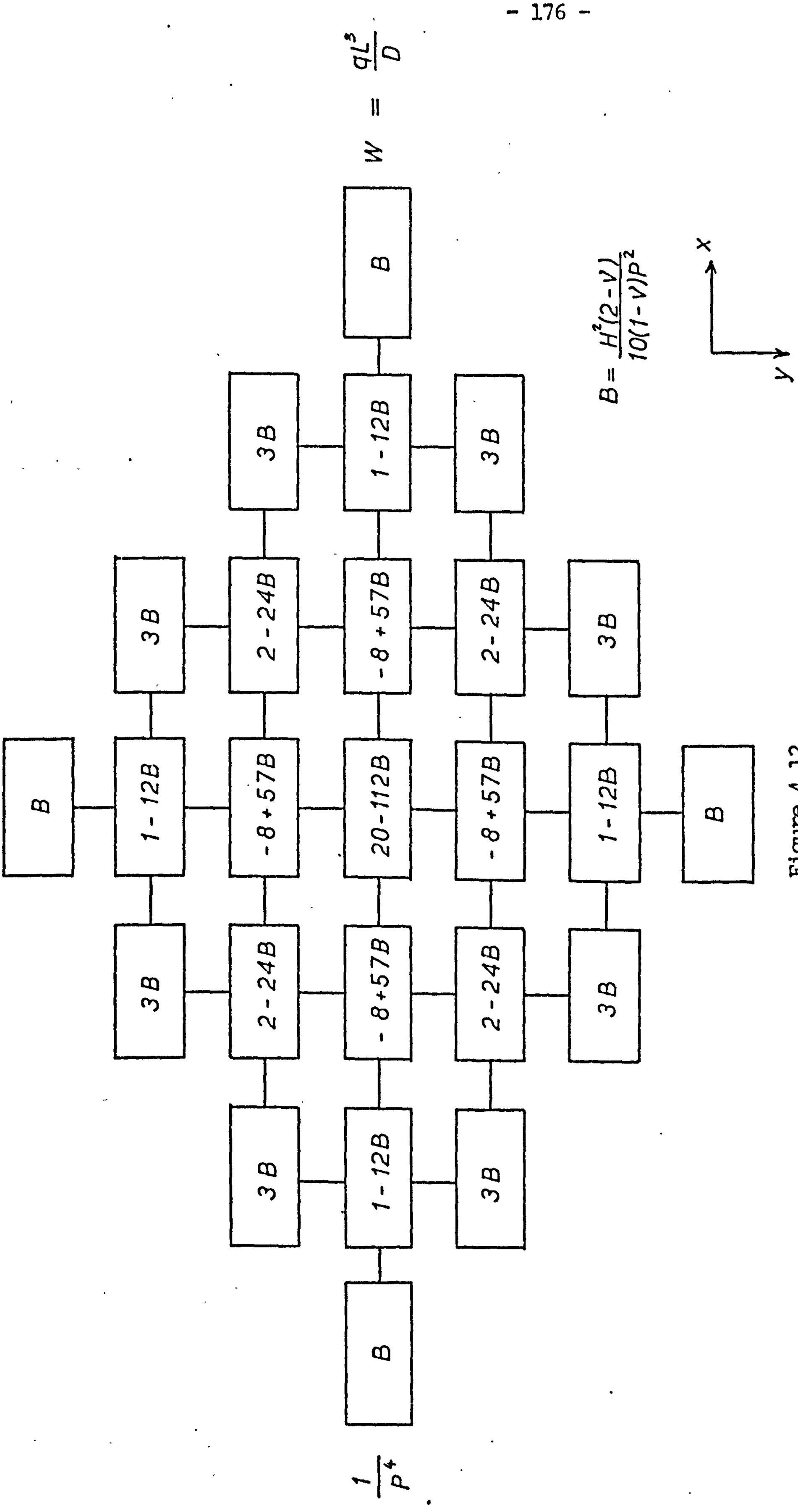

Figure 4.12 Finite difference form of governing equation for W.
Modified Reissner Theory

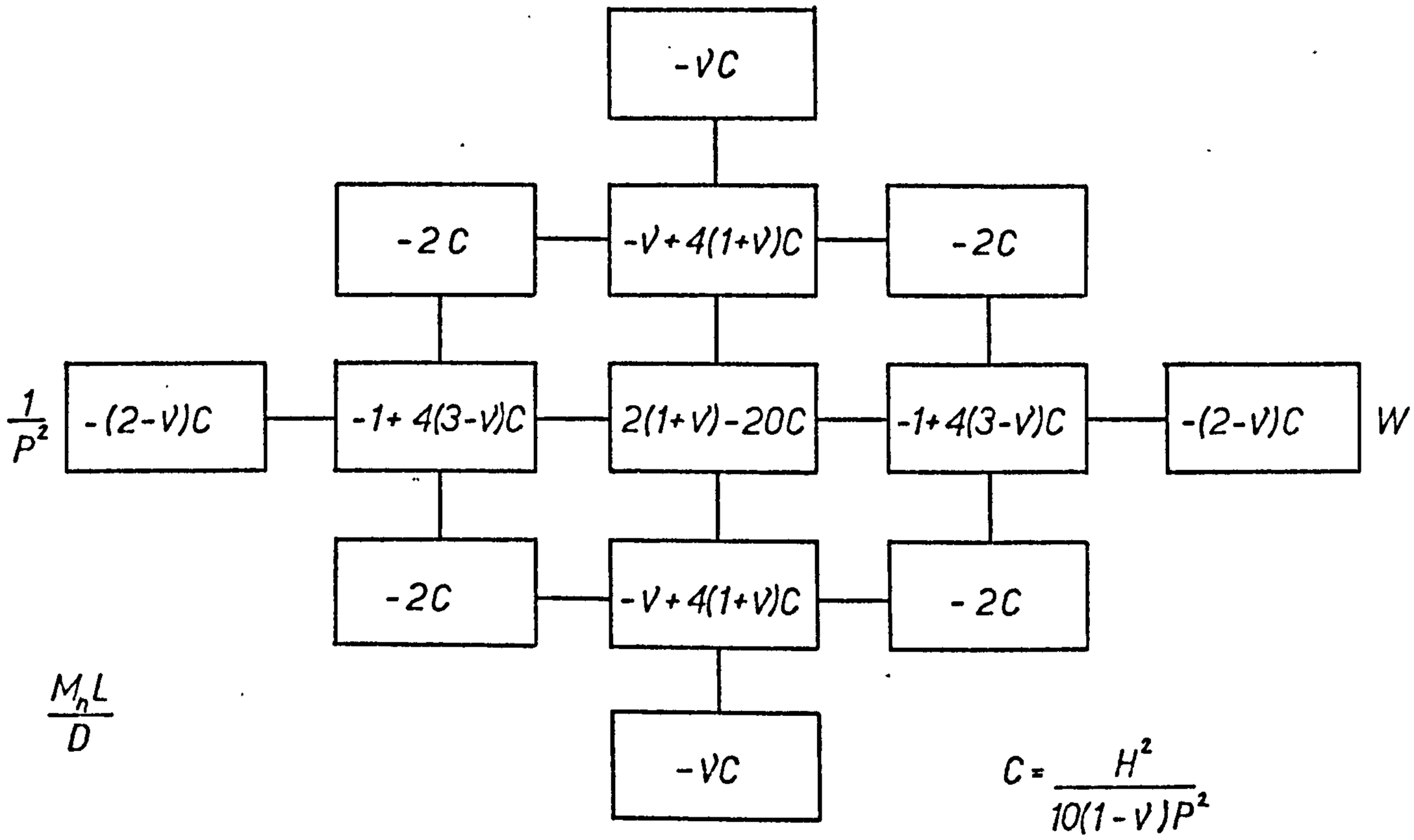

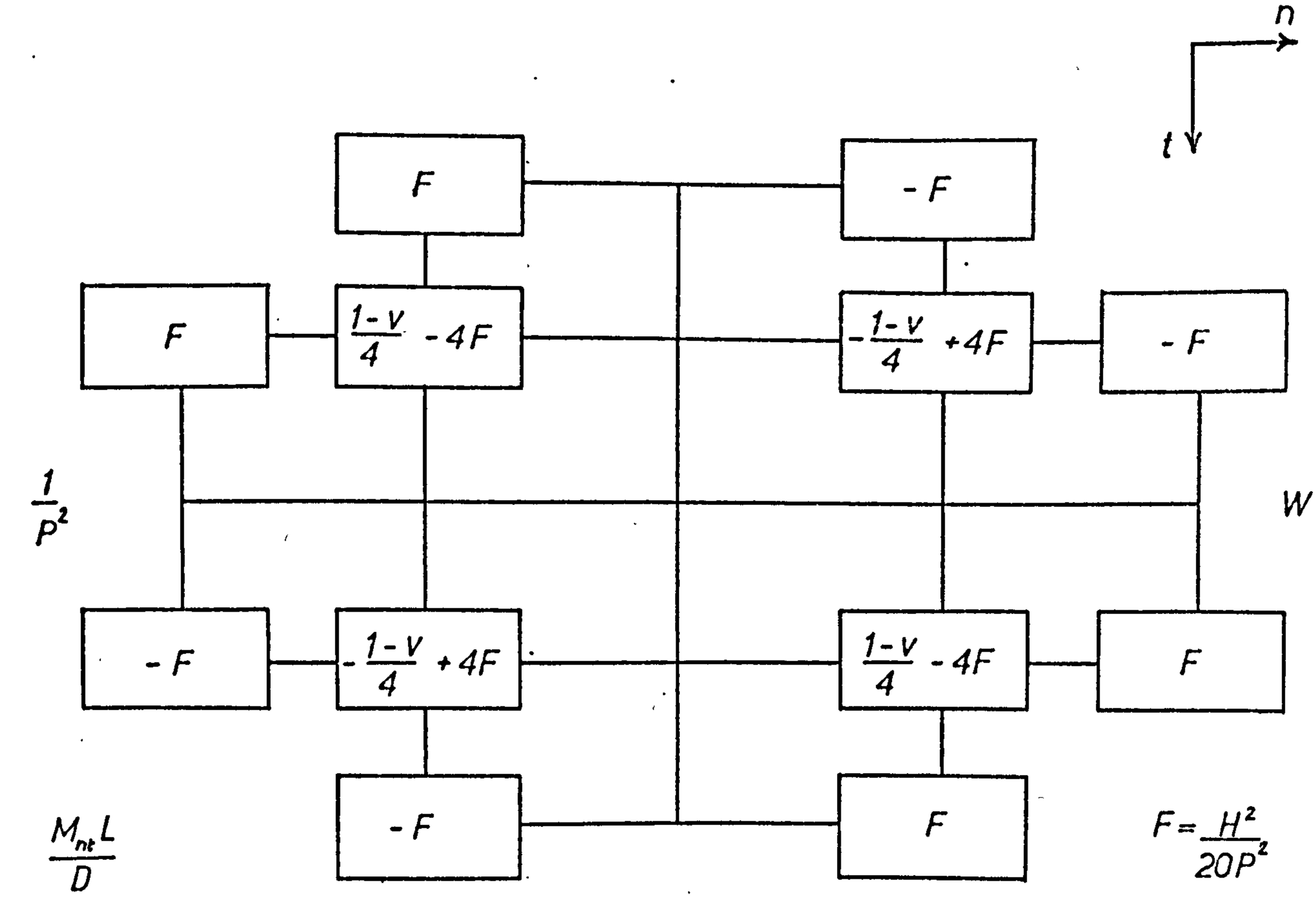

Figure 4.13

Modified Reissner Theory

Finite difference equivalents for bending and twisting moments.

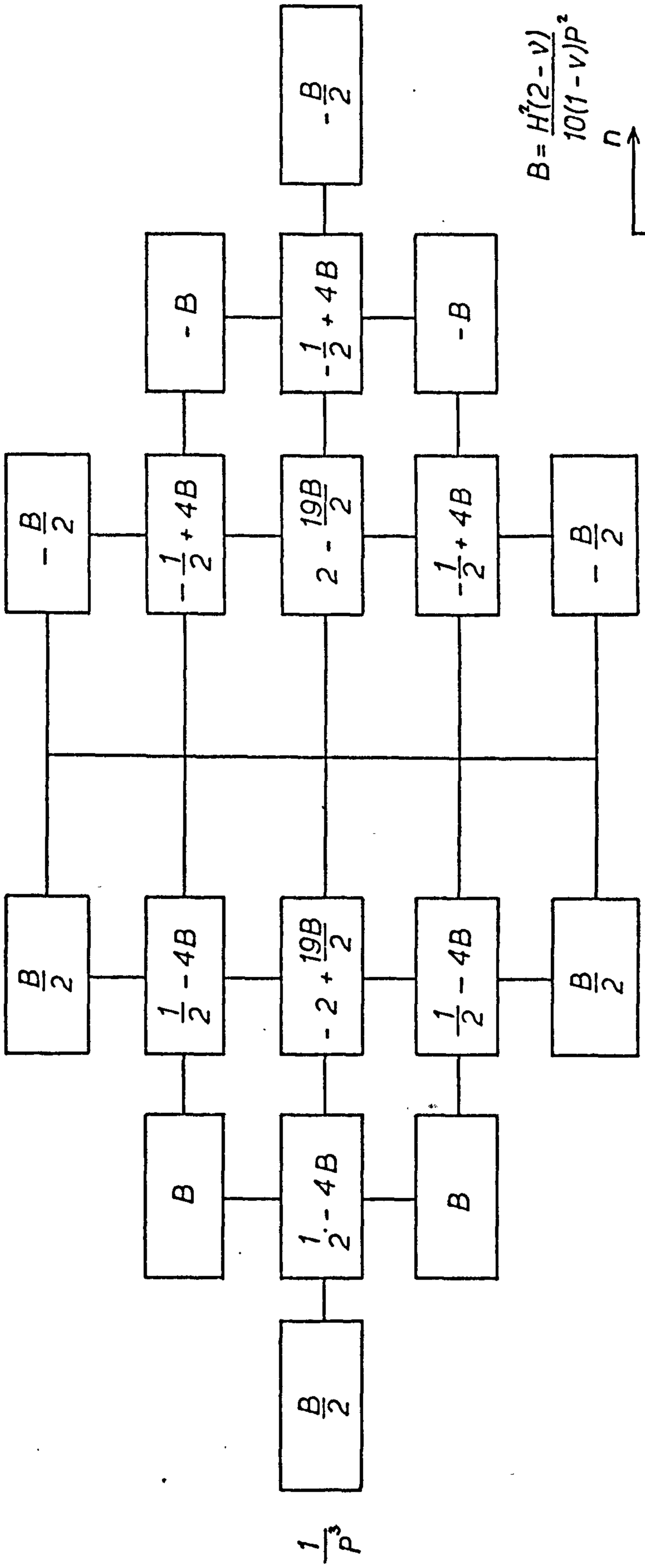

Figure 4.14

Modified Reissner Theory

Finite difference equivalent for shear force

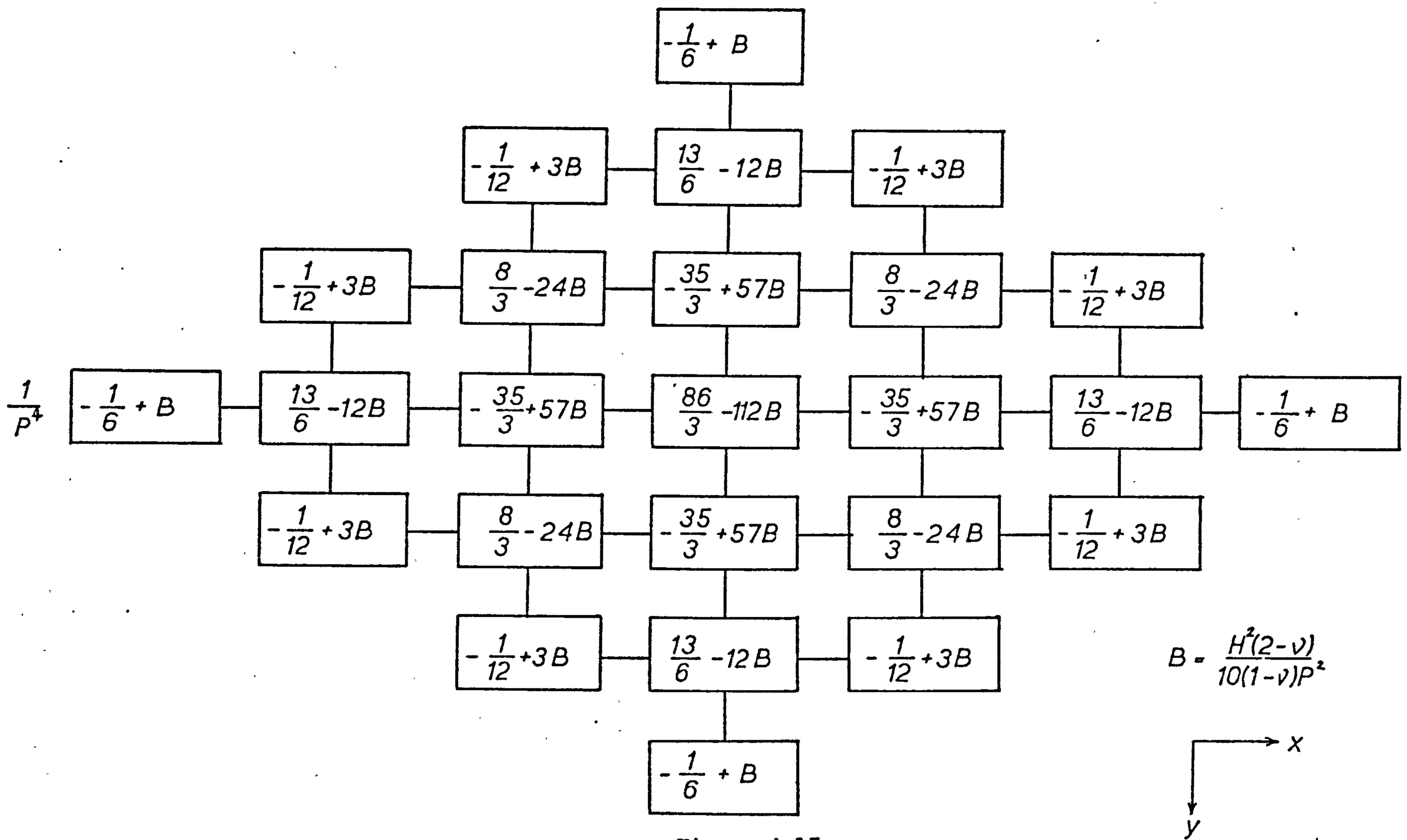

Figure 4.15

Modified Reissner Theory

Finite difference form of governing equation for W

(mixed p^2 and p^4 accuracy)

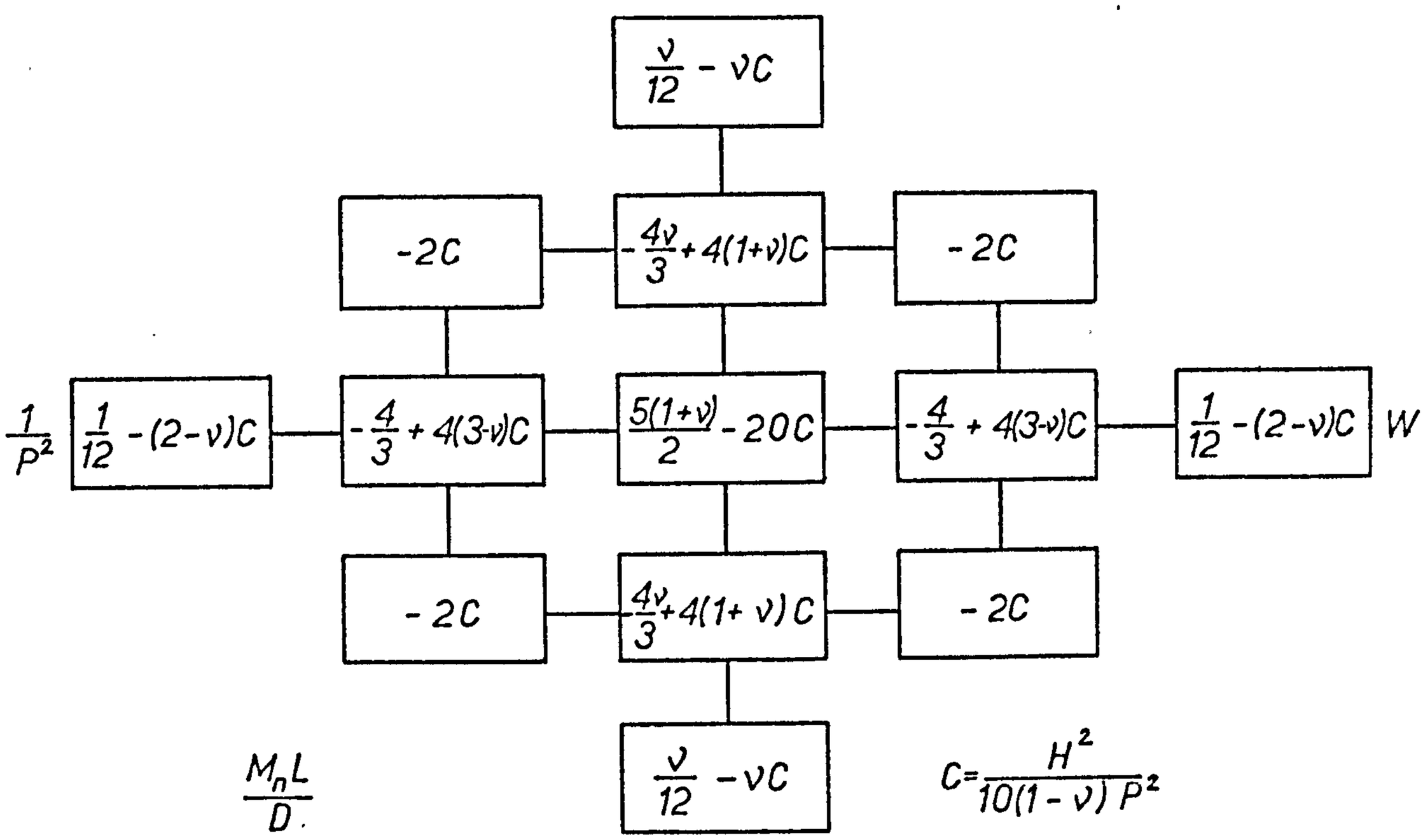

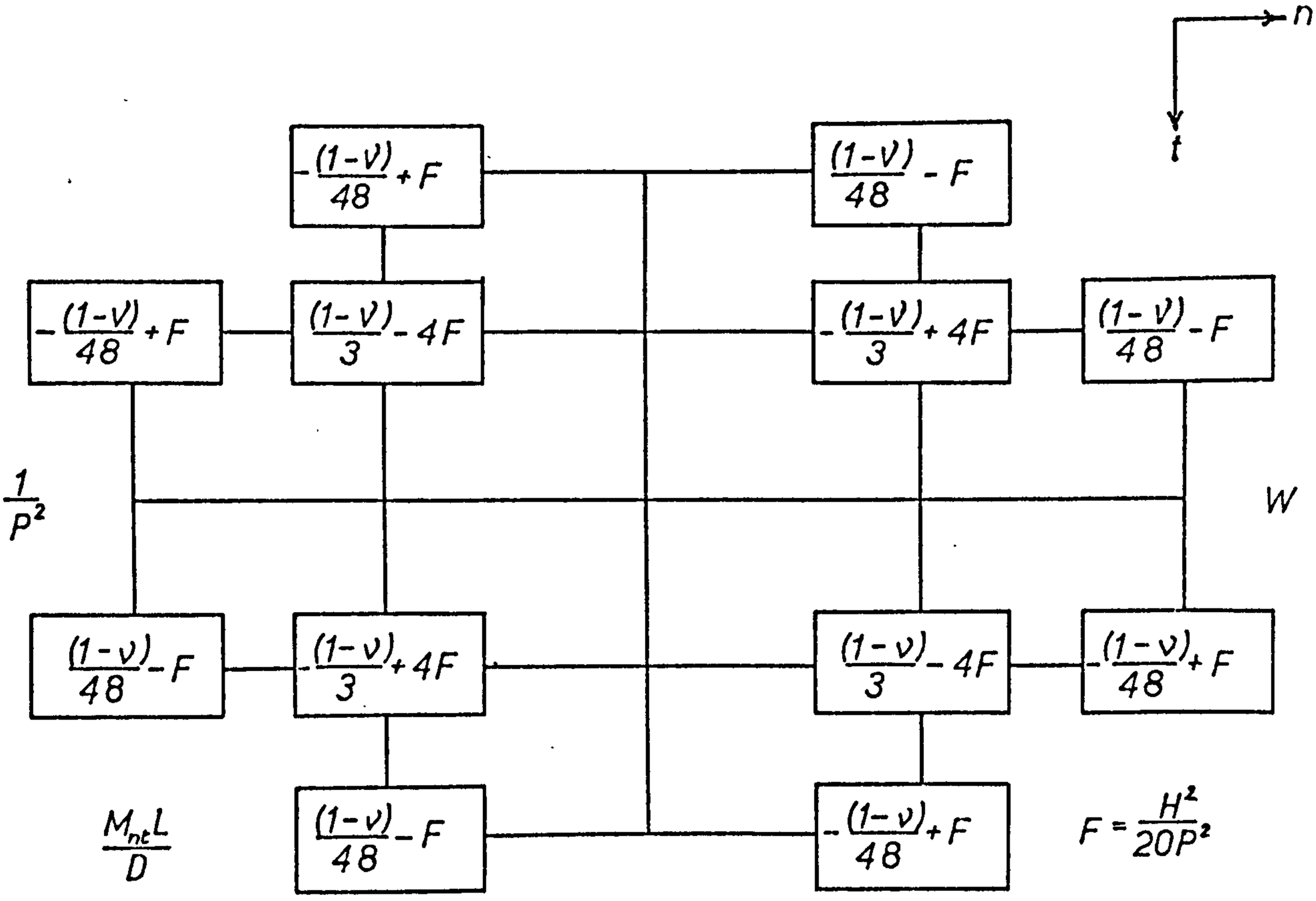

Figure 4.16

: Modified Reissner Theory

Finite difference equivalents for bending and twisting moments (mixed p^2 and p^4 accuracy)

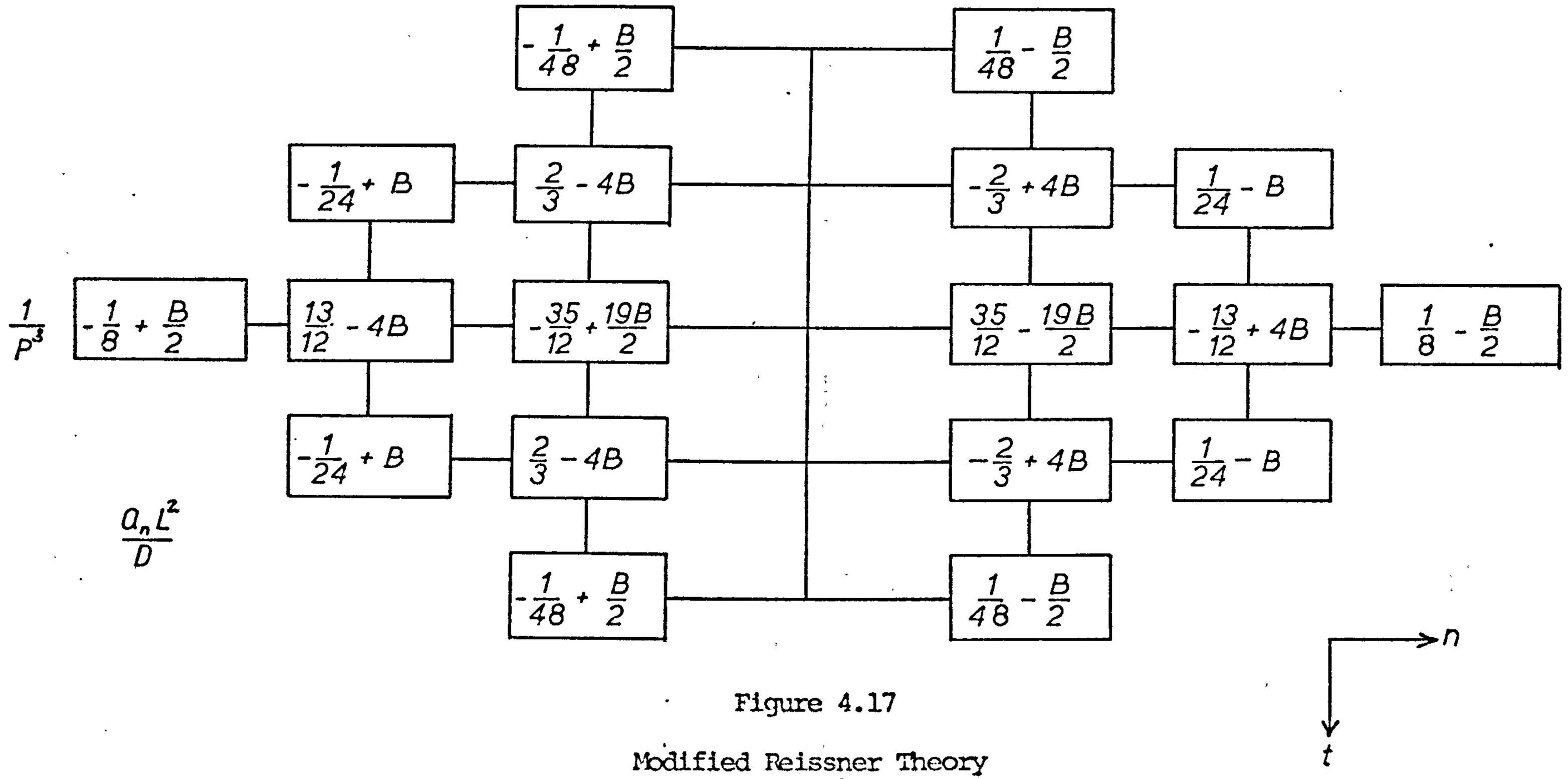

Figure 4.17

Modified Reissner Theory

Finite difference equivalent for shear force

(mixed p^2 and p^4 accuracy)

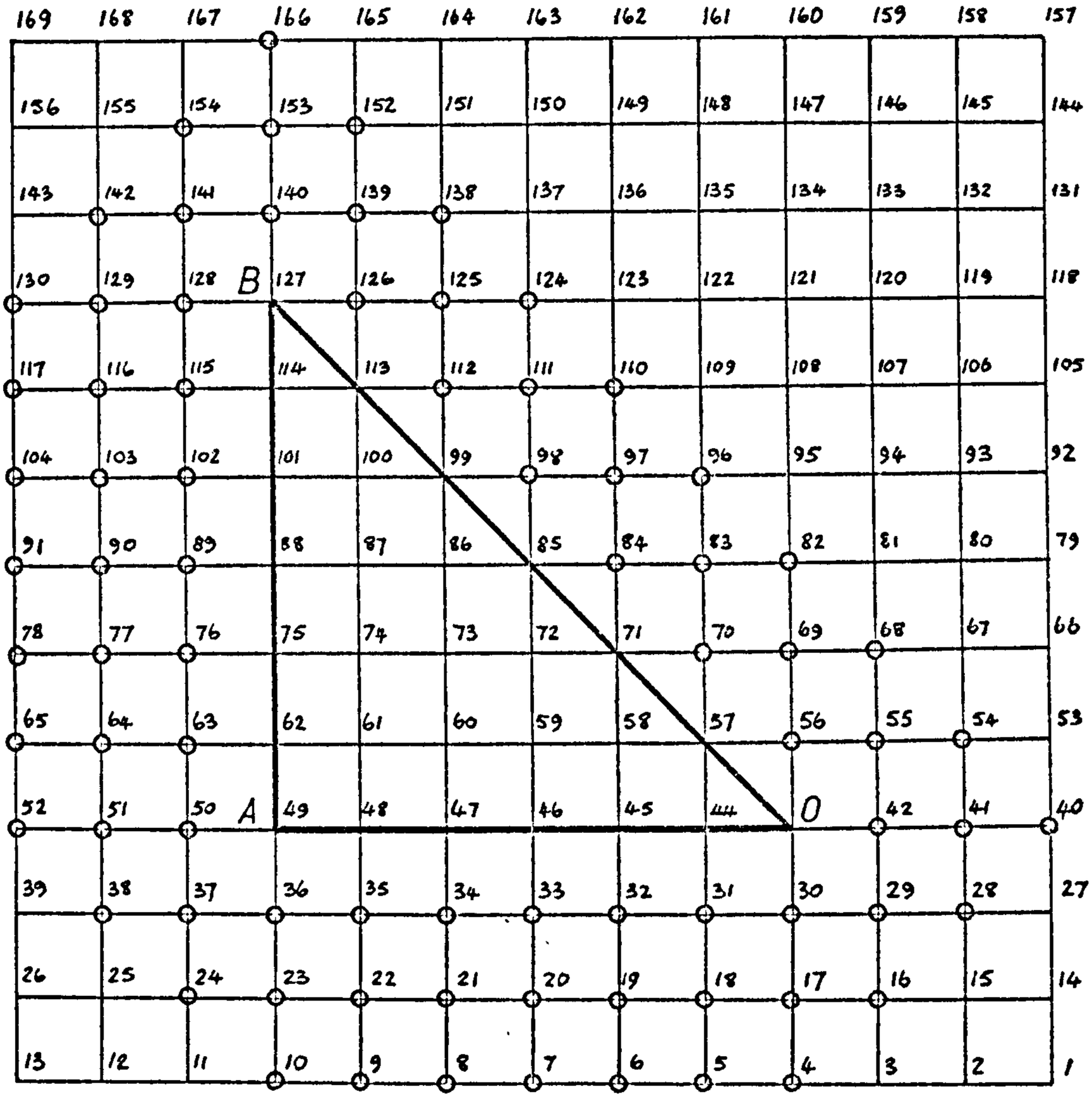

O fictitious values of W

Figure 4.18

Finite difference mesh for modified Reissner theory

Number of unknowns

28 real and 78 fictitious values of W.

Equation	Number
Governing equation for W	28
Boundary equations on AB: W = 0	7
$M_x = 0$	7
$\phi_y = 0$ or $M_{xy} = 0$	6
Symmetry equations	55
Additional equations : W ≐ 0 at mesh points 140, 153 and 166	3
Total	106

Table 4.4

Equations for modified Reissner theory.

The following points should be noted,

(a) Because of general symmetry about OA the third boundary equation on AB is automatically satisfied at mesh point 49, and hence is used as an independent equation only at the remaining mesh points on the boundary.

(b) Three additional equations are required in this case. It was found that the nature of the equations did not automatically produce zero values for the fictitious values of W on AB produced at mesh points 140, 153 and 166. In order that all derivatives of W with respect to Y should be zero at A these three values were set equal to zero, giving the additional equations needed.

4.9 Localised Rayleigh-Ritz solutions

In this section the means by which localised Rayleigh- Ritz techniques can be applied to the modified Reissner theory and the partial deflection method will be described.

4.9.1 Application to the modified Reissner theory

On the basis of the conclusions reached in Section 3.7.2 when discussing the application in connection with beams, displacement functions giving continuity in derivatives up to third order were selected. In the energy function all terms in h^2 and those terms in h^4 arising from the expressions for bending and twisting moment were included. The energy function is then complete with respect to these stress resultants.

The displacement in a local region is defined by the following 64 term polynomial

$$w = a_1 + a_2\xi + a_3\eta + a_4\xi^2 + a_5\xi\eta + a_6\eta^2 + a_7\xi^3 + a_8\xi^2\eta + a_9\xi\eta^2 + a_{10}\eta^3$$

$$+ a_{11}\xi^4 + a_{12}\xi^3\eta + a_{13}\xi^2\eta^2 + a_{14}\xi\eta^3 + a_{15}\eta^4$$

$$+ a_{16}\xi^5 + a_{17}\xi^5\eta + a_{18}\xi^3\eta^2 + a_{19}\xi^2\eta^3 + a_{20}\xi\eta^4 + a_{21}\eta^5$$

$$+ a_{22}\xi^6 + a_{23}\xi^5\eta + a_{24}\xi^4\eta^2 + a_{25}\xi^3\eta^3 + a_{26}\xi^2\eta^4 + a_{27}\xi\eta^5 + a_{28}\eta^6$$

$$+ a_{29}\xi^7 + a_{30}\xi^6\eta + a_{31}\xi^5\eta^2 + a_{32}\xi^4\eta^3 + a_{33}\xi^3\eta^4 + a_{34}\xi^2\eta^5 + a_{35}\xi\eta^6 + a_{36}\eta^7$$

$$+ a_{37}\xi^7\eta + a_{38}\xi^6\eta^2 + a_{39}\xi^5\eta^3 + a_{40}\xi^4\eta^4 + a_{41}\xi^3\eta^5 + a_{42}\xi^2\eta^6 + a_{43}\xi\eta^7$$

$$+ a_{44}\xi^7\eta^2 + a_{45}\xi^6\eta^3 + a_{46}\xi^5\eta^4 + a_{47}\xi^4\eta^5 + a_{48}\xi^3\eta^6 + a_{49}\xi^2\eta^7$$

$$+ a_{50}\xi^7\eta^3 + a_{51}\xi^6\eta^4 + a_{52}\xi^5\eta^5 + a_{53}\xi^4\eta^6 + a_{54}\xi^3\eta^7$$

$$+ a_{55}\xi^7\eta^4 + a_{56}\xi^6\eta^5 + a_{57}\xi^5\eta^6 + a_{58}\xi^4\eta^7$$

$$+ a_{59}\xi^7\eta^5 + a_{60}\xi^6\eta^6 + a_{61}\xi^5\eta^7$$

$$+ a_{62}\xi^7\eta^6 + a_{63}\xi^6\eta^7$$

$$+ a_{64}\xi^7\eta^7$$

or $w = [A]\,[\xi, \eta]$ (4.52)

This will give 16 degrees of freedom at each node, namely w, $\frac{\partial w}{\partial \xi}$, $\frac{\partial w}{\partial \eta}$, $\frac{\partial^2 w}{\partial \xi^2}$, $\frac{\partial^2 w}{\partial \xi \partial \eta}$, $\frac{\partial^2 w}{\partial \eta^2}$, $\frac{\partial^3 w}{\partial \xi^3}$, $\frac{\partial^3 w}{\partial \xi^2 \partial \eta}$, $\frac{\partial^3 w}{\partial \xi \partial \eta^2}$, $\frac{\partial^3 w}{\partial \eta^3}$, $\frac{\partial^4 w}{\partial \xi^3 \partial \eta}$, $\frac{\partial^4 w}{\partial \xi^2 \partial \eta^2}$, $\frac{\partial^4 w}{\partial \xi \partial \eta^3}$, $\frac{\partial^5 w}{\partial \xi^3 \partial \eta^2}$, $\frac{\partial^5 w}{\partial \xi^2 \partial \eta^3}$, $\frac{\partial^6 w}{\partial \xi^3 \partial \eta^3}$

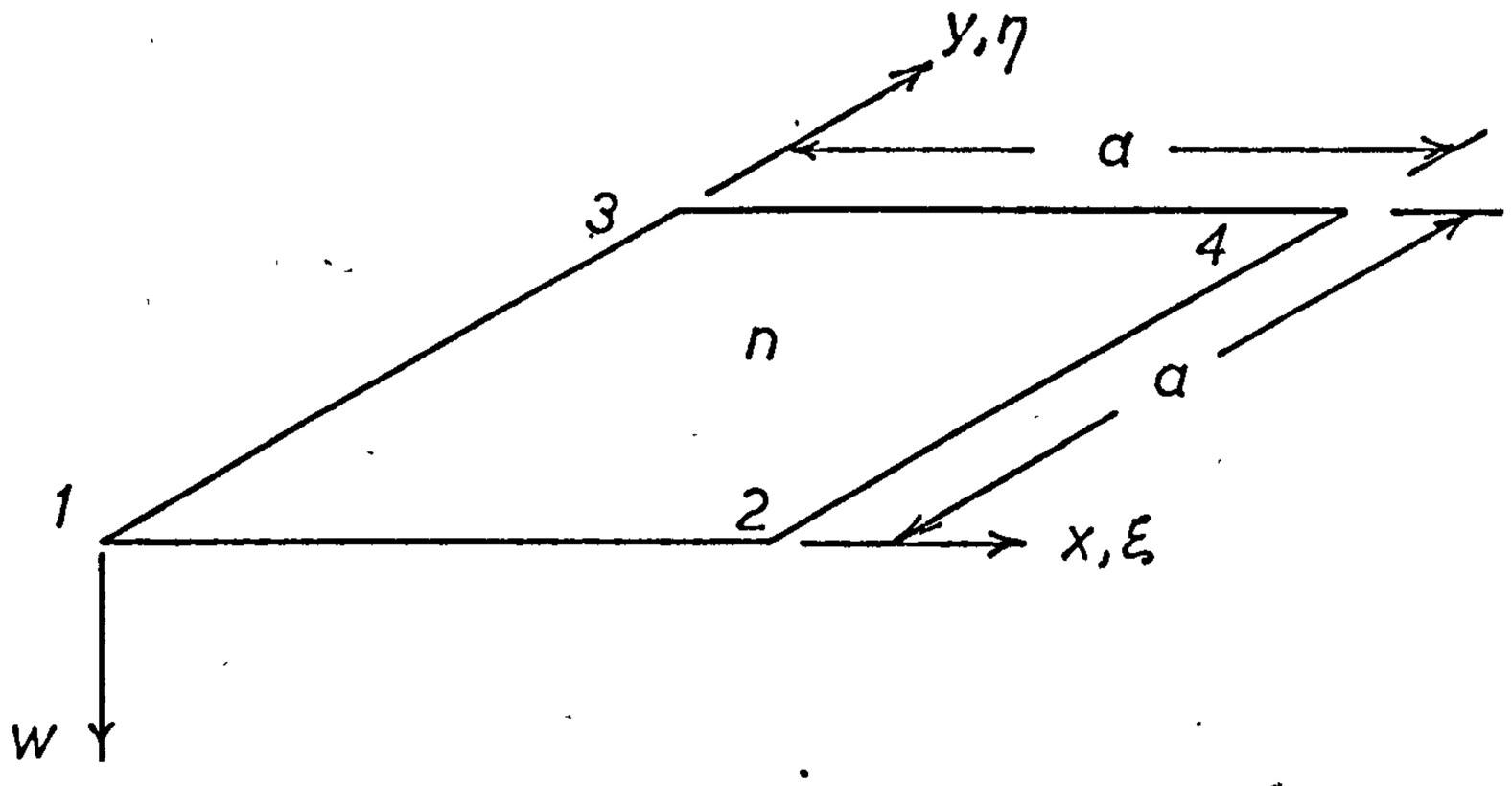

Figure 4.19

Plate region n for localised Rayleigh-Ritz solution.

For the local region n shown in Figure 4.19 the 64 coefficients $[Q]$ giving the 16 degrees of freedom at each node are related to the

coefficients [A] by

$$[A] = [B]\,[Q] \tag{4.53}$$

The coefficient of the 64 x 64 matrix [B] are calculated from those of the matrix [B] used for beams in Figure 3.16a by the method given in Appendix D.

The expression for total strain energy was taken as equation (1.8) with the term σ_z^2 omitted. In terms of the stress resultants this gives the strain energy function as

$$U = \frac{1}{2E}\iint\left[\frac{12}{h^3}\left(M_x^2 + M_y^2 - 2\nu M_x M_y + 2(1+\nu)\,M_{xy}^2\right)\right.$$

$$\left. + \frac{12(1+\nu)}{5Eh}\left(Q_x^2 + Q_y^2\right) - \frac{12\nu q}{5h}\,(M_x + M_y)\right]\,dx\,dy \tag{4.54}$$

In terms of derivatives of w, including only those terms in h^2 and h^4 specified above the strain energy in a region may be written as

$$U = \frac{12D^2}{2Eh^3a^4}\int_0^1\int_0^1\left[(1-\nu^2)\left(\frac{\partial^2 w}{\partial\xi^2}\right)^2 + \left(\frac{\partial^2 w}{\partial\eta^2}\right)^2 + 2(1+\nu)\left(\frac{\partial^2 w}{\partial\xi\,\partial\eta}\right)^2\right)$$

$$+ \beta\left(\left(\frac{\partial^3 w}{\partial\xi^3}\right)^2 + \left(\frac{\partial^3 w}{\partial\eta^3}\right)^2 + 2\frac{\partial^3 w}{\partial\xi^3}\frac{\partial^3 w}{\partial\xi\,\partial\eta^2} + \frac{2\partial^3 w}{\partial\xi^2\partial\eta}\frac{\partial^3 w}{\partial\eta^3} + \left(\frac{\partial^3 w}{\partial\xi\,\partial\eta^2}\right)^2 + \left(\frac{\partial^3 w}{\partial\xi^2\partial\eta}\right)^2\right)$$

$$+ \left(2\alpha(2-\nu)(1-\nu^2) - \nu\gamma\right)\left(\frac{\partial^2 w}{\partial\xi^2}\frac{\partial^4 w}{\partial\xi^4} + \frac{\partial^2 w}{\partial\eta^2}\frac{\partial^4 w}{\partial\eta^4}\right) + \left(4\alpha(1-\nu^2) - 2\nu\gamma\right)\left(\left(\frac{\partial^2 w}{\partial\xi^2} + \frac{\partial^2 w}{\partial\eta^2}\right)\frac{\partial^4 w}{\partial\xi^2\partial\eta^2}\right)$$

$$+ \left(2\alpha\nu(1-\nu^2) - \nu\gamma\right)\left(\frac{\partial^2 w}{\partial\xi^2}\frac{\partial^4 w}{\partial\eta^4} + \frac{\partial^4 w}{\partial\xi^4}\frac{\partial^2 w}{\partial\eta^2}\right) + 4(1-\nu^2)\gamma\left(\left(\frac{\partial^4 w}{\partial\xi^3\partial\eta} + \frac{\partial^4 w}{\partial\xi\,\partial\eta^3}\right)\frac{\partial^2 w}{\partial\xi\,\partial\eta}\right)$$

$$+ 2(1-\nu)(2-\nu^2)\alpha^2\left(\left(\frac{\partial^4 w}{\partial\xi^4}\right)^2 + \left(\frac{\partial^4 w}{\partial\eta^4}\right)^2\right) + 4\nu^2(1-\nu)\alpha^2\frac{\partial^4 w}{\partial\xi^4}\frac{\partial^4 w}{\partial\eta^4}$$

$$+ 8(1-\nu)\alpha^2\left(\left(\frac{\partial^4 w}{\partial\xi^2\partial\eta^2}\right)^2 + \frac{\partial^4 w}{\partial\xi^4}\frac{\partial^4 w}{\partial\xi^2\partial\eta^2} + \frac{\partial^4 w}{\partial\eta^4}\frac{\partial^4 w}{\partial\xi^2\partial\eta^2}\right) + 2(1+\nu)\gamma^2$$

$$\left.\left(\left(\frac{\partial^4 w}{\partial\xi^3\partial\eta}\right)^2 + \left(\frac{\partial^4 w}{\partial\xi\,\partial\eta^3}\right)^2 + \frac{2\partial^4 w}{\partial\xi^3\partial\eta}\frac{\partial^4 w}{\partial\xi\,\partial\eta^3}\right)\right]\,d\xi\,d\eta$$

in which $\alpha = \dfrac{h^2}{10(1-\nu)a^2}$

$\beta = \dfrac{(1+\nu)h^2}{5a^2}$

$\gamma = \dfrac{h^2}{5a^2}$ (4.55)

The analysis now follows the pattern described for beams in Section 3.7.3. The strain energy is expressed as

$$U = \frac{D}{2(1-\nu^2)a^4}\left[A^T C A\right] = \frac{D}{2(1-\nu^2)a^4} Q^T \left[B^T C B\right] Q \qquad (4.56)$$

the total potential energy evaluated as before and thenminimised with respect to each coefficient Q subject to the desired boundary conditions. The calculation of the displacement vector for a uniform load is discussed in Appendix D.

In order to satisfy the minimum condition for convergence, namely that continuity should be achieved for all derivatives up to and including one order lower than those contained in the strain energy expression, continuity of only the first 10 of the 16 derivatives mentioned earlier is required. Numerically it was found that attempts to solve the equations using $[B^T C B]$ as the 64x64 matrix were thwarted by loss of significance at about stage 42 of the elimination. However, when the 6 coefficients from Q relating to the derivatives at each node for which continuity is not necessary and the corresponding terms from $[B^T C B]$ were deleted the system proceeded to a solution without loss of significance, producing extremely accurate results for very thin plates with $a = l/2$. Since only symmetrical support and loading cases were

considered the number of equations to be solved is therefore only 40.

4.9.2 Application to the partial deflection method.

When using the partial deflection method the effects of transverse direct stress are ignored, so that the total strain energy due to bending and shear is

$$U = \frac{1}{2E}\iint\left[\frac{12}{h^3}\left(Mx^2 + My^2 - 2\nu MxMy + 2(1+\nu)\,Mxy^2\right)\right.$$

$$\left. + \frac{12(1+\nu)}{5h}\left(Qx^2 + Qy^2\right)\right]\,dxdy \qquad (4.57)$$

Substituting for these stress resultants from equations (4.34) - (4.38) and setting $S = 5(1-\nu)D/h^2$ as before, gives the following expression for the strain energy of a local region in terms of derivatives of w_b and w_s,

$$U = \frac{D}{2(1-\nu^2)a^4}\int_o^1\int_o^1\left[(1-\nu^2)\left(\left(\frac{\partial^2 w_b}{\partial\xi^2}\right)^2 + \left(\frac{\partial^2 w_b}{\partial\eta^2}\right)^2\right) + 2\nu(1-\nu^2)\frac{\partial^2 w_b}{\partial\xi^2}\frac{\partial^2 w_b}{\partial\eta^2}\right.$$

$$\left. + 2(1+\nu)(1-\nu)^2\left(\frac{\partial^2 w_b}{\partial\xi\partial\eta}\right)^2 + \frac{5(1+\nu)(1-\nu)^2}{h^2}\left(\left(\frac{\partial w_s}{\partial\xi}\right)^2 + \left(\frac{\partial w_s}{\partial\eta}\right)^2\right)\right]d\xi\,d\eta \qquad (4.58)$$

The highest order derivatives involved are second for w_b and first for w_s, and hence the minimum degree of continuity required for w_b is of slope, while w_s need only be continuous itself and may be discontinuous in its derivatives.

Appropriate displacement functions for w_b and w_s are then

$$w_b = a_1 + a_2\xi + a_3\eta + a_4\xi^2 + a_5\xi\eta + a_6\eta^2$$

$$+ a_7\xi^3 + a_8\xi^2\eta + a_9\xi\eta^2 + a_{10}\eta^3 + a_{11}\xi^3\eta + a_{12}\xi^2\eta^2 + a_{13}\xi\eta^3$$

$$+ a_{14}\xi^3\eta^2 + a_{15}\xi^2\eta^3 + a_{16}\xi^3\eta^3$$

or $w_b = [A_b]\,[\xi, \eta]$ (4.59)

giving freedom to w_b, $\frac{\partial w_b}{\partial \xi}$, $\frac{\partial w_b}{\partial \eta}$, and $\frac{\partial^2 w_b}{\partial \xi \partial \eta}$ at each node, and

$$w_s = \alpha_1 + \alpha_2 \xi + \alpha_3 \eta + \alpha_4 \xi \eta$$

or $w_s = [A_s]\,[\xi, \eta]$ (4.60)

Thus a typical region will have a total of 20 degrees of freedom, and in terms of the associated coefficients $[Q_b]$ and $[Q_s]$

$$[A_b] = [B_b][Q_b] \tag{4.61}$$

and $$[A_s] = [B_s][Q_s] \tag{4.62}$$

The coefficients of $[B_b]$ and $[B_s]$ are given in Appendix D.

The strain energy is then evaluated by

$$U = \frac{D}{2(1-\nu^2)a^4}\left(Q_b^T\left[B_b^T C_b B_b\right] Q_b + \frac{5(1+\nu)(1-\nu)^2}{h^2} a^2 Q_s^T \left[B_b^T C_s B_s\right] Q_s\right) \tag{4.63}$$

and the solution proceeds in the usual manner.

4.10 Comparison of numerical results for deflection

4.10.1 General comparison: simply supported square plate carrying uniformly distributed load.

This case was taken as standard for comparing the various methods outlined previously, as a series solution to Reissner due to Salerno and Goldberg (6) is available. The results obtained are shown in Figure 4.20 for $\nu = 0$ and $\nu = 0.3$ and values of depth ratio h/l up to 0.4. They are presented in the form of a ratio to the results given by classical theory.

The results obtained for the central deflection have the following general features:

(a) Partial deflection method

(i) The results obtained using finite differences and localised Rayleigh Ritz techniques are the same within the limits of computing accuracy, differing by less than 1% when P for the finite difference solution is 1/12 and a for the localised Rayleigh Ritz solution is $l/6$.

(ii) When $\nu = 0$ the results are the same as those given by the series solution to Reissner, but are larger than the latter when $\nu = 0.3$. This confirms the earlier conclusion that in adopting average rotations due to shear Reissner's theory effectively simply superimposes bending and shear effects. In ignoring the effects of transverse direct stress, the partial deflection method overestimates the deflection when $\nu \neq 0$.

———— Partial deflections and Reissner (series solution)

—— —— Reissner - finite differences

—— · —— Modified Reissner - finite differences

- - - - - - - - Modified Reissner - localised Rayleigh-Ritz

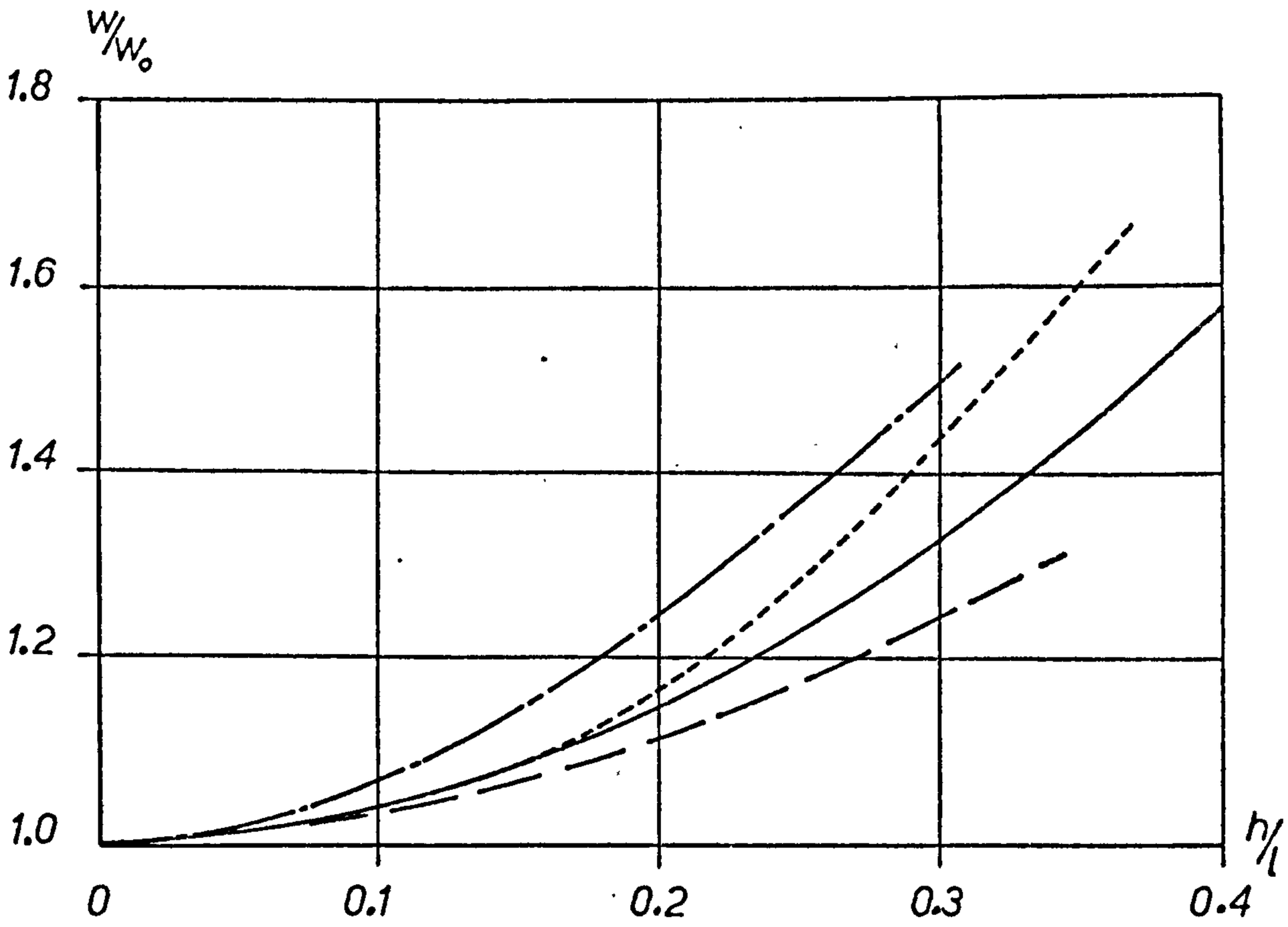

Figure 4.20 (a)

Central deflection ratio.

Simply supported square plate : uniform load ($\nu = 0$)

($w_o = 0.00406\ q l^4/D$)

——·——·—— Reissner (series solution)

———— Partial deflection method

—— —— Reissner - finite differences

——·—·—— Modified Reissner - finite differences

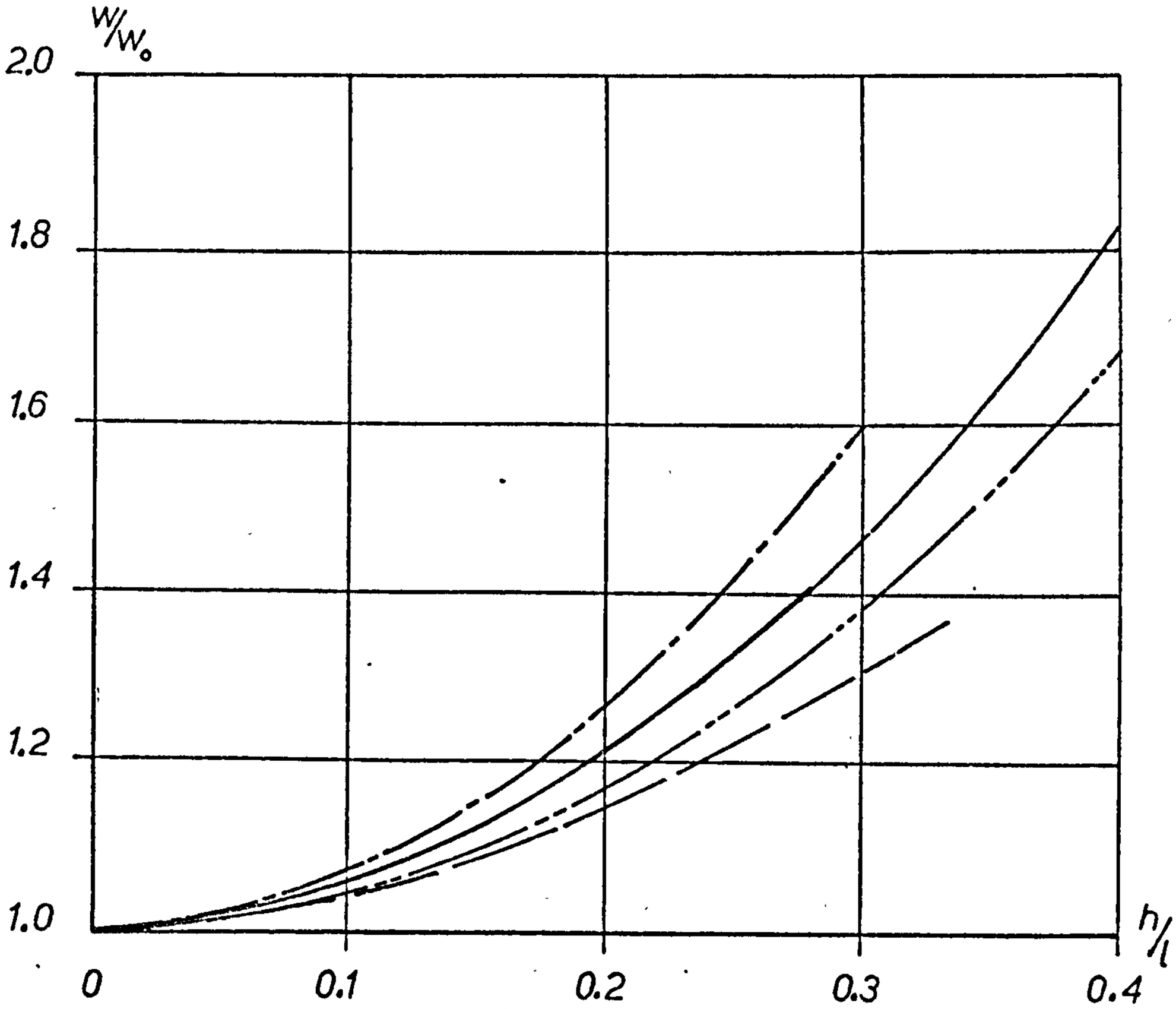

Figure 4.20 (b)

Central deflection ratio

Simply supported square plate : uniform load ($\nu = 0.3$)

($w_o = 0.00406\ q l^4/D$)

The general extent of the disparity may be seen from a typical set of values. For example, when $\nu = 0.3$ and $h/l = 0.3$ the central deflection given by the partial deflection method is 146% of the classical value, while the series solution to Reissner gives 138%. This excess is due to the omission of the effects of transverse direct stress.

(iii) No computing difficulties were encountered using this method for either the finite difference or localised Rayleigh-Ritz solutions.

(b) Reissner Theory - Finite difference solution

(i) Reference to Figure 4.20 shows that this set of results always underestimates the deflection, the difference from the series solution being of the order of 6% when $h/l = 0.3$.

(ii) The results lie on the smooth curves shown in Figure 4.20 for all values of h/l investigated.

(c) Modified Reissner theory

(i) Firstly, comparing the finite difference and localised Rayleigh-Ritz solutions for this theory it can be seen from the graph for $\nu = 0$ that both give an overestimate of the deflection. These differ slightly in that the localised Rayleigh-Ritz results follow the series solution up to $h/l = 0.2$
while the finite difference results are always greater than the series values but do not diverge from them so rapidly at larger values of h/l.

(ii) In the finite difference solution, as the value of the ratio h/l changes there are some coefficients in the solution matrix [A] which change sign and therefore there are values of this ratio for which a critical coefficient may become zero or very small, in which case a totally meaningless solution is obtained.

(iii) In general the localised Rayleigh-Ritz results fit well to the 'smooth curve shown, while the finite difference results show a little scatter.

(iv) In using finite differences no solution was obtainable for values of h/l greater than 0.3.

All the above results have been computed assuming that the boundary conditions are

$$w = M_n = \phi_t = 0$$

The third of these conditions can alternatively be replaced by $M_{nt} = 0$ in the Reissner and modified Reissner theories, and in the former case it was found to result in larger deflections, typically when $h/l = 0.025$ and $\nu = 0$ the increase in central deflection was found to be about 14%. However, it was found that this boundary condition produced very rapid changes in the stress function ψ in the region of the boundary, and thus extremely large values of Q_t along the boundary, a whole order or more greater than values of Q_n. Since Q_t would be zero here in the case of $\phi_t = 0$ being the boundary condition this solution has some unrealistic features at least numerically, and thus the deflection results should be treated with some caution.

In general, the application of $M_{nt} = 0$ as boundary condition seems to generate considerable problems numerically, and when used with the modified Reissner theory the resulting system of equations would not produce a solution which was acceptable from the point of view of boundary values of M_t.

4.10.2 General comparison: simply supported square plate carrying a central point load.

In dealing with a point loaded plate a very significant pattern emerges when the numerical results are compared. Considering each set of results individually in the first instance,

(a) Partial deflection method.

Both numerical methods gave identical results again, and the variation of central deflection with h/l for $\nu = 0$ and $\nu = 0.3$ is shown in Figure 4.21. All results fitted exactly to the curves shown.

(b) Reissner's theory

Attempts to obtain a solution to the point loaded case by finite difference methods were totally unsuccessful.

(c) Modified Reissner theory.

(i) The finite difference method gave results which such a wide scatter that no clear trend emerged.

(ii) The localised Rayleigh-Ritz method gave results throughout the range of values of h/l investigated, and these are shown for $\nu = 0$ in Figure 4.21. However, a serious underestimate of the deflection as predicted by the partial deflection method is found, the increase in deflection due to shear being little over half that

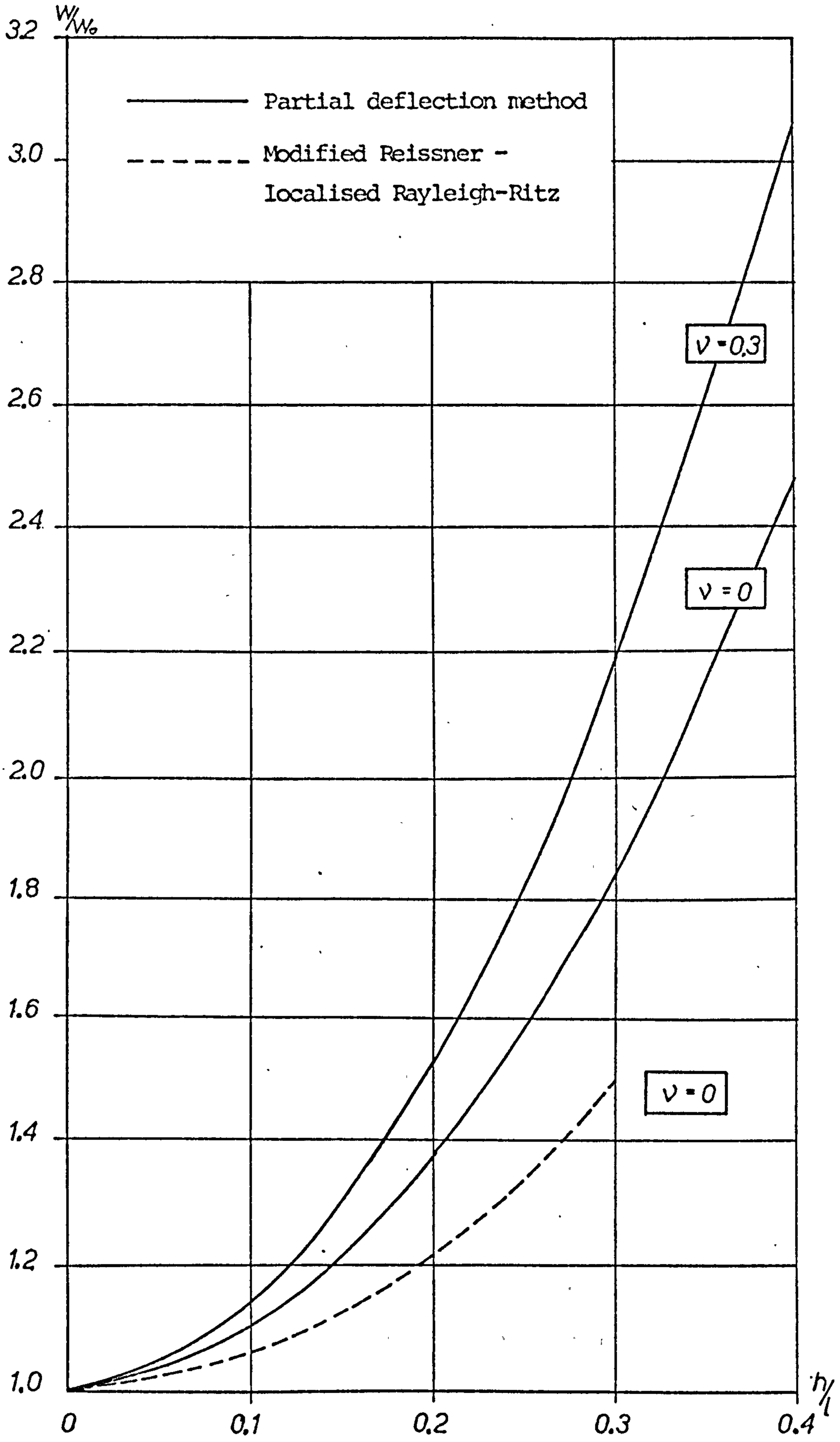

Figure 4.21

Central deflection ratio

Simply supported square plate : central point load

($w_o = 0.01160\ Pl^2/D$)

expected. Further, a fairly significant scatter in the results was found.

4.10.3 General conclusions.

Some general conclusions can be made at this stage before investigating other support and loading cases. From the foregoing section it is clear that both the Reissner and modified Reissner theories have a number of limitations in respect of the application of numerical techniques to them. There are two common features:

(a) In the case of uniform loading, although each method gives a consistent trend of results, some significant differences from the series solution are found.

(b) Concentrated loading presents an extremely problematic situation which presumably derives from attempts to cope with such terms as $\partial Q_x / \partial x$ which are theoretically infinite at the load, and even when Fourier representation of the load was used the variation of these terms between mesh points was still extremely large for a series representing anything near a true point load.

It was therefore concluded that the partial deflection method was likely to be the most generally useful technique to apply to other cases since the effects of bending and shear are completely separated except at certain boundaries, and the resulting systems of equations are perfectly behaved during computing. Attractive though the prospect of working in terms of a single variable may be, in numerical terms it would appear to be impractical in cases of concentrated loading.

In considering results obtained using the partial deflection method, it has to be remembered that the effects of transverse direct stress are not included and that therefore when $\nu \neq 0$ an overestimate of the deflection will result, although this will amount to only a few percent even for relatively large values of Poisson's ratio and depth/span ratio. In estimating the deflection due to shear alone, however, it is as accurate as Reissner's theory and suffers no limitations in the application of numerical techniques.

Further support and loading conditions are investigated in the following sections, in most cases using only the method of partial deflections.

4.10.4 Square plates with clamped boundaries.

Figures 4.22 and 4.23 show the results for central deflection for uniformly distributed loading and a central point load for values of Poisson's ratio of 0 and 0.3.

In plates with clamped and simply supported boundaries the actual increase in deflection due to shear is very nearly the same in both cases, but since the deflection due to bending is much smaller for clamped boundaries the percentage increase due to shear is much greater.

4.10.5 Corner supported plate carrying a central point load.

The results for central deflection for a square plate resting on simple supports at the corners and carrying a central point load are shown in Figure 4.24 and illustrate that the partial deflection method can equally well be applied to cases of point rather than line support, and to a case of free edges.

4.10.6 Square plate with two opposite edges simply supported and the other edges free.

This is another case of some interest since Salerno and Goldberg (6) indicate a series solution to Reissner's theory for it, although they do not include any supporting numerical results in their paper. The results for this case are given in Figure 4.25.

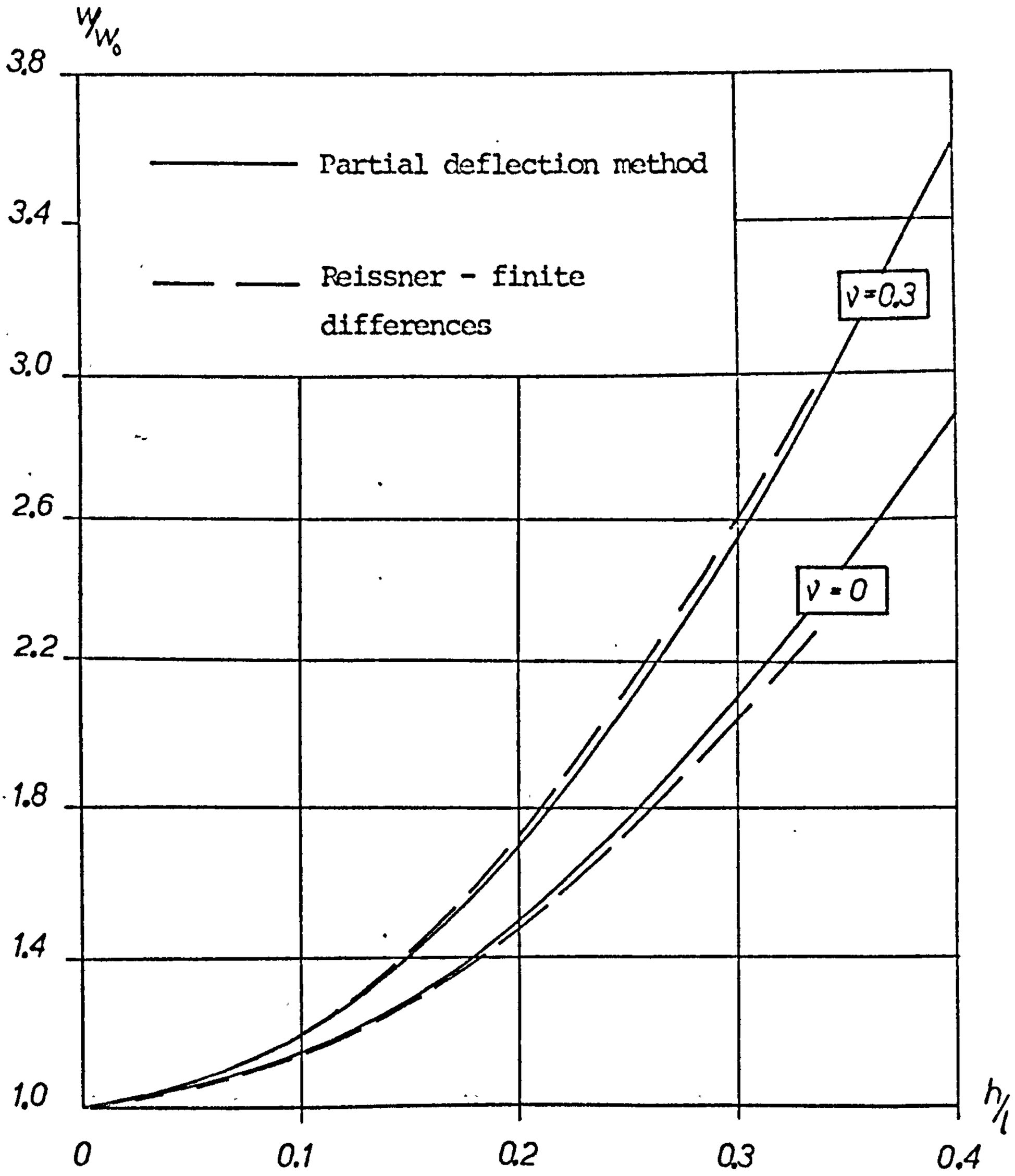

Figure 4.22

Central deflection ratio

Clamped square plate : uniform load

($w_o = 0.00126\ q l^4/D$)

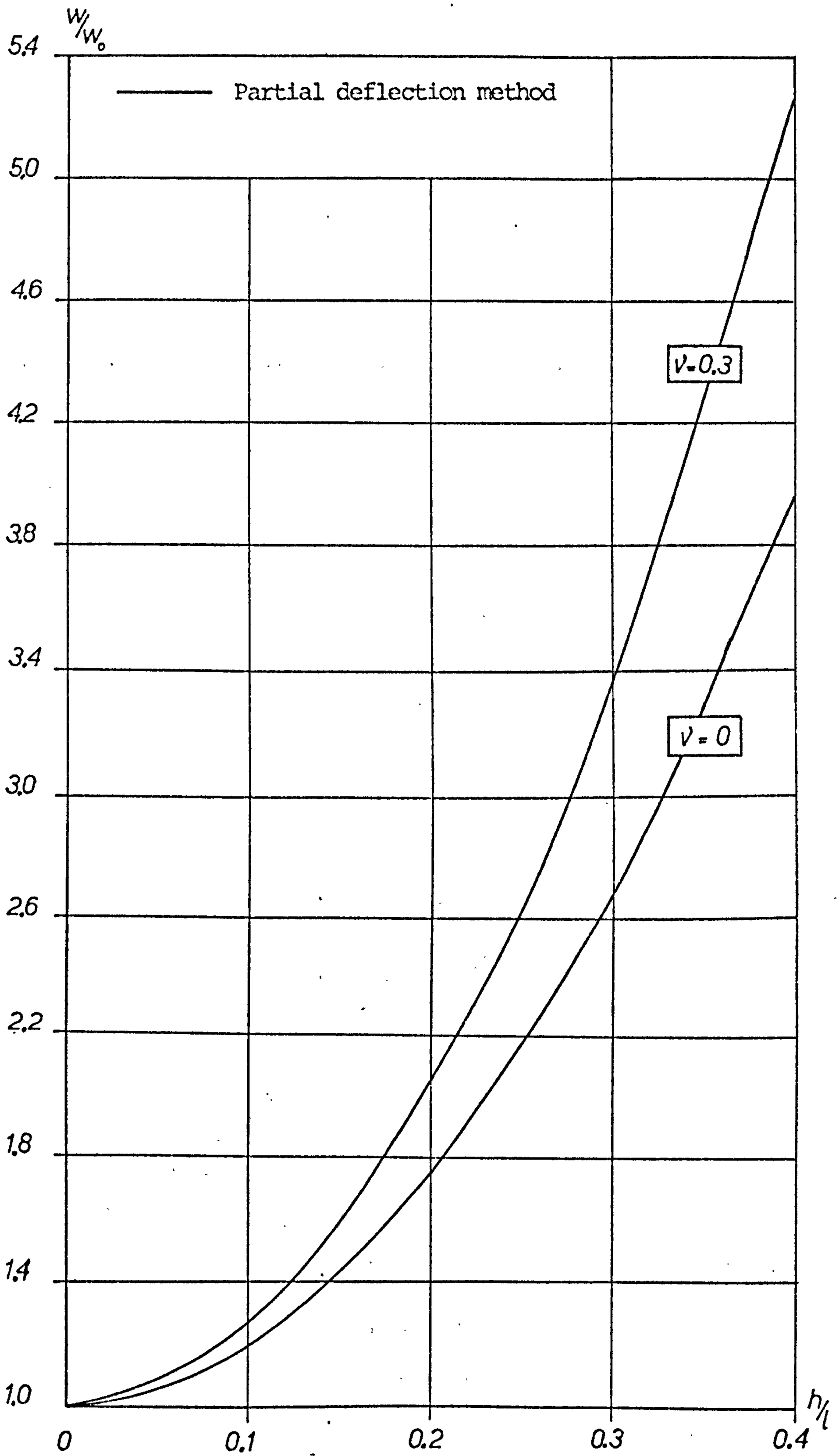

Figure 4.23

Central deflection ratio.

Clamped square plate : central point load

($w_o = 0.00560\ P l^2/D$)

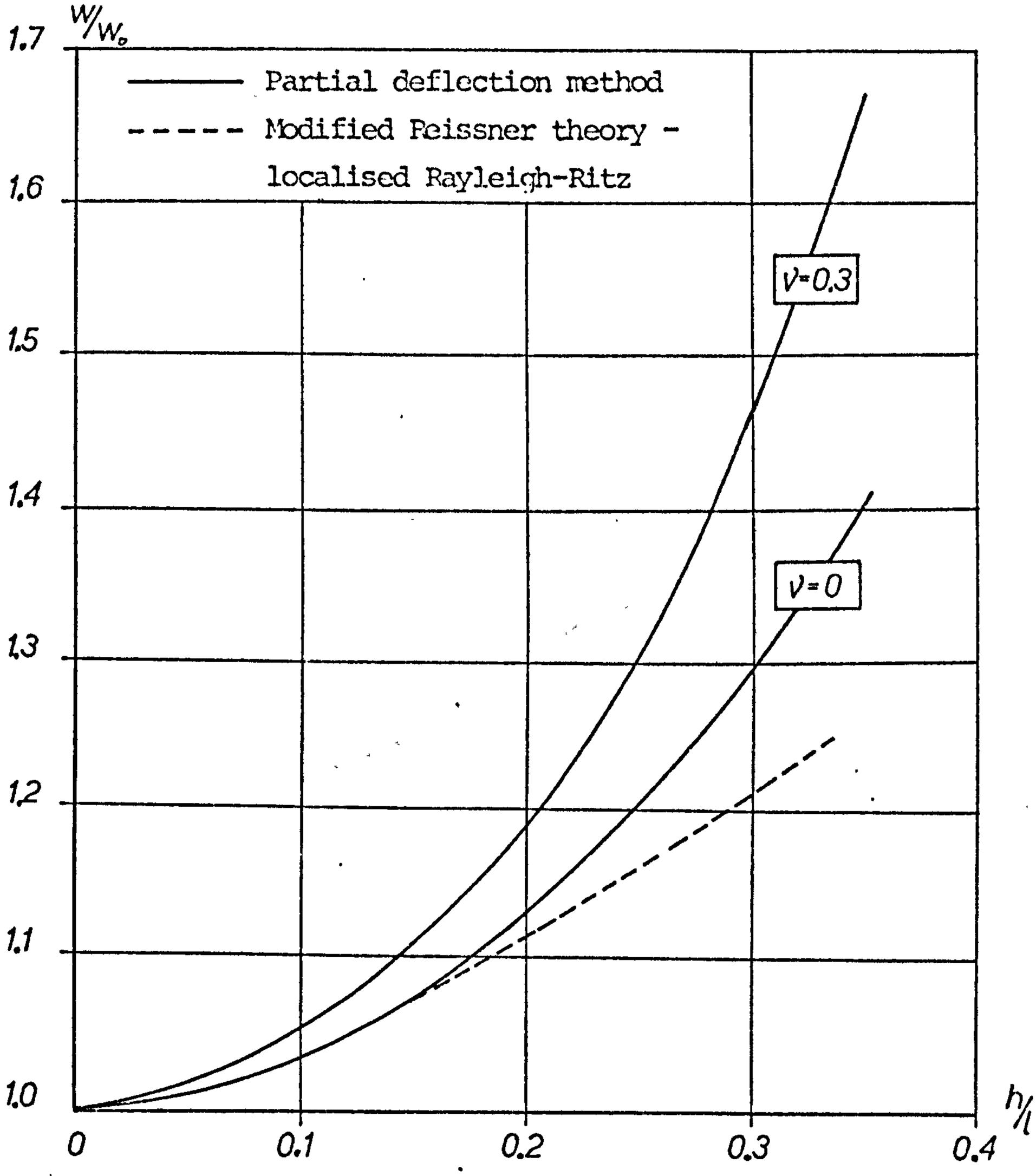

Figure 4.24

Central deflection ratio.

Square plate : corner supports : central point load

$$(\nu = 0, \quad w_o = 0.0449\ P\ell^2/D)$$
$$(\nu = 0.3, w_o = 0.0399\ P\ell^2/D)$$

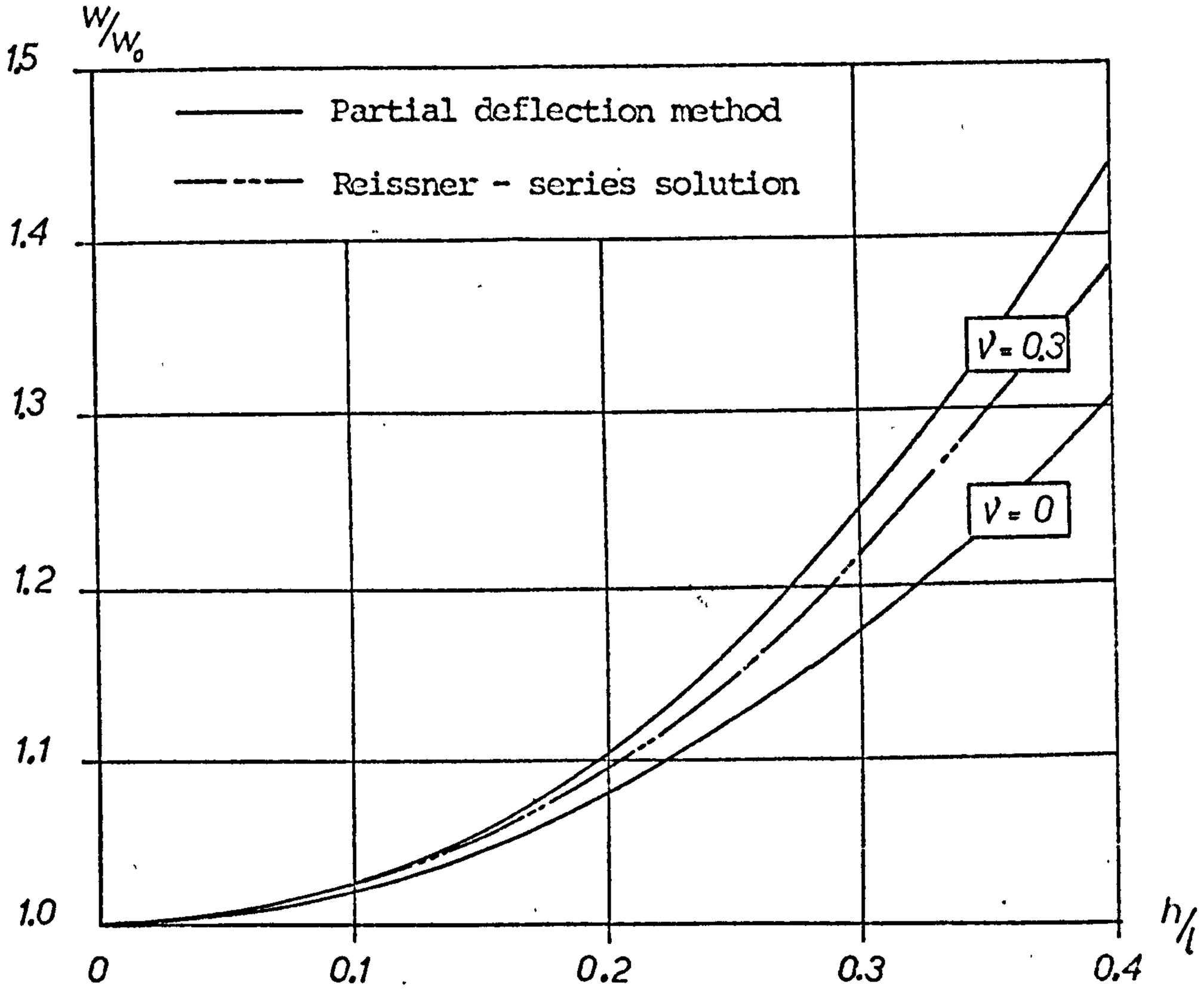

Figure 4.25

Central deflection ratio

Square plate with two opposite edges simply supported and other edges free : uniform load

($w_o = 0.01309\ q l^4/D$)

4.10.7 Summary of central deflection results.

The success in obtaining a solution in the range of problems covered in the foregoing sections indicates that any support or loading condition should be capable of solution by the partial deflection method. Neither the finite difference nor localised Rayleigh-Ritz method seems to have any particular advantage over the other in the cases considered here, but in general it may be that, bearing in mind the manner in which the problem is formulated numerically, the finite difference approach may be more convenient when force boundary conditions are imposed, while the position is reversed when displacement boundary conditions obtain. From a computing point of view the localised Rayleigh-Ritz solution is more compact.

From the graphs of Figures 4.20 - 4.25 of the actual numerical results it is possible to deduce algebraic expressions for the central deflection as given by the partial deflection method, and these are summarised here for the sake of convenience in Table 4.5, and the precise nature of the dependence upon depth/span ratio and Poisson's ratio can be clearly seen.

Boundary conditions	Loading	Classical central deflection, w_o	Central deflection ratio, w/w_o
Simply supported	Uniform load	$0.00406\ ql^4/D$	$1 + \frac{3.62}{(1-\nu)}\frac{h^2}{l^2}$
	Central point load	$0.01160\ Pl^2/D$	$1 + \frac{9.25}{(1-\nu)}\frac{h^2}{l^2}$
Clamped	Uniform load	$0.00126\ ql^4/D$	$1 + \frac{12.35}{(1-\nu)}\frac{h^2}{l^2}$
	Central point load	$0.00560\ Pl^2/D$	$1 + \frac{19.0}{(1-\nu)}\frac{h^2}{l^2}$
Corner supports	Central point load	$\nu = 0$ $0.0149\ Pl^2/D$	$1 + 5.93\frac{h^2}{l^2}$
		$\nu = 0.3$ $0.0399\ Pl^2/D$	$1 + 7.79\frac{h^2}{l^2}$
Two opposite edges simply supported, other edges free	Uniform load	$0.01309\ ql^4/D$	$1 + \frac{1.92}{(1-\nu)}\frac{h^2}{l^2}$

Table 4.5

Summary of central deflection formulae obtained by the partial deflection method.

4.11 Numerical results for stress resultants.

4.11.1 Introduction.

As might be expected from the consideration of beams, the modification to distributions of bending and twisting moments and shear forces are fairly insignificant in most cases. Hence great detail is not appropriate here, and a summary of the general trends is adequate. However, it is necessary to distinguish between the changes caused by a different statement of boundary conditions, by shear deformation and by transverse direct stress. These aspects are now considered for each type of boundary in turn.

4.11.2 Simply supported boundary.

Two different types of simply supported boundary have been noted, depending on the choice of the third boundary condition.

(a) If $\phi_t = 0$ is imposed as the third boundary condition, then the distribution of shear throughout the plate is identical to that of classical theory since precisely the same conditions obtain at the boundary. It follows that the distributions of bending and twisting moment remain unaltered by consideration of shear deformation.

However, in the Reissner type theories, transverse direct stress is shown to cause minor changes to the distribution of bending moment when Poisson's ratio is non-zero. For example, the central moment in a uniformly loaded square plate for $\nu = 0.3$ varies with depth as shown in Table 4.6, and when $h/l = 0.3$ the modification is only about 3%.

h/l	M/ql^2
0	0.0479
0.1	0.0482
0.2	0.0487
0.3	0.0494
0.4	0.0504

Table 4.6

Central bending moment: simply supported square plate: uniform load ($\nu = 0.3$)

(b) Greater changes in the distributions of moments would be expected if the third condition imposed were $M_{xy} = 0$, particularly near the boundary itself. In fact Reissner's theory was found to predict small overall increases in deflection and bending moment throughout the plate when this boundary condition is selected. But this cannot be investigated by the partial deflection method, and, numerically, the modified Reissner theory did not yield consistent results for this type of boundary. The most significant change which occurs is at the boundary itself, since the normal and tangential moments become principal moments, and the latter are no longer zero.

4.11.3 Clamped boundary.

Considering the three factors which may cause changes in the stress resultants in turn:

(a) Different statements of boundary conditions.

The conditions imposed in classical theory result in zero twisting moment along the boundary, and the partial

deflection theory has the same effect. Reissner's theory, however, setting $\phi_n = 0$ instead of the neutral surface slope (or the slope of w_b in the partial deflection method) has the result that the twisting moment is not necessarily zero. In fact it was nevertheless found to have very small values indeed, never exceeding 1% of the normal moment, so that the discrepancy is effectively negligible.

The third boundary condition imposed in using Reissner's theory is $\phi_t = 0$ which results in the elimination of the fairly substantial values of Q_t given by classical theory at the boundary. This in turn has its effect on the distribution of M_t along the boundary. These are very local effects, and the variations vanish rapidly in the interior of the plate.

(c) Effect of shear deformation.

As the partial deflection method takes no account of transverse direct stress the changes in stress resultants found from this theory are due solely to the effects of shear deformation.

Table 4.7 summarises the changes with depth in central bending moment and the normal moment and shear force at the mid-point of a side for $\nu = 0$.

h/l	(central moment)/ql^2	(normal moment)/ql^2	(shear force)/ql
0	0.0178	- 0.0493	0.438
0.1	0.0180	- 0.0491	0.429
0.2	0.0184	- 0.0486	0.411
0.3	0.0190	- 0.0481	0.395

Table 4.7

Variation with depth in central bending moment and normal moment and shear force at mid-point of a side.

Clamped plate: uniformly distributed load: $\nu = 0$.

(c) Transverse direct stress.

Inclusion of this term can have a significant effect on the distributions of bending moment when Poisson's ratio is non-zero, since the clamped support prevents the corresponding straining and hence generates additional stresses. The variation in central bending moment and mid-face normal moment with depth predicted by Reissner's theory are shown in Figure 4.26.

4.11.4 Free Edge

The main point here is the effect of different boundary conditions, since, while in Reissner type theories M_n, Q_n and M_{nt} are separately zero, in the other approaches only M_n and V_n are zero. This obviously makes local modifications, but in the case of the plate simply supported on two opposite faces with the other faces free these were found to have very little effect on the overall behaviour of the plate.

———— Central bending moment

— — — — Normal moment at mid-point of side

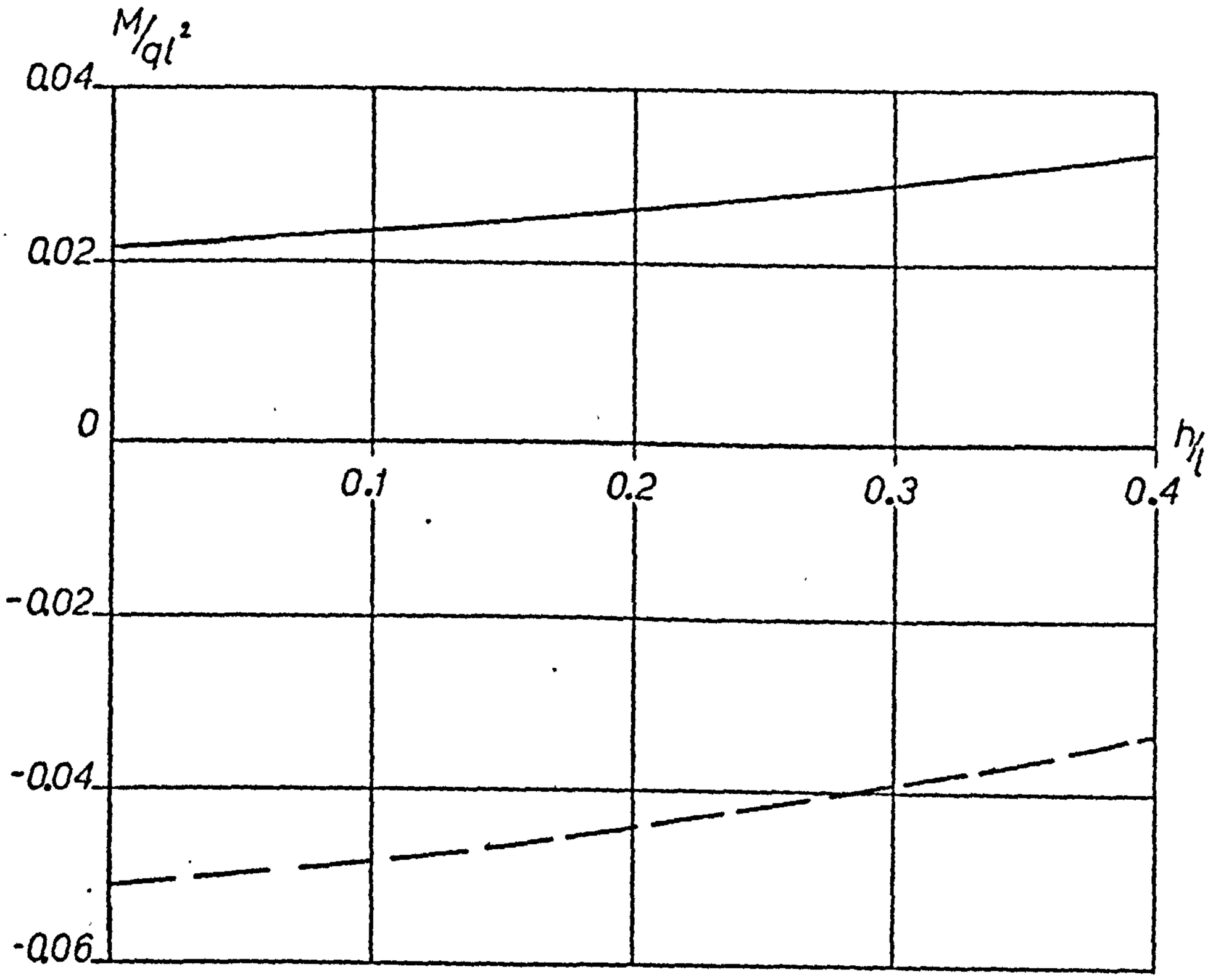

Figure 4.26

Variation in bending moment with depth/span ratio.

Reissner theory : clamped plate : uniform load ($\nu = 0.3$)

4.12 Experimental tests on plates

4.12.1 Description of tests

Tests were carried out on a series of plates 200 mm square and varying in depth from 10 mm to 60 mm, giving a range of depth/span ratios of 0.05 to 0.3. Since the effects being investigated here are of second order it was important that the support conditions chosen should represent exactly the theoretical conditions with which the results were to be compared. To reproduce experimentally the theoretical simple or clamped supports is extremely difficult, and thus the tests were carried out on corner supported plates, loaded at the centre.

The plates were cast from Araldite CY219 in the mould shown in Plate 1. A vacuum pump was connected to the mould to remove any air entrained during mixing. In order that each plate should be cast and cured under identical conditions four castings were made each measuring 300 mm x 300 mm x 80 mm deep. A pair of plates was then cut from the central 200 mm square in the following sequence:

casting 1	Plate depths	10 mm and 60 mm
2		20 mm and 50 mm
3		30 mm and 40 mm
4		25 mm and 35 mm

The excess of cast depth over total plate depth gave an adequate allowance for cutting by the band saw and subsequent machining flat and square. From each casting two beams of 25 mm square section were cut from the discarded edge strips, so that a comparison of the properties of each casting could be made.

The Clockhouse testing machine was again used for the tests and the general arrangement is shown in Plate 3 and Figure 4.27. The main features are

(a) Three of the corner supporting pillars were of fixed height, and the fourth adjustable so that contact at each corner of the plate was ensured at the start of each test. (See detail in Plate 4)

(b) The corners of the plate rest on quadrants of 10 mm diameter circular pads, which in turn rest on a spherical bearing in the top of the pillar, this arrangement permitting free rotation of the corner of the plate. The bearing area is relatively small, but large enough to circumvent the problems of embedment encountered with the beams on roller supports.

(c) The pillars rest on two sets of rollers at right angles so that no in-plane stresses could be generated by any corner restraint. In fact, for the very small deflections occurring in the tests this precaution was found to be unnecessary.

(d) In the beam tests it was found best to use a low load range and very accurate deflection measurement, and the same principle was adopted here. The load was applied through a proving ring for load measurement, and either directly to the plate through a ball bearing, or through a ball and square pad giving a bearing area 16.5 mm square. This latter arrangement simulates the finite difference load application model of the load being uniformly

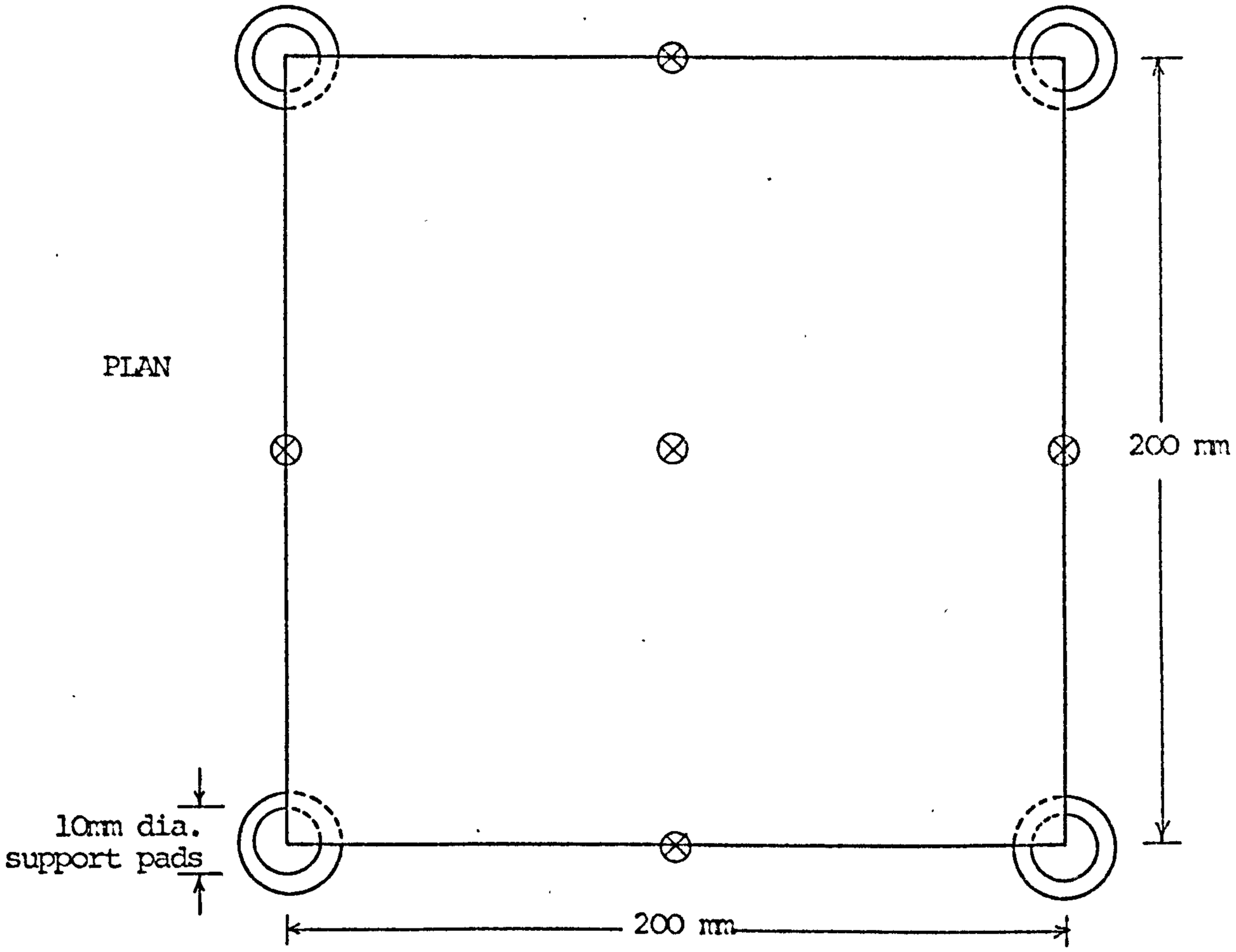

Figure 4.27

General arrangement of plate tests.

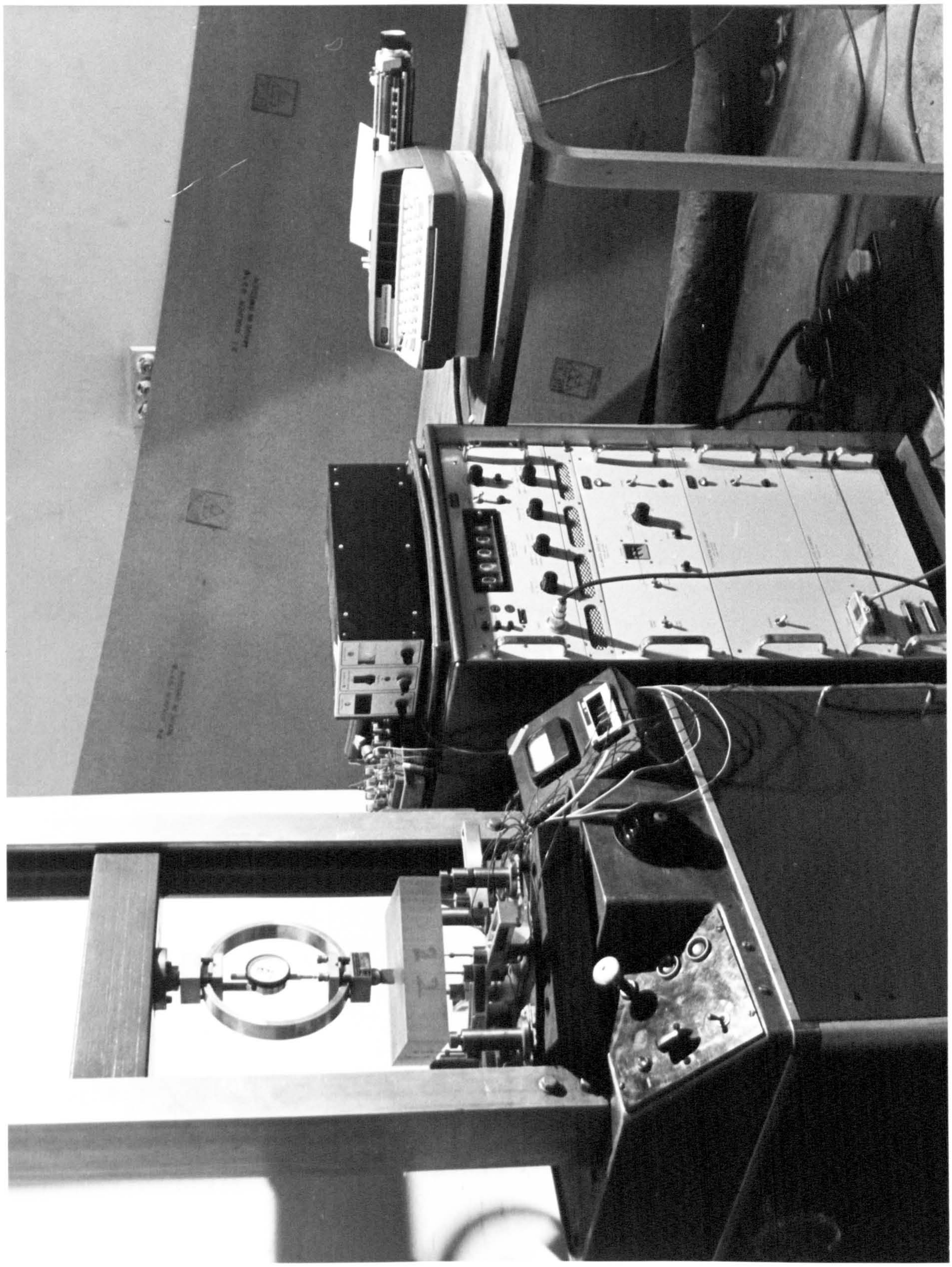

Plate 3

General arrangement for plate tests.

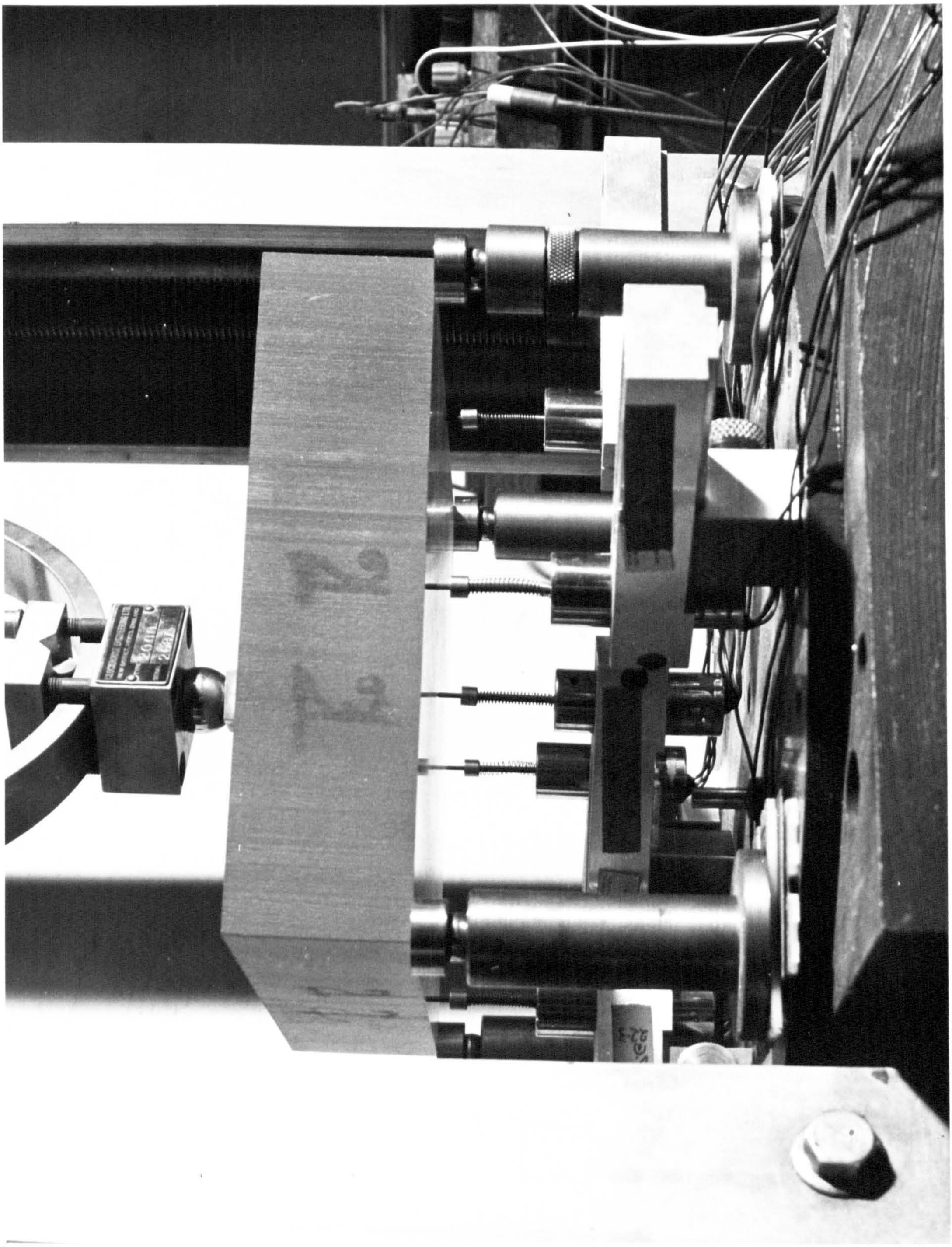

Plate 4

Detail of plate test rig.

distributed over a square of side equal to the mesh length, $l/12$. The load could be measured to an accuracy of 3N.

(e) Deflection was measured at the centre of the plate and at the mid-point of each face, using displacement transducers which enabled the displacement to be measured to an accuracy of 0.002 mm. The mid-point readings were taken to ensure that symmetry was achieved.

4.12.2 Experimental results

Tests on the beams cut from the plate edge strips confirmed that the same material properties were produced in each casting, and thus the deflection rates for the various plates can be compared in simple ratio without any correction for variation in Young's modulus or Poisson's ratio.

The bearing area was found to be adequate to render any embedment undetectable. Also the base was sufficiently rigid to prevent any relative movement between supports and displacement transducer mounting points. Inevitably a certain amount of settlement occurs in the ball seating arrangement, and in view of the extremely small displacements involved for the thicker plates it was necessary to measure this and make an appropriate correction.

Graphs were drawn of deflection against load, and the slopes determined by the method of least squares where necessary, although in nearly all cases the points fitted almost exactly to a straight line. The average values from four sets of readings were taken, and the results obtained are summarised in Table 4.8.

(1) h (mm)	(2) central deflection (mm/N)	(3) (2) x h^3	(4) (3)/4.77
10	4.77×10^{-3}	4.77	1.0
20	0.605×10^{-3}	4.85	1.02
25	0.318×10^{-3}	4.97	1.045
30	0.189×10^{-3}	5.11	1.075
35	0.123×10^{-3}	5.25	1.11
40	0.082×10^{-3}	5.25	1.11
50	0.0455×10^{-3}	5.69	1.195
60	0.0313×10^{-3}	6.78	1.422

Table 4.8

Summary of experimental results

Corner supported plate : central point load

In calculating the values in column (4) it is assumed that the deflection due to shear in the 10 mm plate is insignificant. If there were no shear deformation at all then the values in column (3) ought to be all the same, and hence their ratios in column (4) show clearly the increase in deflection due to shear which actually occurs.

These results are compared with the predictions of the partial deflection method in the graph of Figure 4.28. The validity of this method of presenting the results is, of course, dependent on the accuracy of the value for the deflection of the 10 mm plate, since all the other results are expressed as ratios of this value.

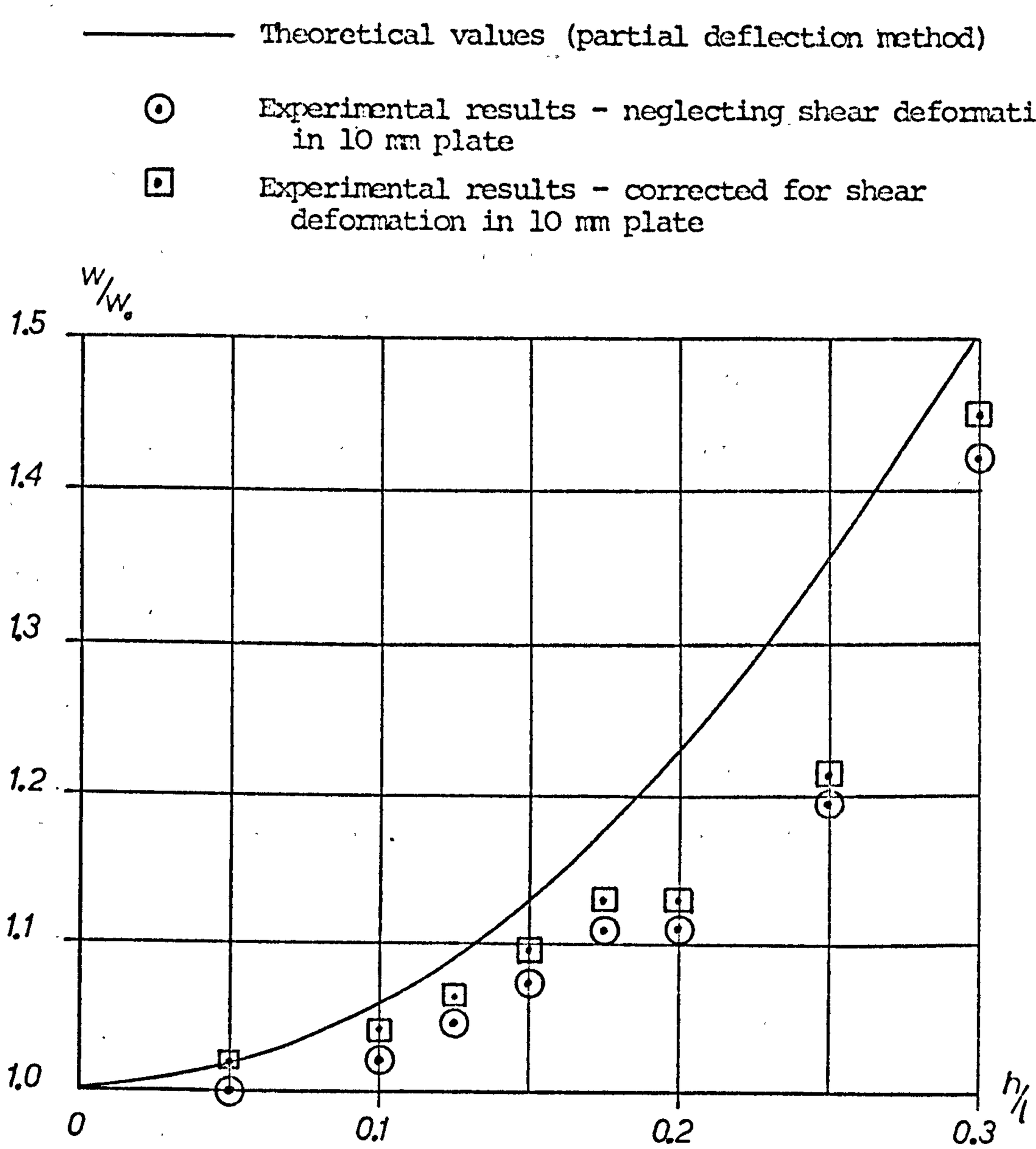

Figure 4.28

Experimental results

Central deflection ratio

Corner supported plate : central point load

The central deflection of this plate as given by the theoretical results for the appropriate values of Young's modulus and Poisson's ratio is 4.85×10^{-3} mm/N compared with the theoretical value of 4.77×10^{-3} mm/N obtained experimentally.

Figure 4.28 shows quite good agreement between the experimental and theoretical results. There are two factors which may explain the fact that all the experimental values are lower than those predicted by the partial deflection method. Firstly, all the results are expressed as ratios of the value for the 10 mm plate assuming that there is no deflection due to shear in this case. If an allowance for this had been made all the results would have been increased slightly as shown by the set of corrected points. The second fact is that in the comparable point loaded beam the partial deflection method was found to give an overestimate of the deflection for non-zero values of Poisson's ratio. In these tests the value of Poisson's ratio is almost 0.4, and it is therefore reasonable to assume that the theoretical results for this case would also be larger than those which might be expected in practice.

4.13 Conclusions

Detailed summaries have been given at various points in this chapter in order to establish the conclusions reached at each stage. Section 4.3.5 summarises the position of Reissner in relation to other theories, and Section 4.6 the place of the modified Reissner and partial deflection approaches developed in this chapter. Discussion of the theoretical results for deflection and stress resultants is given throughout Sections 4.10 and 4.11 and some specific issues are dealt with in Section 4.10.3.

It is convenient now to make a final summing up in very general terms. The principal points are:

(a) A modification to Reissner's theory has been proposed which is a sixth order system of partial differential equations in terms of transverse displacement as the only variable. For uniform loading finite difference and localised Rayleigh-Ritz methods have given quite good results, but as with Reissner's theory itself, there are limitations in dealing with point loads.

(b) The partial deflection method, with an appropriate choice of shear stiffness, can be developed to give a method for dealing with shear deformation which has been shown, from a theoretical point of view, to be identical to Reissner except for some localised boundary effects.

(c) Numerical solutions in terms of a single variable are always subject to occasional random ill-conditioning, since the interaction of bending and shear terms can cause

critical coefficients in the solution matrix to become very small, or even zero, with resulting loss of significance.

(d) In the partial deflection method the bending and shear terms do not interact numerically, and the resulting system of equations is amenable to numerical solution in all support and loading cases considered.

(e) The deflections due to shear deformation have been assessed for a number of cases.

(f) Modifications to the classical distributions of stress resultants have been found to arise from three causes - a different statement of boundary conditions, shear deformation and transverse direct stress. The first of these can cause significant differences at the boundary, but these have little effect on the overall behaviour of the plate. Modifications due to shear deformation alone are relatively minor, but transverse direct stress can have significant effect in clamped plates.

(g) Results for deflection in experimental tests for one loading and support case have shown reasonable agreement with the theoretical results.

CHAPTER 5

CONCLUSIONS

5.1 Introduction

Detailed summaries and discussions have been given at various points in this work so that the conclusions reached at each stage can be clearly seen before proceeding to the next section. It is not intended that this chapter should repeat these detailed conclusions, but rather that a general overall summary should be given in the form of an assessment of the extent to which the objectives stated in Section 1.3 have been achieved.

5.2 Appraisal of existing theories

(a) This investigation has confirmed the position of Reissner's theory as the most comprehensive of the existing two-dimensional approaches for plates, including the effects of both shear and transverse direct stress. It derives its two-dimensional nature from working initially in terms of three average displacements w, ϕ_x and ϕ_y. The last two of these are average rotations of sections initially normal to the neutral surface, and therefore express an average deformation due to shear, which is evaluated from work/energy considerations.

These approximate representations may lead to errors in the evaluation of both the internal state of stress and overall deflection behaviour. The extent of these errors has been assessed by developing a theory for beams which is based on Reissner's assumptions and comparing its predictions with those of the more refined solution of

Timoshenko and Goodier. It was shown that the deviations from linear of the distributions of longitudinal stress and strain are small, and that the consequent error in the overall deflection introduced by ignoring this is minute, even for large values of depth and Poisson's ratio.

It is clear that the fundamental approximations will not lead to any significant error, and the indications are that efforts to improve upon the basic assumptions by, for example, allowing for non-linearity in the distribution of bending stress, are not likely to convey any commensurate advantages.

(b) Reissner's theory has been shown to amount, in effect, to a superposition of curvatures due to bending, shear and transverse direct stress. With respect to shear it can be demonstrated that some other theories (notably that of Libove and Batdorf) lead to the same results providing that an appropriate shear stiffness is chosen.

(c) The principal limitation to Reissner's theory is the difficulty of obtaining analytical solutions, and the most obvious omission in all the theories is an attempt to deal with concentrated loading. Clearly a theory must be amenable to the application of numerical methods if it is to be useable for complex boundary geometry or loading.

(d) The partial deflection method is well established for sandwich beams and plates, and it has been demonstrated that the general approach can be readily applied to homogeneous beams and plates. Although it takes no account of transverse direct stress, in its treatment of shear it can be shown to be the same as Reissner, given a suitable choice of shear stiffness. The situations in whichthis approach amounts to a simple superposition of deflection due to bending and shear have been noted for both beams and plates.
For beams it has been shown analytically that the deflection results given by this method will always be identical with those predicted by the theory based on Reissner's assumptions if only the effects of shear deformation are considered. For plates the situation is not so straightforward, as for clamped and free edges the boundary conditions have to be formulated in a different manner. However, it has been confirmed that apart from some differences in the distributions of stress resultants adjacent to the boundary this has a negligible effect on the overall behaviour of the plate.

5.3 Development of a theory in terms of a single variable.

(a) A theory for plate bending containing the effects of both shear deformation and transverse direct stress has been developed which is based on Reissner's assumptions, and yet is in terms of transverse displacement as the only variable. It has been shown that such a theory can only be stated to a specified order of accuracy, and in this work h^2 has been regarded as adequate, error terms being of order h^4.

(b) This theory is a sixth order system of equations, and therefore requires the satisfaction of three conditions at each boundary.

(c) The theory has been applied to beams for purposes of comparison only, and to the order of accuracy stated the results obtained are identical with those given by the theory based on Reissner's assumptions.

5.4 Application of numerical methods

(a) Finite difference methods have been applied to the solution of Reissner's theory for plates and, together with localised Rayleigh-Ritz techniques, to the

modified Reissner theory and the partial deflection method. Simply supported, clamped and free boundaries have been considered and solutions investigated for uniformly distributed and concentrated loading.

(b) For Reissner's theory, the finite difference method was successfully applied to uniformly loaded plates with simply supported and clamped boundaries. In the first case the results are an underestimate of the deflections given by an existing series solution, while for the second case excellent agreement is found with the results predicted by another method. The error in the first case may illustrate that there are numerical difficulties in dealing with the stress function, which may be very small or zero throughout most of the plate but subject to very rapid changes at the boundary and the external fictitious mesh points. It was found that no useful results could be obtained for cases involving concentrated loads, and it can only be assumed that this is due to failure to cope with terms such as $\partial q/\partial x$, $\partial q/\partial y$ and Δq involved in the formulation of the theory.

(c) Both numerical methods were applied to the modified Reissner theory for beams and plates.

For uniformly loaded beams the finite difference method gave results identical with those obtained analytically, but for point loaded cases results were not obtainable for values of h/l in excess of 0.2. The localised Rayleigh-Ritz solution gave acceptable results for both

uniform and point loading, but the main difficulty is the choice of terms to be included in the energy function. Some inconsistency has to be accepted here, and the best compromise appears to be for each stress resultant to be of specified order of accuracy, although not necessarily the same for moments and shears.
The pattern for plates is similar. For uniformly loaded plates there is a greater spread in the results than in the case of beams, but both numerical methods give consistent trends of results fitting well to smooth curves. While the finite difference method showed a total inability to cope with concentrated loads, the localised Rayleigh-Ritz formulation did yield results, although these were subject to a greater scatter than for uniform loading. It was found to be helpful to mix the order of accuracy of the finite difference equivalents used, giving careful regard to the order of magnitude of the various coefficients.

(d) The partial deflection method keeps the bending and shear effects separate in the computation and as a result solutions by both finite difference and localised Rayleigh-Ritz methods give completely consistent solutions in all cases examined, without any systemmatic or random errors being introduced numerically.
The drawbacks of this approach are that it takes no account of transverse direct stress and that it limits

the number of boundary conditions which can be satisfied to two. However, the work on other theories has identified the effects of transverse direct stress and enabled their magnitudes to be assessed. These are principally to cause a relatively small reduction of deflection in simply supported cases, and a change in the distributions of moments in clamped cases which may be significant for large values of depth and Poisson's ratio together. The boundary condition problem may cause some local differences but certainly is no limitation to an investigation of the overall behaviour. The partial deflection method for plates is a simple superposition of the deflections due to bending and shear only for simply supported boundaries. If a superposition approach is used in other cases the values of w_b and w_s would be incompatible at the boundaries, with incorrect values of shear resulting, and further, changes in the distributions of moments due to shear deformation would not be detected. However, it was found that in spite of these inconsistencies, at the centre of a clamped plate, for example, the error in the deflection would be less than 1% even for large values of h/l. In some situations this apparently crude approach might prove quite useful providing its limitations are understood, since it would enable the effects of shear to be separately assessed and added to a known bending solution.

(e) A random numerical problem has been noted, namely that in any approach in which the bending and shear effects interact in the solution matrix, some critical coefficients may change sign as the ratio h/l is changed, and hence for certain values may be very small or even zero. A corresponding loss of significance in the computation will then result and a spurious solution be obtained.

(f) Finally, it is useful to make an assessment of the relative merits of the finite difference and localised Rayleigh-Ritz approaches for this type of work. Perhaps the only significant point to note about their actual performance is that, apart from the application to the partial deflection theory, the finite difference method is not suitable for dealing with concentrated loading in theories which include the effects of shear deformation. This is presumed to be because of its concern with the high local rate of loading and rate of change, whereas the localised Rayleigh-Ritz method depends upon an evaluation of the work done by the load.

Due to rapid development of the finite element formulation in recent years the finite difference approach has been largely neglected. Certainly for analysis of shapes which would necessitate a variable grid size the computer formulation of a finite difference analysis would prove more cumbersome, but the two methods are certainly of comparable accuracy.

In the particular applications of this work the higher order equations require more fictitious points in the finite difference formulation and hence larger numbers of unknowns. Where the localised Rayleigh-Ritz method uses high order displacement functions the resulting increase in accuracy means that the local regions need not be small and hence the total number of equations involved may be appreciably less than in the finite difference method.

5.5 Experimental results.

(a) The absence of experimental verification of the theoretical predictions has been noted and a series of tests conducted on both beams and plates.

(b) Tests to investigate the deflection due to shear deformation are far from easy to conduct as there are difficulties at both ends of the depth range. At the lower end the effect being investigated is very small, while at the upper end of the scale the overall deflections are very small and hence secondary effects such as embedment and movements in the test equipment become highly significant. Thus throughout the range of depth very accurate deflection measurement is called for and for the deeper specimens very careful investigation of secondary effects is essential.

(c) Having recognised these problems the tests can be regarded as having provided useful confirmation of the theoretical results for one support and load case for beams and plates.

5.6 Applications and suggestions for further work.

5.6.1 Introduction.

Two alternative theoretical formulations are suggested in this section, one for Reissner's theory and the other for the modified Reissner theory, which may have certain advantages when numerical methods are used.

This is followed by a brief review of several fields where shear deformation is known to be important, with an indication of how the theories discussed in this thesis could be employed.

5.6.2 Theoretical approaches.

5.6.2.1 Solution of Reissner in terms of three variables.

Another approach to the solution of Reissner's theory which does not involve the use of the stress function is to work in terms of the three generalised displacements w, ϕ_x, ϕ_y as variables. This has similarities with the finite element approach of Clough and Felippa (30), and also with the solution of Williams and Chapman (24) using the equations of Libove and Batdorf (23) and working in terms of w, Q_x, Q_y.

The governing equilibrium equations (1.10) - (1.12) with the stress resultants written in terms of w, ϕ_x, ϕ_y from equations (4.1) - (4.5) become

$$\frac{\partial \phi_x}{\partial x} + \frac{\partial \phi_y}{\partial y} + \frac{\partial^2 w}{\partial x^2} + \frac{\partial^2 w}{\partial y^2} = - \frac{h^2}{5(1-\nu)} \frac{q}{D} \qquad (5.1)$$

$$\frac{h^2}{5(1-\nu)} \left(\frac{\partial^2 \phi_x}{\partial x^2} + \frac{1+\nu}{2} \frac{\partial^2 \phi_y}{\partial x \partial y} + \frac{1-\nu}{2} \frac{\partial^2 \phi_x}{\partial y^2} \right) - \left(\phi_x + \frac{\partial w}{\partial x} \right) = 0 \qquad (5.2)$$

$$\frac{h^2}{5(1-\nu)} \left(\frac{\partial^2 \phi_y}{\partial y^2} + \frac{1+\nu}{2} \frac{\partial^2 \phi_x}{\partial x \partial y} + \frac{1-\nu}{2} \frac{\partial^2 \phi_y}{\partial x^2} \right) - \left(\phi_y + \frac{\partial w}{\partial y} \right) = 0 \qquad (5.3)$$

These equations are correct for uniform loading including the effects of transverse direct stress. Non-uniform loading would introduce terms such as $\nu\partial q/\partial x$ and in such cases, especially for concentrated loads involving very high rates of change of loading, it would be simpler in the first instance to omit the effects of transverse direct stress.

The solution of Libove and Batdorf in terms of w, Q_x, Q_y in finite difference form involves the complication of having to use backward differences at the boundary in the second and third equilibrium equations, since they involve terms such as $\partial^3 w/\partial x^3$ and only one fictitious value of each variable can be found for each boundary mesh point. Working in terms of w, ϕ_x, ϕ_y as suggested here would avoid this difficulty since no derivatives above second order are included.

5.6.2.2 Solution of the modified Peissner theory in terms of two variables.

The form of the modified Reissner governing equation has been shown to be

$$\triangle^2 w + \frac{h^2(2-\nu)}{10(1-\nu)} \triangle^3 w = \frac{q}{D} \qquad (5.4)$$

If a new variable w_1 is defined as

$$w_1 = w + \frac{h^2(2-\nu)}{10(1-\nu)} \triangle w \qquad (5.5)$$

then (5.4) can be rewritten as

$$\triangle^2 w_1 = q/D \qquad (5.6)$$

Noting (5.5) the shear forces can be written as

$$Q_x = -D\left(\frac{\partial^3 w_1}{\partial x^3} + \frac{\partial^3 w_1}{\partial x \partial y^2}\right) \tag{5.7}$$

$$Q_y = -D\left(\frac{\partial^3 w_1}{\partial y^3} + \frac{\partial^3 w_1}{\partial x^2 \partial y}\right) \tag{5.8}$$

Suitable expressions for bending and twisting moments are found by substituting for q from (1.10) in (4.20) to (4.22) and then for Q_x and Q_y from (5.7) and (5.8) giving finally

$$M_x = -D\left(\frac{\partial^2 w}{\partial x^2} + \nu\frac{\partial^2 w}{\partial y^2}\right) - \frac{h^2 D}{10(1-\nu)}\left((2-\nu)\frac{\partial^4 w_1}{\partial x^4} + 2\frac{\partial^4 w_1}{\partial x^2 \partial y^2} + \nu\frac{\partial^4 w_1}{\partial y^4}\right) \tag{5.9}$$

$$M_y = -D\left(\frac{\partial^2 w}{\partial y^2} + \nu\frac{\partial^2 w}{\partial x^2}\right) - \frac{h^2 D}{10(1-\nu)}\left((2-\nu)\frac{\partial^4 w_1}{\partial y^4} + 2\frac{\partial^4 w_1}{\partial x^2 \partial y^2} + \nu\frac{\partial^4 w_1}{\partial x^4}\right) \tag{5.10}$$

$$M_{xy} = (1-\nu)D\frac{\partial^2 w}{\partial x \partial y} + \frac{h^2 D}{5}\left(\frac{\partial^4 w_1}{\partial x^3 \partial y} + \frac{\partial^4 w_1}{\partial x \partial y^3}\right) \tag{5.11}$$

This formulation would be particularly amenable to a finite difference solution with (5.6) and (5.5) as the governing equations and the boundary conditions being satisfied in the usual manner. It has the advantage of avoiding fifth and sixth order derivatives, and also ensures that coefficients in the finite difference molecules do not contain both a constant and a term in h^2, with the exception of (5.5) where it is quite clear which, if any, values of h might cause difficulties.

5.6.3 Sandwich and cellular structures.

5.6.3.1 Existing approaches.

Excellent summaries and bibliographies on this topic are given by Plantema (21) and Allen (22), and it is sufficient here to

note one or two points relevant to the theme of this work. The principal objective has been to describe the overall behaviour of beams and plates, and Reissner (34) concludes that the effects of transverse direct stress are negligible in this context. Allen also concludes that general theories including transverse core deformation have proved more or less intractable in practice. They are of much greater significance in local effects where, for example, the transverse core flexibility might result in short wave wrinkling instability of the faces.

For an overall treatment the partial deflection method has been used effectively and is subject only to the various constraints noted in this work. Although a uniform shear strain through the depth of the core is generally assumed this is not essential and any appropriate method of assessing the shear stiffness could be used.

5.6.3.2 A form of the modified Reissner theory suitable for sandwich structures.

Assuming that for sandwich structures the effects of transverse direct stress can be ignored then the equations derived from Reissner are identical in form with those of Libove and Batdorf, since both are then a superposition of curvatures due to bending and shear. (see Section 4.3.1) If the shear stiffness is defined as S the resulting system of equations can be subjected to the modifying procedure used in Section 4.4, repeatedly substituting for derivatives of shear forces and neglecting terms in $(D/S)^2$ or higher powers which are the equivalent of the h^4 terms in the homogeneous case.

For an isotropic sandwich plate the following equations are then obtained:

the governing equation is

$$\Delta^2 w + \frac{1}{S}\Delta^3 w = q/D \qquad (5.12)$$

the bending and twisting moments are

$$M_x = -D\left(\frac{\partial^2 w}{\partial x^2} + \nu\frac{\partial^2 w}{\partial y^2}\right) - \frac{D}{S}\left(\frac{\partial^4 w}{\partial x^4} + (1+\nu)\frac{\partial^4 w}{\partial x^2\partial y^2} + \nu\frac{\partial^4 w}{\partial y^4}\right) \qquad (5.13)$$

$$M_y = -D\left(\frac{\partial^2 w}{\partial y^2} + \nu\frac{\partial^2 w}{\partial x^2}\right) - \frac{D}{S}\left(\frac{\partial^4 w}{\partial y^4} + (1+\nu)\frac{\partial^4 w}{\partial x^2\partial y^2} + \nu\frac{\partial^4 w}{\partial x^4}\right) \qquad (5.14)$$

$$M_{xy} = D(1-\nu)\frac{\partial^2 w}{\partial x\partial y} + \frac{D(1-\nu)}{S}\left(\frac{\partial^4 w}{\partial x^3\partial y} + \frac{\partial^4 w}{\partial x\partial y^3}\right) \qquad (5.15)$$

and the shear forces

$$Q_x = -D\left(\frac{\partial^3 w}{\partial x^3} + \frac{\partial^3 w}{\partial x\partial y^2}\right) - \frac{D}{S}\left(\frac{\partial^5 w}{\partial x^5} + \frac{2\partial^5 w}{\partial x^3\partial y^2} + \frac{\partial^5 w}{\partial x\partial y^4}\right) \qquad (5.16)$$

$$Q_y = -D\left(\frac{\partial^3 w}{\partial y^3} + \frac{\partial^3 w}{\partial x^2\partial y}\right) - \frac{D}{S}\left(\frac{\partial^5 w}{\partial y^5} + \frac{2\partial^5 w}{\partial x^2\partial y^3} + \frac{\partial^5 w}{\partial x^4\partial y}\right) \qquad (5.17)$$

5.6.3.3 Box and cellular structures.

The overall behaviour of box and cellular structures can be represented by an equivalent sandwich system, and this has been the subject of some recent work. The discussion on Morley (25) brings together some relevant references on this topic from which it is clear that the principal difficulties are the determination of appropriate stiffness parameters and the effect of stiff end diaphrams.

5.6.4 Non-linear and time-dependent problems.

The present work has been confined to linear elastic problems, but it could profitably be extended to materials with non-linear elastic stress/strain relationships. The solution for this type of problem would require an incremental approach considering the cumulative effect of successive changes of loading.

Research could also be usefully carried out in connection with materials subject to creep. Where bending and shear are both significant the time-dependent problem may be complicated by creep due to bending and shear proceeding at different rates. There is the need for both the provision of experimental data within this area, and the establishment of a theoretical method for incorporating this in the analysis of the behaviour of such structures.

5.6.5 Beams and plates on elastic foundation.

Ratcliffe (35) suggests that shear deformation can become significant when beams are supported on elastic foundations, even for large values of span/depth ratio. Investigation of this effect in connection with plates could readily be conducted using the methods developed in this work.

Structures on soil foundations could be considered here, and also mining structures where subsidence can result in loss of contact over part of the structure, shear deformation being of potential importance in both cases.

5.6.6 Lower bound solutions.

Parkhill (36) suggests a method of establishing lower bounds by evaluating the elastic moments throughout the segments bounded by a given yield line pattern along which yield moments are applied. The case he considered is a square slab, uniformly loaded and simply supported, but the discussion points out that the method is not of general application since in cases other than this one it would not be possible to maintain continuity of M_n, M_{nt} and Q_n across the yield line, as this would require a plate theory which enables the satisfaction of three conditions at each boundary.

It was this problem which initiated the work in this thesis, since Parkhill's general approach clearly calls for the use of a Reissner type theory. However, early attempts to apply Reissner's theory showed that there were difficulties from both theoretical and numerical viewpoints. Hence the objectives of this work were directed towards an examination of theories which include shear deformation, and their use in conjunction with numerical methods. An early interest in Parkhill's work, which used finite difference methods, explains the slight predominance of the same approach in this work.

Returning briefly to the lower bound problem, the shape of the finite difference molecules involved make the investigation using Reissner's theory practically intractable since the molecules for stress resultants involve mesh points outside the basic biharmonic.

However, in the modified Reissner theory no mesh points other than those incorporated in the molecule for the governing equation are required for the stress resultants, making it suitable for examining lower bound solutions.

The partial deflection method would not be applicable since it would not allow the necessary continuity to be satisfied.

5.6.7 Vibration and buckling problems.

Timoshenko (37) gives a solution to the vibration of a beam in which the effects of shear deformation are included. In essence the governing elemental equation

$$\frac{\partial^2 M}{\partial x^2}\,dx = -\rho A\,dx\,\frac{\partial^2 y}{\partial t^2} \qquad (5.18)$$

is written in such a way that shear deformation is taken into account so that M is no longer proportional to the curvature. The effect begins to assume some importance for higher modes of vibration, where the depth of the beam is a more significant fraction of the wavelength.

A similar situation arises in buckling problems, and in the typical equation

$$\frac{d^2 M}{dx^2} + P\frac{d^2 w}{dx^2} = 0 \qquad (5.19)$$

M would be redefined to allow for the shear component of curvature. The buckling load is found to be modified to

$$P = \frac{n^2\pi^2 EI/l^2}{1 - n^2\pi^2 EI/(l^2 S)} \qquad (5.20)$$

and is equal to the Euler load when the shear stiffness, S, is infinite.

The modification is unlikely to be significant in practical cases, but a promising field of further research is in the field of post-buckling behaviour where shear deformation may lead to a further reduction in stiffness.

APPENDICES

APPENDIX A

DEVELOPMENT OF A THEORY FOR BEAMS BASED ON REISSNER'S ASSUMPTIONS

A.1 Introduction

A theory for beams is developed here which includes the effects of shear deformation and transverse direct stress. It is based on Reissner's assumptions and follows the general approach he originally used for plates.

A.2 Elastic properties in two dimensions

The elastic stress/strain relationships in two dimensions are

$$\epsilon_x = \frac{1}{E}(\sigma_x - \nu\sigma_z) \tag{A.1}$$

$$\epsilon_y = -\frac{\nu}{E}(\sigma_x + \sigma_z) \tag{A.2}$$

$$\epsilon_z = \frac{1}{E}(-\nu\sigma_x + \sigma_z) \tag{A.3}$$

$$\gamma_{xz} = \frac{\tau_{xz}}{G} \tag{A.4}$$

with $\sigma_y = \tau_{xy} = \tau_{yz} = 0$.

A.3 Strain energy and complementary energy

The strain energy for a two dimensional system is

$$U = \iiint (\sigma_x\epsilon_x + \sigma_z\epsilon_z + \tau_{xz}\gamma_{xz})\, dxdydz \tag{A.5}$$

and substituting for strains in terms of stresses from equations (A.1) to (A.4) gives

$$U = \frac{1}{2E}\iiint (\sigma_x^2 + \sigma_z^2 - 2\nu\sigma_x\sigma_z + 2(1+\nu)\tau_{xz}^2)dxdydz \tag{A.6}$$

The following distributions of stress are now assumed

$$\sigma_x = \frac{Mz}{I} \qquad (I = \frac{h^3}{12}) \tag{A.7}$$

$$\sigma_z = -\frac{3q}{4}\left(\frac{2}{3} - \frac{2z}{h} + \frac{1}{3}\left(\frac{2z}{h}\right)^3\right) \tag{A.8}$$

$$\tau_{xz} = \frac{3Q}{2h}\left(1 - \left(\frac{2z}{h}\right)^2\right) \tag{A.9}$$

So that the strain energy (A.6) can be rewritten in terms of stress resultants as

$$U = \frac{1}{2EI}\int\left(M^2 + \frac{h^2(1+\nu)}{5}Q^2 - \frac{\nu q h^2 M}{5}\right)dx + \iiint\frac{\sigma_z^2}{2E}\,dxdydz \tag{A.10}$$

The boundary work is $\oint (M\bar{\beta} + Q\bar{w})ds$ where $\bar{\beta}$ and $\bar{w}$ are generalised boundary displacements, and hence the complementary energy is

$$C = U + \oint (M\bar{\beta} + Q\bar{w})ds \tag{A.11}$$

A.4 Minimization of complementary energy

The equilibrium equations are multiplied by Lagrangian multipliers λ_a and λ_c and added to the complementary energy and the variation of the resulting expression set equal to zero.

$$\text{i.e. } \delta\left[\, C + \int\left(\lambda_a\left(\frac{dQ}{dx} + q\right) + \lambda_c\left(\frac{dM}{dx} - Q\right)\right) dxdy \,\right] = 0 \tag{A.12}$$

which gives

$$\int\left(\frac{M\delta M}{EI} + \frac{h^2(1+\nu)}{5EI}Q\delta Q - \frac{\nu q h^2}{10EI}\,\delta M + \lambda_a\,\delta\left(\frac{dQ}{dx} + q\right)\right.$$

$$\left. + \lambda_c\,\delta\left(\frac{dM}{dx} - Q\right)\right)dx + \oint(\bar{\beta}\delta M + \bar{w}\,\delta Q)ds = 0 \tag{A.13}$$

Reissner identifies the Lagrangian multipliers as

$$\lambda_a = w \quad \text{and} \quad \lambda_c = \beta \tag{A.14}$$

Integrating terms by parts where necessary gives

$$\int w\delta\left(\frac{dQ}{dx}\right)\,dx = w\delta Q - \int \frac{dw}{dx}\,\delta Q\,dx \qquad (A.15)$$

$$\int \beta\delta\left(\frac{dM}{dx}\right)\,dx = \beta\delta M - \int \frac{d\beta}{dx}\,\delta M\,dx \qquad (A.16)$$

so that equation (A.13) finally becomes

$$\int \left[\left(\frac{M}{EI} - \frac{\nu q h^2}{10EI} - \frac{d\beta}{dx}\right)\delta M + \left(\frac{h^2(1+\nu)}{5EI}Q - \frac{dw}{dx} - \beta\right)\delta Q\right]dx = 0 \qquad (A.17)$$

Hence $$\frac{M}{EI} = \frac{d\beta}{dx} + \frac{\nu q h^2}{10EI} \qquad (A.18)$$

and $$\beta = -\frac{dw}{dx} + \frac{h^2(1+\nu)}{5EI}Q \qquad (A.19)$$

Differentiating (A.19) and substituting in (A.18) and noting that $\frac{dQ}{dx} = -q$ gives

$$M = -EI\frac{d^2w}{dx^2} - \frac{h^2(2+\nu)}{10}q \qquad (A.20)$$

and $$Q = \frac{dM}{dx} = -EI\frac{d^3w}{dx^3} - \frac{h^2(2+\nu)}{10}\frac{dq}{dx} \qquad (A.21)$$

The governing equilibrium equation is therefore given by

$$EI\frac{d^4w}{dx^4} = q - \frac{h^2(2+\nu)}{10}\frac{d^2q}{dx^2} \qquad (A.22)$$

APPENDIX B

ORTHOTROPIC FORM OF THE MODIFIED REISSNER THEORY

For an orthotropic plate the strain energy is given by

$$U = \frac{1}{2}\iiint\left(\frac{\sigma_x^2}{E_x} + \frac{\sigma_y^2}{E_y} + \frac{\sigma_z^2}{E_z} - 2\sigma_x\sigma_y\frac{\nu_{xy}}{E_x} - 2\sigma_y\sigma_z\frac{\nu_{yz}}{E_y} - 2\sigma_z\sigma_x\frac{\nu_{zx}}{E_z}\right.$$

$$\left. + \frac{\tau_{xy}^2}{G_{xy}} + \frac{\tau_{yz}^2}{G_{yz}} + \frac{\tau_{zx}^2}{G_{zx}}\right) \quad dxdydz \qquad (B.1)$$

Following exactly the same procedure as Reissner gives for homogeneous plates (3) the following expressions for stress resultants are found

$$M_x = -D_x\left(\frac{\partial^2 w}{\partial x^2} + \nu_{yx}\frac{\partial^2 w}{\partial y^2}\right) + D_x\left(\frac{\partial Q_x}{\partial x}\left(\frac{1}{S_x} - \lambda\right) + \frac{\partial Q_y}{\partial y}\left(\frac{\nu_{yx}}{S_y} - \lambda\right)\right) \qquad (B.2)$$

$$M_y = -D_y\left(\frac{\partial^2 w}{\partial y^2} + \nu_{xy}\frac{\partial^2 w}{\partial x^2}\right) + D_y\left(\frac{\partial Q_y}{\partial y}\left(\frac{1}{S_y} - \mu\right) + \frac{\partial Q_x}{\partial x}\left(\frac{\nu_{xy}}{S_x} - \mu\right)\right) \qquad (B.3)$$

$$M_{xy} = D_{xy}\left(-2\frac{\partial^2 w}{\partial x\partial y} + \frac{1}{S_x}\frac{\partial Q_x}{\partial y} + \frac{1}{S_y}\frac{\partial Q_y}{\partial x}\right) \qquad (B.4)$$

$$Q_x = -D_x\left(\frac{\partial^3 w}{\partial x^3} + \nu_{yx}\frac{\partial^3 w}{\partial x\partial y^2}\right) - 2D_{xy}\frac{\partial^3 w}{\partial x\partial y^2} + \frac{\partial^2 Q_x}{\partial x^2}\ D_x\left(\frac{1}{S_x} - \lambda\right)$$

$$+ \frac{\partial^2 Q_x}{\partial y^2}\frac{D_{xy}}{S_x} + \frac{\partial^2 Q_y}{\partial x\partial y}\left(D_x\left(\frac{\nu_{yx}}{S_y} - \lambda\right) + \frac{D_{xy}}{S_y}\right) \qquad (B.5)$$

$$Q_y = -D_y\left(\frac{\partial^3 w}{\partial y^3} + \nu_{xy}\frac{\partial^3 w}{\partial x^2\partial y}\right) - 2D_{xy}\frac{\partial^3 w}{\partial x^2\partial y} + \frac{\partial^2 Q_y}{\partial y^2}D_y\left(\frac{1}{S_y} - \mu\right)$$

$$+ \frac{\partial^2 Q_y}{\partial x^2}\frac{D_{xy}}{S_y} + \frac{\partial^2 Q_x}{\partial x\partial y}\left(D_y\left(\frac{\nu_{xy}}{S_x} - \mu\right) + \frac{D_{xy}}{S_x}\right) \qquad (B.6)$$

where $\frac{1}{D_x} = \frac{12}{h^3}\left(\frac{1}{E_x} - \frac{\nu_{yx}^2}{E_y}\right)$; $\frac{1}{D_y} = \frac{12}{h^2}\left(\frac{1}{E_y} - \frac{\nu_{xy}^2}{E_x}\right)$; $\frac{1}{D_{xy}} = \frac{12}{h^3 G_{xy}}$

$$\frac{1}{S_x} = \frac{6}{5hG_{zx}} \; ; \; \frac{1}{S_y} = \frac{6}{5hG_{yz}}$$

$$\lambda = \frac{12}{10h}\left(\frac{\nu_{xz}}{E_x} + \frac{\nu_{yz}\nu_{yx}}{E_y}\right) \; ; \quad \mu = \frac{12}{10h}\left(\frac{\nu_{yz}}{E_y} + \frac{\nu_{xz}\nu_{xy}}{E_x}\right) \qquad \text{(B.7)}$$

Differentiating (B.5) and (B.6) as required to find $\frac{\partial^2 Q_x}{\partial x^2}$ etc, substituting back and neglecting terms in h^4 and higher powers the following expressions for shear forces result,

$$Q_x = -D_x\frac{\partial^3 w}{\partial x^3} - (\nu_{yx}D_x + 2D_{xy})\frac{\partial^3 w}{\partial x \partial y^2} - q_1\frac{\partial^5 w}{\partial x^5} - q_2\frac{\partial^5 w}{\partial x^3 \partial y^2} - q_3\frac{\partial^5 w}{\partial x \partial y^4} \qquad \text{(B.8)}$$

$$Q_y = -D_y\frac{\partial^3 w}{\partial y^3} - (\nu_{xy}D_y + 2D_{xy})\frac{\partial^3 w}{\partial x^2 \partial y} - q_4\frac{\partial^5 w}{\partial y^5} - q_5\frac{\partial^5 w}{\partial x^2 \partial y^3} - q_6\frac{\partial^5 w}{\partial x^4 \partial y} \qquad \text{(B.9)}$$

where $q_1 = D_x^2\left(\frac{1}{S_x} - \lambda\right)$ $\qquad$ $q_4 = D_y^2\left(\frac{1}{S_y} - \mu\right)$

$$q_2 = (\nu_{yx}D_x + 2D_{xy})D_x\left(\frac{1}{S_x} - \lambda\right) + \frac{D_x D_{xy}}{S_x} + (\nu_{xy}D_x + 2D_{xy})\left(D_x\left(\frac{\nu_{yx}}{S_y} - \lambda\right) + \frac{D_{xy}}{S_y}\right)$$

$$q_5 = (\nu_{xy}D_y + 2D_{xy})D_y\left(\frac{1}{S_y} - \mu\right) + \frac{D_y D_{xy}}{S_y} + (\nu_{yx}D_y + 2D_{xy})\left(D_y\left(\frac{\nu_{xy}}{S_x} - \mu\right) + \frac{D_{xy}}{S_x}\right)$$

$$q_3 = (\nu_{yx}D_x + 2D_{xy})\frac{D_{xy}}{S_x} + D_y\left(D_x(\frac{\nu_{yx}}{S_y} - \lambda) + \frac{D_{xy}}{S_y}\right)$$

$$q_6 = (\nu_{xy}D_y + 2D_{xy})\frac{D_{xy}}{S_y} + D_x\left(D_y(\frac{\nu_{xy}}{S_x} - \mu) + \frac{D_{xy}}{S_y}\right) \qquad \text{(B.10)}$$

Substituting (B.8) and (B.9) in (B.2) - (B.4) and again omitting terms in h^4 gives for the bending and twisting moments

$$M_x = -D_x(\frac{\partial^2 w}{\partial x^2} + \nu_{yx}\frac{\partial^2 w}{\partial y^2}) - D_x\left[\frac{\partial^4 w}{\partial x^4}D_x(\frac{1}{S_x} - \lambda) + \frac{\partial^4 w}{\partial y^4}D_y(\frac{\nu_{yx}}{S_y} - \lambda)\right.$$

$$\left. + \frac{\partial^4 w}{\partial x^2\partial y^2}\left(\nu_{yx}D_x(\frac{1}{S_x} - \lambda) + \nu_{xy}D_y(\frac{\nu_{yx}}{S_y} - \lambda) + 2D_{xy}(\frac{1}{S_x} + \frac{\nu_{yx}}{S_y} - 2\lambda)\right)\right] \qquad \text{(B.11)}$$

$$M_y = -D_y(\frac{\partial^2 w}{\partial y^2} + \nu_{xy}\frac{\partial^2 w}{\partial x^2}) - D_y\left[\frac{\partial^4 w}{\partial y^4}D_y(\frac{1}{S_y} - \mu) + \frac{\partial^4 w}{\partial x^4}D_x(\frac{\nu_{xy}}{S_x} - \mu)\right.$$

$$\left. + \frac{\partial^4 w}{\partial x^2\partial y^2}\left(\nu_{xy}D_y(\frac{1}{S_y} - \mu) + \nu_{yx}D_x(\frac{\nu_{xy}}{S_x} - \mu) + 2D_{xy}(\frac{1}{S_y} + \frac{\nu_{xy}}{S_x} - 2\mu)\right)\right] \qquad \text{(B.12)}$$

$$M_{xy} = -D_{xy}\left[\frac{2\partial^2 w}{\partial x\partial y} + \frac{\partial^4 w}{\partial x^3\partial y}(\frac{D_x}{S_x} + \frac{\nu_{xy}D_y}{S_y} + \frac{2D_{xy}}{S_y}) + \frac{\partial^4 w}{\partial x\partial y^3}(\frac{D_y}{S_y} + \frac{\nu_{yx}D_x}{S_x} + \frac{2D_{xy}}{S_x})\right]$$

(B.13)

Finally the governing equation for w is found by substituting (B.8) and (B.9) in (1.10) which gives

$$D_x\frac{\partial^4 w}{\partial x^4} + (\nu_{yx}D_x + \nu_{xy}D_y + 4D_{xy})\frac{\partial^4 w}{\partial x^2\partial y^2} + D_y\frac{\partial^4 w}{\partial y^4}$$

$$+ q_1\frac{\partial^6 w}{\partial x^6} + (q_2 + q_6)\frac{\partial^6 w}{\partial x^4\partial y^2} + (q_3 + q_5)\frac{\partial^6 w}{\partial x^2\partial y^4} + q_4\frac{\partial^6 w}{\partial y^6} = q \qquad \text{(B.14)}$$

APPENDIX C

NOTES ON ASPECTS OF THE FINITE DIFFERENCE SOLUTIONS.

C.1 Non-dimensionalisation.

A finite difference analysis is conveniently carried out in a non-dimensional form, and the usual procedure is followed here. Lengths and linear displacements are expressed as ratios of a representative dimension, in this case L, the span of the beam or side of the plate, so that non-dimensional forms for co-ordinates, displacement, plate thickness and mesh length are

$$X = \frac{x}{L} \ , \ Y = \frac{y}{L} \ , \ W = \frac{w}{L} \ , \ H = \frac{h}{L} \ , \ P = \frac{p}{L}$$

Derivatives of w then become

$$\frac{\partial^n w}{\partial x^n} = \frac{1}{L^{n-1}} \frac{\partial^n W}{\partial X^n}$$

and all derivatives of the type $\partial^n W/\partial X^n$ are then non-dimensional. Inspection of the form of the equations for bending and twisting moments and shear forces shows that in non-dimensional form these become

$$\frac{M_x L}{D} \ , \ \frac{M_y L}{D} \ , \ \frac{M_{xy} L}{D} \ , \ \frac{Q_x L^2}{D} \ , \ \frac{Q_y L^2}{D}$$

and the load per unit area is qL^3/D.

C.2 Finite difference equivalents for 5th and 6th order derivatives.

Application of the modified Reissner theory involves the use of 5th and 6th order derivatives of W, and as the finite difference equivalents for these are not commonly in use the molecules for $\partial^5 W/\partial X^5$ and $\partial^6 W/\partial X^6$ accurate to order P^2 are shown in Figure C.1.

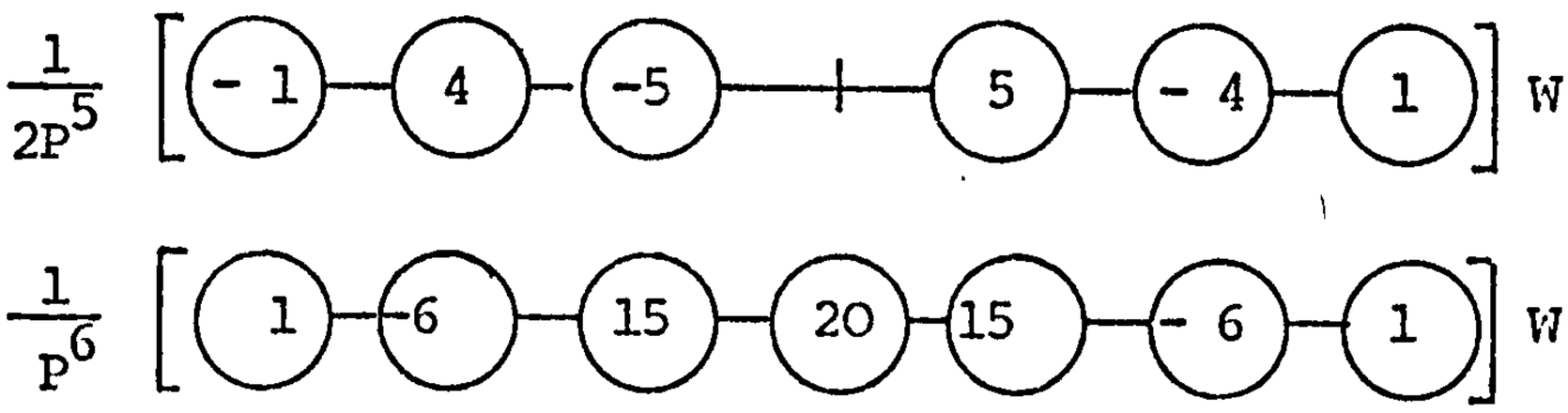

Figure C.1

Finite difference molecules for $\partial^5 W/\partial X^5$ and $\partial^6 W/\partial X^6$

The appropriate expressions for the other higher order derivatives, $\partial^5 W/\partial X^n \partial Y^{5-n}$, $\partial^6 W/\partial X^n \partial Y^{6-n}$ are then found in the usual manner.

C.3 Finite difference equivalents of order of accuracy p^4

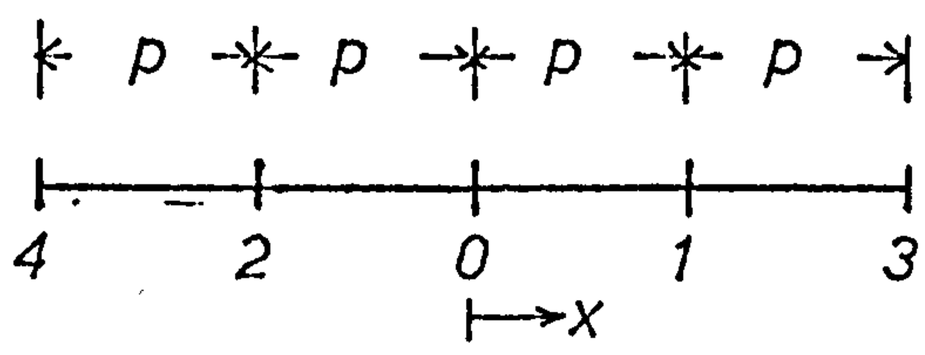

First and second order derivatives of w at mesh point 0 can be written in finite difference form to accuracy p^4 in terms of the values of w at the five points shown.

Taylor's series are used to express w at mesh points 1, 2, 3 and 4 in terms of w and its derivatives at mesh point 0 as follows:

$$w_1 = w_o + pw_o' + \frac{p^2}{2} w_o'' + \frac{p^3}{6} w_o''' + \frac{p^4}{24} w_o'''' + \ldots.$$

$$w_2 = w_o - pw_o' + \frac{p^2}{2} w_o'' - \frac{p^3}{6} w_o''' + \frac{p^4}{24} w_o'''' - \ldots.$$

$$w_3 = w_o + 2pw_o' + 2p^2 w_o'' + \frac{4p^3}{3} w_o''' + \frac{2p^4}{3} w_o'''' + \ldots.$$

$$w_4 = w_o - 2pw_o' + 2p^2 w_o'' - \frac{4p^3}{3} w_o''' + \frac{2p^4}{3} w_o'''' - \ldots.$$

where primes denote differentiation with respect to x. From these equations it can be seen that

$$8(w_1 - w_2) - (w_3 - w_4) = 12pw'_o$$

and hence $(\frac{\partial w}{\partial x})_o = \frac{1}{12p} (8w_1 - 8w_2 - w_3 + w_4)$ (C.1)

The next term in the series would be of order p^5 giving an error of order p^4.

The corresponding expression for the curvature at mesh point O is found by observing from the Taylor's series that

$$16(w_1 + w_2) - (w_3 + w_4) = 30w_o + 12p^2w''_o$$

and hence

$$(\frac{\partial^2 w}{\partial x^2})_o = \frac{1}{12p^2} (-30w_o + 16w_1 + 16w_2 - w_3 - w_4) \quad (C.2)$$

In order to form the finite difference equivalents of this order of accuracy for third and fourth order derivatives the two mesh points at distance $3p$ from mesh point O are involved, and the Taylor's series expanded to the term in p^6. The derivation is then as before, and the resulting molecules are shown in Figure D.2.

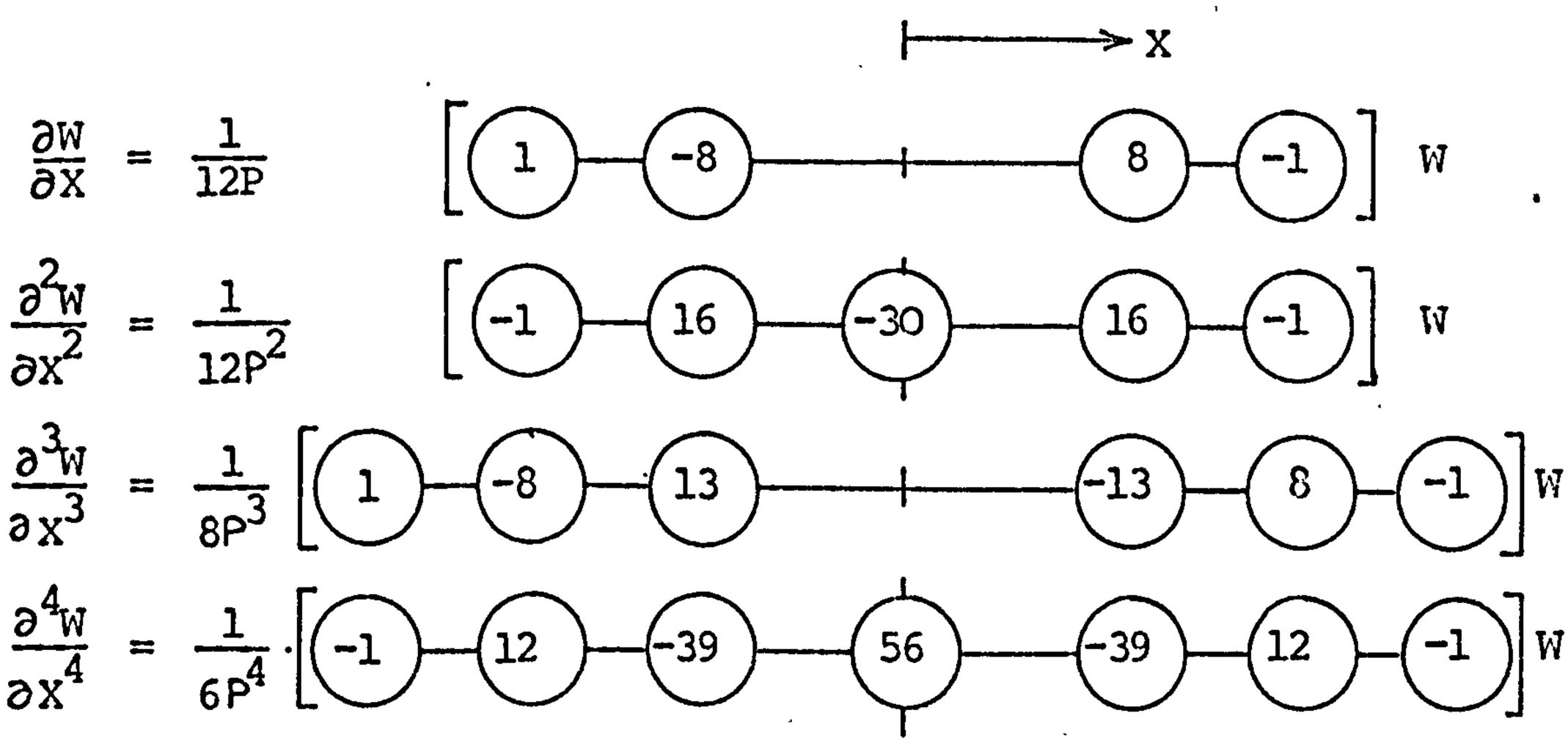

Figure C.2

Finite difference molecules accurate to order p^4

Cross derivatives are then found from these in the usual way, or, where mixed order accuracy is used, in conjunction with the normal derivatives of order of accuracy p^2.

APPENDIX D

COMPUTER FORMULATION FOR LOCALISED RAYLEIGH-RITZ SOLUTIONS

D.1 Introduction.

Localised Rayleigh-Ritz techniques have been used to apply the modified Reissner theory to beams (Section 3.7.3) and plates (Section 4.9.1) and the partial deflection method to plates. This Appendix discusses the computer formulation of some of the matrices and vectors involved.

D.2 Matrix[C].

The strain energy in a local region is written as

$$U = k\ [\Lambda^T C A]$$

where the displacement function is

$$w = [A][\xi]$$

D.2.1 Matrix [C] for beams - continuity to third order derivative.

In this case the deflection function is

$$w = \sum_{i=1}^{8} a_i \xi^{m_i} \qquad (D.1)$$

and hence the kth derivative is

$$\frac{d^k w}{d\xi^k} = \sum_{i=1}^{8} m_i(m_i - 1).....(m_i - k + 1)a_i\ \xi^{m_i - k} \qquad (D.2)$$

$$m_i \geqslant k \text{ for each term}$$

The energy function contains N terms each of which is the product of two derivatives,

$$U = \sum_{p=1}^{N} \alpha_p \int_0^1 \frac{d^{k_p} w}{d\xi^{k_p}} \cdot \frac{d^{l_p} w}{d\xi^{l_p}}\ d\xi \qquad (D.3)$$

$$\text{Now } \frac{d^k w}{d\xi^k} \cdot \frac{d^l w}{d\xi^l} = \sum_{i=1}^{8} \sum_{j=1}^{8} \frac{m_i (m_i-1)\ldots(m_i-k+1) m_j (m_j-1)\ldots(m_j-l+1)}{m_i+m_j-k-l+1} a_i a_j$$

$$m_i \geqslant k \text{ and } m_j \geqslant l \qquad \text{(D.4)}$$

and hence the coefficients of matrix [C] are given by

$$c_{ij} = \sum_{p=1}^{N} \alpha_p \frac{m_i (m_i-1)\ldots(m_i-k+1) m_j (m_j-1)\ldots(m_j-l_p+1)}{m_i + m_j - k_p - l_p + 1}$$

$$m_i \geqslant k \text{ and } m_j \geqslant l \qquad \text{(D.5)}$$

D.2.2 Matrix C for plates - continuity to third order derivatives.

The local deflection function for a plate region is

$$W = \sum_{i=1}^{64} a_i \xi^{r_i} \eta^{s_i} \qquad \text{(D.6)}$$

from which a typical derivative may be written as

$$\frac{\partial^{k+l} w}{\partial \xi^k \partial \eta^l} = \sum_{i=1}^{64} r_i (r_i-1)\ldots(r_i-k+1) s_i (s_i-1)\ldots(s_i-l+1) a_i \xi^{r_i-k} \eta^{s_i-l}$$

$$r_i \geqslant k \text{ and } s_i \geqslant l \qquad \text{(D.7)}$$

The strain energy function in terms of derivatives of w has the form

$$U = \sum_{p=1}^{N} \alpha_p \int_0^1 \int_0^1 \frac{\partial^{k+l} w}{\partial \xi^k \partial \eta^l} \frac{\partial^{m+n} w}{\partial \xi^m \partial \eta^n} \, d\xi \, d\eta \qquad \text{(D.8)}$$

Integrating a single term gives

$$\int_0^1 \int_0^1 \frac{\partial^{k+l} w}{\partial \xi^k \partial \eta^l} \frac{\partial^{m+n} w}{\partial \xi^m \partial \eta^n} =$$

$$\sum_{i=1}^{64} \sum_{j=1}^{64} \frac{r_i (r_i-1)\ldots(r_i-k+1) s_i (s_i-1)\ldots(s_i-l+1) r_j (r_j-1)\ldots(r_j-m+1) s_j (s_j-1)\ldots(s_j-n+1)}{(r_i+r_j-k-m+1)(s_i+s_j-l-n+1)}$$

$$r_i \geqslant k,\ s_i \geqslant l,\ r_j \geqslant m \text{ and } s_j \geqslant n \qquad \text{(D.9)}$$

and hence the coefficients of matrix C are given by

$$C_{ij} = \sum_{p=1}^{N} \alpha_p \frac{r_i \ldots (r_i - k_p + 1) s_i \ldots (s_i - \ell_p + 1) r_j \ldots (r_j - m_p + 1) s_j (s_j - n_p + 1)}{(r_i + r_j - k_p - m_p + 1)(s_i + s_j - \ell_p - n_p + 1)}$$

$$r_i \geqslant k_p,\ s_i \geqslant \ell_p,\ r_j \geqslant m_p \text{ and } s_j \geqslant n_p \qquad \text{(D.10)}$$

D.3 Matrix B.

D.3.1 Matrix B for plates with continuity in third derivatives.

Freedom is given to a typical derivative $\frac{\partial^{k+\ell} w}{\partial \xi^k \partial \eta^\ell}$ by forming the product of $f_q^k(\xi)$ and $f_q^\ell(\eta)$, the functions which give freedom to the kth and ℓth derivatives at node q. These functions are

$$f_q^k(\xi) = \sum_{i=1}^{8} \alpha_i \xi^i \qquad \text{(D.11)}$$

$$f_q^\ell(\eta) = \sum_{j=1}^{8} \alpha_j \eta^j \qquad \text{(D.12)}$$

where the coefficients α_i and α_j are the relevant values from matrix [B] for beams shown in Figure 3.16a. The 64 term expression giving freedom to the general derivative $\frac{\partial^{k+\ell} w}{\partial \xi^k \partial \eta^\ell}$ is

$$f_q^k(\xi) . f_q^\ell(\eta) = \sum_{i=1}^{8} \sum_{j=1}^{8} \alpha_i \alpha_j \xi^i \eta^j \qquad \text{(D.13)}$$

If the deflection in the local region is

$$w = \sum_{p=1}^{64} a_p \xi^{m_p} \eta^{n_p} \qquad \text{(D.14)}$$

then the pth element of the column of [B] relating to freedom of $\frac{\partial^{k+\ell} w}{\partial \xi^k \partial \eta^\ell}$ at node q is $\alpha_i \alpha_j$ when $i = m_p$ and $j = n_p$

D.4 Matrix [B] for partial deflection method.

Matrix [B] for the partial deflection method is compiled from the matrices $[B_b]$ and $[B_s]$ shown in Figures D.1 and D.2. $[B_b]$ gives freedom to w_b, $\frac{\partial w_b}{\partial \xi}$, $\frac{\partial w_b}{\partial \eta}$, $\frac{\partial^2 w_b}{\partial \xi \partial \eta}$ and $[B_s]$ to w_s at each node.

$$\begin{bmatrix}
1 & 0 & 0 & 0 & 0 & 0 & 0 & 0 & 0 & 0 & 0 & 0 & 0 & 0 & 0 & 0 \\
0 & 1 & 0 & 0 & 0 & 0 & 0 & 0 & 0 & 0 & 0 & 0 & 0 & 0 & 0 & 0 \\
0 & 0 & 1 & 0 & 0 & 0 & 0 & 0 & 0 & 0 & 0 & 0 & 0 & 0 & 0 & 0 \\
-3 & -2 & 0 & 0 & 3 & -1 & 0 & 0 & 0 & 0 & 0 & 0 & 0 & 0 & 0 & 0 \\
0 & 0 & 0 & 1 & 0 & 0 & 0 & 0 & 0 & 0 & 0 & 0 & 0 & 0 & 0 & 0 \\
-3 & 0 & -2 & 0 & 0 & 0 & 0 & 0 & -3 & 0 & -1 & 0 & 0 & 0 & 0 & 0 \\
2 & 1 & 0 & 0 & -2 & 1 & 0 & 0 & 0 & 0 & 0 & 0 & 0 & 0 & 0 & 0 \\
0 & 0 & -3 & -2 & 0 & 0 & 3 & -1 & 0 & 0 & 0 & 0 & 0 & 0 & 0 & 0 \\
0 & -3 & 0 & -2 & 0 & 0 & 0 & 0 & 0 & 3 & 0 & -1 & 0 & 0 & 0 & 0 \\
2 & 0 & 1 & 0 & 0 & 0 & 0 & 0 & -2 & 0 & 1 & 0 & 0 & 0 & 0 & 0 \\
0 & 0 & 2 & 1 & 0 & 0 & -2 & 1 & 0 & 0 & 0 & 0 & 0 & 0 & 0 & 0 \\
9 & 6 & 6 & 4 & -9 & 3 & -6 & 2 & -9 & -6 & 3 & 2 & 9 & -3 & -3 & 1 \\
0 & 2 & 0 & 1 & 0 & 0 & 0 & 0 & 0 & -2 & 0 & 1 & 0 & 0 & 0 & 0 \\
-6 & -3 & -4 & -2 & 6 & -3 & 4 & -2 & 6 & 3 & -2 & -1 & -6 & 3 & 2 & -1 \\
-6 & -4 & -3 & -2 & 6 & -2 & 3 & -1 & 6 & 4 & -3 & -2 & -6 & 2 & 3 & -1 \\
4 & 2 & 2 & 1 & -4 & 2 & -2 & 1 & -4 & -2 & 2 & 1 & 4 & -2 & -2 & 1
\end{bmatrix}$$

Figure D.1

Matrix $[B_b]$

$$\begin{bmatrix}
1 & 0 & 0 & 0 \\
-1 & 1 & 0 & 0 \\
-1 & 0 & 1 & 0 \\
1 & -1 & -1 & 1
\end{bmatrix}$$

Figure D.2

Matrix $[B_s]$

D.5 Loading vector for uniformly distributed load.

The displacement of a local region of a beam where continuity of the third order derivative is prescribed is defined by

$$w = \sum_{i=1}^{8} a_i \xi^{m_i} \quad \text{where} \quad a_i = \sum_{j=1}^{8} B_{ij} Q_j \tag{D.15}$$

and hence a load of q per unit length will suffer a loss of potential energy in the region of

$$V = -\int_0^1 qw\,d\xi = -q \sum_{i=1}^{8} \sum_{j=1}^{8} \frac{1}{m_i + 1} B_{ij} Q_j \tag{D.16}$$

Minimizing this with respect to Q_j will lead to expressions of the form

$$\frac{\partial V}{\partial Q_j} = -q \frac{B_{ij}}{m_i + 1} \tag{D.17}$$

from which the total right hand side vector is formed by addition of such terms for each local region.

For plates subjected to a uniform loading of q per unit area where continuity of third order derivatives is prescribed the following three equations apply in place of equations (D.15) - (D.17) respectively

$$w = \sum_{i=1}^{64} a_i \xi^{m_i} \eta^{n_i} \quad \text{where} \quad a_i = \sum_{j=1}^{64} B_{ij} Q_j \tag{D.18}$$

$$V = -\int_0^1 \int_0^1 qw\,d\xi\,d\eta = -q \sum_{i=1}^{64} \sum_{j=1}^{64} \frac{B_{ij}}{(m_i + 1)(n_i + 1)} Q_j \tag{D.19}$$

$$\frac{\partial V}{\partial Q_j} = -q \sum_{i=1}^{64} \frac{B_{ij}}{(m_i + 1)(n_i + 1)} \tag{D.20}$$

APPENDIX E

COMPUTATION AND NUMERICAL ANALYSIS

All computation was carried out on the IBM 360 at University College, London, or the CDC 7600 at the University of London Computer Centre. Gaussian elimination was used to solve the systems of simultaneous equations using a subroutine from the IBM SSP3 library, which was available on both computers in single and double precision form. Because of the relatively short word length of the IBM 360 most of the calculations on this machine were carried out in double precision, while single precision was found to be adequate on the CDC 7600.

Any possible loss of numerical significance in the solution is determined using a tolerance defined by

$$tol = a_{ij}\epsilon$$

where a_{ij} is the largest element of the left hand side coefficient matrix [A] and ϵ is a relative tolerance which may range from 10^{-7} in single precision to 10^{-14} in double precision. If at any stage of the elimination the absolute value of the pivotal element falls below tol a warning is given that possible loss of significance has occurred, although this does not necessarily invalidate the solution values.

Table F.1 gives a comparison of the storage and CPU times required for the various plate solutions.

Finite difference solutions - IBM 360			
	No. of equations	Storage	CPU time
Partial deflection method	126	104kB	29 sec
Reissner's theory	150+	218kB	50 sec
Modified Reissner theory	106+	126kB	18 sec
Localised Rayleigh-Ritz solutions - CDC 7600			
Modified Reissner theory	40	24K	5 sec
Partial deflection method	45*	16K	2 sec

+ double precision

* Using a 4x4 mesh for w_b and w_s. Since the sets of equations for w_b and w_s are independent in the superposition approach the same size mesh need not necessarily be used for both.

Table E.1

Storage requirements and CPU times.

For purposes of comparison 1K of storage and 1 sec CPU time for the CDC 7600 roughly equivalent to 4kB and 20 sec CPU time for the IBM 360.

REFERENCES

1. Timoshenko S.P. and Woinowsky-Krieger S. Theory of Plates and Shells. (Second Edition) McGraw Hill, 1959.

2. Reissner E. On the theory of bending of elastic plates. J. Mathematics and Physics, Vol. 23, 1944.

3. Reissner E. The Effect of transverse shear deformation on the bending of elastic plates. J. App. Mech. June, 1944.

4. Reissner E. On bending of elastic plates. Q. App. Maths. Vol. 5, 1947.

5. Green A.E. On Reissner's theory of bending of elastic plates. Q. App. Maths. Vol. 7, 1949.

6. Salerno V.L. and Goldberg M.A. Effect of shear deformation on the bending of rectangular plates. J. App. Mech. Mar. 1960.

7. Koeller R.C. and Essenburg F. Shear deformation in rectangular plates. Proc. 4th U.S. Nat. Cong. Appl. Mech. 1962.

8. Schäfer M. Über eine Verfeinerung der klassischen Theorie dünner schwach gebogener Platten. Z. für Ang. Math. und Mech. Vol. 32, 1952.

9. Carley T.G. and Langhaar H.L. Transverse shearing stress in rectangular plates. J. Eng. Mech. Div. Proc. ASCE, Feb. 1968.

10. Frederick D. On some problems in bending of thick circular plates on an elastic foundation. J. Appl. Mech. Vol. 23, 1936.

11. Frederick D. Thick rectangular plates on an elastic foundation. Trans ASCE Vol. 122, 1957.

12. Langhaar H.L. Energy theorems in Applied Mechanics. Wiley, 1962.

13. Love A.E.H. The Mechanical Theory of Elasticity. 4th Edition. Cambridge University Press, 1927.

14. Kromm A. Verallgemeinerte Theory der Plattenstatik. Ingenieur-Archiv Vol. 21, 1953.

15. Kromm A. Über die Rand querkrafte bei Gestutaten Platten. Z. für Ang. Math. und Mech. Vol. 35, 1955.

16. Goldenveiser A.L. and Kolos A.V. On the derivation of two dimensional equations in the theory of thin elastic plates. J. Appl. Math. Mech. Vol. 29,1 1965.

17. Kolos A.V. Methods of refining the classical theory of bending and extension of plates. J. Appl. Math. Mech. Vol. 29,4 1965.

18. Goldenveiser A.L. Derivation of an approximate theory of bending of a plate by the method of asymptotic integration of the equations. J. Appl. Math. Mech. Vol. 26,4. 1962.

19. Ambartsumyan S.A. Theory of Anisotropic Plates. Technomic Publishing Co. Inc. 1970.

20. Haberland G. Photoelastic analysis of plates applying the theory of E. Reissner. 1964 - see Applied Mechanics Reviews, 3457.

21. Plantema F.J. Sandwich Construction. Wiley, 1966.

22. Allen H.G. Analysis and Design of Structural Sandwich Panels. Pergamon, 1969.

23. Libove C. and Batdorf S.B. A general small deflection theory for flat sandwich plates. NACA Report No. 899.

24. Williams D.G. and Chapman J.C. Effect of shear deformation on uniformly loaded rectangular orthotropic plates. Suppl. Proc. ICE, 1969.

25. Morley C.T. Allowing for shear deformation in orthotropic plate theory. Suppl. Proc. ICE, 1971.

26. Timoshenko S.P. and Goodier J.N. Theory of Elasticity. Second Edition, McGraw Hill, 1951.

27. Timoshenko S.P. Strength of Materials (Second Edition) Vol. 1.

28. Sechler E.E. Elasticity in Engineering. Dover, 1952.

29. Thomson J.M.T. Localised Rayleigh functions for structural and stress analysis. Int. J. Solids and Structures. Vol. 3, 1967.

30. Clough R.F. and Felippa C.A. A refined quadrilateral element for analysis of plate bending. Second Conference on Matrix Methods in Structural Mechanics. Wright-Patterson Air Force Base, 1968.

31. Basu A.K. and Dawson J.M. Orthotropic sandwich plates. Suppl. Proc. ICE, 1971.

32. Pryor C.W. Barker R.M. and Frederick D. Finite element bending of Reissner plates. J. Eng. Mech. Div. ASCE EM6 Dec. 1970.

33. Smith I.M. A finite element analysis for 'moderately thick' rectangular plates in bending. Int. J. Mech. Sci. Vol. 10, 1968.

34. Reissner E. Finite deflections of sandwich plates. J. Aero. Sci. Vol. 15, July 1948; Vol. 17, Feb. 1950 (erratum)

35. Ratcliffe A.T. Effect of shear deformation in a beam on an elastic foundation. Int. J. Mech. Sci. Vol. 15, June 1973.

36. Parkhill D.L. The flexural behaviour of slabs at ultimate load. Mag. of Concrete Research. Vol. 18, No. 56 : Sept. 1966.

37. Timoshenko S.P. Young D.H. and Weaver W. Vibration problems in Engineering. 4th Ed. Wiley 1974.